Towards glycomimetic derivatives of *N*-Acetyl-D-Fucosamine

By

Sara J. Duncan

Submitted in Partial Fulfillment of the Requirements

for the Degree of

Master of Science

in the

Chemistry

Program

YOUNGSTOWN STATE UNIVERSITY

August, 2006

Towards glycomimetic derivatives of *N*-Acetyl-D-Fucosamine

Sara J. Duncan

I hereby release this thesis to the public. I understand that this thesis will be made available from the OhioLINK ETD Center and the Maag Library Circulation Desk for public access. I also authorize the University or other individuals to make copies of this thesis as needed for scholarly research.

Signature:

Sara J. Duncan — 8/3/06 Date

Approvals:

Dr. Peter Norris — 8/3/06 Date
Thesis Advisor

Dr. John A. Jackson — 8/3/06 Date
Committee Member

Dr. Timothy R. Wagner — 8/3/06 Date
Committee Member

Dr. Peter J. Kasvinsky — 8/9/06 Date
Dean of Graduate Studies and Research

Thesis Abstract

The following work describes an attempted synthesis towards making *N*-Acetyl-D-Fucosamine from *N*-Acetyl-D-Glucosamine. The bacterium *Staphylococcus aureus* depends on a capsular polysaccharide to protect it from being destroyed by the body's immune defense system. Thus, if the rare sugar *N*-Acetyl-D-Fucosamine can be made, more experiments can be done to make small molecule glycomimetics that will possibly inhibit capsular polysaccharide formation.

Acknowledgements

First I would like to thank Youngstown State University and the graduate school for the wonderful opportunity that I was given to come here to get my Master's degree. I would also like to thank the Chemistry Department and in particular Dr. Timothy Wagner and Dr. John Jackson for being members of my committee. Their feedback on my thesis was greatly appreciated.

I of course want to thank Dr. Peter Norris for being my thesis advisor. All the pushing to get things done and obtain results really paid off when I went to find a job. Thank you so much Doc for all the hard work as well as all the coffee. I also want to thank so many members of the Norris group. All of the graduates who were here when I started, Craig, Dave, Travis, and especially Mat for being a great friend. I want to thank Iulia and Monica because we were the three girls in lab and even though having three girls together usually made us clash, you two are great friends. I want to thank Basit for always being the happy guy in the group and always having a smile on his face, and Ryan for being my lab buddy and a great friend.

I especially want to thank my mom and Tony for supporting me through thick and thin and always believing in anything I ever did. I love you both so much.

Table of Contents

List of Tables

List of Schemes

List of Equations

List of Figures

Introduction

Sugars, in one form or another, can be traced back to the early times of civilization. Simple sugars had the formula $C_x(H_2O)_y$ and were therefore thought to be hydrates of carbon. They were then called carbohydrates although the word sugar is slowly being replaced by the word saccharide meaning "sugarlike."[1] Carbohydrates have been used extensively as starting materials in enantioselective syntheses because they are generally inexpensive. Many of the syntheses start with D-glucose, however since glucose does not normally resemble the desired final product, many of the syntheses involve multi-step processes.[2] The importance of carbohydrates is exemplified by their uses in many different industries. In manufacturing, there are obvious major uses for sucrose and paper, in the food industry starch is used frequently for baked goods and staples such as pasta, and in the textile industry cellulose is used to make clothes in the form of cotton and wool.[1] In the pharmaceutical industry, carbohydrates are found frequently as components of antibiotics. In this industry, optical purity is important because a racemic drug in biological systems behaves like a mixture of the two compounds, often with only one of the enantiomers having the desired properties.[2] Other areas that highlight the importance of carbohydrates are the fine chemical industry that markets pure sugars to consumers, and the nutrition industry that markets them as dietary supplements. Carbohydrates are also the most abundant organic components in plants and they play key roles in the processes of life.[1]

With the importance of carbohydrates established, it is important to understand why they are used in synthetic chemistry. One of the main reasons to use carbohydrates is that the price of these materials is often so low that syntheses can usually be carried out

on any scale. The greatest use for these is as synthons for compounds with carbon chains with contiguous or noncontiguous secondary alcohols. Another advantage to these molecules is the stereocontrol possible when manipulating functions. A major advantage of carbohydrates as starting materials is that they come from renewable natural sources. Some of these sources are various polysaccharides such as starch, mannans, and xylans.[2] One of the few drawbacks though of carbohydrates from a synthetic perspective is that they can be overfunctionalized.[2]

Carbohydrates are organized into four main classes according to their degree of polymerization, which include *monosaccharides*, *oligosaccharides*, *polysaccharides*, and the class that includes DNA, RNA, nucleotides, and nucleosides.[1] The first class, monosaccharides, are chiral polyhydroxyalkanals or polyhydroxyalkanones that exist in hemiacetal forms; an example of one is in Figure 1.

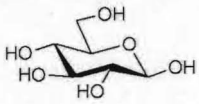

Figure 1: Monosaccharide example, β-D-glucopyranose.

There are two groups of these forms that are determined by whether the acyclic forms possess an aldehyde or keto group and are thus called *aldoses* or *ketoses* with examples of each shown in Figure 2.[1]

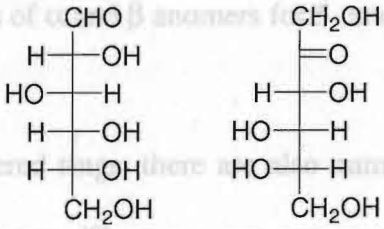

Figure 2: Examples of an aldose (D-glucose) and a ketose (L-fructose).

The D and L notations refer to the orientation of the hydroxyl group on the bottom stereocenter in the Fischer projection. If the hydroxyl group is on the left of the chain, this represents the L enantiomer and if the hydroxyl group is on the right of the chain this represents the D enantiomer. If the Fischer projections are then transformed into the cyclic ring orientation, the hydroxyl groups will be given either α or β notations based on their orientations. Based on the orientation of the anomeric center, which is the atom at C-1, if the hydroxyl at this anomeric center is positioned below the ring it is given the α notation. If the hydroxyl group is above the cyclic ring, it is given the β notation. The monosaccharides are also grouped according to the size of the rings into five-membered furanoses or six-membered pyranoses.[1] Examples of α (**A** and **C**) and β (**B** and **D**) anomers for both 5- (**C** and **D**) and 6- (**A** and **B**) membered rings are shown in Figure 3.

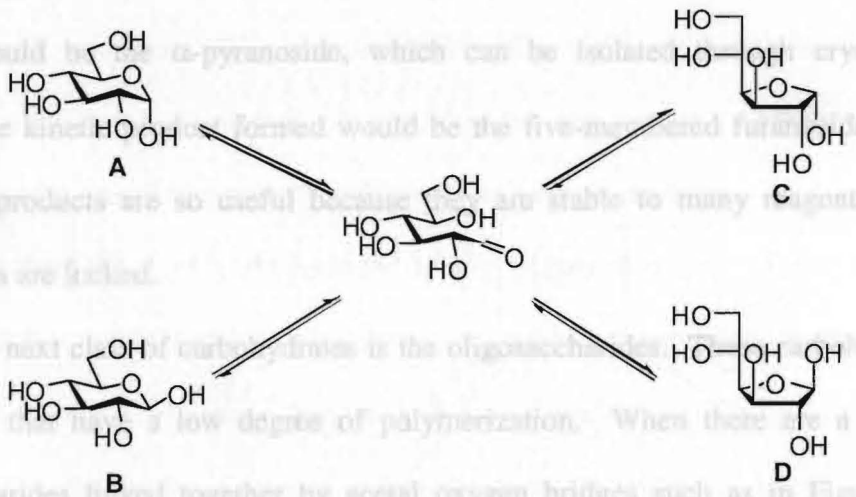

Figure 3: Examples of α and β anomers for 5- and 6-membered rings.

Within the six-membered rings, there are also numerous conformations possible when dealing with carbohydrates. The two most extreme forms would include the $^4C_1$

and the $^1C_4$ forms shown in Figure 4.[3,4,5] The form that the current research involves the most is the $^4C_1$ form.

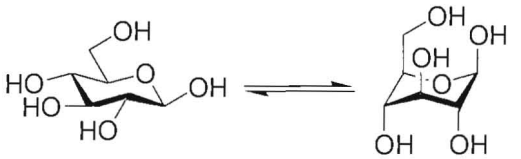

Figure 4: $^4C_1$ and the $^1C_4$ forms of D-glucopyranose.

Monosaccharides cannot be depolymerized by hydrolysis into simple sugars.[1] An example of a monosaccharide reaction would be the reaction with an alcohol and an acid, which would convert into a monomethyl acetal (or a *methyl glycoside*), which is called a Fisher glycosidation.[6] This type of reaction can be complicated and can lead to four isomeric products. For D-glucose, for example, the most thermodynamically stable product would be the α-pyranoside, which can be isolated through crystallization; however the kinetic product formed would be the five-membered furanoside.[7,8] These glycosidic products are so useful because they are stable to many reagents and their cyclic forms are locked.

The next class of carbohydrates is the oligosaccharides. These carbohydrates are polyacetals that have a low degree of polymerization. When there are a number of monosaccharides linked together by acetal oxygen bridges such as in Figure 5, their overall composition can be seen.[1]

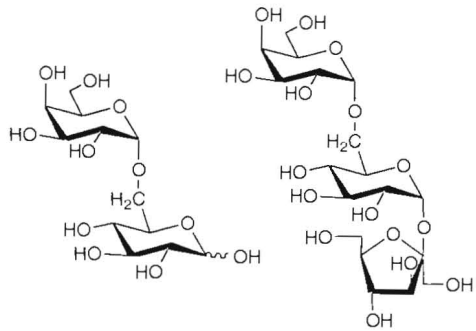

Figure 5: Examples of a disaccharide and a trisaccharide.

Oligosaccharides with a lower degree of polymerization often have a sweet taste to them; if their degree of polymerization is above four monosaccharide units though the oligosaccharides are generally tasteless. There are two types of oligosaccharides; simple oligosaccharides and conjugate oligosaccharides. Simple (or "true") oligosaccharides are oligomers and polymers of monosaccharides that yield only monosaccharides on complete hydrolysis. Conjugate oligosaccharides are oligomers and polymers of monosaccharides linked to nonsaccharides such as lipids or peptides.[1]

The third class of carbohydrates is the polysaccharides. These differ from oligosaccharides in the degree of polymerization; polysaccharides can reach a degree of polymerization of 10^5, whereas oligosaccharides only reach a degree of polymerization of 10 units. The higher the degree of polymerization, the more the physical properties change; the solubility of the material will start to decrease and the viscosity will start to increase.[1] There are also two general classes of polysaccharides. The first is *homopolysaccharides*, which are simple polymers having only one type of monosaccharide as a repeating unit. The other class is *heteropolysaccharides*, which are made up of more than one type of monosaccharide.[1]

The final major class of carbohydrate materials include; DNA, RNA, nucleotides, and nucleosides. The main difference between this class and the other classes is that it consists of units that are linked by phosphate esters, and not through glycosidic linkages as occurs in oligo- and polysaccharides.[1]

One of the main reasons we are so interested in carbohydrates is that they are found in the opportunistic bacteria *Staphylococcus aureus*. This bacterium is a pathogen responsible for a variety of human and animal diseases. It is also a major cause of wound infections and has the persistent potential to induce osteomyelitis, endocarditis, and bacteremia, leading to secondary infections in many of the major organs.[9] *S. aureus* is the number one cause of infections in hospitalized patients. Those most susceptible to *staph* infections are those who abuse drugs, patients undergoing surgical procedures, those with prosthetic devices, and immunocompromised hosts.[10,11] Some of the conditions the bacteria causes include scalded-skin syndrome, toxic shock syndrome, septic arthritis, and food poisioning.[13] *S. aureus* is a major cause of community-acquired infection and it is most common in hosts with compromised or defective immune systems.[9] *Staphylococci* that cause disease in humans and animals are not inherently pathogenic organisms. Rather the purpose of a given virulence factor is not to cause disease but to enhance the survival of the bacterium in adverse environments. A virulence factor would be a factor produced by a bacterium that is not essential for growth but allows survival within or on a host organism in a non-symbiotic manner meaning that this factor is extremely infectious. The bacterial survival during the infection depends on the ability of the bacterium to enclose or entrap the host's defenses, which would primarily mean our body's immune system.[14]

S. aureus is a versatile pathogen that has evolved resistance to all antibiotic classes.[15] It is one of the most dangerous pathogens due to its ability to cause sepsis and even death.[10,16] Other infections *S. aureus* causes are necrotizing fasciitis, which is a life threatening infection that needs medical therapy and urgent surgery,[17] and acute bacterial endocarditis, which leads to disseminated intravascular coagulation or septic shock.[18] In this case mortality ranges from 40-80%.[18] In some areas, more than 95% of *S. aureus* isolates are now resistant to penicillin or ampicillin and more than 50% have developed resistance to methicillin, which are all penicillin-type antibiotics.[19] There are an increasing number of microorganisms that have evolved strains which can defeat a lot of modern medicine's weapons such as antibiotics.[20] The current mortality rates associated with the *staph* infections are 20-25% even with active antimicrobial agents.[21,22,23] A significant number of the isolates are also resistant to lincosamides, macrolides, aminoglycosides, and fluoroquinolones.[16] Due to this frequency of antibiotic-resistant strains, and the recent emergence of clinical isolates resistant to vancomycin also, attempts to overcome *S. aureus* have become increasingly more difficult.

The bacterial components and secreted products that affect the pathogenesis of *S. aureus* infections are abundant and include surface-associated adhesions, a capsular polysaccharide, exoenzymes, and exotoxins. This collection of bacterial products allows *S. aureus* to stick on to eukaryotic membranes, resist opsonophagocytosis, lyse or break up eukaryotic cells, and cause a loss of host immunomodulating molecules.[24] The organism makes its first contact with humoral and cellular host factors through surface molecules adhering to the host's tissues and through colonization.[25] Eleven serotypes have been identified, but strains 5 and 8 are clinically prevalent.[26-30] The majority of

clinical *S. aureus* isolates produce either a type 5 or type 8 capsule, which makes the organisms resistant to phagocytic uptake.[24]

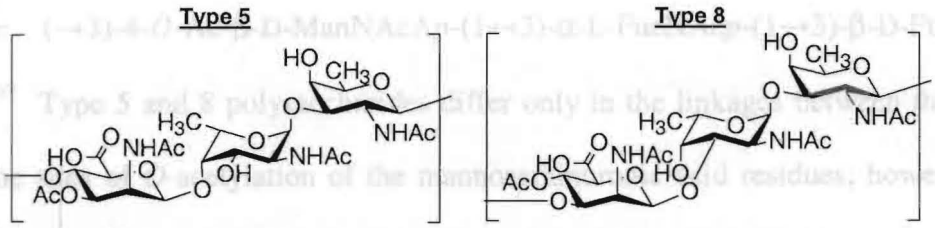

Figure 6: Structures of the repeating units of the microcapsules of Type 5 and Type 8 serotypes of *Staphylococcus aureus*.

Polysaccharides from *Staphylococcus aureus* serotypes 5 and 8 (Figure 6) are built of 2-acetamido-D-mannosamineuronic acid (*N*-acetyl-D-mannosaminuronic acid or D-ManAcA), 2-acetamido-2,6-dideoxy-L-galactose (*N*-acetyl-L-fucosamine or L-FucNAc), and 2-acetamido-2,6-dideoxy-D-galactose (*N*-acetyl-D-fucosamine or D-FucNAc) residues (Figure 7).

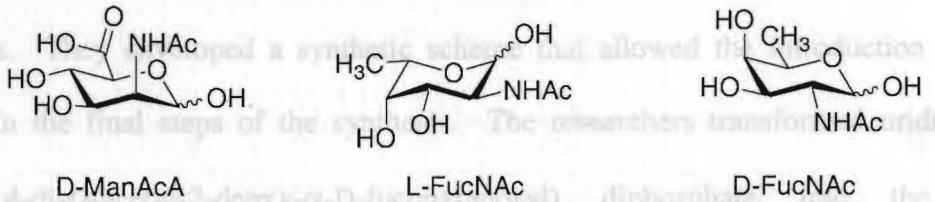

Figure 7: Structures of saccharide residues in *S. aureus* serotypes 5 and 8.

The production of these microcapsules is influenced by environmental factors such as oxygen and carbon dioxide availability.[31] More than 70% of clinical isolates of *staphylococci* belong to these serotypes.[32] The serotype 5 capsular polysaccharide produced by *S. aureus* has a trisaccharide repeating unit structure of (→4)-3-*O*-Ac-β-D-

ManNAcA*p*-(1→4)-α-L-FucNAc*p*-(1→3)-β-D-FucNAc*p*-(1→). Type 5 and 8 capsular polysaccharides are structurally very similar to each other. Type 8 has the following structure: (→3)-4-*O*-Ac-β-D-ManNAcA*p*-(1→3)-α-L-FucNAc*p*-(1→3)-β-D-FucNAc*p*-(1→).[33-37] Type 5 and 8 polysaccharides differ only in the linkages between the sugars and in the sites of *O*-acetylation of the mannosaminuronic acid residues; however they are serologically distinct meaning the characteristics of the disease are shown by studying the blood.[9]

N-Acetyl-D-fucosamine is the third sugar residue in serotypes 5 and 8 in *S. aureus*. The residue's activated form is uridine 5'(2-acetamido-2,6-dideoxy-α-D-galacto-pyranosyl diphosphate).[32] In the block mechanism,[38] which is an assembly of trisaccharide repeating units on a polyprenyl phosphate acceptor, this sugar acts as the monosaccharide initiating the chain growth.[32] Research that has already been carried out with this monosaccharide is with the use of a radioactive label. Illarionov *et al.* used a tri-*O*-acetyl derivative of *N*-acetyl-D-fucosamine as the starting material in their synthesis. They developed a synthetic scheme that allowed the introduction of [^{14}C] acetate in the final steps of the synthesis. The researchers transformed uridine 5'(2-amino-3,4-di-*O*-acetyl-2-deoxy-α-D-fucopyranosyl) diphosphate into the target nucleoside diphosphate sugar, which was the activated form of *N*-acetyl-D-fucosamine. Research that can now be performed is the introduction of a radioactive label into the two products formed that have different groups off of C-1 but with the *N*-acetyl-D-fucosamine form from [^{14}C]-acetate and open up possibilities for biosynthetic studies.[32]

N-Acetyl-D-fucosamine is not a commercially available carbohydrate. However, if *N*-acetyl-D-glucosamine is used as the starting material, it may be possible to obtain the

desired *N*-acetyl-D-fucosamine in several synthetic steps such as in the following scheme (Scheme 1):

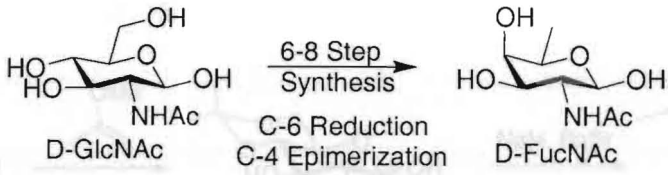

Scheme 1: Possible synthesis of *N*-acetyl-D-fucosamine.

One of the syntheses that will be adapted for our use is the Horton synthesis.[39] In this synthesis, Horton starts with *N*-acetyl-D-glucosamine and, by a series of protection-deprotection and functional group manipulations, arrives at an orthogonally protected *N*-acetyl-D-fucosamine (Scheme 2).

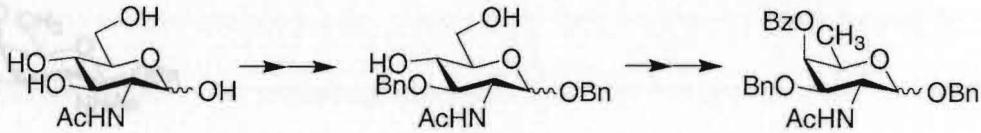

Scheme 2: Horton synthesis of *N*-acetyl-D-fucosamine.[39]

The full version of the Horton synthesis is shown in Scheme 3. The first three steps of the synthesis involve a series of protection and deprotection reactions. The first step is to protect O-4 and O-6 with an isopropylidene protecting group, the second is to protect O-3 with a benzyl protecting group, and the third is then to remove the isopropylidene protecting group at O-4 and O-6. The next two steps involve activating C-4 and C-6 using methanesulfonyl chloride and then doing a reduction reaction that will only reduce C-6 due to deoxygenation occurring selectively with primary sulfonates and

not secondary sulfonates. The final step is an S_N2 reaction epimerizing C-4 resulting in the C-4 axial product.

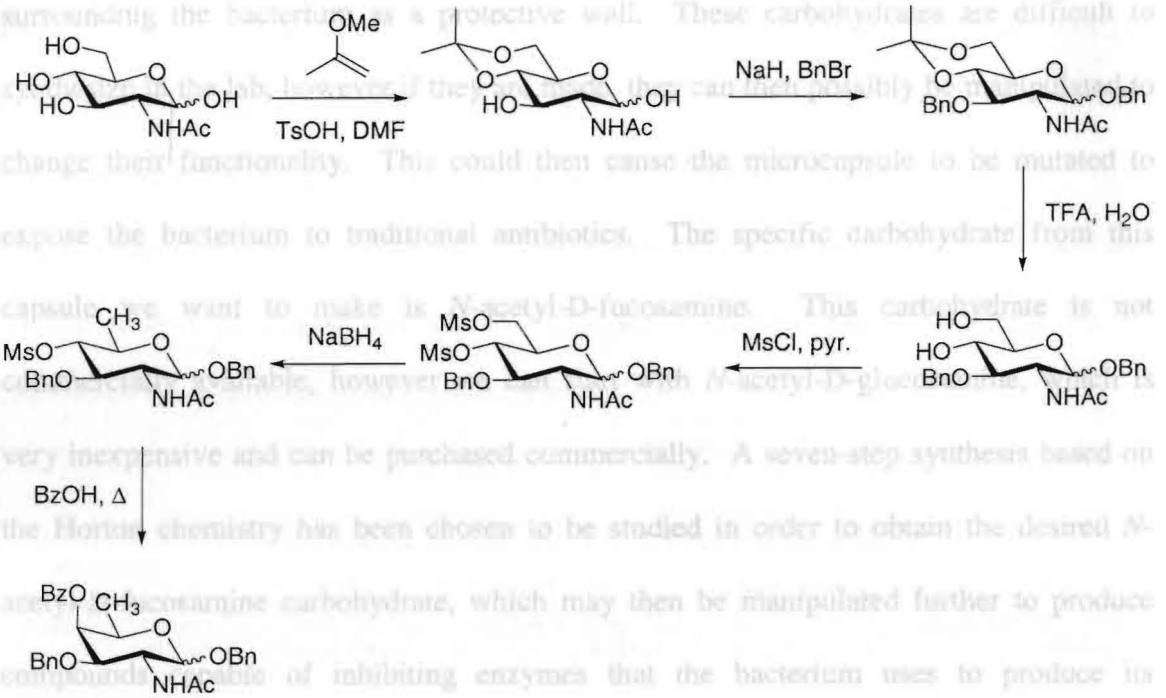

Scheme 3: Complete Horton synthesis of *N*-acetyl-D-fucosamine.[39]

The main goal of this project is to adapt this synthesis to develop novel *O*- and *N*-glycosides that may serve as inhibitors of capsular polysaccharide formation in *S. aureus*.

Statement of Problem

Carbohydrates have very important uses in the development of new antibiotics. In the *Staphylococcus aureus* bacterium, carbohydrates make up the microcapsule surrounding the bacterium as a protective wall. These carbohydrates are difficult to synthesize in the lab, however if they are made, they can then possibly be manipulated to change their functionality. This could then cause the microcapsule to be mutated to expose the bacterium to traditional antibiotics. The specific carbohydrate from this capsule we want to make is *N*-acetyl-D-fucosamine. This carbohydrate is not commercially available, however we can start with *N*-acetyl-D-glucosamine, which is very inexpensive and can be purchased commercially. A seven-step synthesis based on the Horton chemistry has been chosen to be studied in order to obtain the desired *N*-acetyl-D-fucosamine carbohydrate, which may then be manipulated further to produce compounds capable of inhibiting enzymes that the bacterium uses to produce its microcapsule.

Results and Discussion:

The major goal of the project is to develop a synthetic pathway from *N*-acetyl-D-glucosamine, which is cheap, to the much rarer *N*-acetyl-D-fucosamine that can be used in future work towards small molecule glycomimetics. The main reason for attempting to make these molecules would be to possibly inhibit the enzymes that make the capsular polysaccharide of *S. aureus* where *N*-acetyl-D-fucosamine is one of the three main sugars. The route taken to form this molecule, and analogs, branches off in two different directions; both an *O*-glycoside and an *N*-glycoside[40] scaffold will be investigated using the known Horton synthesis as a guide (Scheme 3).[39]

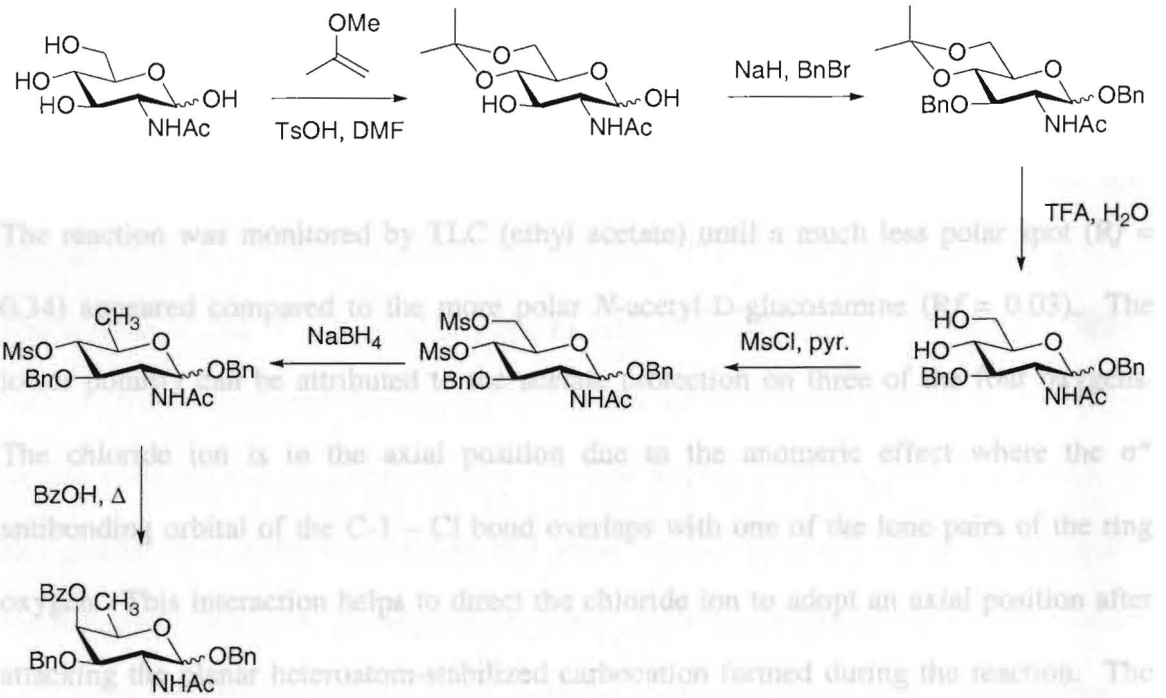

Scheme 3: Horton synthesis of *N*-acetyl-D-fucosamine.

1. *N*-Glycoside Synthesis

The first step in the synthesis of *N*-glycoside analogs of *N*-acetyl-D-fucosamine from the starting material *N*-acetyl-D-glucosamine (GlcNAc, **1**) was the reaction with acetyl chloride[41,42] to block O-3, O-4, and O-6 with acetate protecting groups. The chloride in the product **2** is in the axial or α position due to the anomeric effect (Equation 1).[43]

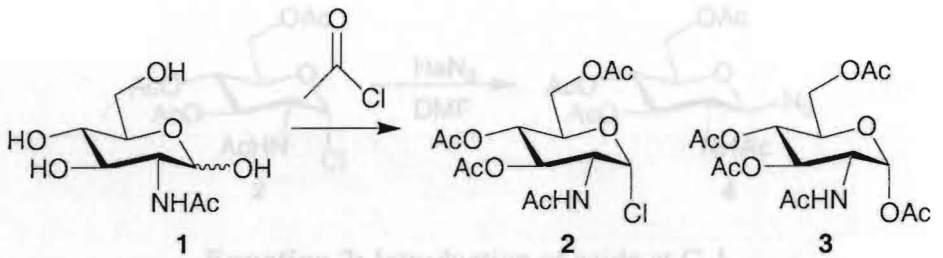

Equation 1: Formation of glycosyl chloride **2**.

The reaction was monitored by TLC (ethyl acetate) until a much less polar spot (R*f* = 0.34) appeared compared to the more polar *N*-acetyl-D-glucosamine (R*f* = 0.03). The lower polarity can be attributed to the acetate protection on three of the four oxygens. The chloride ion is in the axial position due to the anomeric effect where the σ* antibonding orbital of the C-1 – Cl bond overlaps with one of the lone pairs of the ring oxygen. This interaction helps to direct the chloride ion to adopt an axial position after attacking the planar heteroatom-stabilized carbocation formed during the reaction. The result is then the α-anomer as the thermodynamically favored product of the reversible reaction. Compound **3** is also formed in this reaction in a mixture with **2** due to the

reaction not going to completion. Compounds **2** and **3** are used in the next step as a mixture.

After a work-up and evaporation to a brown syrup, the ^{1}H NMR spectrum proved that the alpha anomer had been formed based on a coupling constant of 3.8 Hz between H-1 and H-2. The crude product **2**, isolated in 96% yield, was used in the next step; the introduction of an azide group at C-1 to form an *N*-glycoside (Equation 2).[40,44]

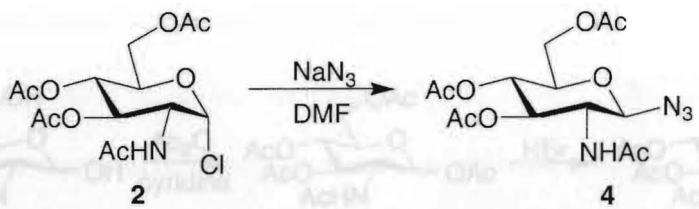

Equation 2: Introduction of azide at C-1.

The reaction was monitored by TLC (ethyl acetate) showing a slightly less polar spot with an R*f* value of 0.33 compared to the chloride. The ^{1}H NMR spectrum of product **4** was similar to that of the chloride with the only major differences being the coupling constant from the doublet representing H-1; where for the chloride this value was 3.8 Hz, for the azide the H-1 coupling constant was then 9.2 Hz, and the chemical shifts for the H-1 proton itself where the chloride H-1 value was 6.2 ppm and for the azide the H-1 value shifted to 4.8 ppm. Based on these values, it can be concluded that the azide indeed was in the equatorial position. If the coupling constant value is small, the relationship between H-1 and H-2 is *gauche*, which would mean the proton at C-1 is in the beta or equatorial orientation thus the C-1 substituent would be in the axial orientation. If the coupling constant is large, then the alignment between H-1 and H-2 is either eclipsed

(unlikely in a $^4C_1$ ring) or *anti* meaning the proton at C-1 is in the alpha orientation thus the C-1 substituent is in the beta orientation. After column chromatography had been performed, the desired azide product **4** was isolated as a white solid in 51% yield.

The synthesis of the azide was also attempted in a different manner. Product **3** was made purposely through an acetylation reaction with *N*-acetyl-D-glucosamine (**1**) as the starting material, acetic anhydride as the reagent, and pyridine as the solvent. Once product **3** was formed it was reacted with hydrobromic acid to obtain bromide **5** (Scheme 4).

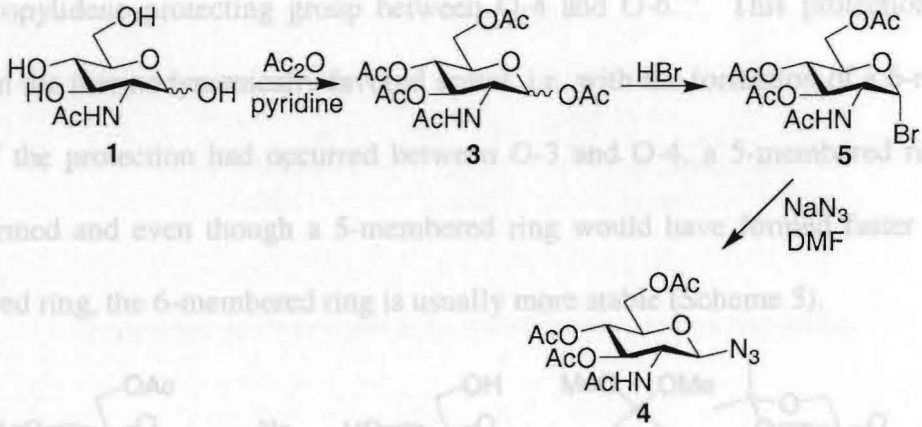

Scheme 4: Alternative route to form azide **4**.

Bromide **5** is very similar to **2** in terms of their NMR spectra and we can assume that they will behave in the same manner chemically.[43] Once bromide **5** was formed; an S_N2 reaction was carried out with sodium azide to make the azide **4**. Even though product **4** is formed, two different routes were investigated to determine the most efficient way of making the azide. The route shown in Scheme 4 was not as clean to perform as the route shown in Equations 1 and 2; thus the glycosyl chloride route to azide **4** was chosen.

Azide **4** was then deprotected to unblock O-3, O-4, and O-6 using sodium methoxide in methanol.[45] The reaction was monitored by TLC (3:1 ethyl acetate – methanol) until the consumption of starting material was seen and a much more polar spot with an R*f* value of 0.31 was observed when compared to the azide spot. Since the three acetate protecting groups were now gone, the polarity of the molecule would increase. The reaction mixture was evaporated down to give a white solid in 95% yield. The ^{1}H NMR spectrum showed the disappearance of the three acetate singlet signals at 2.0 ppm confirming azide **6** was formed. This crude material **6** was then protected with an isopropylidene protecting group between O-4 and O-6.[46] This protection reaction results in the thermodynamically favored acetal, i.e. with the formation of a 6-membered ring. If the protection had occurred between O-3 and O-4, a 5-membered ring would have formed and even though a 5-membered ring would have formed faster than a 6-membered ring, the 6-membered ring is usually more stable (Scheme 5).

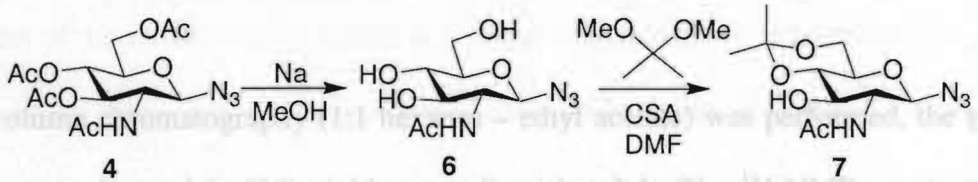

Scheme 5: Deprotection and O-4 – O-6 protection on azide product **6**

After TLC (3:1 ethyl acetate – methanol) showed consumption of starting material, and a less polar spot was formed compared to azide **6**, the reaction was evaporated to give crude **7** in ~90% yield as a yellow-brown syrup. The ^{1}H NMR spectrum showed two singlets at 1.3 and 1.45 ppm representing the two methyl groups of the isopropylidene group confirming that the protecting group had been introduced successfully.

With the isopropylidene protecting group masking O-4 and O-6 on azide **7**, the next position to be blocked on the molecule was O-3 with a benzyl protecting group.[47] This ether group works well with the planned reaction scheme because the benzyl protecting group is acid and base stable. This will help with reaction conditions later when the isopropylidene protecting group is to be removed because the acetal protecting group is only base stable thus it can be removed later on in the synthesis by an acid without affecting the benzyl O-3 group. TLC (ethyl acetate) was performed on compound **8** showing consumption of starting material and a spot less polar than azide **7** due to the hydroxyl group at O-3 now carrying the benzyl protecting group (Equation 3).

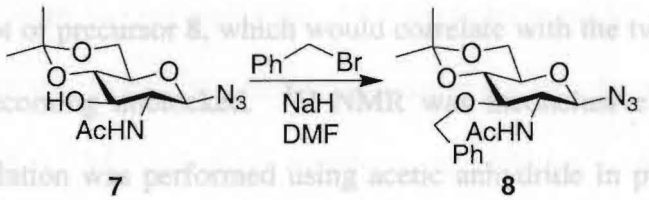

Equation 3: Protection at O-3 with benzyl protecting group.

After column chromatography (1:1 hexanes – ethyl acetate) was performed, the purified product was obtained in 51% yield as a yellowish solid. The ^{1}H NMR spectrum again showed two singlets at 1.3 and 4.5 ppm indicating that the isopropylidene protecting group was still intact blocking O-4 and O-6. The NMR spectrum also showed the protons on the benzene ring of the benzyl group at 7.3 ppm indicating that the protecting group was attached to the molecule blocking O-3. All other proton NMR signals agreed with the assigned structure for **8**.

The next step of the planned synthesis was to remove the isopropylidene protecting group and unblock O-4 and O-6. The route taken to achieve this step was to

follow Horton's precedent;[39] however, the reaction conditions (trifluoroacetic acid and water) did not work and we were unable to deprotect compound **8** to form **9** (X = N_3, Scheme 6).

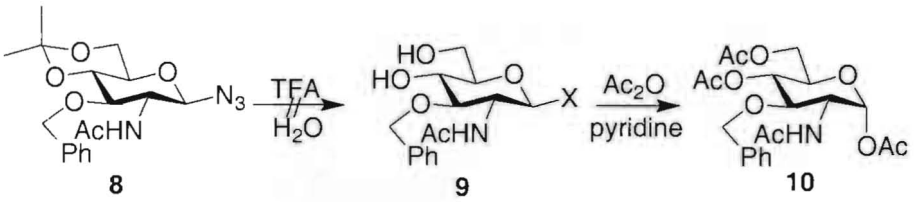

Scheme 6: Attempted deprotection of azide **8**.

TLC (ethyl acetate) of the reaction did show a more polar spot with an R_f value of 0.25 compared to the spot of precursor **8**, which would correlate with the two hydroxyl groups at O-4 and O-6 becoming unblocked. ^{1}H NMR was inconclusive as to the product formed so an acetylation was performed using acetic anhydride in pyridine to see how many acetate protecting groups would be introduced on compound **9**. The ^{1}H NMR spectrum of **10** showed four singlets at 2.0 ppm indicating that there were four acetate groups on the ring. One acetate group at C-2 should have still been intact, i.e. the amide NHAc group, but two more acetate groups would have indicated that the isopropylidene protecting group had been deprotected to hydroxyl groups, and two acetate groups would have then blocked these hydroxyls. There was however one more acetate group showing up in the NMR spectrum indicating that the azide at C-1 had been cleaved during the reaction with acid in the attempt to form product **9** (X = N_3). Thus, the group at C-1 was now confirmed to be an acetate group, which inferred that the product from the attempted hydrolysis of acetal **8** was in fact **9** where X = OH. The mass spectrum of peracetate **10** indicated as well that the desired glycosyl azide product **9** (X = N_3) had not been formed

and the molecular weight of 460, plus sodium, did represent tetraacetate **10**. At this point we have been unable to find appropriate conditions for the cleavage of the O-4 – O-6 acetal in **8** that leaves the azide functional group intact. Attention will now be turned to the *O*-glycoside variation.

2. *O*-Glycoside Synthesis

The first step in the synthesis of *O*-glycoside[48] analogs of *N*-acetyl-D-fucosamine uses the same starting material as in the attempted *N*-glycoside synthesis. *N*-Acetyl-D-glucosamine (**1**) was reacted with HCl gas in methanol in an acid-catalyzed glycosylation. This is an S_N1 reaction where HCl gas is bubbled through methanol for a few minutes and then the methanolic GlcNAc mixture is put into the acidic methanol and allowed to stir. Once TLC (3:1 ethyl acetate – methanol) showed that the starting material had been consumed, and there was a less polar spot with an R*f* value of 0.20 compared to the very polar GlcNAc, the reaction was evaporated to give crude **11** as a brown syrup in 90% yield (Scheme 7). In the ^{1}H NMR, the peaks of interest were the two singlets around 3.4 ppm that represented the two methyl groups at C-1 in the axial and equatorial positions indicating that the desired product **11** was formed. With **11α/β** in hand, an acetylation with acetic anhydride and pyridine was performed to block the O-3, O-4, and O-6 groups with acetate protecting groups (Scheme 7).

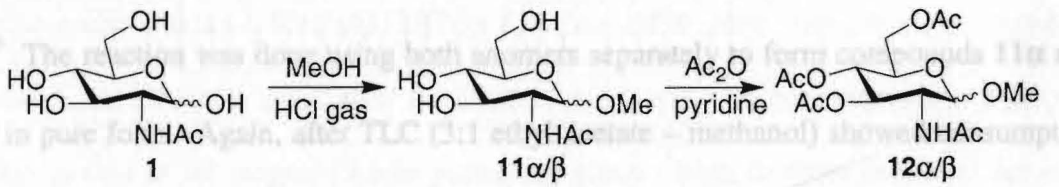

Scheme 7: GlcNAc to methyl glycoside mixture and subsequent acetylation.

The reason for introducing the acetate groups to block O-3, O-4, and O-6 was to make column chromatography easier to perform when separating the α and β mixture. After the acetylation had been performed and monitored by TLC (ethyl acetate), to show two much less polar spots representing **12α/β**, column chromatography (ethyl acetate) was used to separate the mixture of anomers and obtain compounds **12α** and **12β**. In the NMR spectra of both **12α** and **12β** there were four singlets at ~2 ppm indicating that the acetylation performed had been successful; these signals represented the three new acetate groups at O-3, O-4, and O-6 along with the NHAc acetate group at C-2. The only way to tell the difference between both anomers was to determine the coupling constants for the doublet between 4-5 ppm that represented the proton at C-1 of each isomer. Compounds **12α** and **12β** only differed in the position of this proton thus this is the only significant difference seen between the two NMR spectra. The two coupling constants were found to be 3.7 Hz for compound **12α** and 8.4 Hz for compound **12β**. Based on previous explanations of the angles between H-1 and H-2, the α and β anomers were identified. After the separation, both anomers were used individually in the rest of the synthesis to ensure that the reactions to follow will work on either stereoisomer.

The next three steps of the synthesis use the same conditions that were performed on the *N*-glycosyl azide previously. The next reaction carried out was the deprotection with sodium methoxide in methanol to remove the acetate protecting groups (Equation 4).[45] The reaction was done using both anomers separately to form compounds **11α** and **11β** in pure form. Again, after TLC (3:1 ethyl acetate – methanol) showed consumption of starting material and a more polar spot ($R_f\alpha = 0.31$ and $R_f\beta = 0.24$) appeared compared with **12α** and **12β**, the reactions were evaporated to give yields of 99% for the α-anomer

and 95% for the β-anomer with both as yellow solids. ^{1}H NMR showed the disappearance of three singlets at 2.0 ppm indicating that O-3, O-4, and O-6 had been unblocked.

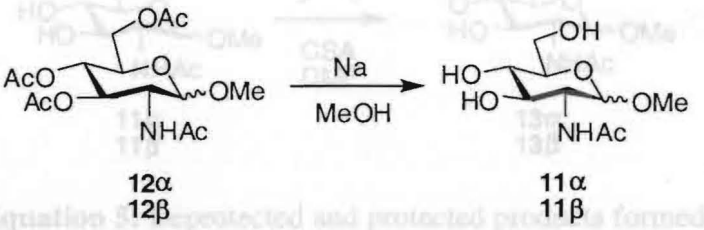

Equation 4: Deacetylation of individual anomers or tetraacetates **12**.

The next step of the synthesis was to block O-4 and O-6 of each anomer of **11** with the isopropylidene protecting group.[46] The first attempt of this reaction used the same reagents and conditions as in the Horton synthesis,[39] namely 2-methoxypropene and *p*-toluenesulfonic acid. When this reaction was performed on **11α** and after evaporation of the solvent, the ^{1}H NMR of what was hoped to be **12α** proved the material to be only **11α**. The reaction was then performed again using the same reagents used with the *N*-glycoside azide, i.e. 2,2-dimethoxypropane and CSA. The reaction was performed using both the α and β anomers of **11** separately, and once TLC (3:1 ethyl acetate – methanol) showed consumption of starting material (both had less polar spots; $R_f\alpha = 0.60$ and $R_f\beta = 0.63$) compared with the starting materials (**11α** and **11β**), the reactions were evaporated to give crude products **13α** and **13β** in 83% and 88% yield respectively. Important signals in the ^{1}H NMR again were the singlets at 1.3 and 1.45 ppm representing the two methyl groups of the isopropylidene protecting group. Both of these singlet peaks were

present in both NMR spectra of both products thus confirming **13α** and **13β**, had indeed been formed (Equation 5).

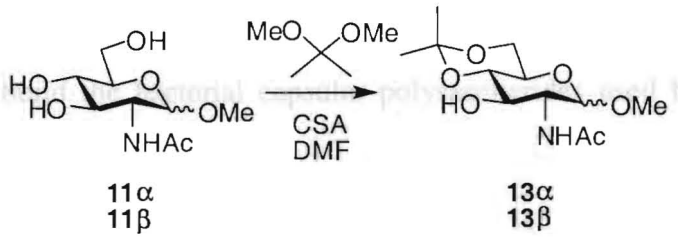

Equation 5: Deprotected and protected products formed.

The final step of the *O*-glycoside synthesis that was performed at this point was the blocking of O-3 with a benzyl protecting group thus forming compounds **14α** and **14β** (Equation 6).[47] The reaction was performed with both anomers separately and TLC (ethyl acetate) showed consumption of starting material; both had less polar spots, with R_f values of 0.42 for **14α** and 0.45 for **14β**, compared with the starting materials **13α** and **13β**, respectively. After column chromatography (1:1 hexanes – ethyl acetate) was performed, the ^{1}H NMR spectra of each compound still had two singlets at ~1.3 and 1.45 ppm confirming the isopropylidene groups were still intact in both compounds.

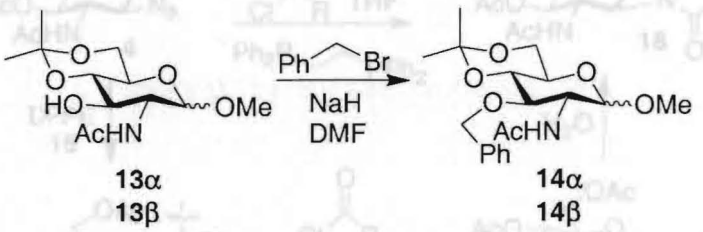

Equation 6: 3-*O*-Benzyl-protected methyl glycosides.

At 7.3 ppm, the protons on the aryl ring were represented in a multiplet, again proving the introduction of the benzyl ether into the desired products, **14α** and **14β**. With

the successful formation of these orthogonally protected intermediates *en route* to analogs of *N*-acetyl-D-fucosamine, attention was turned to the synthesis of *N*-glycosides from glycosyl azide **4** (See Equation 2), which may themselves serve as inhibitors of the enzymes used to build the bacterial capsular polysaccharides used by *Staphylococcus aureus*.

3. Amide Synthesis

Formation of amides from azide **4** was achieved using a modified Staudinger reaction with bis(diphenylphosphino)ethane (DPPE) (**15**) and an acylating agent. The transformation starts with the reaction between the azide **4** and DPPE (Scheme 9) to generate an aza-ylide intermediate (**16**) after the loss of nitrogen. The nucleophilic nitrogen of the ylide will then attack the carbonyl carbon of an acylating agent, with loss of the bis(phosphineoxide), to give an imidoyl chloride intermediate **17** that will then undergo hydrolysis to give the *N*-linked glycosyl amides **18** (Scheme 8).[49,50,51]

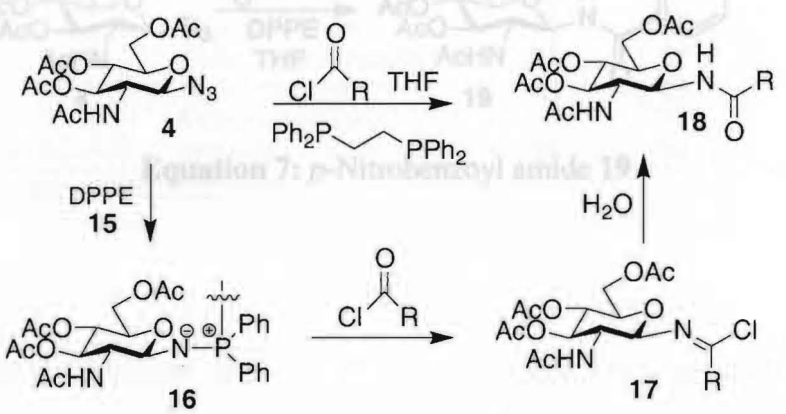

Scheme 8: Modified Staudinger reaction to produce glycosyl amides.

What was investigated next in the research was to introduce amide substitutents at C-1 of the GlcNAc ring in a potentially stereoselective synthesis of these molecules. DPPE was used in the reactions because its very polar oxide byproduct allows for easy purification through column chromatography or recrystallization.[52] The reaction of azide **4** with DPPE and *p*-nitrobenzoyl chloride (Equation 7) gave product **19** with a yield of 33% as a white solid after recrystallization (Table 1). The TLC plate showed a UV-active spot indicating that the benzoyl group had been introduced compared to the azide starting material (**4**). The ^{1}H NMR spectrum indicated two sets of doublets of double intensity at 8.01 and 8.30 ppm that represent the four protons of the aryl ring. A peak at 8.22 ppm was also present representing the new N-H bond that was formed as part of the amide group. The crystal structure of **19** in Figure 8 proves further that the amide bond was indeed formed and in the β-GlcNAc orientation as desired.

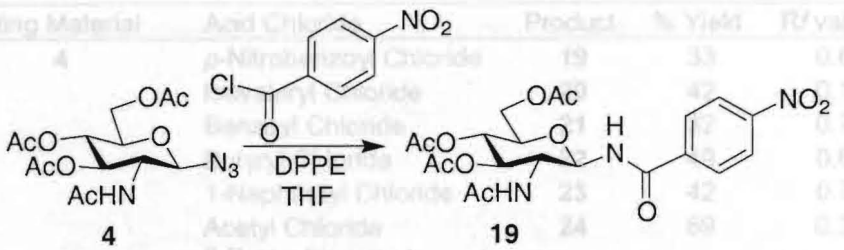

Equation 7: *p*-Nitrobenzoyl amide **19**.

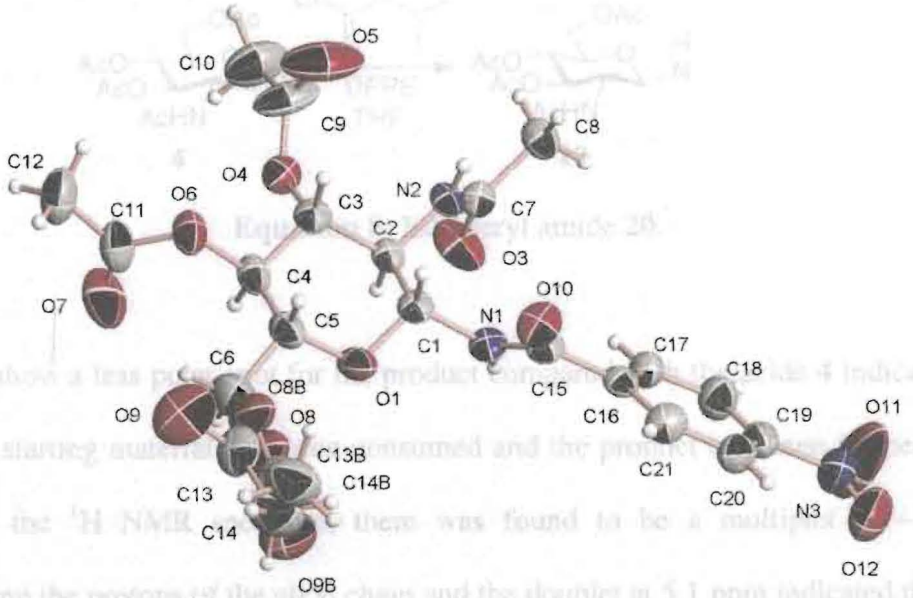

Figure 8: X-Ray structure of amide **19**.

Table 1: Synthesis of amides *via* modified Staudinger reaction from GlcNAc azide **4**.

Starting Material	Acid Chloride	Product	% Yield	R*f* value*
4	*p*-Nitrobenzoyl Chloride	**19**	33	0.66
	Isovaleryl Chloride	**20**	42	0.15
	Benzoyl Chloride	**21**	32	0.75
	Butyryl Chloride	**22**	49	0.65
	1-Naphthoyl Chloride	**23**	42	0.72
	Acetyl Chloride	**24**	69	0.35
	6-Bromohexanoyl Chloride	**25**	70	0.42

*Solvent system - Ethyl acetate

The reaction between azide **4**, DPPE, and isovaleryl chloride gave a yellow solid after recrystallization with a yield of 42% that was identified as compound **20** (Equation 8).

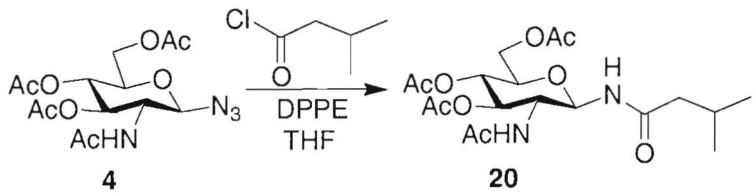

Equation 8: Isovaleryl amide **20**.

TLC did show a less polar spot for the product compared with the azide **4** indicating that all of the starting material had been consumed and the product had been formed. After obtaining the ^{1}H NMR spectrum, there was found to be a multiplet at ~1.0 ppm representing the protons of the alkyl chain and the doublet at 5.1 ppm indicated the amide was in the β orientation with a coupling constant of 7.9 Hz. ESI mass spectral data also confirmed the formation of the amide product with a mass of 453.0 representing the calculated molecular ion (plus sodium).

In the reaction of azide **4** with DPPE and benzoyl chloride, a yield of 32% was obtained after recrystallization giving product **21** (Equation 9).

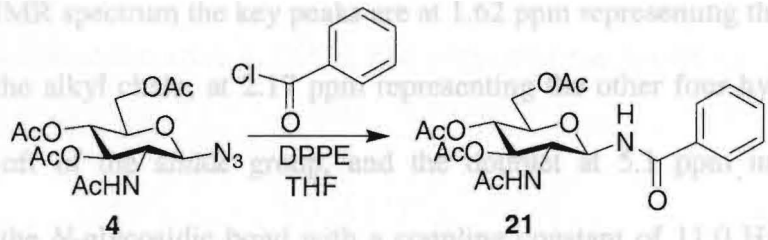

Equation 9: Benzoyl amide **21**.

TLC showed a less polar UV-active spot compared with the starting material indicating that the reaction had gone to completion. Once the ^{1}H NMR spectrum had been obtained, it was confirmed that the correct product had been formed. There were three peaks between 7.45 and 7.83 ppm representing the five protons of the phenyl ring and a doublet

at 5.2 ppm with a coupling constant of 9.9 Hz indicated the β orientation at C-1 of the sugar. A doublet at 7.88 ppm represented the proton on the nitrogen atom at C-1 indicating that the amide bond had also been formed. ^{13}C NMR also showed peaks between 125-135 ppm, which are representative of the carbons in the phenyl ring. ESI mass spectral data also confirmed the correct product with a molecular weight of 451 (plus hydrogen).

In the reaction to form the butyryl amide **22**, azide **4**, butyryl chloride, and DPPE were all reacted in a round bottom flask in THF to give **22** in a yield of 49% after recrystallization (Equation 10).

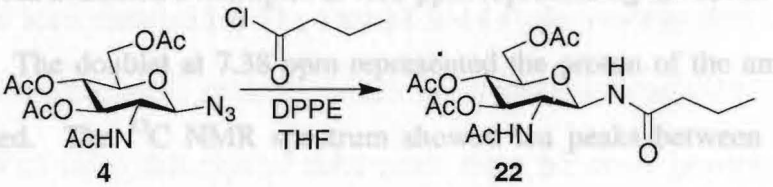

Equation 10: Butyryl amide **22**.

From the ^{1}H NMR spectrum the key peaks are at 1.62 ppm representing the methyl group at the end of the alkyl chain, at 2.17 ppm representing the other four hydrogens on the carbon chain off of the amide group, and the doublet at 5.1 ppm indicating the β orientation of the *N*-glycosidic bond with a coupling constant of 11.0 Hz. The peak at 6.92 ppm indicates that the amide bond was formed with this doublet corresponding to the proton of the glycosyl amide N-H bond. The ESI mass spectral data also proved the correct product had been formed with a value of 416 for M^{+}.

In the reaction between the azide **4**, DPPE, and 1-naphthoyl chloride TLC showed a UV-active spot that was more polar than the starting material. After column

chromatography had been performed, the product was a yellow solid isolated in 42% yield identified as **23** (Equation 11).

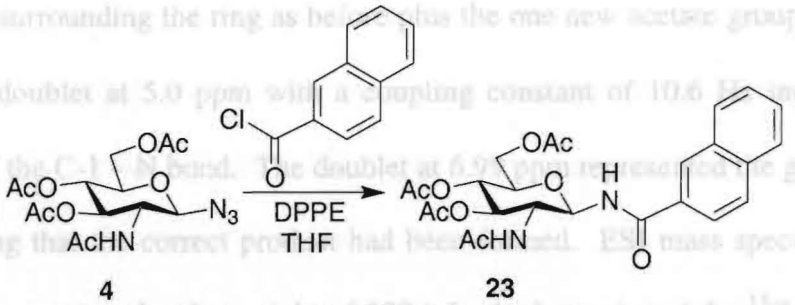

Equation 11: 1-Naphthoyl amide **23**.

^{1}H NMR spectrum indicated a multiplet at 7.35 ppm representing the seven protons of the two aryl rings. The doublet at 7.38 ppm represented the proton of the amide bond that had been formed. The ^{13}C NMR spectrum showed ten peaks between 120-135 ppm representing the ten carbon atoms found in the two aryl rings. The ESI mass spectral data showed a molecular weight of 501 (M^{+} plus hydrogen) representing the correct molecular weight of compound **23**.

The reaction of the azide **4**, DPPE, and acetyl chloride resulted in product **24** in a yield of 69% (Equation 12).

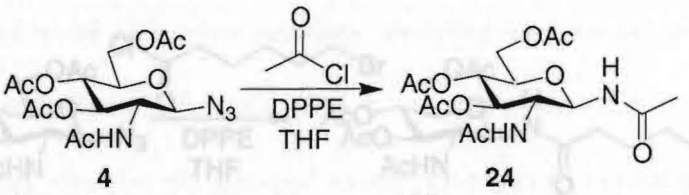

Equation 12: Acetyl amide **24**.

After column chromatography was performed, the product was obtained as a white solid. The ^{1}H NMR spectrum showed five singlets between 1.97 and 2.10 ppm representing the four acetates surrounding the ring as before plus the one new acetate group on the amide bond, and a doublet at 5.0 ppm with a coupling constant of 10.6 Hz indicating the β orientation of the C-1 – N bond. The doublet at 6.99 ppm represented the glycosyl amide N-H indicating that the correct product had been formed. ESI mass spectral data again indicated the correct molecular weight of 389 (plus hydrogen), and the ^{13}C NMR showed five peaks between 20.7 and 26.6 ppm for the five acetate groups now around the ring.

The next amide reaction performed was slightly different compared to the other amides that had been made so far. The chloride used in this reaction with the azide **4** and DPPE was 6-bromohexanoyl chloride, which has a bromine attached to the end of the alkyl chain. With using this type of compound, there are many possibilities of further derivatives that could be made from the resultant amide **25**, (Equation 13) due to the Br atom at the end of the chain being a good leaving group in substitution reactions. In the following reaction one of these possibilities will be seen. After column chromatography was performed on the crude material, compound **25** was obtained in a yield of 70% (Equation 13).

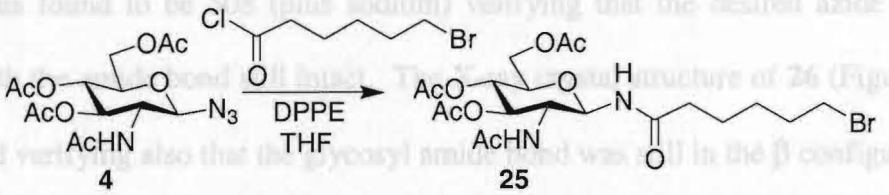

Equation 13: 6-Bromohexanoyl amide **25**.

The ^{1}H NMR spectrum of **25** showed four sets of multiplets between 1.43 and 2.20 ppm representing eight of the ten protons on the carbon chain. The triplet at 3.4 ppm represented the two other protons closest to the Br atom at the end of the chain. The doublet at 6.97 ppm indicated that the amide bond had been formed between the sugar ring and the acyl chain carbons. ESI mass spectral data showed a mass of 523.1 representing the actual mass of the desired product.

The final reaction that was performed with amides was reacting product **25** and sodium azide together in DMF. The isolated product proved to be **26**, formed by azide displacing the bromine atom from **25** (Equation 14).

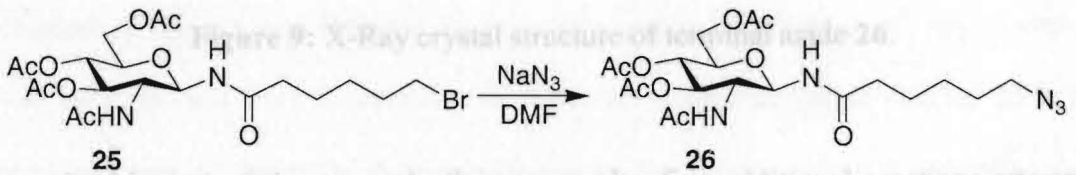

Equation 14: 6-Azidohexanoyl amide **26**.

Azide **26** was formed as a white solid in 40% yield after workup. The ^{1}H NMR spectrum was very similar to that of the bromide precursor thus the ESI mass spectral data was more useful to determining the identity of the product. The molecular weight of the product was found to be 508 (plus sodium) verifying that the desired azide had been formed with the amide bond still intact. The X-ray crystal structure of **26** (Figure 9) was determined verifying also that the glycosyl amide bond was still in the β configuration.

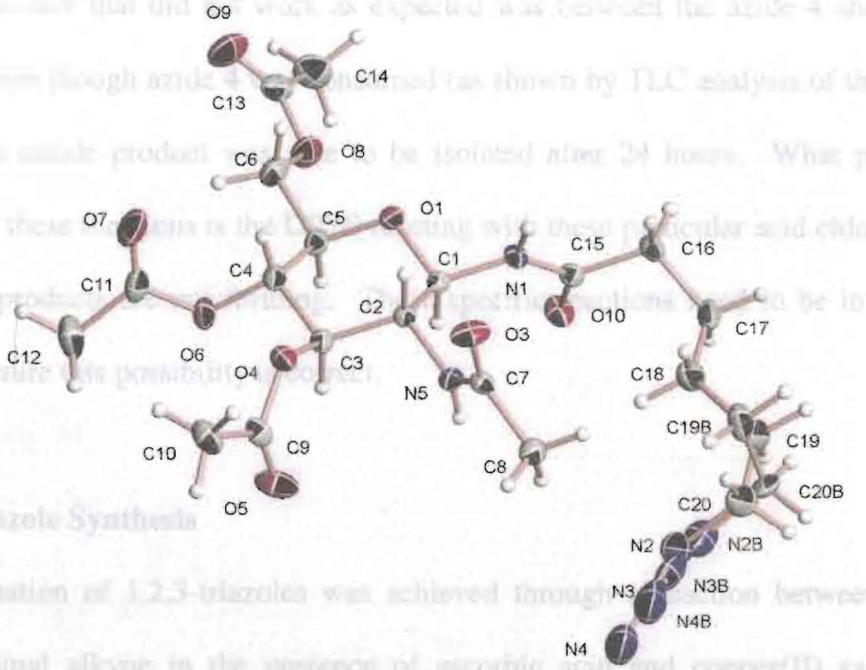

Figure 9: X-Ray crystal structure of terminal azide **26**.

In this part of the research, there were also five additional reactions attempted with other acylating agents that were unsuccessful. The acid chlorides used and the outcomes are listed in Table 2 (SM = starting material).

Table 2: Unsuccessful attempted syntheses of amides *via* Staudinger reaction.

Starting Material	Acid Chloride	Expected Product	% Yield
4	Succinyl Chloride	**27**	SM
	p-Toluenesulfonyl Chloride	**28**	SM
	Oxalyl Chloride	**29**	SM
	2-Furoyl Chloride	**30**	SM
9	Benzoyl Chloride	**31**	SM

(Structures of compounds **27-31** can be found in the experimental section, pg. 67-69).

A reaction that did not work as expected was between the azide **4** and 2-furoyl chloride. Even though azide **4** was consumed (as shown by TLC analysis of the reaction mixture), no amide product was able to be isolated after 24 hours. What possibly is occurring in these reactions is the DPPE reacting with these particular acid chlorides thus the desired products are not forming. These specific reactions need to be investigated further to ensure this possibility is correct.

4. 1,2,3-Triazole Synthesis

Formation of 1,2,3-triazoles was achieved through a reaction between azide **4** with a terminal alkyne in the presence of ascorbic acid and copper(II) salt.[53] The mechanism of this reaction (Scheme 9), as determined by Sharpless *et al.*, begins with an alkyne, **32**, reacting with a copper(I) to form the copper acetylide species **33**. The internal nitrogen of the azide then coordinates to the copper of the acetylide to form product **34**. The azide terminus then attacks at C-2 of the acetylide forming a metallocycle that collapses into a copper-triazole species **35**. Proteolysis then occurs and the 1,4-disubstituted 1,2,3-triazole **36** is formed.[54,55]

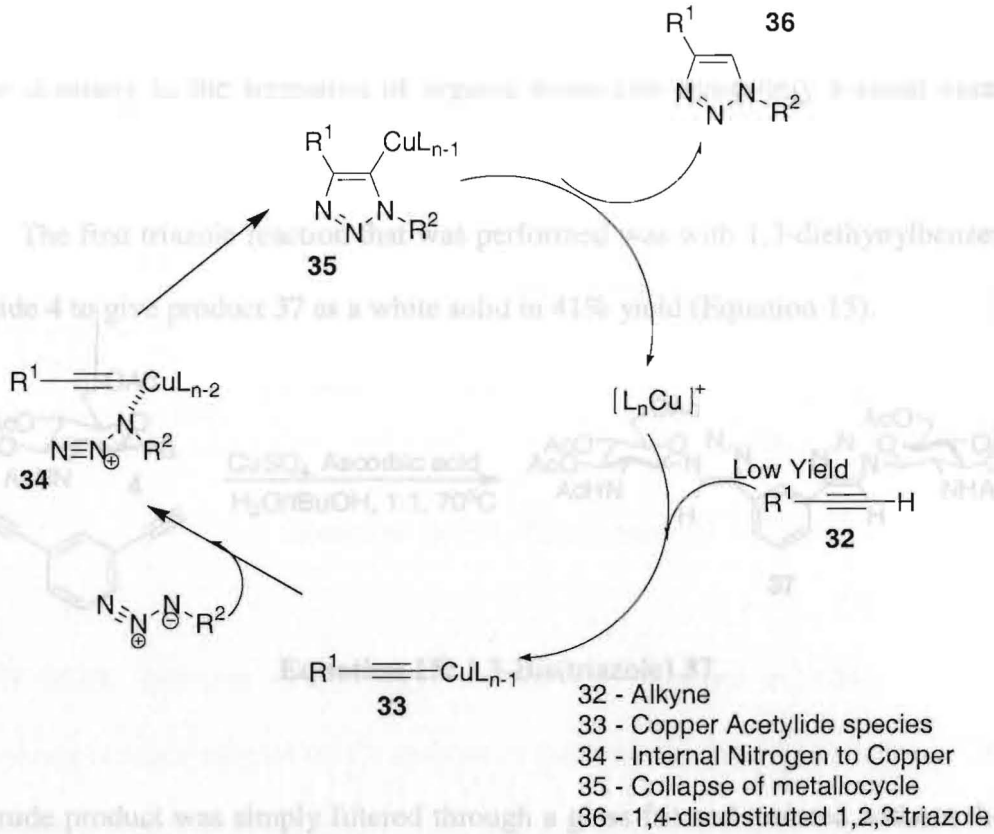

Scheme 9: Proposed mechanism for Cu(I)-catalyzed triazole formation.[54, 55]

A useful fact about these triazoles is that they are essentially insoluble in solvents such as water at low temperatures thus it is very easy to isolate these products through filtration. Also, Sharpless has reported that a catalytic amount of Cu(I) salts will increase the rate of reaction, through the above mechanism, which also increases the regioselectivity of addition to afford only the 1,4-disubstituted products.[55] These copper(I)-catalyzed reactions are becoming so important because they represent a powerful linking method due to their degree of dependability and complete regiospecificity. The synthesis of 1,2,3-triazoles underpins the idea of "click chemistry."[56] With these types of reactions, the conditions involved must included the following; they must give high yields, be easy to perform, be insensitive to oxygen and water, use only readily available reagents, and

workup and isolation must be simple.[56,57,58] This type of synthesis is expected to bring greater diversity to the formation of organic molecules using only a small number of reactions.

The first triazole reaction that was performed was with 1,3-diethynylbenzene and the azide **4** to give product **37** as a white solid in 41% yield (Equation 15).

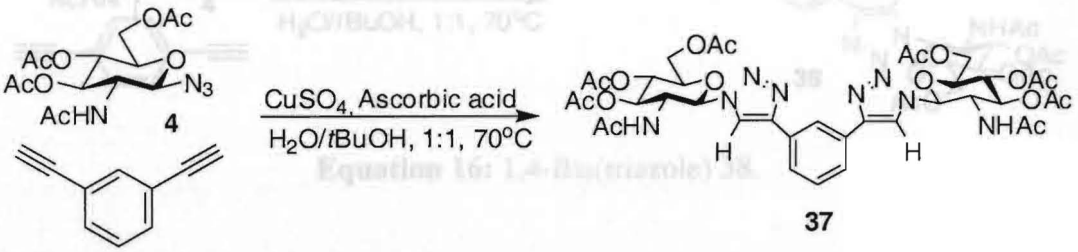

Equation 15: 1,3-Bis(triazole) **37**.

The crude product was simply filtered through a glass frit and isolated without the need for crystallization or column chromatography. The ^{1}H NMR spectrum revealed a triplet at 7.39 ppm and two doublets at 7.47 and 7.84 ppm representing the four protons on the aryl ring. The singlet at 8.11 ppm corresponded to the proton attached to the triazole ring and was a double intensity peak due to the two triazole rings formed on both sides of the aromatic ring. The β-stereochemistry of the azide precursor was retained in **37**; the H-1 – H-2 coupling constant of 9.9 Hz for the H-1 signal at 6.0 ppm corresponding to an *anti* relationship between H-1 and H-2. The ESI mass spectral data also proved the product was formed with a molecular ion of 869.5 found representing the molecular weight of compound **37**.

Bis(triazole) product **38** was also formed with the azide **4** and 1,4-diethynyl benzene, which gave very similar spectral results to product **37**, with a yield of 54% (Equation 16).

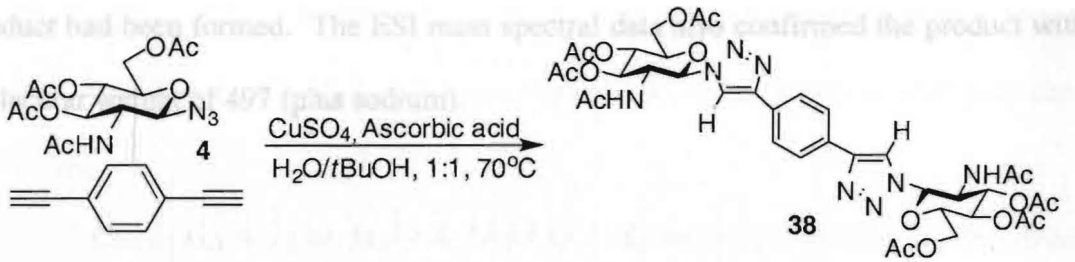

Equation 16: 1,4-Bis(triazole) **38**.

The ^{1}H NMR spectrum of **38** again showed two doublets at 7.84 and 8.13 ppm representing the four protons on the carbons in the benzene ring. The singlet at 7.93 ppm represented the proton on the triazole ring and was double intensity due to the symmetry of the molecule.

The final triazole that was made involved the reaction between azide **4** and phenyl acetylene to form compound **39** (Equation 17).

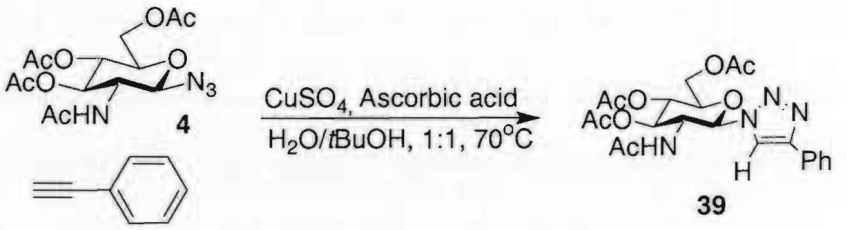

Equation 17: Phenyl acetylene-derived triazole **39**.

Triazole **39** was made according to the typical procedure and gave a very clean ^{1}H NMR spectrum without any type of purification after filtering and an 86% isolated yield. The spectrum showed three signals at 7.4-7.8 ppm representing the five protons for the phenyl

ring, and a doublet at 6.0 ppm with a coupling constant of 10.1 Hz for the H-1 proton indicating the β configuration of the amide. The most significant peak at 8.09 ppm was a singlet representing the proton on the triazole ring confirming that the 1,2,3-triazole product had been formed. The ESI mass spectral data also confirmed the product with a molecular weight of 497 (plus sodium).

Conclusion

Development of a synthetic route to making *N*-acetyl-D-fucosamine was unsuccessful in that the route was brought to a standstill. The fifth step of the synthesis, deprotecting the isopropylidene at C-4 and C-6, in an attempt to produce **9** (X = N_3), was unsuccessful. The synthesis may still be successful once the problem at this step can be overcome.

The compounds made from the GlcNAc azide **4** through both the amide synthesis and the triazole synthesis, were very successful in the products that were formed. The chemistry from these syntheses will be useful to us in the future due to the new chemical handle at the C-1 position. The azide at this position can now be linked to other molecules or compounds to form possible inhibitors to the *S. aureus* bacterium.

Future work on this synthesis may continue on in two ways to still prove the route successful. What first may be attempted is to try other reagents that are known to deprotect an isopropylidene protecting group without destroying the azide. In the synthesis performed, only two reagents were tried in different quantities. The other route that may be attempted is to put the azide at C-1 on at a later step in the synthesis. Since the azide is the only part of the product being destroyed in deprotecting the isopropylidene group, if it is put onto C-1 after this step, it may no longer be a problem to the synthesis.

Experimental

General Procedures

A Varian Gemini 2000 NMR spectrometer was used to obtain 400 MHz ^{1}H and 100 MHz ^{13}C spectra using $CDCl_3$ (0.1% w/v TMS) and DMSO (d_6, 99.9 atom % D) as the solvents. Chemical shifts (δ) are recorded in parts per million (ppm). Multiplicities for NMR spectra are listed as follows: s (singlet), d (doublet), t (triplet), q (quartet), dd (doublet of doublets), ddd (doublet of doublets of doublets), dq (doublet of quartets), m (multiplet), and all coupling constants (*J*) are labeled in Hz. A Bruker Esquire-HP 1100 LC/MS was used to obtain mass spectra. Whatman aluminum-backed plates were used for thin layer chromatography. Flash chromatography was performed with 32-60 mesh 60-Å silica gel.

Preparation of 2-Acetamido-3,4,6-tri-*O*-acetyl-α-D-glucopyranosyl chloride (2) and Pentaacetate 3 from *N*-Acetyl-D-Glucosamine (1).

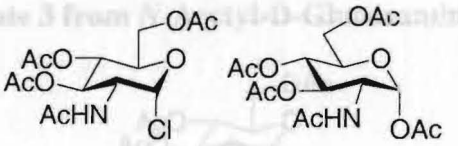

2 **3**

In a 250 mL round-bottom flask equipped with a magnetic stir bar, *N*-acetyl-D-glucosamine (5.016 g, 22.68 mmol) was dissolved in acetyl chloride (25 mL) at RT. The reaction was refluxed for 1 h. Heat was then removed and the reaction continued to stir for 17 h until TLC (ethyl acetate) showed consumption of starting material. The reaction was diluted with $CHCl_3$ (25 mL) through the condenser. The reaction was diluted more

with an ice/water mix (200 mL). The organic phase was washed with aqueous $NaHCO_3$ (200 mL). The aqueous phase was washed with $CHCl_3$ (2 x 25 mL), the organic layers were collected and dried over anhydrous $MgSO_4$. Evaporation of the solvent gave 7.91 g of crude product as a brown syrup in 96% yield.

^{1}H NMR ($CDCl_3$): δ 1.95 (s, 3H, -CH_3), 2.00 (s, 3H, -CH_3), 2.05 (s, 3H, -CH_3), 2.06 (s, 3H, -CH_3), 2.07 (s, 3H, -CH_3), 2.09 (s, 3H, -CH_3), 2.10 (s, 3H, -CH_3), 2.11 (s, 3H, -CH_3), 2.20 (s, 3H, -CH_3), 4.06 (m, 2H, H-5(**2**), H-5(**3**)), 4.28 (m, 4H, H-6(**2**), H-6'(**2**), H-6(**3**), H-6'(**3**)), 4.55 (m, 2H, H-2(**2**), H-2(**3**)), 5.26 (m, 4H, H-3(**2**), H-4(**2**), H-3(**3**), H-4(**3**)), 5.70 (d, 1H, N<u>H</u>Ac(**3**), J = 9.2 Hz), 5.92 (d, 1H, N<u>H</u>Ac(**2**), J = 9.0Hz), 6.18 (d, 1H, H-1(**3**), J = 3.7 Hz), 6.20 (d, 1H, H-1(**2**), J = 3.8 Hz).

Melting Point: Syrup

Preparation of Pentaacetate 3 from *N*-Acetyl-D-Glucosamine (1).

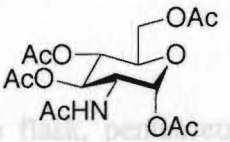

In a 250 mL round-bottom flask fitted with a septum and magnetic stir bar, *N*-acetyl-D-glucosamine (1.006 g, 4.55 mmol) was dissolved in pyridine (15 mL). Acetic anhydride (5 mL) was added dropwise into the reaction while in an ice bath and the reaction was stirred overnight. After TLC (ethyl acetate) showed consumption of starting material, the reaction was poured over a water/ice mix (75 mL) and then extracted with

CH_2Cl_2 (3 x 25 mL). The organic layer was washed with 5% H_2SO_4 (2 x 25 mL) and H_2O (25 mL). The organic layer was dried over anhydrous $MgSO_4$ and evaporated to give 1.43 g of product with an 81% yield. The ^{1}H NMR spectrum proved this material to be mainly the α-pentaacetate ($J_{1,2}$ = 3.7 Hz).

^{1}H NMR ($CDCl_3$): δ 1.95 (s, 3H, -CH_3), 2.05 (s, 3H, -CH_3), 2.06 (s, 3H, -CH_3), 2.09 (s, 3H, -CH_3), 2.20 (s, 3H, -CH_3), 3.99 (ddd, 1H, H-5, J = 3.7, 5.9, 5.9 Hz), 4.07 (dd, 1H, H-6, J = 2.6, 12.45 Hz), 4.26 (dd, 1H, H-6', J = 4.1, 12.4 Hz), 4.49 (m, 1H, H-2), 5.22 (t, 1H, H-4, J = 3.3 Hz), 5.24 (t, 1H, H-3, J = 3.5 Hz), 5.53 (d, 1H, N<u>H</u>Ac, J = 9.3 Hz), 6.18 (d, 1H, H-1, J = 3.7 Hz).

Preparation of 2-Acetamido-3,4,6-tri-*O*-acetyl-3,4,6-tri-*O*-acetyl-α-D-glucopyranosyl bromide (5) from Pentaacetate (3).

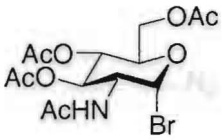

In a 100 mL round-bottom flask, pentaacetate (**3**) (0.503 g, 1.29 mmol) was dissolved in hydrobromic acid (11 mL) and allowed to spin for 21 h until TLC (ethyl acetate) showed the reaction was complete. The reaction was evaporated down and dissolved in $CHCl_3$ (15 mL). Cold, saturated $NaHCO_3$ (15 mL) and H_2O (15 mL) were added to the reaction, the layers separated, and then the organic layer was collected. The organic layer was dried over anhydrous $MgSO_4$, and evaporated to give 0.50 g of product

with a yield of 94%. The proton spectrum was somewhat similar to the mixture of product **2** and **3**; the spectrum of **5** did contain some product **3** also.

^{1}H NMR ($CDCl_3$): δ 1.98 (s, 3H, -CH_3), 2.05 (s, 3H, -CH_3), 2.06 (s, 3H, -CH_3), 2.09 (s, 3H, -CH_3), 2.10 (s, 3H, -CH_3), 2.12 (s, 3H, -CH_3), 2.12 (s, 3H, -CH_3), 2.20 (s, 3H, -CH_3), 2.34 (s, 3H, -CH_3), 3.75 (m, 4H, H-2(**5**), H-2(**3**), H-5(**5**), H-5(**3**)), 4.25 (m, 4H, H-6(**5**), H-6'(**5**), H-6(**3**), H-6'(**3**)), 5.16 (m, 4H, H-3(**5**), H-3(**3**), H-4(**5**), H-4(**3**)), 5.76 (d, 1H, N<u>H</u>Ac, J = 9.0 Hz), 6.25 (d, 1H, N<u>H</u>Ac, J = 7.1 Hz), 6.52 (d, 1H, H-1(**5**), J = 3.8 Hz), 6.64 (d, 1H, H-1(**3**), J = 3.5 Hz).

Preparation of 2-*N*-Acetyl-3,4,6-tri-*O*-acetyl-2-aminodeoxy-β-D-glucopyranosyl azide (4) from 2-*N*-Acetyl-3,4,6-tri-*O*-acetyl-2-aminodeoxy-α-D-glucopyranosyl chloride (2).

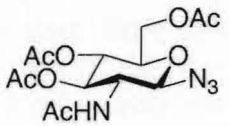

In a 250 mL round-bottom flask fitted with a septum and magnetic stir bar, the crude acetate-protected chloride **2** (7.08 g, 19.36 mmol) was dissolved in DMF (115 mL). NaN_3 (5.018 g, 77.19 mmol) was added to the reaction and allowed to stir for 18 h at RT until TLC (ethyl acetate) showed consumption of the starting material. CH_2Cl_2 (70 mL), 5% H_2SO_4 (70 mL), and H_2O (70 mL) were added to the reaction and the organic layer was collected. The organic layer was washed with 5% H_2SO_4 (70 mL) and then H_2O (200 mL). The organic layer was dried over anhydrous $MgSO_4$, evaporated, and purified

on a column of silica gel (1:6 hexanes – ethyl acetate) to give 3.95 g of product as a white solid in 51% yield.

^{1}H NMR ($CDCl_3$): δ 1.99 (s, 3H, -CH_3), 2.04 (s, 3H, -CH_3), 2.05 (s, 3H, -CH_3), 2.11 (s, 3H, -CH_3), 3.79 (ddd, 1H, H-5, J = 3.3, 6.2, 6.2 Hz), 3.92 (q, 1H, H-2, J = 9.5 Hz), 4.17 (dd, 1H, H-6, J = 2.1, 12.4 Hz), 4.28 (dd, 1H, H-6', J = 4.8, 12.5 Hz), 4.76 (d, 1H, H-1, J = 9.2 Hz), 5.11 (t, 1H, H-3, J = 9.7 Hz), 5.25 (t, 1H, H-4, J = 10.0 Hz), 5.63 (d, 1H, N<u>H</u>Ac, J = 9.0 Hz).

^{13}C NMR ($CDCl_3$): δ 20.67, 20.72, 20.81, 23.30, 54.04, 61.82, 67.99, 72.06, 73.86, 88.33, 169.12, 170.37, 170.56, 170.80.

m/z calculated: 372.33 *m/z* found: 395.1 (M + Na)

Melting Point: 166-168 °C

Preparation of 2-*N*-Acetyl-3,4,6-tri-*O*-acetyl-2-aminodeoxy-β-D-glucopyranosyl azide (4) (other route) from 2-*N*-Acetyl-3,4,6-tri-*O*-acetyl-2-aminodeoxy-α-D-glucopyranosyl bromide (5).

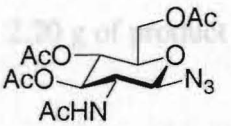

In a 2-neck 50 mL round-bottom flask, 2-*N*-Acetyl-3,4,6-tri-*O*-acetyl-2-aminodeoxy-α-D-glucopyranosyl bromide (**5**) (0.47 g, 1.15 mmol) was dissolved in DMF (15 mL) and

NaN_3 (0.507 g, 7.799 mmol) was added. The reaction was heated at 70 °C for 75 min until TLC (ethyl acetate) showed starting material was consumed. The reaction mixture was evaporated down, dissolved in CH_2Cl_2 (10 mL), and washed with H_2O (20 mL). The organic layer was washed with H_2O (20 mL), and then dried with anhydrous $MgSO_4$. The reaction mix was evaporated and gave 0.15 g of product with a yield of 36%. The NMR signals matched those of product **4** formed from the chloride, however it was not as clean of a spectrum.

Preparation of 2-*N*-Acetyl-2-aminodeoxy-β-D-glucopyranosyl azide (6) from 2-*N*-Acetyl-3,4,6-tri-*O*-acetyl-2-aminodeoxy-β-D-glucopyranosyl azide (4).

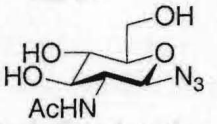

In a 500 mL round-bottom flask fitted with a septum and magnetic stir bar, acetate-protected azide (**4**) (3.32 g, 9.266 mmol) was dissolved in CH_3OH (80 mL). In a 50 mL Erlenmeyer flask, sodium metal (1/2 a pellet) was dissolved in CH_3OH (20 mL). The sodium methoxide solution was added to the sugar solution and allowed to stir for 2 h until TLC (3:1 ethyl acetate – methanol) showed total consumption of starting material. The reaction was evaporated to give 2.20 g of product as a white solid in 87.1% yield.

^{1}H NMR (d_6-DMSO): δ 1.82 (s, 3H, NHAc), 3.22 (m, 2H, H-2, H-5), 3.47 (m, 3H, H-3, H-4, H-6), 3.67 (dd, 1H, H-6', J = 1.8, 12.0 Hz), 4.36 (d, 1H, H-1, J = 9.3 Hz), 7.86 (d, 1H, NHAc, J = 9.2 Hz).

^{13}C NMR (d_6-DMSO): δ 23.01, 54.82, 60.76, 70.04, 73.77, 79.36, 88.51, 169.30.

m/z calculated: 246.22 *m/z* found: 269.0 (M + Na)

Melting Point: 138 °C, decomposes

Preparation of 2-*N*-Acetyl-2-aminodeoxy-4,6-*O*-isopropylidene-β-D-glucopyranosyl azide (7) from 2-*N*-Acetyl-2-aminodeoxy-β-D-glucopyranosyl azide (6).

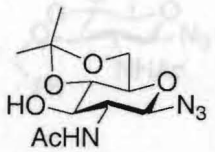

In a 100 mL round-bottom flask fitted with a septum and magnetic stir bar, azide **6** (0.92 g, 3.736 mmol) was dissolved in DMF (15 mL). D(+)-10-Camphorsulfonic acid (0.186 g, 0.801 mmol) and 2,2-dimethoxypropane (25 mL) were added and the mixture was allowed to stir for 3 h until TLC (3:1 ethyl acetate – methanol) showed disappearance of compound **6**. The residue after evaporation afforded a brown syrup weighing 0.93 g giving product **7** in 87% yield.

^{1}H NMR ($CDCl_3$): δ 1.30 (s, 3H, -CH_3), 1.43 (s, 3H, -CH_3), 1.83 (s, 3H, NHAc), 3.30 (ddd, 1H, H-5, *J* = 5.3, 9.8, 9.8 Hz), 3.44 (m, 2H, H-4, H-6), 3.61 (q, 1H, H-2, *J* = 9.2 Hz), 3.71 (t, 1H, H-3, *J* = 10.3 Hz), 3.81 (dd, 1H, H-6', *J* = 5.2, 10.4 Hz), 4.50 (d, 1H, H-1, *J* = 9.5 Hz), 7.94 (d, 1H, NHAc, *J* = 9.0 Hz).

m/z calculated: 286.1 *m/z* found: 309.1 (M + Na)

Melting Point: Syrup

Preparation of 2-*N*-Acetyl-2-aminodeoxy-3-*O*-benzyl-4,6-*O*-isopropylidene-β-D-glucopyranosyl azide (8) from 2-*N*-Acetyl-2-aminodeoxy-4,6-*O*-isopropylidene-β-D-glucopyranosyl azide (7).

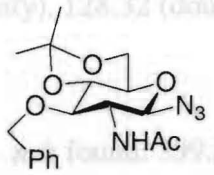

In a 100 mL round-bottom flask, DMF (30 mL) was added to azide **7** (1.245 g, 4.349 mmol) to dissolve it. Sodium hydride (0.354 g, 14.75 mmol) was added to the reaction and the mixture was allowed to sit until bubbling ceased. Benzyl bromide (0.52 mL) was then added and the reaction was stirred overnight until TLC (ethyl acetate) showed consumption of starting material. The reaction was then poured into 100 mL of H_2O/ice mixture. The product was extracted with CH_2Cl_2 (1 x 35 mL), washed with ammonium chloride (1 x 45 mL), and washed with $NaHCO_3$ (1 x 45 mL). The organic layer was finally washed with H_2O (1 x 70 mL), dried with anhydrous $MgSO_4$ and the solvent was then evaporated off. Column chromatography was then performed (1:1 hexane – ethyl acetate) to give 0.83 g of product as a white solid in 50.7% yield.

^{1}H NMR ($CDCl_3$): δ 1.44 (s, 1H, -CH_3), 1.51 (s, 1H, -CH_3), 1.90 (s, 3H, NHAc), 3.32 (q, 1H, H-2, J = 9.1 Hz), 3.41 (ddd, 1H, H-5, J = 5.3, 10.0, 10.0 Hz), 3.72 (t, 1H, H-4, J = 9.3 Hz), 3.79 (t, 1H, H-3, J = 10.6 Hz), 3.95 (m, 2H, H-6, H-6'), 4.59 (d, 1H, H-8, J = 12.0 Hz), 4.83 (d, 1H, H-7, J = 12.0 Hz), 5.02 (d, 1H, H-1, J = 9.2 Hz), 5.42 (d, 1H, NHAc, J = 7.9 Hz), 7.32 (m, 5H, Ar-H).

^{13}C NMR ($CDCl_3$): δ 19.15, 23.57, 29.15, 56.46, 61.90, 69.07, 74.02, 74.99, 76.58, 88.28, 99.39, 127.77, 128.09 (double intensity), 128.32 (double intensity), 138.21, 170.44.

m/z calculated: 376.41 *m/z* found: 399.2 (M + Na)

Melting Point: 142-160 °C

Attempted Preparation of 2-*N*-Acetyl-2-aminodeoxy-3-*O*-benzyl-β-D-glucopyranosyl azide (9) from 2-*N*-Acetyl-2-aminodeoxy-3-*O*-benzyl-4,6-*O*-isopropylidene-β-D-glucopyranosyl azide (8).

In a 100 mL round-bottom flask fitted with a rubber septum and magnetic stir bar, 2-*N*-Acetyl-2-aminodeoxy-3-*O*-benzyl-4,6-*O*-isopropylidene-β-D-glucopyranosyl azide (**8**) (0.218 g, 0.579 mmol) was dissolved in a mixture of TFA and H_2O (9:1) and allowed to stir until TLC (ethyl acetate) showed consumption of starting material. The reaction was then evaporated to give 0.16 g of product as a syrup in 82% yield. ^{1}H NMR showed a different product suggesting that the azide group at C-1 had been cleaved off. The reaction was also attempted using ratios of TFA: H_2O with 1:1, 1:9, and 1:99 with the

same results suggesting to us that the azide had in fact been removed and replaced with an –OH group which we attempted to prove by an acetylation in the next step.

Acetylation of crude deprotection product (10) from the previous experiment.

In a 100 mL round-bottom flask fitted with a rubber septum and magnetic stir bar, the crude product from the previous reaction (0.287 g) was dissolved in pyridine (3 mL). Acetic anhydride (1 mL) was added dropwise and the reaction was stirred until TLC (ethyl acetate) showed consumption of starting material. The reaction was then put into a water/ice (10 mL) mixture and extracted with CH_2Cl_2 (3 x 5 mL). The combined organic layers were washed with 5% H_2SO_4 (3 x 5 mL) and H_2O (15 mL). The organic layer was then dried over anhydrous $MgSO_4$ and after evaporation gave 0.18 g of product as a solid in 50.2% yield. NMR proved that the desired deprotected glycosyl azide product in the previous experiment in fact had not been formed and that the group at C-1 was in fact now an –OAc group, which was also proven by mass spectrometry.

^{1}H NMR ($CDCl_3$): δ 1.85 (s, 3H, -CH_3), 2.07 (s, 3H, -CH_3), 2.09(s, 3H, -CH_3), 2.14 (s, 3H, -CH_3), 2.23 (s, 3H, -CH_3), 3.86 (m, 2H, H-2, H-5), 4.17 (m, 2H, H-6, H-6'), 4.60 (m, 2H, H-3, H-4), 5.05 (d, 1H, N<u>H</u>Ac, J = 7.9 Hz), 6.18 (d, 1H, H-1, J = 3.7 Hz), 7.33 (m, 5H, Aromatic H's)

m/z calculated: 437.2 *m/z* found: 460.2 (M + Na)

Melting Point: syrup

Preparation of Methyl 2-*N*-acetyl-2-aminodeoxy-α/β-D-glucopyranosides (11α/β) from *N*-Acetyl-D-glucosamine (1).

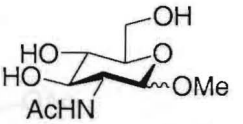

In a 250 mL round-bottom flask equipped with a rubber septum and magnetic stir bar, *N*-acetyl-D-glucosamine (5.103 g, 22.66 mmol) was dissolved in anhydrous CH_3OH (60 mL). In another 250 mL round-bottom flask, HCl gas was bubbled through anhydrous CH_3OH (60 mL) for 5 min. The sugar solution was poured into the flask containing CH_3OH and HCl gas. The reaction was stirred until TLC (3:1 ethyl acetate – methanol) showed no starting material remaining. The solution was evaporated to give 0.96 g of product as a brown syrup in 90.4% yield and a 2:1 α:β ratio.

^{1}H NMR (d_6-DMSO): δ 1.78 (s, 3H, NHAcβ), 1.81 (s, 3H, NHAcα), 3.15 (s, 3H, -OMeα), 3.22 (s, 3H, -OMeβ), 4.15 (d, 1H, H-1β, J = 8.4 Hz), 4.51 (d, 1H, H-1α, J = 3.5 Hz), 7.73 (d, 1H, NHAcβ, J = 8.8 Hz), 7.79 (d, 1H, NHAcα, J = 8.2 Hz).

Melting Point: Syrup

Preparation of Methyl 2-*N*-acetyl-3,4,6-tri-*O*-acetyl-2-aminodeoxy-α/β-D-glucopyranosides (12α/β) from Methyl 2-*N*-acetyl-2-aminodeoxy-α/β-D-glucopyranosides (11α/β).

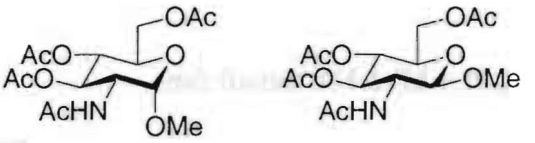

In a 250 mL round-bottom flask, methyl 2-*N*-acetyl-2-aminodeoxy-α/β-D-glucopyranosides (**11α/β**) (6.59 g, 28.02 mmol) was dissolved in pyridine (75 mL) and acetic anhydride (25 mL) and was equipped with a septum and magnetic stir bar. The reaction was allowed to stir in an ice bath for 2 h until TLC (ethyl acetate) showed consumption of starting material. The reaction was poured over a water/ice mix (300 mL) and then extracted with CH_2Cl_2 (3 x 80 mL). The combined organic layers were washed with 5% H_2SO_4 (2 x 80 mL) and then with H_2O (200 mL). The organic layer was dried over anhydrous $MgSO_4$, evaporated, and separated on a column of silica gel (ethyl acetate as eluent) to afford 3.66 g of the α anomer in 36.2% yield and 1.76 g of the β anomer in 17.4% yield with both products being white solids.

β-Methyl glycoside

^{1}H NMR ($CDCl_3$): δ 1.96 (s, 3H, -CH_3), 2.03 (s, 3H, -CH_3), 2.04 (s, 3H, -CH_3), 2.09 (s, 3H, -CH_3), 3.50 (s, 3H, -OCH_3), 3.71 (ddd, 1H, H-5, J = 2.4, 4.9, 4.9 Hz), 3.87 (q, 1H, H-2, J = 9.2 Hz), 4.15 (dd, 1H, H-6, J = 2.8, 12.5 Hz), 4.28 (dd, 1H, H-6', J = 4.8, 12.3 Hz), 4.59 (d, 1H, H-1, J = 8.4 Hz), 5.09 (t, 1H, H-4, J = 9.7 Hz), 5.28 (t, 1H, H-3, J = 10.0 Hz), 5.51 (d, 1H, N<u>H</u>Ac, J = 8.4 Hz).

^{13}C NMR ($CDCl_3$): δ 20.68, 20.73, 20.79, 23.37, 54.50, 56.76, 62.08, 68.59, 71.72, 72.40, 101.48, 169.20, 170.16, 170.54, 170.69.

m/z calculated: 361.34 *m/z* found: 384.1 (M + Na)

Melting Point: 148-152 °C

α-Methyl glycoside

^{1}H NMR ($CDCl_3$): δ 1.96 (s, 3H, -CH_3), 2.02 (s, 3H, -CH_3), 2.03 (s, 3H, -CH_3), 2.11 (s, 3H, -CH_3), 3.41 (s, 3H, -OCH_3), 4.42 (ddd, 1H, H-5, *J* = 2.3, 4.7, 4.9 Hz), 4.11 (dd, 1H, H-6, *J* = 2.4, 12.4 Hz), 4.25 (dd, 1H, H-6', *J* = 4.6, 12.3 Hz), 4.35 (ddd, 1H, H-2, *J* = 2.3, 6.7 Hz), 4.74 (d, 1H, H-1, *J* = 3.5 Hz), 5.13 (t, 1H, H-4, *J* = 9.8 Hz), 5.22 (t, 1H, H-3, *J* = 10.1 Hz), 5.72 (d, 1H, N<u>H</u>Ac, *J* = 9.5 Hz).

^{13}C NMR ($CDCl_3$): δ 20.57, 20.68 (double intensity), 23.12, 51.70, 55.32, 61.91, 67.49, 68.02, 71.15, 98.12, 169.03, 169.72, 170.42, 171.00.

m/z calculated: 361.34 *m/z* found: 384.1 (M + Na)

Melting Point: 120-128 °C

Preparation of Methyl 2-*N*-acetyl-2-aminodeoxy-α/β-D-glucopyranosides (11α/11β) from Methyl 2-*N*-acetyl-3,4,6-tri-*O*-acetyl-2-aminodeoxy-α/β-D-glucopyranosides (12α/12β).

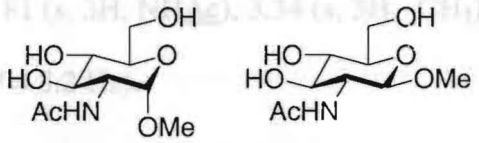

In a 500 mL round-bottom flask fitted with a septum and magnetic stir bar, the tetraacetate (**12α**) (3.95 g, 10.93 mmol) or (**12β**) (1.26 g, 3.487 mmol) was dissolved in CH_3OH (80 mL). In a 50 mL Erlenmeyer flask, sodium metal (1/2 a pellet) was dissolved in CH_3OH (20 mL). The sodium methoxide solution was added to the sugar solution and allowed to stir for 2 h until TLC (3:1 ethyl acetate – methanol) showed total consumption of starting material. The reactions were evaporated to give crude yellow solids with 2.54 g of the α anomer in 98.8% yield and 0.78 g of the β anomer in 95% yield.

Methyl 2-*N*-acetyl-2-aminodeoxy-β-D-glucopyranoside

^{1}H NMR (d_6-DMSO): δ 1.77 (s, 3H, NH<u>Ac</u>), 3.22 (m, 2H, H-2, H-5), 3.30 (s, 3H, -CH_3), 3.44 (m, 4H, H-3, H-4, H-6, H-6') 4.15 (d, 1H, H-1, J = 8.4 Hz), 7.71 (d, 1H, N<u>H</u>Ac, J = 9.2 Hz).

^{13}C NMR (d_6-DMSO): δ 23.18, 55.00, 55.69, 60.91, 70.45, 74.16, 76.97, 101.84, 168.88.

m/z calculated: 235.23 *m/z* found: 258.1 (M + Na)

Melting Point: 76 °C, decomposes

Methyl 2-*N*-acetyl-2-aminodeoxy-α-D-glucopyranoside

^{1}H NMR (d_6-DMSO): δ 1.81 (s, 3H, NHAc), 3.34 (s, 3H, -CH_3), 4.51 (d, 1H, H-1, J = 3.5 Hz), 7.82 (d, 1H, NHAc, J = 8.2 Hz).

^{13}C NMR (d_6-DMSO): δ 22.73, 53.80, 54.28, 60.86, 70.65, 70.81, 72.73, 97.87, 169.33.

m/z calculated: 235.23 *m/z* found: 259.1 (M + Na + H)

Melting Point: 80 °C, decomposes

Attempted Preparation of Methyl 2-*N*-acetyl-2-aminodeoxy-4,6-*O*-isopropylidene-β-D-glucopyranoside (13β) from Methyl 2-*N*-acetyl-2-aminodeoxy-β-D-glucopyranoside (11β).

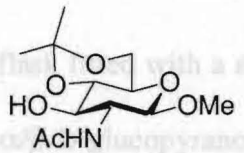

In a 125 mL round-bottom flask, methyl 2-*N*-acetyl-2-aminodeoxy-β-D-glucopyranoside (**11β**) (0.100 g, 0.425 mmol), DMF (1 mL), and 2-methoxypropene (0.3 mL) were mixed and then *p*-toluenesulfonic acid (0.017 g, 0.099 mmol) was added and stirred until TLC (3:1 ethyl acetate – methanol) apparently showed reaction to be complete. The reaction was evaporated and CH_2Cl_2 (5 mL) and H_2O (5 mL) were added

to the residue. The aqueous layer was extracted further with CH_2Cl_2 (2 x 5 mL) and washed with $NaHCO_3$ (2 x 5 mL) and H_2O (5 mL). The solution was dried over anhydrous $MgSO_4$ and evaporated, but gave no product. It was thought that the organic material was possibly lost in the aqueous layer. After evaporating the aqueous layer, NMR again showed no product only possible starting material. The reaction did not work possibly due to an inefficient amount of 2-methoxypropene being added to the reaction.

Preparation of Methyl 2-*N*-acetyl-2-aminodeoxy-4,6-*O*-isopropylidene-α- and β-D-glucopyranosides (13α/13β) from Methyl 2-*N*-acetyl-2-aminodeoxy-α/β-D-glucopyranosides (11α/11β).

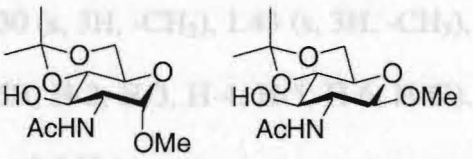

In a 100 mL round-bottom flask fitted with a septum and magnetic stir bar, either methyl 2-*N*-acetyl-2-aminodeoxy-α/β-D-glucopyranosides (**11α/11β**) (2.96 g, 12.58 mmol or 1.489 g, 6.330 mmol, respectively) were dissolved in DMF (10 mL). D(+)-10-Camphorsulfonic acid (0.593 g, 2.553 mmol or 0.301 g, 1.296 mmol) and 2,2-dimethoxypropane (20 mL) were added and the mixture was allowed to stir until TLC (3:1 ethyl acetate – methanol) showed disappearance of compound **11α/11β**. The residue

after evaporation afforded **13α** and **13β** as brown syrups, 3.08 g of the α anomer in 88.9% yield and 1.524 g of the β anomer in 87.5% yield.

Methyl 2-*N*-acetyl-2-aminodeoxy-4,6-*O*-isopropylidene-β-D-glucopyranoside

^{1}H NMR (d_6-DMSO): δ 1.03 (s, 3H, -CH_3), 1.24 (s, 3H, -CH_3), 1.78 (s, 3H, NHAc), 3.30 (s, 3H, -OMe), 3.31 (m, 6H, H-2, H-3, H-4, H-5, H-6, H-6'), 4.15 (d, 1H, H-1, J = 8.4 Hz), 7.69 (d, 1H, NHAc, J = 9.0 Hz).

m/z calculated: 275.3 *m/z* found: 277.0 (M + 2H)

Melting Point: syrup

Methyl 2-*N*-acetyl-2-aminodeoxy-4,6-*O*-isopropylidene-α-D-glucopyranoside

^{1}H NMR (d_6-DMSO): δ 1.30 (s, 3H, -CH_3), 1.43 (s, 3H, -CH_3), 1.82 (s, 3H, NHAc), 3.23 (s, 3H, -OCH_3), 3.62 (m, 6H, H-2, H-3, H-4, H-5, H-6, H-6'), 4.54 (d, 1H, H-1 J = 3.5 Hz), 7.87 (d, 1H, NHAc, J = 8.6 Hz).

m/z calculated: 275.3 *m/z* found: 298.1 (M + Na)

Melting Point: syrup

Preparation of Methyl 2-*N*-acetyl-2-aminodeoxy-3-*O*-benzyl-4,6-*O*-isopropylidene-α-D-glucopyranoside and Methyl 2-*N*-acetyl-2-aminodeoxy-3-*O*-benzyl-4,6-*O*-

isopropylidene-β-D-glucopyranoside (14α and 14β) from Methyl 2-*N*-acetyl-2-aminodeoxy-4,6-*O*-isopropylidene-α/β-D-glucopyranosides (13α/13β).

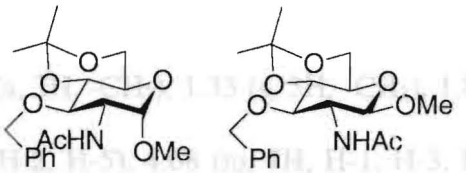

In a 100 mL round-bottom flask, DMF (30 mL) was added to either methyl 2-*N*-acetyl-2-aminodeoxy-4,6-*O*-isopropylidene-α/β-D-glucopyranosides (**13α/13β**) (1.02 g, 3.71 mmol or 1.26 g, 4.58 mmol, respectively) to dissolve it. Sodium hydride (0.306 g, 12.75 mmol or 0.373g, 15.54 mmol) was added to the reaction and the mixture was allowed to sit until bubbling ceased. Benzyl bromide (0.44 mL or 0.54 mL) was then added and the reaction was stirred overnight until TLC (ethyl acetate) showed consumption of starting material. The reaction mixture was then poured into 50 mL of H_2O/ice mixture. The organic layer was extracted out with CH_2Cl_2 (1 x 25 mL), washed with ammonium chloride (1 x 30 mL), and washed with $NaHCO_3$ (1 x 30 mL). The organic layer was washed with H_2O (1 x 50 mL) dried with anhydrous $MgSO_4$ and the solvent was then evaporated off. Column chromatography was then performed (1:1 hexane – ethyl acetate) to give 0.43 g of a white solid in 36.0% yield for the α anomer and 0.36 g of product for a 15.3% yield for the β anomer.

Methyl 2-*N*-acetyl-2-aminodeoxy-3-*O*-benzyl-4,6-*O*-isopropylidene-β-D-glucopyranoside

^{1}H NMR ($CDCl_3$): δ 1.26 (s, 3H, -CH_3), 1.33 (s, 3H, -CH_3), 1.86 (s, 3H, NHAc), 3.49 (s, 3H, -OMe), 3.72 (m, 2H, H-2, H-5), 4.68 (m, 7H, H-1, H-3, H-4, H-6, H-6', H-7, H-8) 5.54 (d, 1H, NHAc, J = 8.1 Hz), 7.32 (m, 5H, Ar-H).

m/z calculated: 365.42 *m/z* found: 387.0 (M + H)

Melting Point: 113-121 °C

Methyl 2-*N*-acetyl-2-aminodeoxy-3-*O*-benzyl-4,6-*O*-isopropylidene-α-D-glucopyranoside

^{1}H NMR ($CDCl_3$): δ 1.45 (s, 3H, -CH_3), 1.51 (s, 3H, -CH_3), 1.92 (s, 3H, NHAc), 3.32 (s, 3H, -OMe), 3.51 (q, 1H, H-2, J = 6.4 Hz), 3.61 (ddd, 1H, H-5, J = 5.3, 10.1, 10.1 Hz), 3.82 (m, 2H, H-3, H-4), 4.21 (dd, 1H, H-6, J = 2.4, 7.9 Hz), 4.24 (dd, 1H, H-6', J = 2.4, 7.9 Hz), 4.59 (d, 1H, H-8, J = 12.5 Hz), 4.65 (d, 1H, H-7, J = 3.9 Hz), 4.83 (d, 1H, H-1, J = 12.5 Hz), 5.35 (d, 1H, NHAc, J = 9.2), 7.32 (m, 5H, Ar-H).

m/z calculated: 365.42 *m/z* found: 388.1 (M + H)

Melting Point: 130-133°C

Attempted Preparation of Methyl 2-*N*-acetyl-2-aminodeoxy-3-*O*-pivaloyl-4,6-*O*-isopropylidene-β-D-glucopyranoside from Methyl 2-*N*-acetyl-2-aminodeoxy-4,6-*O*-isopropylidene-β-D-glucopyranoside (13β).

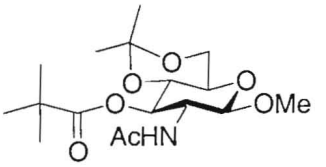

In a 100 mL round-bottom flask, methyl 2-*N*-acetyl-2-aminodeoxy-4,6-*O*-isopropylidene-β-D-glucopyranoside (**13β**) (0.15 g, 0.545 mmol) was dissolved in pyridine (5 mL) and then trimethyl acetyl chloride (1 mL) was added to the reaction, which was allowed to stir overnight until TLC (ethyl acetate) appeared to show consumption of starting material. The reaction was put into water/ice (40 mL) and extracted with CH_2Cl_2 (3 x 10 mL). The organic layer was washed with 5% H_2SO_4 (2 x 10 mL) and H_2O (20 mL). The solution was dried over anhydrous $MgSO_4$, evaporated, and purified on a column of silica gel (ethyl acetate) to give material, the structure of which was inconclusive by NMR spectroscopy.

Preparation of methyl 2-*N*-acetyl-2-aminodeoxy-4,6-*O*-benzylidene-α-D-glucopyranoside from Methyl 2-*N*-acetyl-2-aminodeoxy-α-D-glucopyranoside (11α).

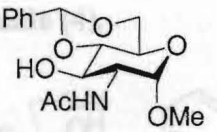

Methyl 2-*N*-acetyl-2-aminodeoxy-α-D-glucopyranoside (**11α**) (0.511 g, 2.172 mmol) was placed in a 100 mL round-bottom flask. Freshly distilled benzaldehyde (2 mL) and fused zinc chloride (0.511 g, 3.749 mmol) were added to the reaction, which was stirred overnight until TLC (3:1 ethyl acetate – methanol) appeared to show consumption of starting material. The reaction was placed on a high vacuum pump to remove all solvent and column chromatography was performed (3:1 ethyl acetate – methanol) to give what was concluded to be starting material according to ^{1}H NMR.

Typical procedure for the synthesis of *N*-glycosyl amides using the modified Staudinger reaction. 2-Acetamido-glucosyl azide (**4**) (1.0 mmol), acylating agent (2.0 mmol), and ethylenebis(diphenylphosphine) (0.65 mmol) were all put into a round bottom flask, and then dry THF (0.1 g/mL) was added dropwise to dissolve the reagents. The mixture was stirred at RT for 4 h until TLC showed the disappearance of the intermediate ylid. Saturated $NaHCO_3$ was then added and the mixture was stirred overnight. After THF was removed under vacuum, the residue was dissolved in $CHCl_3$ (3 x 20 mL) and then washed with H_2O (1 x 20 mL). The organic layer was dried over anhydrous $MgSO_4$, filtered, evaporated to dryness, and the crude product was purified by recrystallization.

Preparation of *p*-Nitrobenzoic acid amide (19) from 2-*N*-Acetyl-3,4,6-tri-*O*-acetyl-2-aminodeoxy-β-D-glucopyranosyl azide (4).

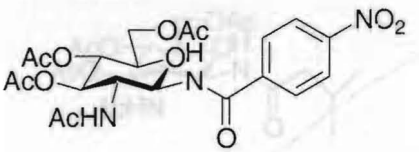

2-*N*-Acetyl-3,4,6-tri-*O*-acetyl-2-aminodeoxy-β-D-glucopyranosyl azide (**4**) (0.377 g, 1.01 mmol), *p*-nitrobenzoyl chloride (0.379 g, 2.04 mmol), and DPPE (0.262 g, 0.66 mmol) were reacted in THF according to the typical procedure. Purification by recrystallization (ethanol) yielded 0.163 g of product as a white solid in 32.5% yield.

^{1}H NMR ($CDCl_3$): δ 1.97 (s, 3H, -CH_3), 2.08 (s, 3H, -CH_3), 2.10 (s, 3H, -CH_3), 2.12 (s, 3H, -CH_3), 3.85 (ddd, 1H, H-5, J = 2.1, 6.0, 5.9 Hz), 4.13 (dd, 1H, H-6, J = 2.3, 12.5 Hz), 4.24 (q, 1H, H-2, J = 9.3 Hz), 4.36 (dd, 1H, H-6', J = 4.2, 12.6 Hz), 5.11 (t, 1H, H-4, J = 10.1 Hz), 5.19 (d, 1H, H-1, J = 2.9 Hz), 5.21 (t, 1H, H-3, J = 3.8 Hz), 6.20 (d, 1H, N<u>H</u>Ac, J = 7.3 Hz), 8.01 (d, 2H, H-8 and H-9, J = 9.2 Hz), 8.22 (d, 1H, N-H, J = 7.1 Hz), 8.30 (d, 2H, H-10 and H-11, J = 9.0 Hz).

^{13}C NMR ($CDCl_3$): δ 20.70, 20.85, 20.86, 23.28, 53.81, 61.57, 67.40, 72.79, 73.54, 81.42, 123.80 (double intensity), 128.55 (double intensity), 138.04, 149.83, 165.21, 169.07, 170.52, 172.21, 172.72

m/z calculated: 495.4 *m/z* found: 518.2 (M + Na)

Melting Point: 280-282 °C, decomposes

Preparation of Isovaleryl amide (20) from 2-*N*-Acetyl-3,4,6-tri-*O*-acetyl-2-aminodeoxy-β-D-glucopyranosyl azide (4).

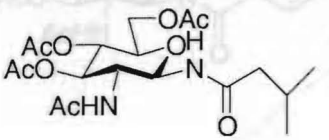

2-*N*-Acetyl-3,4,6-tri-*O*-acetyl-2-aminodeoxy-β-D-glucopyranosyl azide (**4**) (0.376 g, 1.01 mmol), isovaleryl chloride (0.25 mL, 2.03 mmol), and DPPE (0.263 g, 0.66 mmol) were dissolved in THF according to the typical procedure. Purification by recrystallization (ethanol) yielded 0.182 g of product as a solid in 41.9% yield.

^{1}H NMR ($CDCl_3$): δ 0.90 (d, 6H, -CH_3 x 2, *J* = 6.4 Hz), 0.93 (d, 2H, -CH_2, J = 6.2 Hz), 2.00 (m, 1H, -CH), 2.05 (s, 3H, -CH_3), 2.07 (s, 3H, -CH_3), 2.09 (s, 3H, -CH_3), 3.76 (ddd, 1H, H-5, *J* = 2.1, 4.7, 4.8 Hz), 4.08 (dd, 1H, H-6, *J* = 2.2, 12.5 Hz), 4.14 (q, 1H, H-2, *J* = 9.6 Hz), 4.32 (dd, 1H, H-6', *J* = 4.3, 12.5 Hz), 5.04 (t, 1H, H-4, *J* = 9.0 Hz), 5.08 (d, 1H, H-1, *J* = 7.9 Hz), 5.14 (t, 1H, H-3, *J* = 9.6 Hz), 6.02 (d, 1H, N<u>H</u>Ac, *J* = 8.2 Hz), 6.90 (d, 1H, N-H, *J* = 8.6 Hz).

^{13}C NMR ($CDCl_3$): δ 20.67, 20.81, 23.09, 25.95, 45.87, 53.06, 61.76, 67.88, 72.93, 73.34, 79.84, 128.71, 130.63, 131.96, 169.14, 170.54, 171.47, 171.71, 173.21

m/z calculated: 430.4 *m/z* found: 453.0 (M + Na)

Melting Point: 236-238 °C

Preparation of Benzoyl amide (21) from 2-*N*-Acetyl-3,4,6-tri-*O*-acetyl-2-aminodeoxy-β-D-glucopyranosyl azide (4).

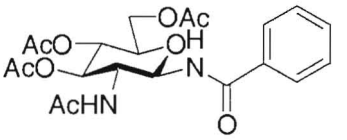

2-*N*-Acetyl-3,4,6-tri-*O*-acetyl-2-aminodeoxy-β-D-glucopyranosyl azide (**4**) (0.374 g, 1.00 mmol), benzoyl chloride (0.23 mL, 2.00 mmol), and DPPE (0.266 g, 0.67 mmol) were reacted in THF according to the typical procedure. Purification by recrystallization (ethanol) yielded 0.144 g of product as a solid in 31.9% yield.

^{1}H NMR ($CDCl_3$): δ 1.94 (s, 3H, -CH_3), 2.07 (s, 3H, -CH_3), 2.10 (s, 3H, -CH_3), 2.11 (s, 3H, -CH_3), 3.86 (ddd, 1H, H-5, *J* = 2.1, 4.7, 4.6 Hz), 4.12 (dd, 1H, H-6, *J* = 2.2, 12.5 Hz), 4.28 (q, 1H, H-2, *J* = 9.5 Hz), 4.36 (dd, 1H, H-6', *J* = 4.1, 12.4 Hz), 5.12 (t, 1H, H-4, *J* = 10.0 Hz), 5.19 (d, 1H, H-1, *J* = 9.9 Hz), 5.26 (t, 1H, H-3, *J* = 8.9 Hz), 6.15 (d, 1H, N<u>H</u>Ac, *J* = 7.9 Hz), 7.45 (t, 1H, H-12, *J* = 7.7 Hz), 7.53 (t, 2H, H-10 and H-11, *J* = 7.4 Hz), 7.83 (d, 2H, H-8 and H-9, *J* = 7.1 Hz), 7.88 (d, 1H, N-H, *J* = 8.1 Hz).

^{13}C NMR ($CDCl_3$): δ 20.72, 20.86 (double intensity), 23.21, 53.51, 61.71, 67.67, 72.94, 73.49, 81.10, 127.27 (double intensity), 128.59 (double intensity), 132.14, 132.57, 167.34, 169.12, 170.58, 171.92, 172.18.

m/z calculated: 450.4 *m/z* found: 451.1 (M + H)

Melting Point: 247-249 °C

Preparation of Butyryl amide (22) from 2-*N*-Acetyl-3,4,6-tri-*O*-acetyl-2-aminodeoxy-β-D-glucopyranosyl azide (4).

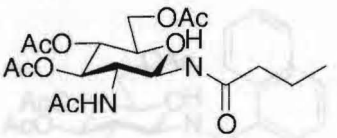

2-*N*-Acetyl-3,4,6-tri-*O*-acetyl-2-aminodeoxy-β-D-glucopyranosyl azide (**4**) (0.377 g, 1.01 mmol), butyryl chloride (0.21 mL, 2.02 mmol), and DPPE (0.270 g, 0.68 mmol) were reacted in THF according to the typical procedure. Purification by recrystallization (ethanol) yielded 0.206 g of product as a solid in 48.9% yield.

^{1}H NMR ($CDCl_3$): δ 1.62 (m, 3H, -CH_3), 1.95 (s, 3H, -CH_3), 2.05 (s, 3H, -CH_3), 2.08 (s, 3H, -CH_3), 2.09 (s, 3H, -CH_3), 2.17 (m, 4H, H8-H11), 3.7 (ddd, 1H, H-5, J = 2.2, 4.7, 4.7 Hz), 4.09 (dd, 1H, H-6, J = 2.3, 12.5 Hz), 4.14 (q, 1H, H-2, J = 8.3 Hz), 4.31 (dd, 1H, H-6', J = 4.4, 12.5 Hz), 5.05 (t, 1H, H-3, J = 8.2 Hz), 5.09 (d, 1H, H-1, J = 11.0 Hz), 5.13 (t, 1H, H-4, J = 7.6 Hz), 6.08 (d, 1H, NHAc, J = 8.2 Hz), 6.92 (d, 1H, N-H, J = 8.4 Hz).

^{13}C NMR ($CDCl_3$): δ 13.66, 18.70, 20.69, 20.81, 20.85, 23.17, 38.55, 53.29, 61.74, 67.74, 72.91, 73.42, 80.10, 169.12, 170.55, 171.67, 171.69, 173.59.

m/z calculated: 416.4 *m/z* found: 431.1 (M + -CH_3)

Melting Point: 219-221 °C

Preparation of 1-Naphthoyl amide (23) from 2-*N*-Acetyl-3,4,6-tri-*O*-acetyl-2-aminodeoxy-β-D-glucopyranosyl azide (4).

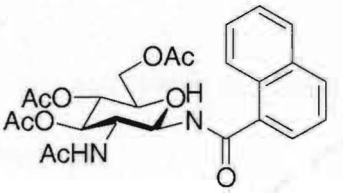

2-*N*-Acetyl-3,4,6-tri-*O*-acetyl-2-aminodeoxy-β-D-glucopyranosyl azide (**4**) (0.377 g, 1.01 mmol), 1-naphthoyl chloride (0.30 mL, 1.99 mmol), and DPPE (0.264 g, 0.66 mmol) were reacted in THF according to the typical procedure. Purification by recrystallization (ethanol) and then through a column of silica gel (ethyl acetate as eluent) yielded 0.211 g of product as a solid in 41.6% yield.

^{1}H NMR ($CDCl_3$): δ 1.96 (s, 3H, -CH_3), 2.08 (s, 3H, -CH_3), 2.10 (s, 3H, -CH_3), 2.11 (s, 3H, -CH_3), 3.89 (ddd, 1H, H-5, J = 2.1, 4.4, 4.7 Hz), 4.17 (dd, 1H, H-6, J = 2.1, 12.5 Hz), 4.29 (q, 1H, H-2, J = 9.6 Hz), 4.37 (dd, 1H, H-6', J = 4.3, 12.5 Hz), 5.16 (d, 1H, H-1, J = 10.1 Hz), 5.21 (t, 1H, H-3, J = 9.5 Hz), 5.40 (t, 1H, H-4, J = 9.3 Hz), 6.09 (d, 1H, N<u>H</u>Ac, J = 8.6 Hz), 7.38 (d, 1H, N-H, J = 8.6 Hz), 7.35 (m, 7H, Ar-H).

^{13}C NMR ($CDCl_3$): δ 20.72, 20.83, 20.87, 23.08, 53.35, 61.80, 67.86, 73.08, 73.73, 77.32, 80.28, 124.59, 125.21, 125.37, 126.35, 127.15, 128.25, 130.05, 131.50, 132.06, 133.60, 169.15, 169.50, 170.58, 171.58.

m/z calculated: 500.50 *m/z* found: 501.2 (M + H)

Melting Point: 259-261 °C, decomposes

Preparation of Acetyl amide (24) from 2-*N*-Acetyl-3,4,6-tri-*O*-acetyl-2-aminodeoxy-β-D-glucopyranosyl azide (4).

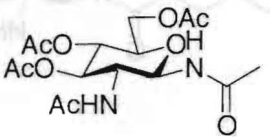

2-*N*-Acetyl-3,4,6-tri-*O*-acetyl-2-aminodeoxy-β-D-glucopyranosyl azide (**4**) (0.372 g, 1.00 mmol), acetyl chloride (0.14 mL, 1.97 mmol), and DPPE (0.263 g, 0.66 mmol) were reacted in THF according to the typical procedure. Purification through a column of silica gel (ethyl acetate as eluent) yielded 0.270 g of product as a solid in 69.8% yield.

^{1}H NMR ($CDCl_3$): δ 1.97 (s, 3H, -CH_3), 1.98 (s, 3H, -CH_3), 2.05 (s, 3H, -CH_3), 2.08 (s, 3H, -CH_3), 2.10 (s, 3H, -CH_3), 3.76 (ddd, 1H, H-5, J = 2.1, 4.8, 4.8 Hz), 4.09 (dd, 1H, H-6, J = 1.9, 12.5 Hz), 4.13 (q, 1H, H-2, J = 6.0 Hz), 4.31 (dd, 1H, H-6', J = 4.3, 12.5 Hz), 5.037 (d, 1H, H-1, J = 10.6 Hz), 5.043 (t, 1H, H-3, J = 9.1 Hz), 5.14 (t, 1H, H-4, J = 9.7 Hz), 5.93 (d, 1H, N<u>H</u>Ac, J = 8.2 Hz), 6.99 (d, 1H, N-H, J = 7.9 Hz).

^{13}C NMR ($CDCl_3$): δ 20.70, 20.84, 23.24, 23.50, 26.57, 53.49, 61.69, 67.50, 70.61, 72.91, 73.45, 80.38, 169.09, 170.56, 170.71, 171.89.

m/z calculated: 387.33 *m/z* found: 411.1 (M + Na + H)

Melting Point: 235-238 °C, decomposes

Preparation of 6-Bromohexanoyl amide (25) from 2-*N*-Acetyl-3,4,6-tri-*O*-acetyl-2-aminodeoxy-β-D-glucopyranosyl azide (4).

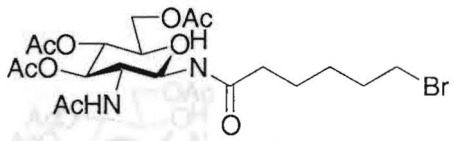

2-*N*-Acetyl-3,4,6-tri-*O*-acetyl-2-aminodeoxy-β-D-glucopyranosyl azide (**4**) (1.002 g, 2.69 mmol), 6-bromohexanoyl chloride (0.82 mL, 5.36 mmol), and DPPE (0.699 g, 1.75 mmol) were reacted in THF according to the typical procedure. Purification through a column of silica gel (ethyl acetate as eluent) yielded 0.99 g of product as a white solid in 70.3% yield.

^{1}H NMR ($CDCl_3$): δ 1.43 (m, 2H, -CH_2), 1.62 (m, 2H, -CH_2), 1.87 (m, 2H, -CH_2), 1.96 (s, 3H, -CH_3), 2.05 (s, 3H, -CH_3), 2.08 (s, 3H, -CH_3), 2.09 (s, 3H, -CH_3), 2.20 (m, 2H, -CH_2), 3.40 (t, 2H, Br-CH_2, J = 6.7 Hz), 3.76 (ddd, 1H, H-5, J = 2.0, 4.6, 4.6 Hz), 4.10 (m, 2H, H-2, H-6) 4.31 (dd, 1H, H-6', J = 4.1, 12.5 Hz), 5.04 (m, 2H, H-1, H-3) 5.14 (t, 1H, H-4, J = 9.5 Hz), 5.97 (d, 1H, N<u>H</u>Ac, J = 7.9 Hz), 6.97 (d, 1H, N-H, J = 8.4 Hz).

m/z calculated: 523.37 *m/z* found: 523.1

Melting Point: 138-146 °C, decomposes

Preparation of 6-Bromohexanoyl amide azide (26) from 6-Bromohexanoyl amide (25).

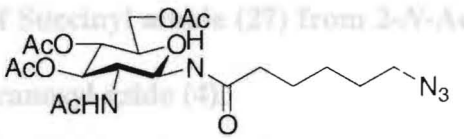

In a 250 mL round-bottom flask fitted with a septum and magnetic stir bar, 6-bromohexanoyl amide (**25**) (0.99 g, 1.892 mmol) was dissolved in DMF (15 mL). NaN_3 (0.620 g, 9.537 mmol) was added and the reaction was allowed to stir for 18 h when TLC (ethyl acetate) showed consumption of the starting material. CH_2Cl_2 (30 mL), 5% H_2SO_4 (30 mL), and water (30 mL) were added to the reaction and the organic layer was collected. The organic layer was washed with H_2O (100 mL) and was dried over anhydrous $MgSO_4$, evaporated, and then dissolved into methylene chloride (25 mL) again and washed with water (2 x 25 mL) again to remove residual DMF. The organic solution was again dried over anhydrous $MgSO_4$ and evaporated to give 0.359 g of product as a white solid in 39.1% yield.

^{1}H NMR ($CDCl_3$): δ 1.37 (m, 2H, -CH_2), 1.60 (m, 4H, -CH_2 x 2), 2.18 (m, 2H, -CH_2), 1.96 (s, 3H, -CH_3), 2.05 (s, 3H, -CH_3), 2.08 (s, 3H, -CH_3), 2.10 (s, 3H, -CH_3), 3.27 (t, 2H, N-CH_2, J = 7.1 Hz), 3.75 (ddd, 1H, H-5, J = 2.1, 4.6, 4 8 Hz), 4.10 (m, 2H, H-2, H-6) 4.31 (dd, 1H, H-6', J = 4.1, 12.4 Hz), 5.04 (m, 2H, H-1, H-3) 5.15 (t, 1H, H-4, J = 9.7 Hz), 5.95 (d, 1H, N<u>H</u>Ac, J = 8.2 Hz), 6.97 (d, 1H, N-H, J = 8.1 Hz).

m/z calculated: 485.49 *m/z* found: 508.2 (M + Na)

Melting Point: 167-169 °C, decomposes

Attempted Preparation of Succinyl amide (27) from 2-*N*-Acetyl-3,4,6-tri-*O*-acetyl-2-aminodeoxy-β-D-glucopyranosyl azide (4).

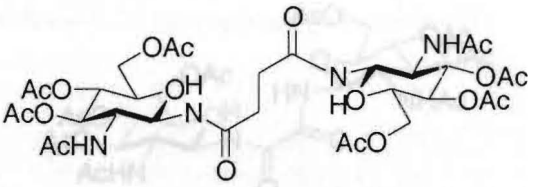

2-*N*-Acetyl-3,4,6-tri-*O*-acetyl-2-aminodeoxy-β-D-glucopyranosyl azide (**4**) (0.378 g, 1.02 mmol), succinyl chloride (0.22 mL, 2.00 mmol), and DPPE (0.265 g, 0.67 mmol) were reacted in THF according to the typical amide procedure. After extraction with $CHCl_3$ and washing with H_2O, the organic solution was evaporated to dryness; the residue proved to be only starting material by NMR spectroscopy.

Attempted Preparation of *p*-Toluenesulfonyl amide (28) from 2-*N*-Acetyl-3,4,6-tri-*O*-acetyl-2-aminodeoxy-β-D-glucopyranosyl azide (4).

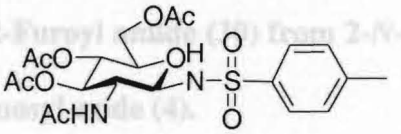

2-*N*-Acetyl-3,4,6-tri-*O*-acetyl-2-aminodeoxy-β-D-glucopyranosyl azide (**4**) (0.378 g, 1.02 mmol), *p*-toluenesulfonyl chloride (0.380 g, 1.99 mmol), and DPPE (0.262 g, 0.66 mmol) were reacted in THF according to the typical procedure. After extraction with

$CHCl_3$ and washing with H_2O, the organic layer was evaporated to dryness and the residue was found to be only starting material by NMR spectroscopy.

Attempted Preparation of Oxalyl amide (29) from 2-*N*-Acetyl-3,4,6-tri-*O*-acetyl-2-aminodeoxy-β-D-glucopyranosyl azide (4).

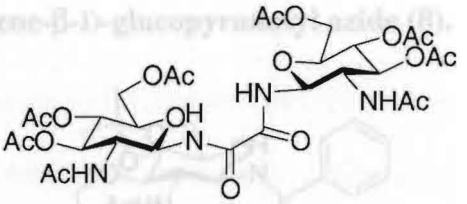

2-*N*-Acetyl-3,4,6-tri-*O*-acetyl-2-aminodeoxy-β-D-glucopyranosyl azide (**4**) (0.745 g, 2.00 mmol), oxalyl chloride (0.10 mL, 1.15 mmol), and DPPE (0.399 g, 1.00 mmol) were reacted in THF according to the typical procedure. After extraction with $CHCl_3$ and washing with H_2O, the organic layer was evaporated to dryness and column chromatography (ethyl acetate as eluent) was performed to afford only starting material by NMR spectroscopy.

Attempted Preparation of 2-Furoyl amide (30) from 2-*N*-Acetyl-3,4,6-tri-*O*-acetyl-2-aminodeoxy-β-D-glucopyranosyl azide (4).

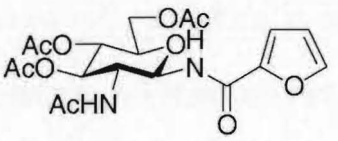

2-*N*-Acetyl-3,4,6-tri-*O*-acetyl-2-aminodeoxy-β-D-glucopyranosyl azide (**4**) (0.374 g, 1.00 mmol), 2-furoyl chloride (0.20 mL, 2.02 mmol), and DPPE (0.266 g, 0.67 mmol)

were reacted in THF according to the typical procedure. The crude product was purified with column chromatography (1:1, hexanes – ethyl acetate) to give a mixture containing starting material but not the desired product.

Attempted Preparation of Benzoyl amide (31) from 2-*N*-Acetyl-2-aminodeoxy-3-*O*-benzyl-4,6-*O*-isopropylidene-β-D-glucopyranosyl azide (8).

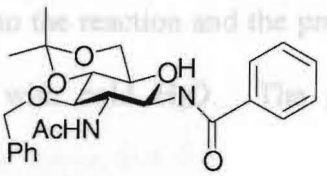

2-*N*-Acetyl-2-aminodeoxy-3-*O*-benzyl-4,6-*O*-isopropylidene-β-D-glucopyranosyl azide (**8**) (0.520 g, 1.381 mmol), benzoyl chloride (0.25 mL, 2.152 mmol), and DPPE (0.304 g, 0.763 mmol) were reacted in THF according to the typical procedure. Purification by column chromatography (ethyl acetate as eluent) afforded mostly starting material by NMR spectroscopy.

Typical procedure for the formation of triazoles from 2-*N*-Acetyl-3,4,6-tri-*O*-acetyl-2-aminodeoxy-β-D-glucopyranosyl azide (4).

The azide and an alkyne were suspended in a mixture of *t*-BuOH and water (1:1). An aqueous solution of ascorbic acid (1M) and an aqueous solution of $CuSO_4$ (1M) were added and the mixture was heated to 60 °C until TLC showed consumption of starting material. The mixture was allowed to cool to RT and most of the *t*-BuOH was removed *in vacuo*. Ice water was added to the reaction and the product was filtered off through a glass frit funnel and washed with cold H_2O. The product was then purified by recrystallization.

Preparation of bis(triazole) (37) from 1,3-Diethynylbenzene and 2-*N*-Acetyl-3,4,6-tri-*O*-acetyl-2-aminodeoxy-β-D-glucopyranosyl azide (4).

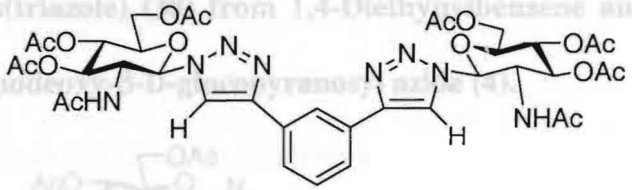

2-*N*-Acetyl-3,4,6-tri-*O*-acetyl-2-aminodeoxy-β-D-glucopyranosyl azide (**4**) (0.205 g, 0.5505 mmol) and 1,3-diethynyl benzene (0.09 mL, 0.6769 mmol) were dissolved in 5 mL of a *t*-BuOH and H_2O solution (1:1) according to the typical procedure. Ascorbic acid (0.15 mL of 1 M aqueous solution, 1.448 mmol) and copper sulfate (0.03 mL of 1 M aqueous solution, 0.1954 mmol) were added and the mixture was heated until TLC (ethyl acetate) showed consumption of starting material. Ice H_2O (15 mL) was added and the product filtered off to give 0.196 g of product as a crude white solid in 40.9% yield.

^{1}H NMR ($CDCl_3$): δ 1.58 (s, 3H, -CH_3), 1.78 (s, 3H, -CH3), 2.09 (s, 3H, -CH_3), 2.10 (s, 3H, -CH_3), 4.01 (ddd, 1H, H-5, *J* = 2.4, 5.1, 5.0 Hz), 4.16 (dd, 1H, H-6, *J* = 2.1, 12.6 Hz), 4.32 (dd, 1H, H-6', *J* = 5.0, 12.7 Hz), 4.65 (q, 1H, H-2, *J* = 10.0 Hz), 5.28 (t, 1H, H-4, *J* = 9.8 Hz), 5.44 (t, 1H, H-3, *J* = 9.9 Hz), 5.80 (d, 1H, N<u>H</u>Ac, *J* = 9.0 Hz), 7.39 (t, 1H, Ar-H, *J* = 7.7 Hz), 7.47 (d, 1H, Ar-H, *J* = 7.6 Hz), 7.84 (d, 1H, Ar-H, *J* = 7.9 Hz), 8.11 (s, 1H, triazole-H).

m/z calculated: 870.8 *m/z* found: 869.5

Melting Point: 341 °C, decomposes

Preparation of bis(triazole) (38) from 1,4-Diethynylbenzene and 2-*N*-Acetyl-3,4,6-tri-*O*-acetyl-2-aminodeoxy-β-D-glucopyranosyl azide (4).

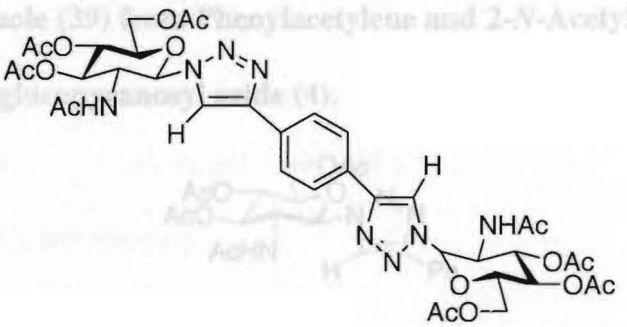

2-*N*-Acetyl-3,4,6-tri-*O*-acetyl-2-aminodeoxy-β-D-glucopyranosyl azide (**4**) (0.209 g, 0.5613 mmol) and 1,4-diethynylbenzene (0.072 g, 0.5707 mmol) were dissolved in 5 mL of a *t*-BuOH and H_2O solution (1:1) according to the typical procedure. Ascorbic

acid (0.15 mL of 1 M aqueous solution, 1.448 mmol) and copper sulfate (0.03 mL of 1 M aqueous solution, 0.1954 mmol) were added and the mixture heated until TLC (ethyl acetate) showed consumption of starting material. Ice H_2O (15 mL) was added and the product filtered off to give 0.261 g of product as an orange solid in 53.4% yield.

^{1}H NMR ($CDCl_3$): δ 1.59 (s, 3H, -CH_3), 1.96 (s, 3H, -CH_3), 2.00 (s, 3H, -CH_3), 2.02 (s, 3H, -CH_3),4.21 (m, 3H, H-5, H-6, H-6'), 4.64 (q, 1H, H-2, J = 9.8 Hz), 5.11 (t, 1H, H-4, J = 9.7 Hz), 5.39 (t, 1H, H-3, J = 9.8 Hz), 6.38 (m, 2H, H-1, N<u>H</u>Ac), 7.57 (d, 1H, N<u>H</u>Ac (monomer), J = 8.1 Hz), 7.84 (d, 2H, Ar-H (monomer), J = 8.6 Hz), 7.93 (s, 4H, Ar-H), 8.13 (d, 2H, Ar-H (monomer), J = 8.8 Hz), 8.91 (s, 1H, triazole-H), 8.93 (s, 1H, triazole-H (monomer))

Melting Point: 330 °C, decomposes

Preparation of triazole (39) from Phenylacetylene and 2-*N*-Acetyl-3,4,6-tri-*O*-acetyl-2-aminodeoxy-β-D-glucopyranosyl azide (4).

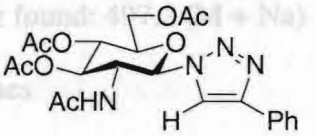

2-*N*-Acetyl-3,4,6-tri-*O*-acetyl-2-aminodeoxy-β-D-glucopyranosyl azide (**4**) (0.201 g, 0.5398 mmol) was dissolved in 5 mL of a *t*-BuOH and H_2O solution (1:1) and Phenyl acetylene (0.01 mL, 0.9085 mmol) was added according to the typical procedure. Ascorbic acid (0.15 mL of 1 M aqueous solution, 1.448 mmol) and copper sulfate (0.03

mL of 1 M aqueous solution, 0.1954 mmol) were added and the reaction was heated until TLC (ethyl acetate) showed consumption of starting material. Ice H_2O (15 mL) was added and the product filtered off as a white solid with a weight of 0.221 g in 86.0% yield.

^{1}H NMR ($CDCl_3$): δ 1.78 (s, 3H, -CH_3), 2.08 (s, 3H, -CH_3), 2.09 (s, 3H, -CH_3), 2.09 (s, 3H, -CH_3), 4.01 (ddd, 1H, H-5, J = 2.4, 5.1, 4.9 Hz), 4.16 (dd, 1H, H-6, J = 2.2, 12.5 Hz), 4.32 (dd, 1H, H-6', J = 4.9, 12.7 Hz), 4.66 (q, 1H, H-2, J = 9.9 Hz), 5.28 (t, 1H, H-4, J = 9.6 Hz), 5.46 (t, 1H, H-3, J = 9.9 Hz), 5.83 (d, 1H, N<u>H</u>Ac, J = 9.2 Hz), 6.04 (d, 1H, H-1, J = 10.1 Hz), 7.35 (t, 1H, Ar-H, J = 7.4 Hz), 7.43 (t, 2H, Ar-H, J = 7.4 Hz), 7.84 (d, 2H, Ar-H, J = 7.1 Hz), 8.09 (s, 1H, triazole-H).

^{13}C NMR ($CDCl_3$): δ 20.14 (double intensity), 20.24, 22.24, 51.99, 61.28, 67.69, 72.12, 73.95, 85.20, 118.03, 125.09 (double intensity), 127.62, 128.12 (double intensity), 129.53, 146.92, 168.62, 169.39, 169.71, 169.73.

m/z calculated: 474.5 *m/z* found: 497.2 (M + Na)

Melting Point: 270 °C, decomposes

References:

1. El Khadem, H. S. *Carbohydrate Chemistry: Monosaccharides and Their Oligomers*; Academic Press: San Diego, 1988; pp.1-5, 7.
2. Bols, M. *Carbohydrate Building Blocks*; John Wiley & Sons, Inc.: New York, 1996; pp.1-2, 11.
3. Collins, P., Ferrier, R. *Monosaccharides: Their Chemistry and Their Roles in Natural Products*; John Wiley & Sons: New York, 1995.
4. Barton, D.H.R. *Experientia*, **1950**, *6*, 316-320.
5. Eliel, E.L. *Conformational Analysis*, Wiley-Interscience, New York, 1965.
6. Bochkov, A. F., Zaikov, G. E. *Chemistry of the O-Glycosidic Bond*. Pergamon Press, Oxford, 1979, pp.11-16.
7. Augestad, I., Berner, E. *Acta. Chem. Scand.* **1954**, *8*, 251-256.
8. Mowery Jr., D. F. *Methods Carbohydr. Chem.* **1963**, *2*, 328-331.
9. O'Riordan, K.; Lee, J. C. *J. Clin. Microbiol. Rev.* **2004**, *17*, 218-234.
10. Lowy, F. D. *N. Engl. J. Med.* **1998**, *339*, 520-532.
11. Archer, G. L. *Clin. Infect. Dis.* **1998**, *26*, 1179-1181.
12. *Staphylococcus aureus: Infection and Disease*; Honeyman, A., Friedman, H., Bendinelli, M., Eds.; Plenum Publishers: New York, 2001.
13. Alexander, E.; Hudson, M. *Appl. Microbiol. Biotechnol.* **2001**, *56*, 361-366.
14. Potter, K. N., Li, Y., Pascual, V., Capra, J.D. *Infect. Immun.* **1997**, *14*, 291-308.
15. Enright, M. *Curr. Opin. Pharmacol.* **2003**, *3*, 474-479.

16. Wladvogel, F. A. *Staphylococcus aureus in: Principles and Practice of Infectious Diseases*, Mandell, G.L., Bennett, J.E., Dolan, R. eds. Churchill Livingstone, New York, 1995; pp.1754-1777.

17. Miller, L. G., Perdreau-Remington, F., Rieg, G., Mehdi, S., Perlroth, J., Bayer, A., Tang, A. W., Phung, T. O., Spellberg, B. *N. Engl. J. Med.* **2005**, *352*, 1445-1453.

18. Hochkeppel, H. K., Braun, D. G., Vischer, W., Imm, A., Sutter, S., Staeubli, U., Guggenheim, R., Kaplan, E. L., Boutonnier, A., Fournier, J. M. *J. Clin. Microbiol.* **1987**, *25*, 526-530.

19. Fattom, A.; Horwith, G.; Fuller, S.; Propst, M.; Naso, R. *Vaccine* **2004**, *22*, 880-887.

20. Stein, R. "Dangerous Germ Becoming More Common." *Washington Post*, April 7, 2005, p A11.

21. Fridkin, S. K., Hageman, J. C., Morrison, M., Sanza, L. T., Como-Sabetti, K., Jernigan, J. A., Harriman, K., Harrison, L. H., Lynfield, R., Farley, M. M. *N. Engl. J. Med.* **2005**, *352*, 1436-1444.

22. Cosgrove, S. E., Sakoulas, G., Perencevich, E. N., Schwaber, M. J., Karchmer, A. W., Carmeli, Y. *Clin. Infect. Dis.* **2003**, *36*, 53-59.

23. Chambers, H. F. *Emerg. Infect. Dis.* **2001**, *7*, 178-182.

24. Kneidinger, B.; O'Riordan, K.; Li, J.; Brisson, J.; Lee, J.; Lam, J. *J. Biol. Chem.* **2003**, *278*, 3615-3627.

25. Sompolinsky, D., Samra, Z., Karakawa, W. W., Vann, W. F., Schneerson, R., Malik, Z. *J. Clin. Microbiol.* **1985**, *22*, 828-834.

26. Albus, A. Fournier, J.M., Wolz, C., Boutonnier, A., Ranke, M., Hoiby, N., Hochkeppel, H., Doring, G. *J. Clin. Microbiol.* **1988**, *26*, 2505-2509.

27. Arbeit, R. D., Karakawa, W. W., Vann, W. F., Robbins, J. B. *Diagn. Microbiol. Infect. Dis.* **1984**, *2*, 85-91.

28. Karakawa, W. W., Sutton, A., Schneerson, R., Karpas, A., Vann, W. F. *Infect. Immun.* **1988**, *56*, 1090-1095.

29. Karakawa, W. W., Vann, W. F. *Semin. Infect. Dis.* **1982**, *4*, 285-293.

30. Poutrel, B., Boutonnier, A., Sutra, L., Fournier, J. M. *J. Clin. Microbiol.* **1988**, *26*, 38-40.

31. Ohlsen, K., Koller, K. P., Hacker, J. *Infect. Immun.* **1997**, *65*, 3606-3614.

32. Illarionov, P.; Torgov, V.; Hancock, I.; Shibaev, V. *Russ. Chem. Bull.* **2001**, *181*, 1303-1308.

33. Wilkinson, B. J. *Staphylococci and staphylococcal infections*; Academic Press: New York, 1983.

34. Fournier, J. M., Vann, W. F., Karakawa, W. W. *Infect. Immun.* **1984**, *45*, 87-93.

35. Hanessian, S., Haskell, T. H. *J. Biol. Chem.* **1964**, *239*, 2758-2764.

36. Moreau, M. Richards, J.C., Fournier, J.M., Byrd, R.A. Karakawa, W.W., Vann, W.F. *Carbohydr. Res.* **1990**, *201*, 285-297.

37. Murthy, S. V., Melly, M. A., Harris, T. M., Hellerqvist, C. G., Hash, J. H. *Carbohydr. Res.* **1983**, *201*, 113-123.

38. Sau, S., Bagga, N., Wann, E. R., Lee, J. C., Foster, T. J., Lee, C. Y. *Microbiology* **1997**, *143*, 2395-2405.

39. Horton, D.; Saeki, H. *Carbohydr. Res.* **1978**, *63*, 270-276.

40. Garcia-Lopez, J. J., Santoyo-Gonzalez, F., Vargas-Berenguel, A., Gimenez-Martinez, J. J. *Chem. Eur. J.* **1999**, *5*, 1775-1784.

41. Horton, D. *Org. Synth. Coll.* **1966**, *46*, 1-5.

42. Roth, W., Pigman, W. *J. Am. Chem. Soc.* **1960**, *82*, 4608-4611.

43. Baker, B. R., Joseph, J. P., Schaub, R. E., Williams, J. H. *J. Org. Chem.* **1954**, *19*, 1786-1792.

44. Brase, S. Gil, C., Knepper, K., Zimmermann, V. *Angew. Chem. Int. Ed.* **2005**, *44*, 5188-5240.

45. Kovac, P., Edgar, K. J. *J. Org. Chem.* **1992**, *57*, 2455-2467.

46. Mulard, L. A., Costachel, C., Sansonetti, P. J. *J. Carbohydr. Chem.* **2000**, *19*, 849-877.

47. Emmerson, D. P. G., Hems, W. P., Davis, B. G. *Tetrahedron: Asymmetry* **2005**, *16*, 213-221.

48. Knirel, Y. A., Paramonov, N. A., Vinogradov, E. V., Shashkov, A. S., Dmitriev, B. A., Kochetkov, N. K., Kholodkova, E. V., Stanislavsky, E. S. *Eur. J. Biochem.* **1987**, *167*, 549-561.

49. Root, Y. Y., Bailor, M. S., Norris, P. *Synth. Commun.* **2004**, *34*, 2499-2506.

50. Temelkoff, D. P. Approaches to the efficient synthesis of N-glycosyl amides and triazoles. M.S. Thesis, Youngstown State University, Youngstown, OH, August 2005.

51. Pleuss, N. Kunz, H. *Synthesis* **2005**, *1*, 122-130.

52. Temelkoff, D. P., Smith, C. R., Kibler, D. A., McKee, S., Duncan, S. J., Zeller, M., Hunsen, M., Norris, P. *Carbohydr. Res.* **2006**, *341*, 1645-1656.

53. Rostovtsev, V. V., Green, L. G., Fokin, V. V., Sharpless, K. B. *Angew. Chem. Int. Ed.* **2002**, *41*, 2596-2599.

54. Wu, P., Feldman, A. K., Nugent, A. K., Hawker, C. J., Scheel, A., Voit, B., Pyun, J., Frechet, J. M. J., Sharpless, K. B., Fokin, V. V. *Agnew. Chem. Int. Ed.* **2004**, *43*, 3928-3932.

55. Freeze, S., Norris, P. *Heterocycles* **1999**, *51*, 1807-1817.

56. Kolb, H.; Sharpless, K. B. *Drug Discovery Today* **2003**, *8*, 1128-1137.

57. Akula, R. A., Temelkoff, D. P., Artis, N. D., Norris, P. *Heterocycles* **2004**, *63*, 2719-2725.

58. Miner, P. L., Wagner, T. R., Norris, P. *Heterocycles* **2005**, *65*, 1035-1049.

Appendix A

Appendix A

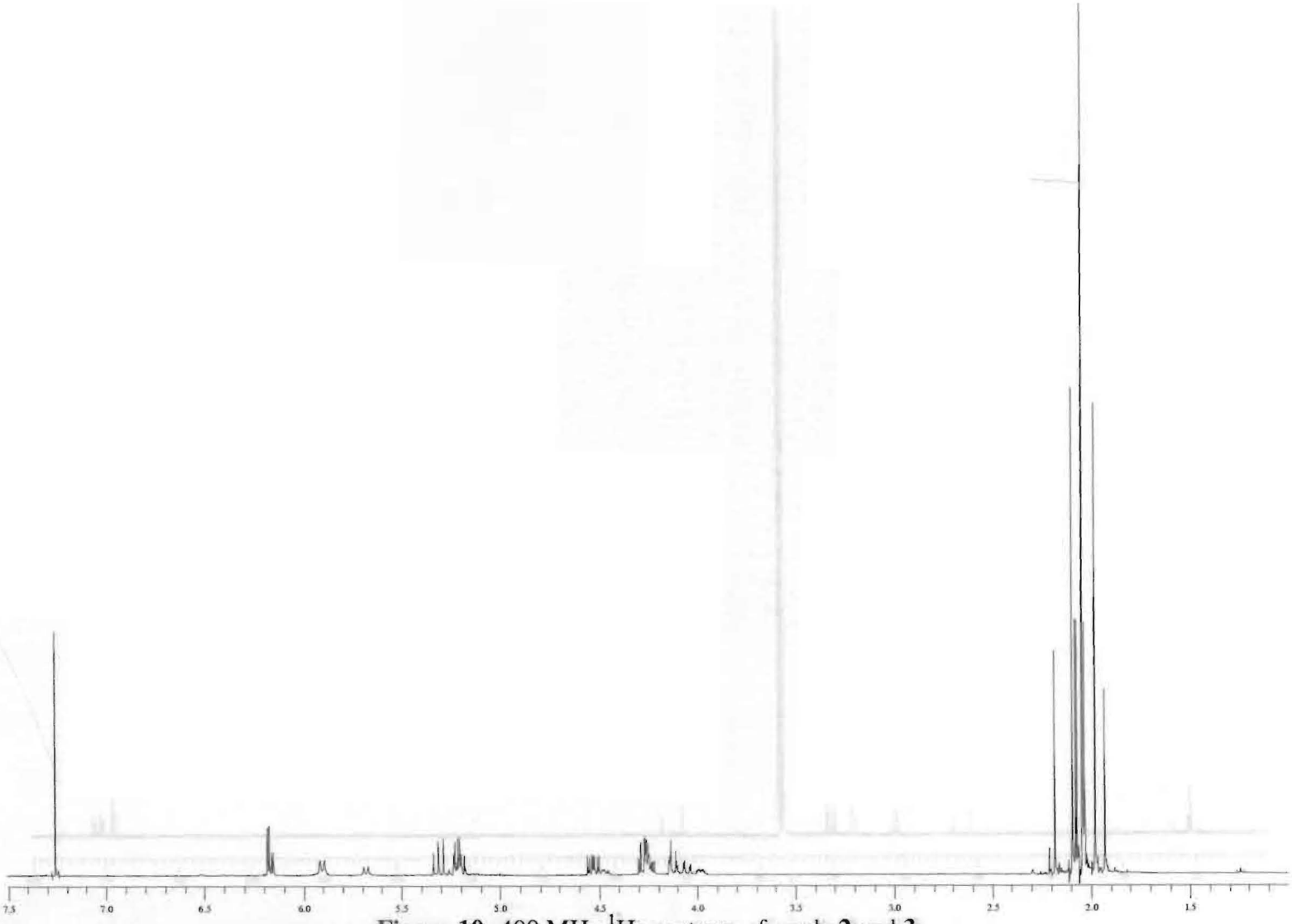

Figure 10: 400 MHz ^{1}H spectrum of crude **2** and **3**

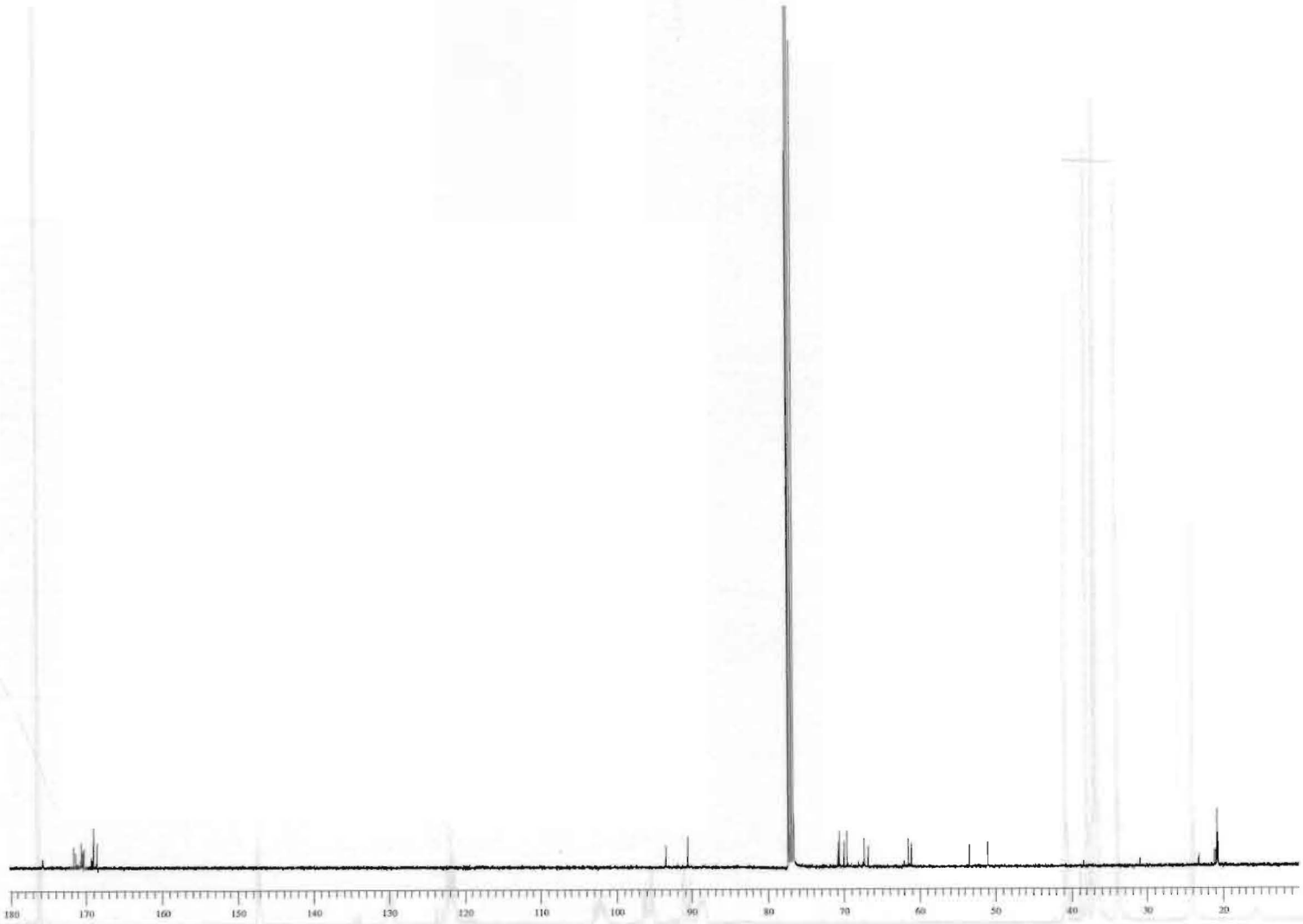

Figure 11: 100 MHz ^{13}C spectrum of crude **2** and **3**

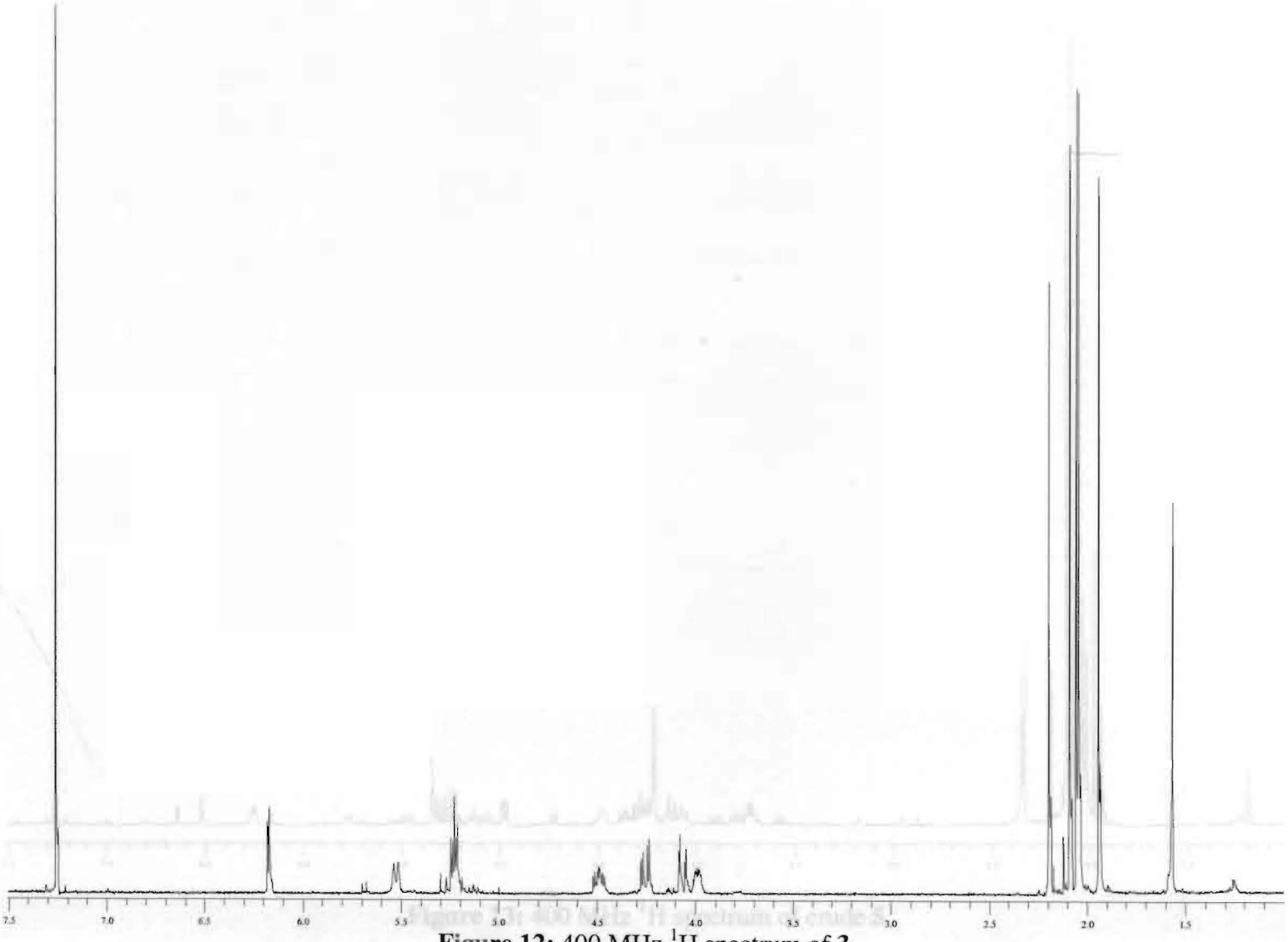

Figure 12: 400 MHz ^{1}H spectrum of **3**

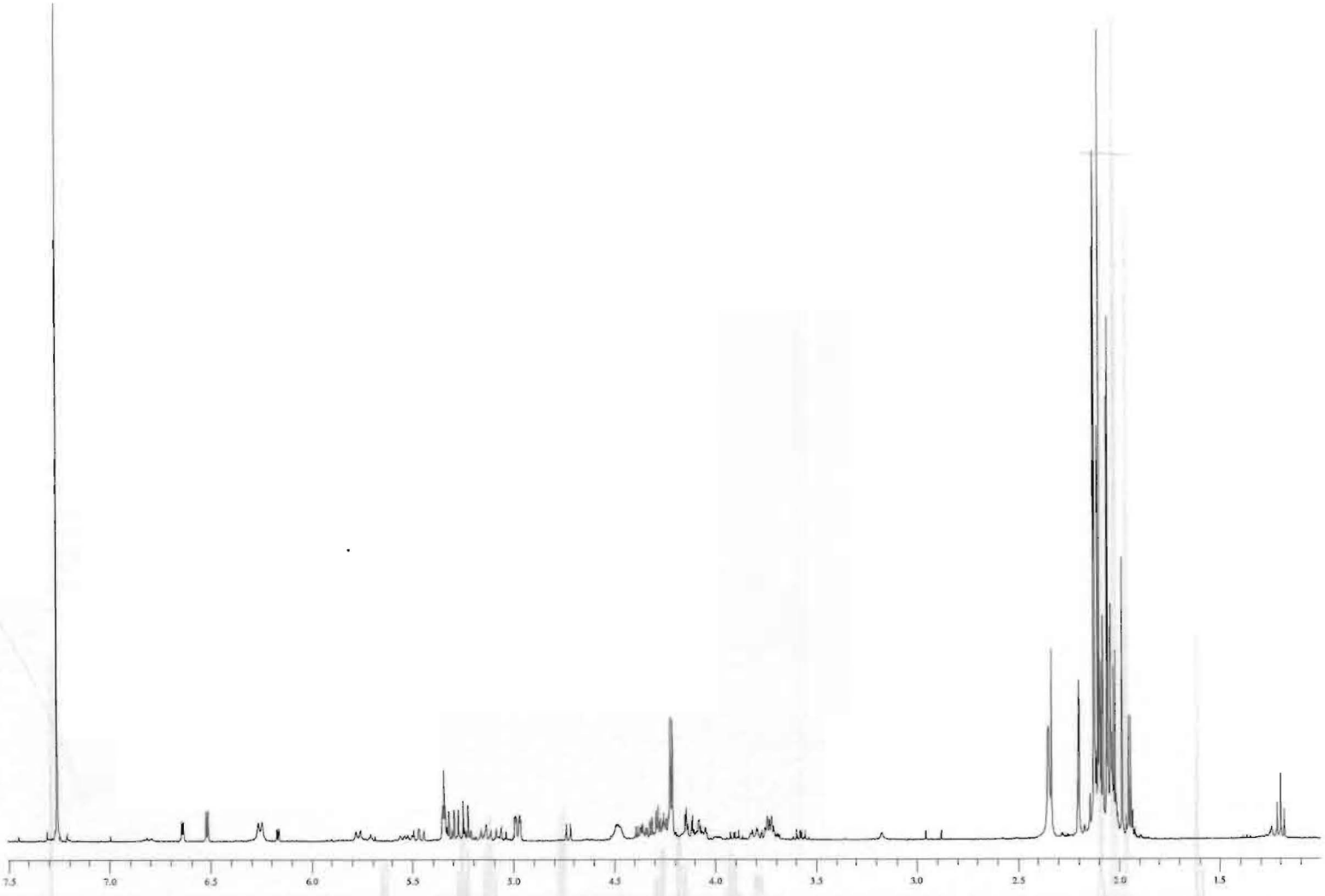

Figure 13: 400 MHz ^{1}H spectrum of crude **5**

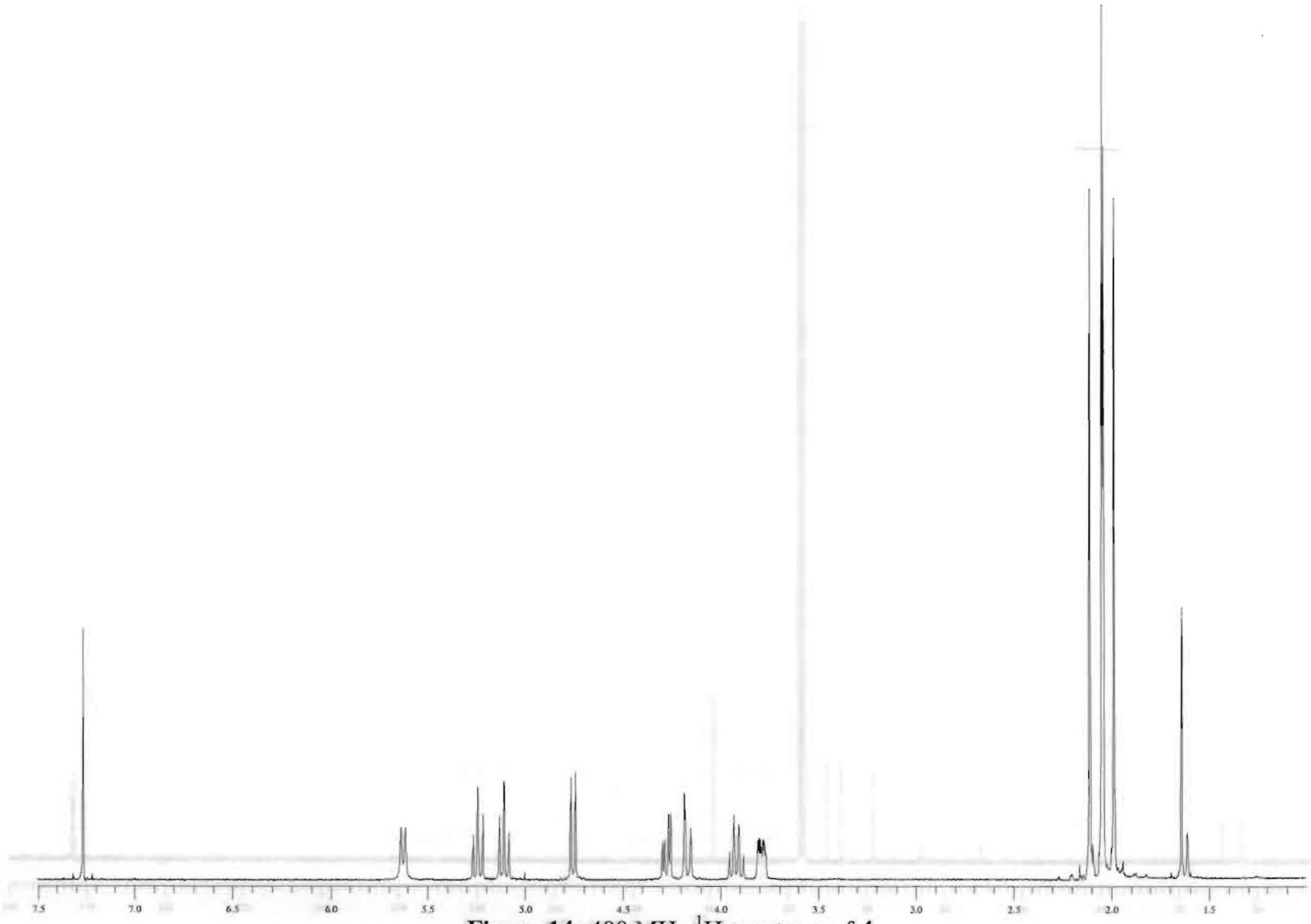

Figure 14: 400 MHz ^{1}H spectrum of **4**

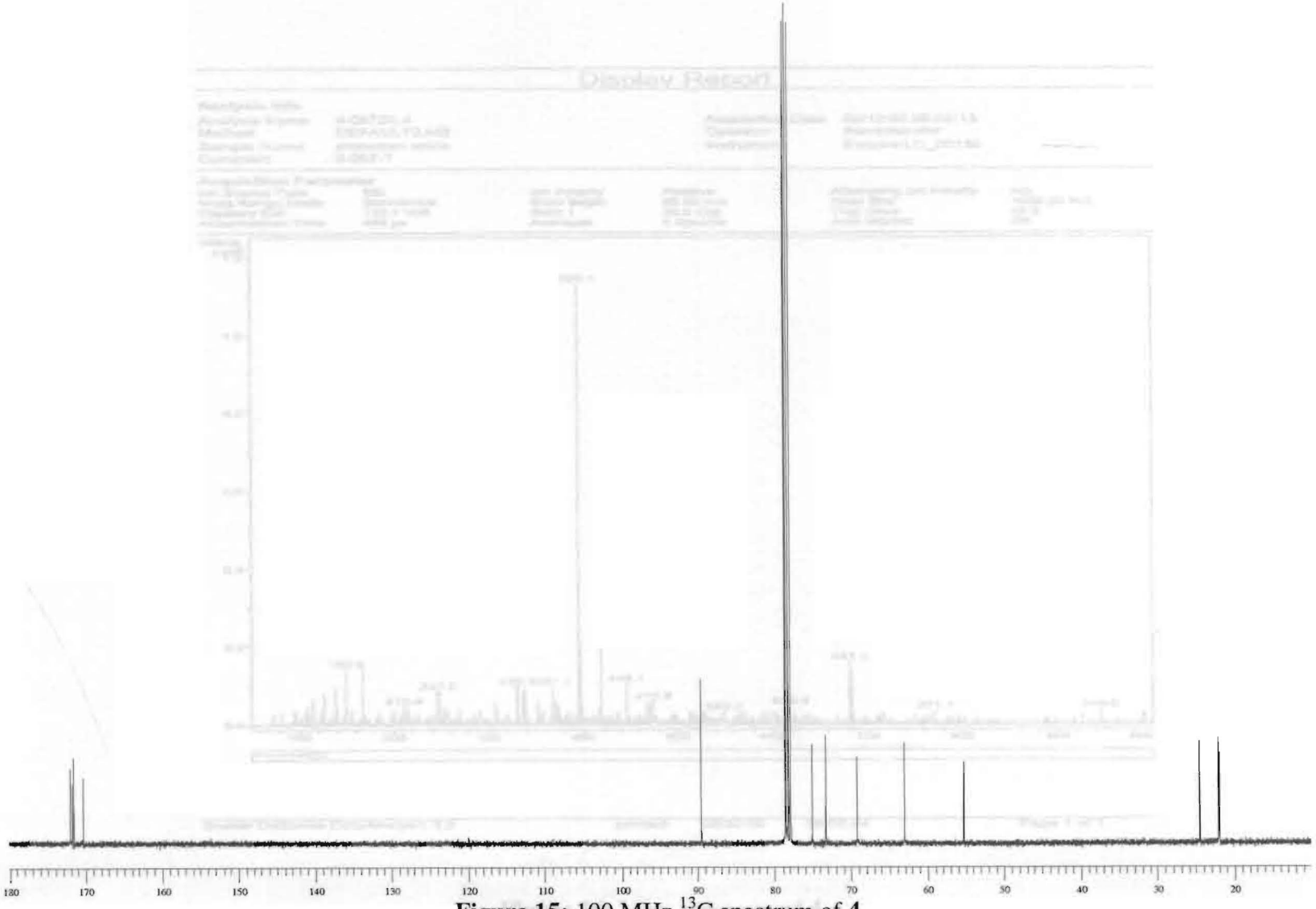

Figure 15: 100 MHz ^{13}C spectrum of **4**

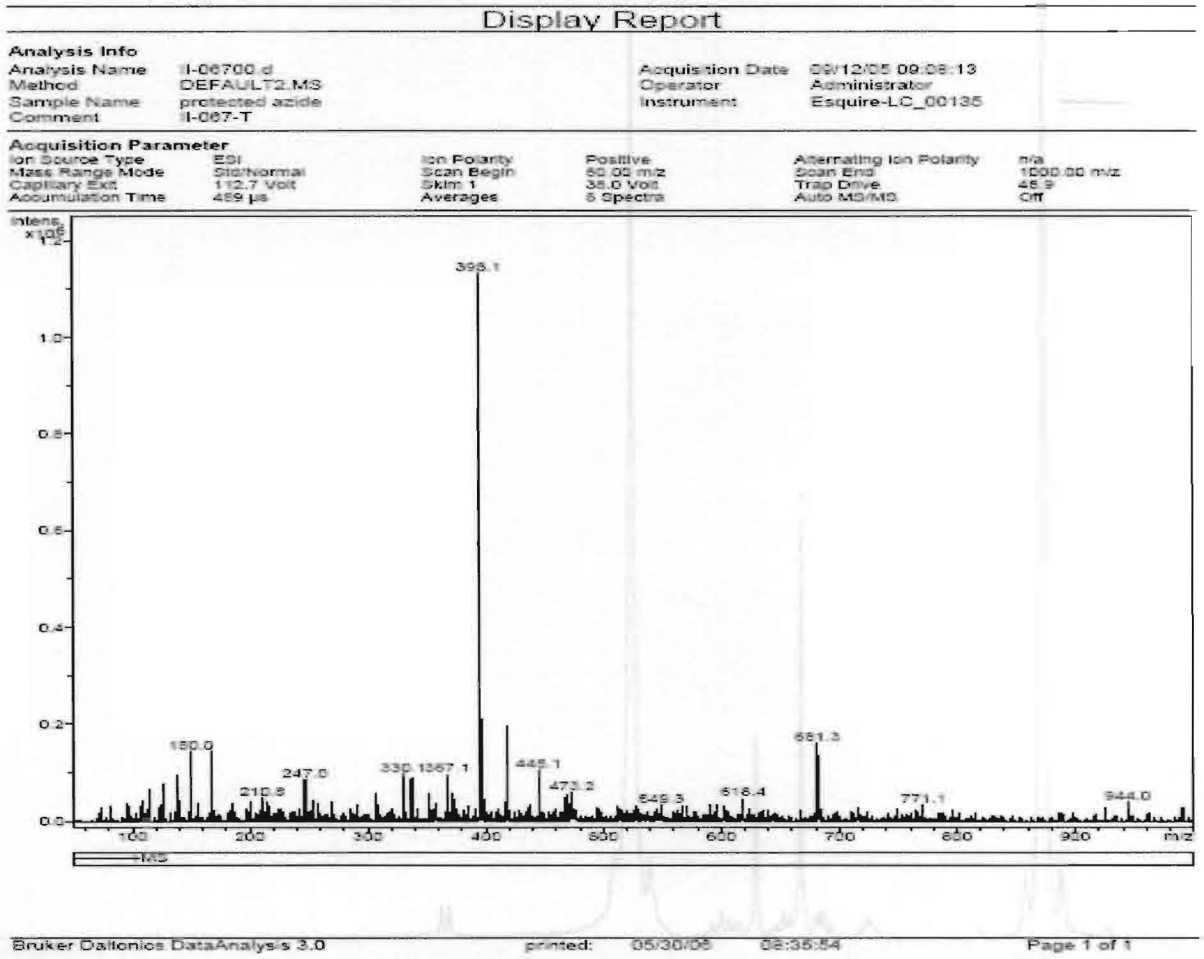

Figure 16: Mass spectrum of **4**

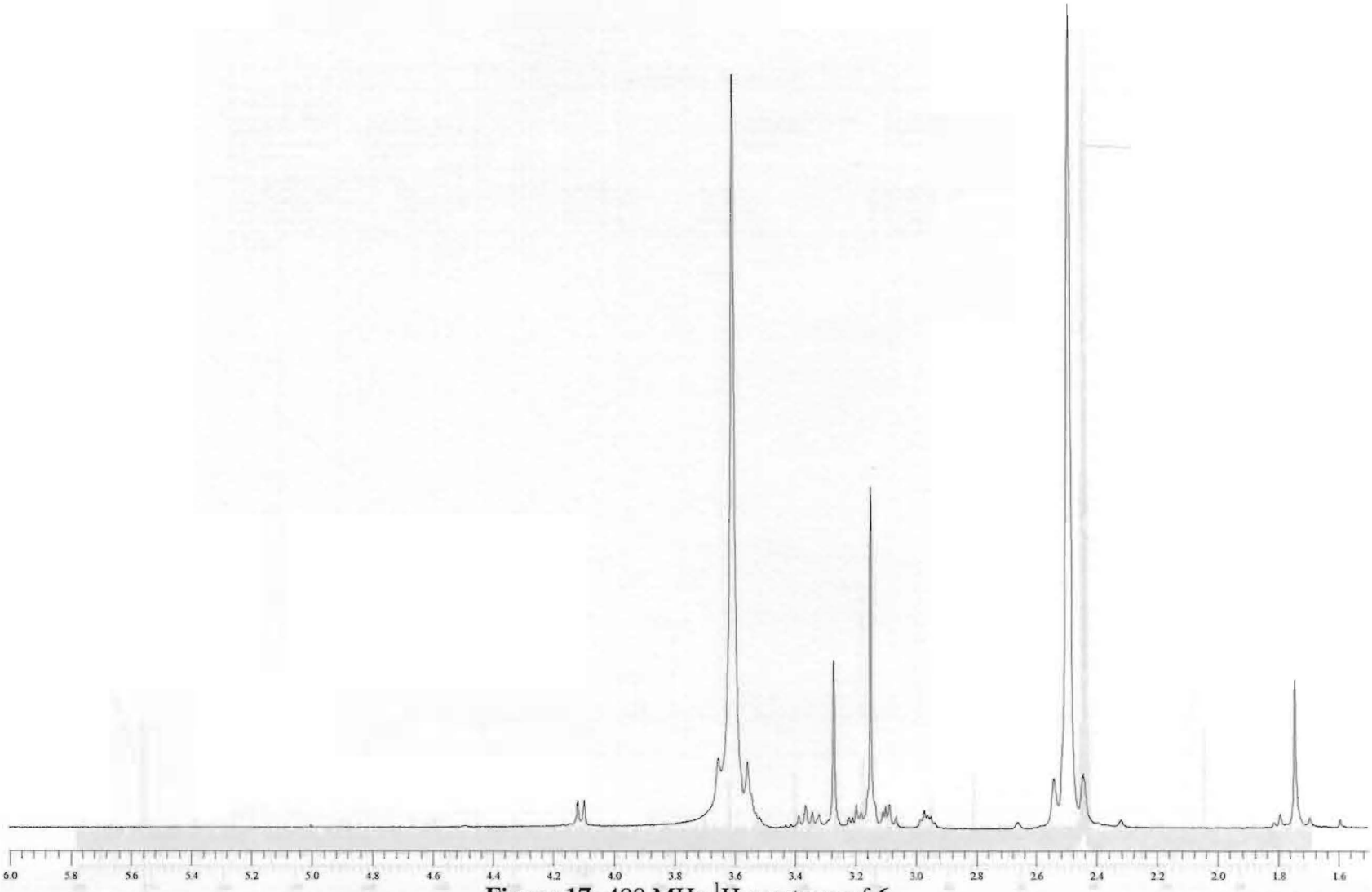

Figure 17: 400 MHz ^{1}H spectrum of **6**

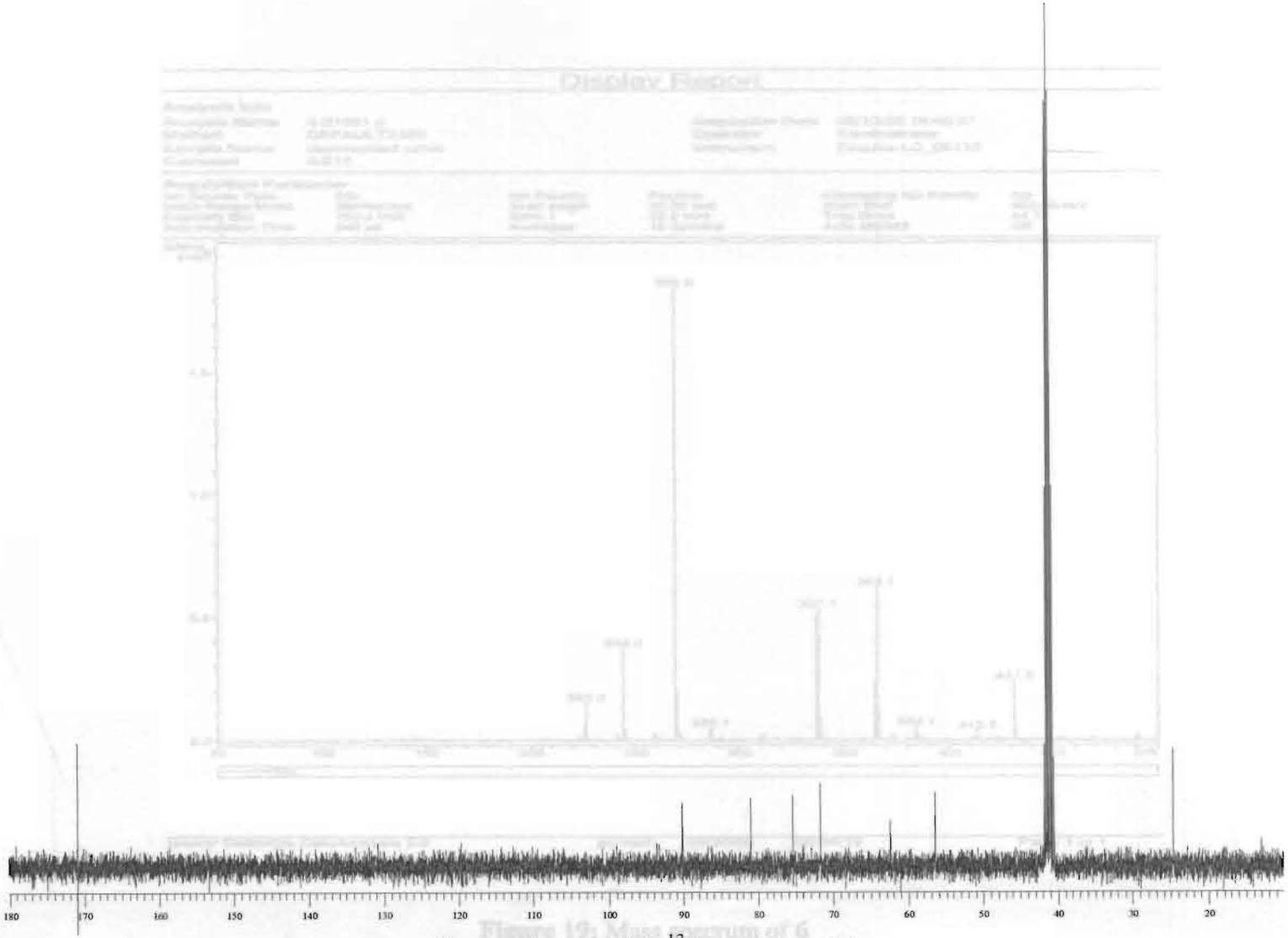

Figure 18: 100 MHz ^{13}C spectrum of **6**

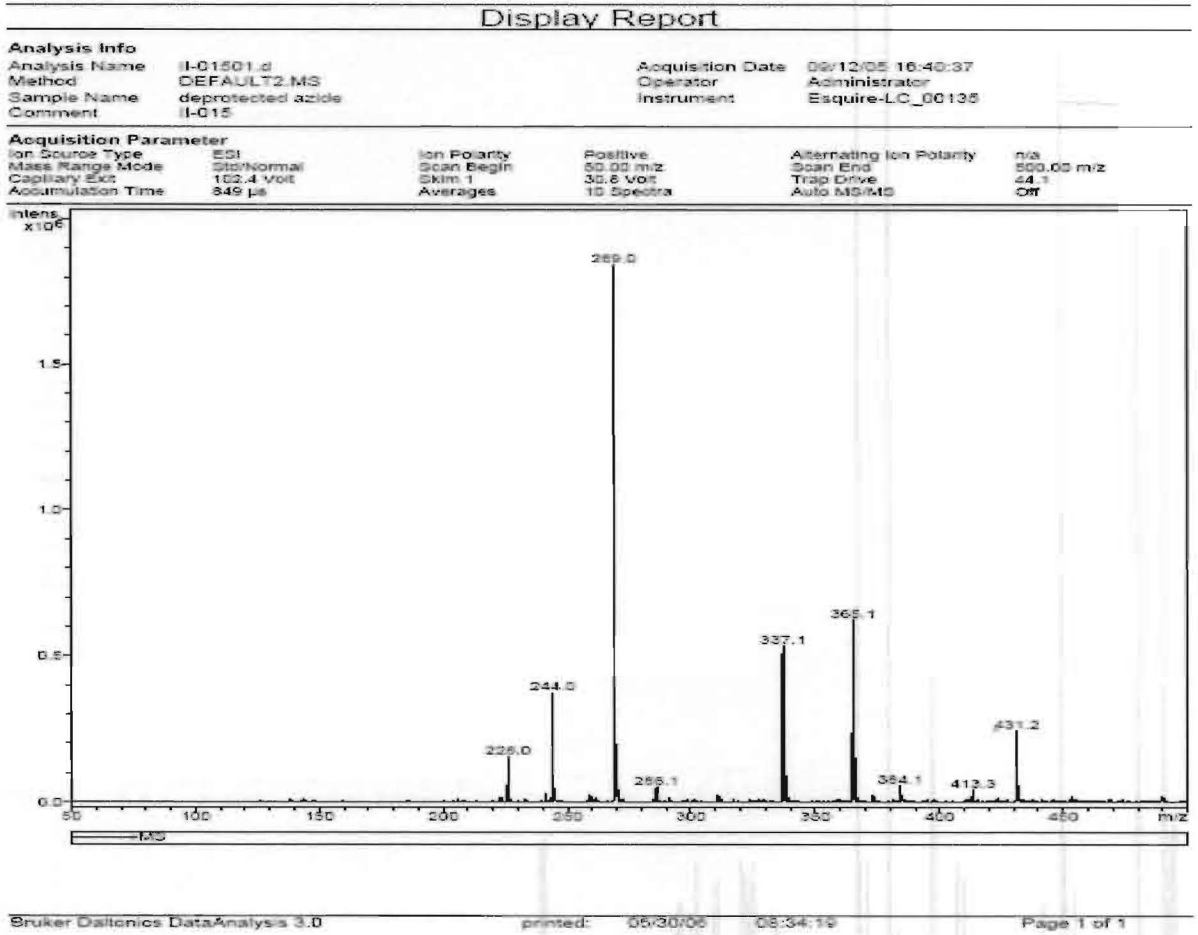

Figure 19: Mass specrum of **6**

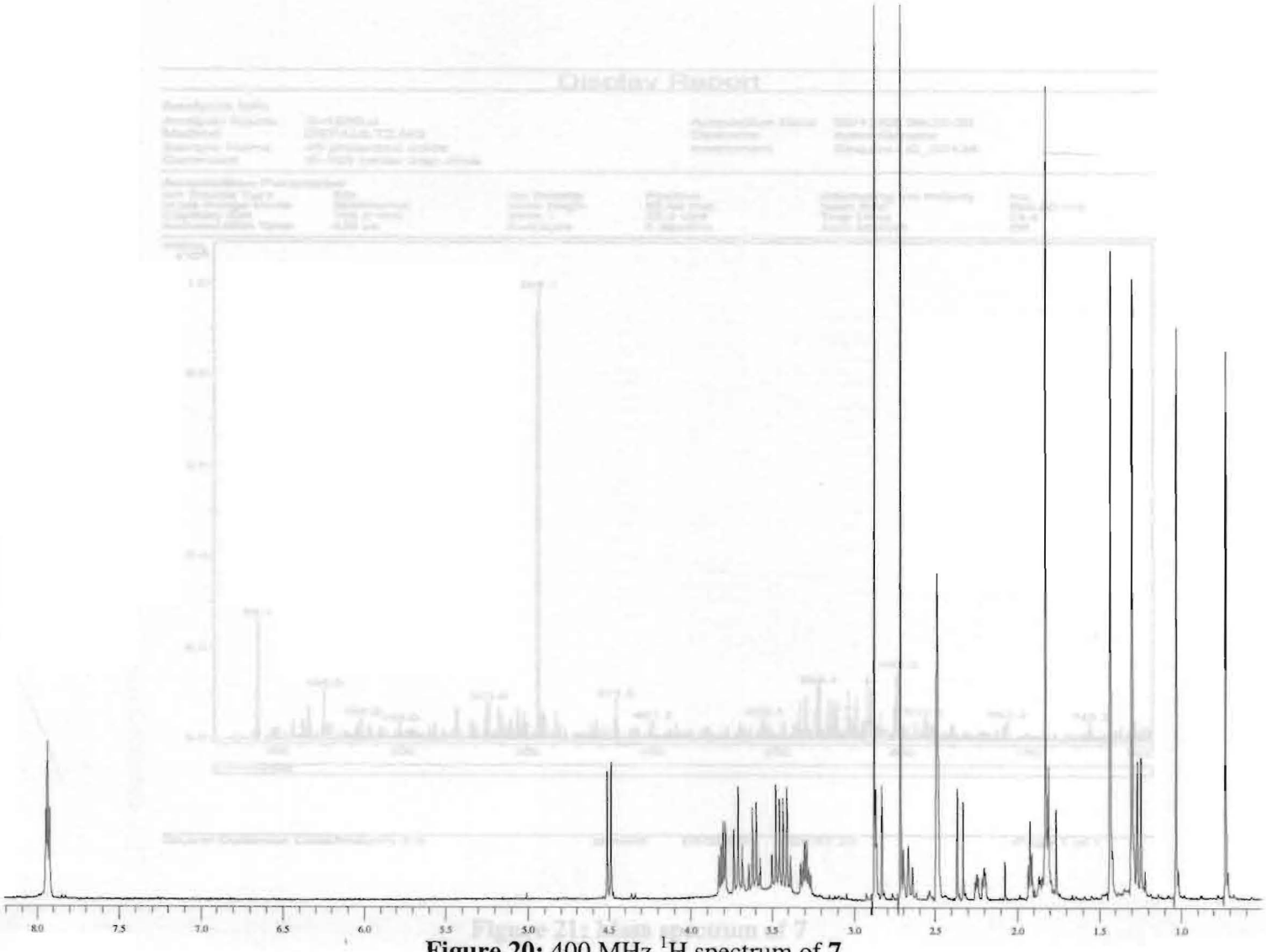

Figure 20: 400 MHz ^{1}H spectrum of **7**

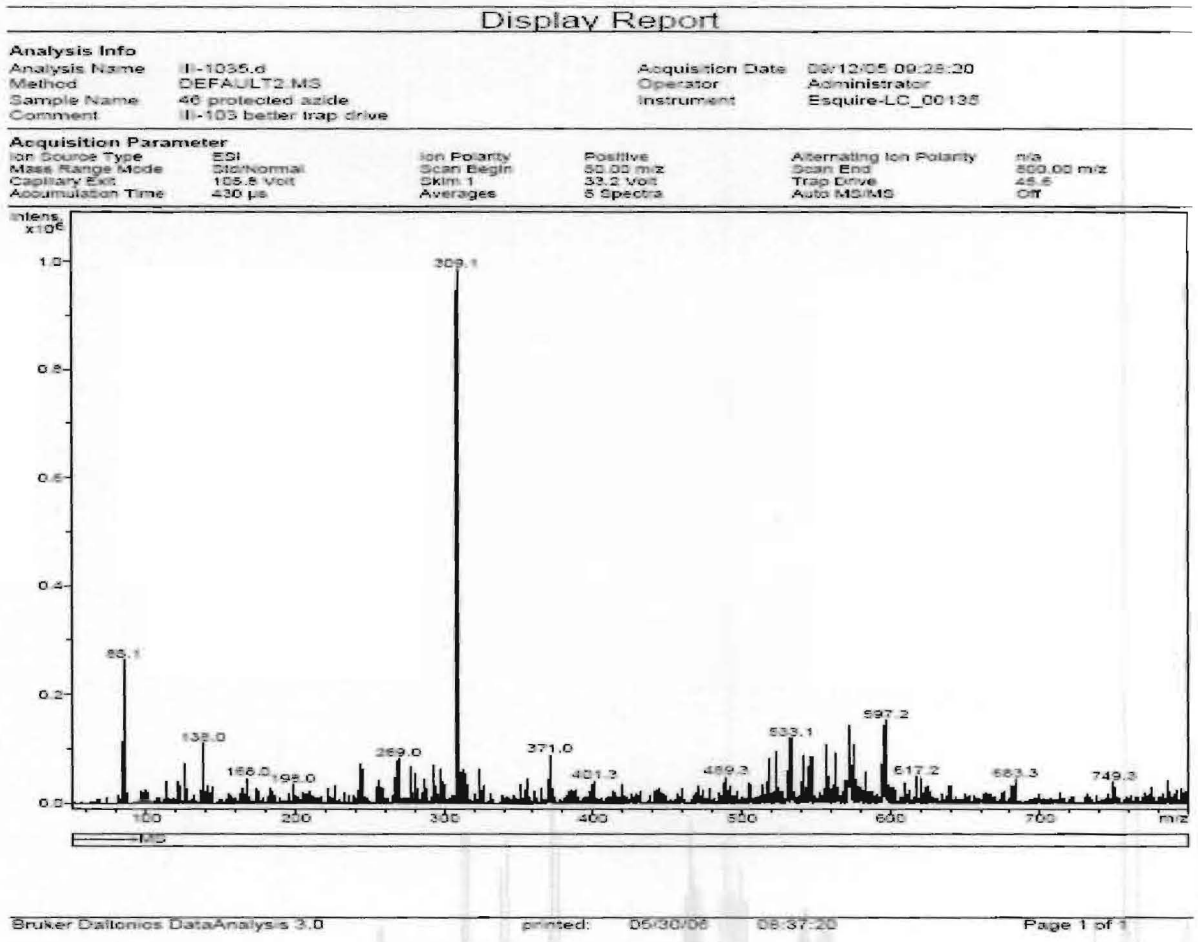

Figure 21: Mass spectrum of **7**

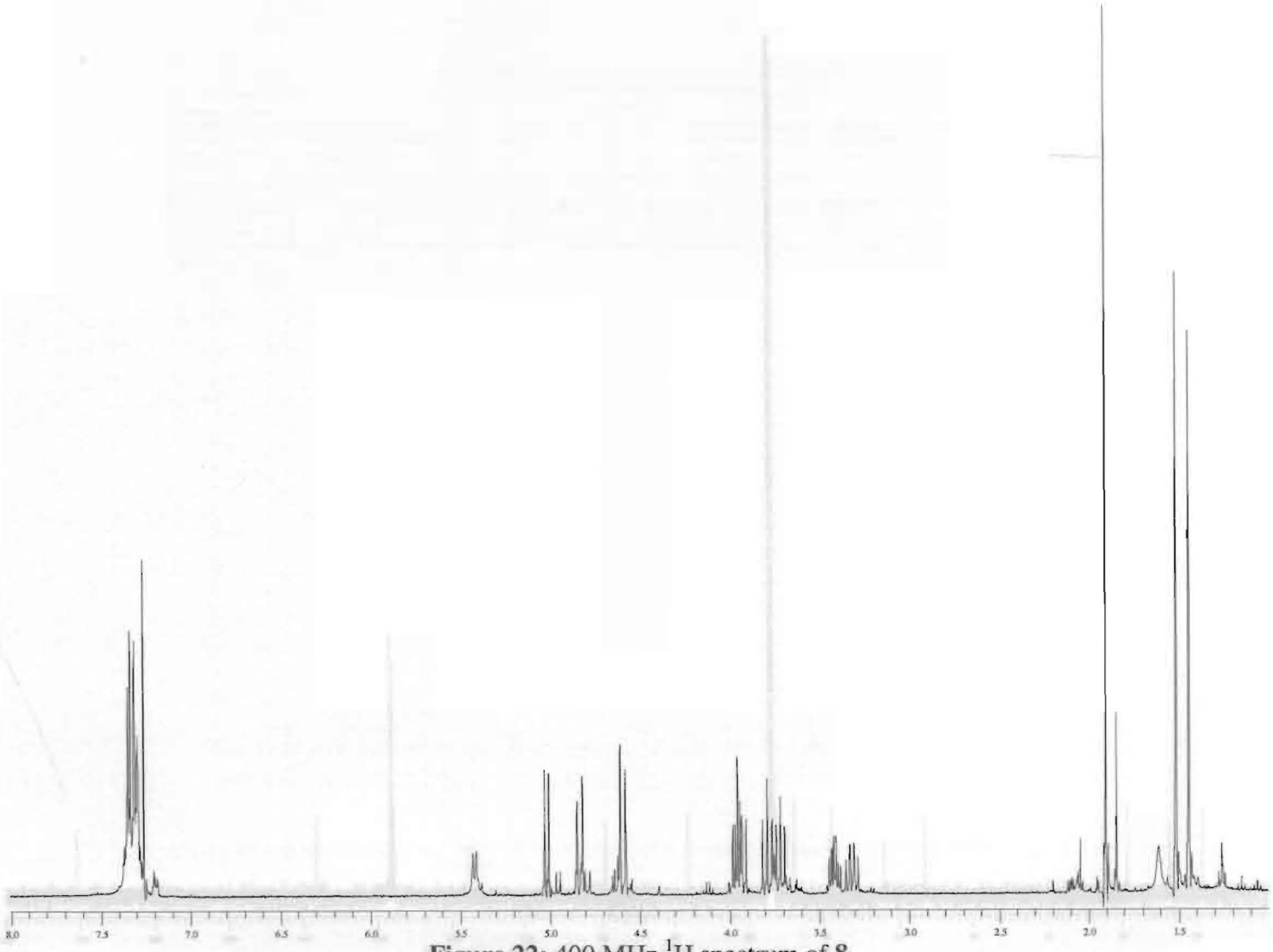

Figure 22: 400 MHz ^{1}H spectrum of **8**

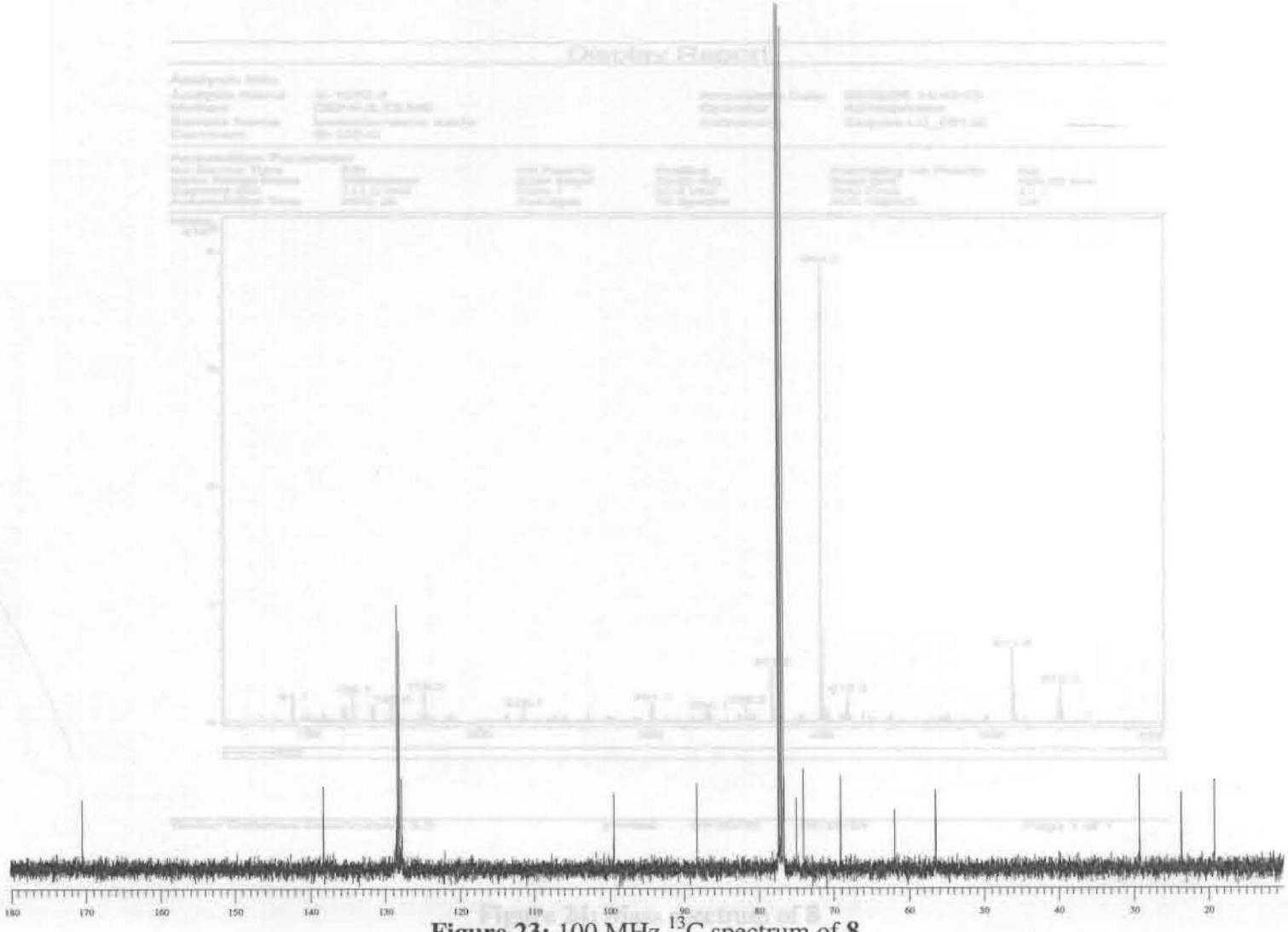

Figure 23: 100 MHz ^{13}C spectrum of **8**

Display Report

Analysis Info

Analysis Name	II-1050.d	Acquisition Date	09/09/05 14:49:03
Method	DEFAULT2.MS	Operator	Administrator
Sample Name	bromobenzene azide	Instrument	Esquire-LC_00135
Comment	II-105-C		

Acquisition Parameter

Ion Source Type	ESI	Ion Polarity	Positive	Alternating Ion Polarity	n/a
Mass Range Mode	Std/Normal	Scan Begin	50.00 m/z	Scan End	600.00 m/z
Capillary Exit	111.2 Volt	Skim 1	37.0 Volt	Trap Drive	41.1
Accumulation Time	2978 µs	Averages	10 Spectra	Auto MS/MS	Off

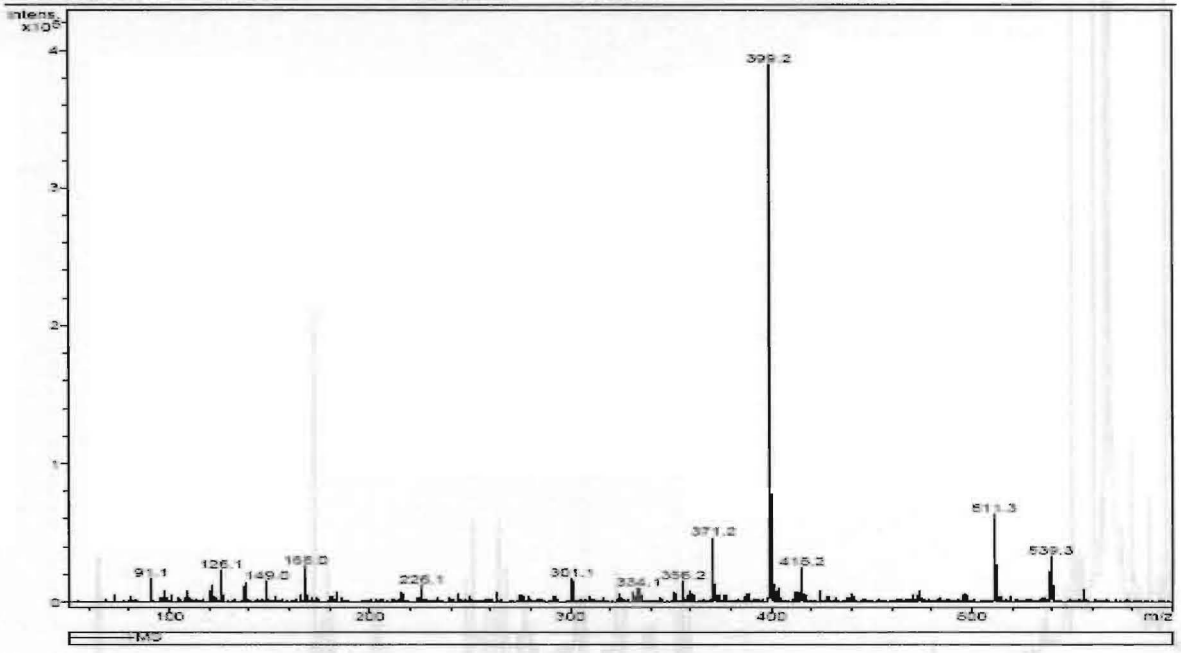

Bruker Daltonics DataAnalysis 3.0 printed: 05/30/06 08:38:24 Page 1 of 1

Figure 24: Mass spectrum of **8**

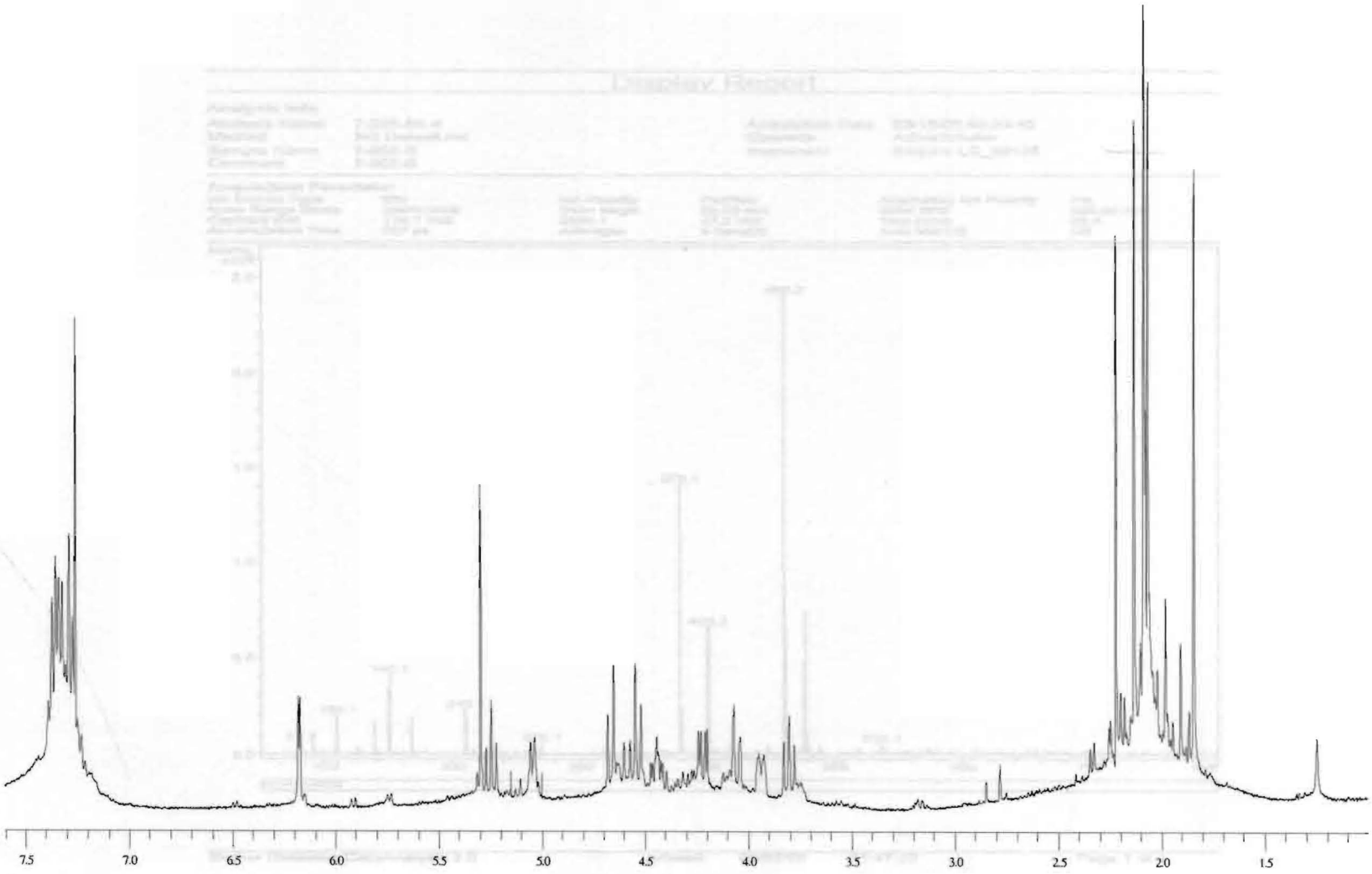

Figure 25: 400 MHz ^{1}H spectrum of **10**

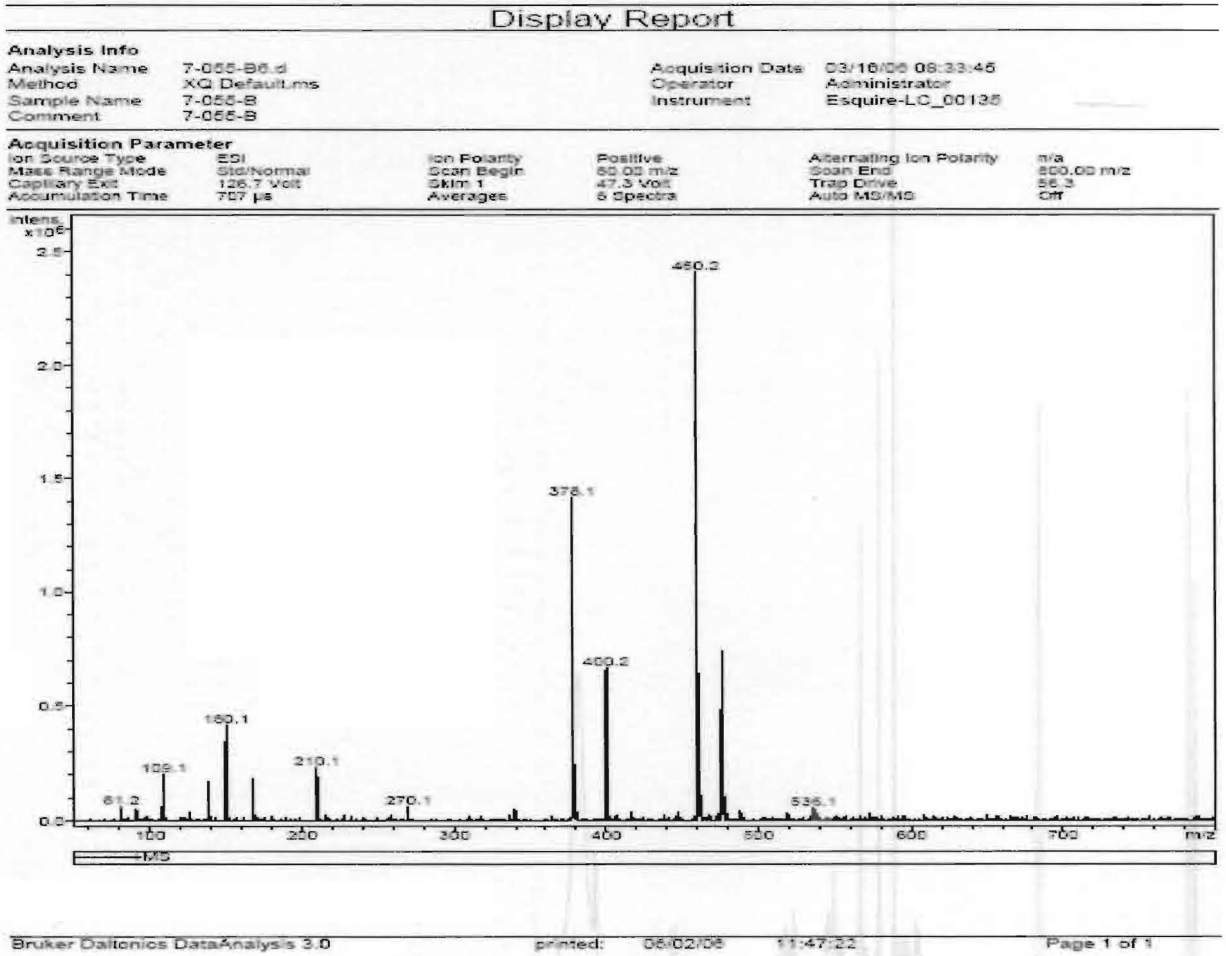

Figure 26: Mass spectrum of **10**

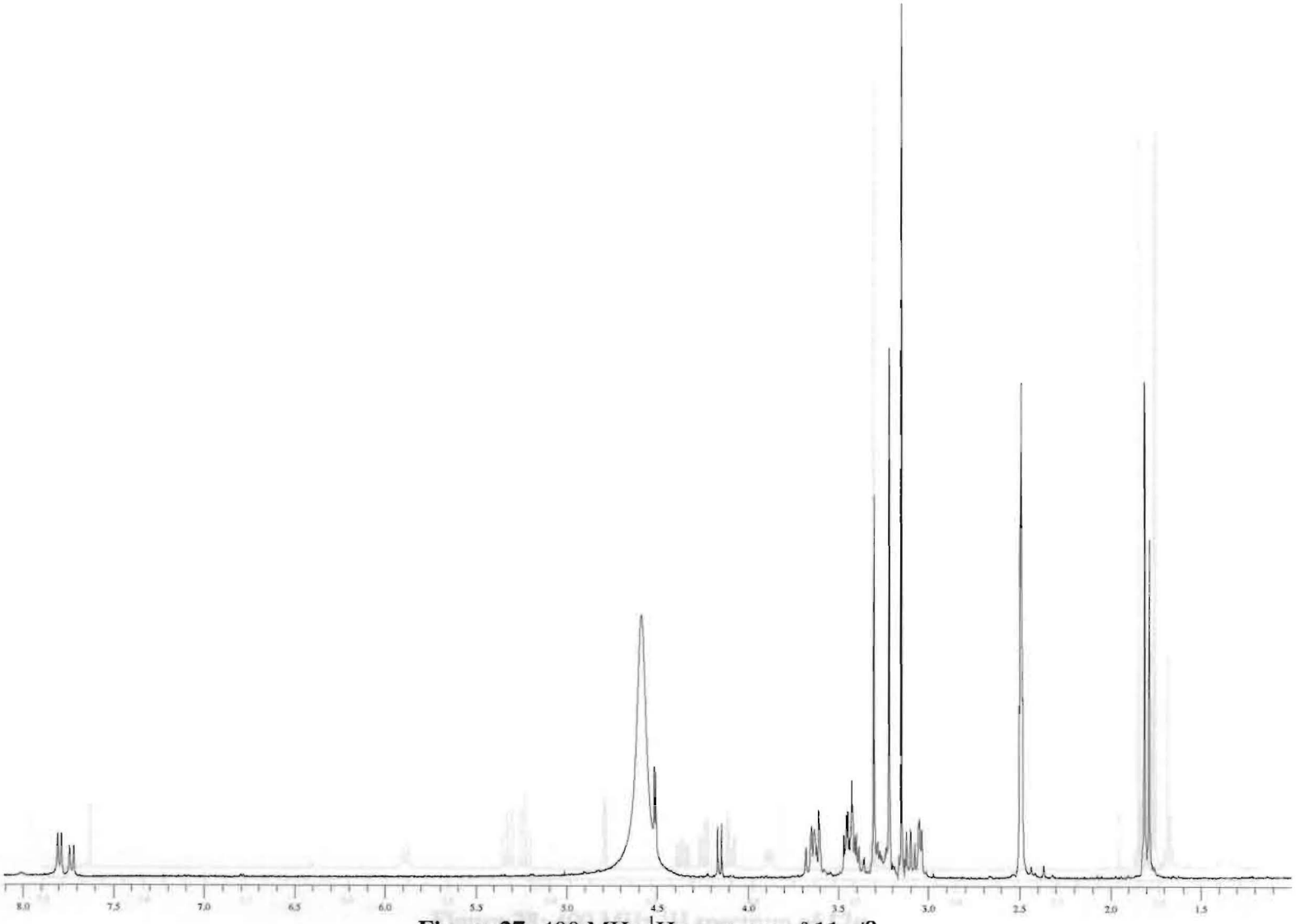

Figure 27: 400 MHz ^{1}H spectrum of **11α/β**

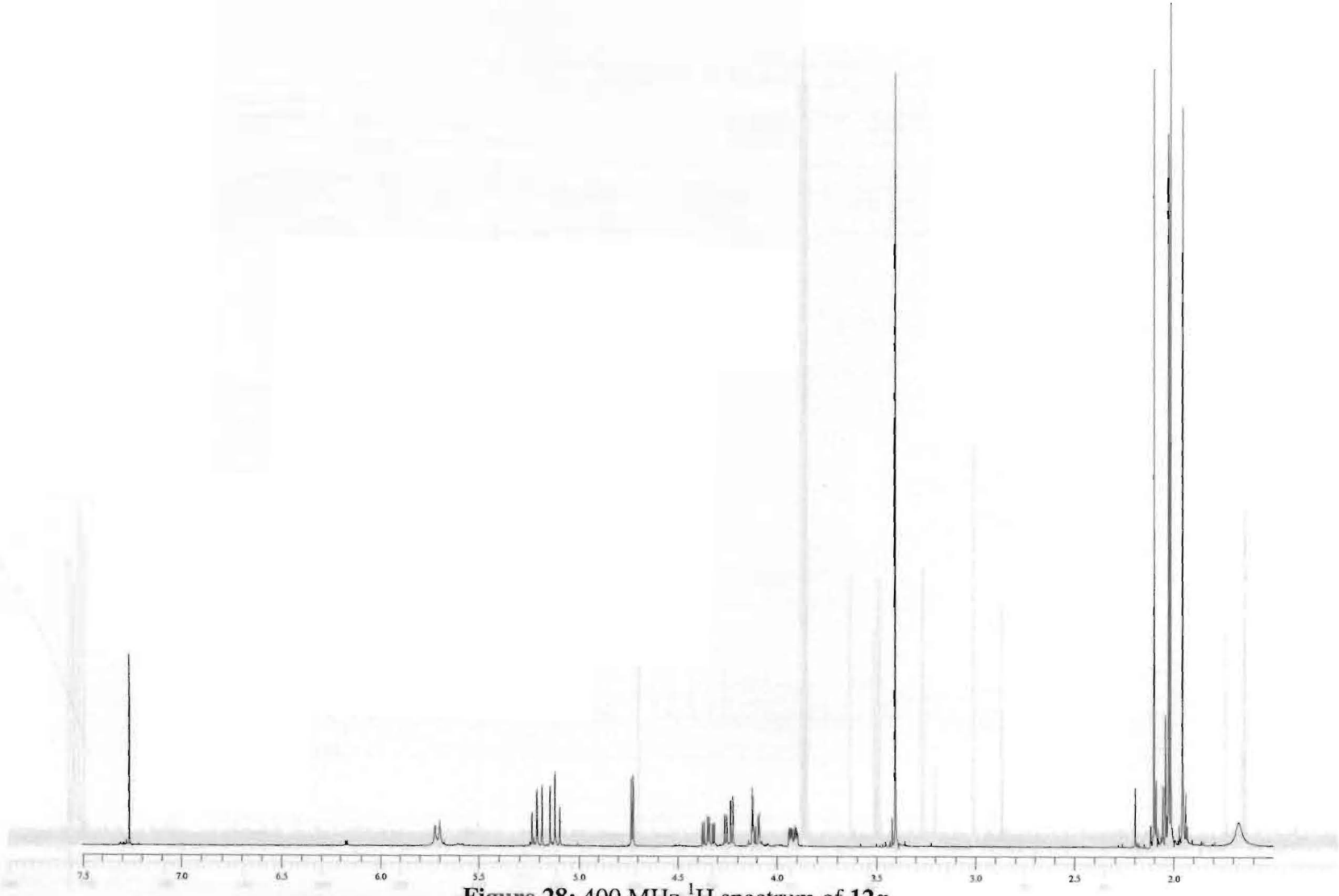

Figure 28: 400 MHz ^{1}H spectrum of **12α**

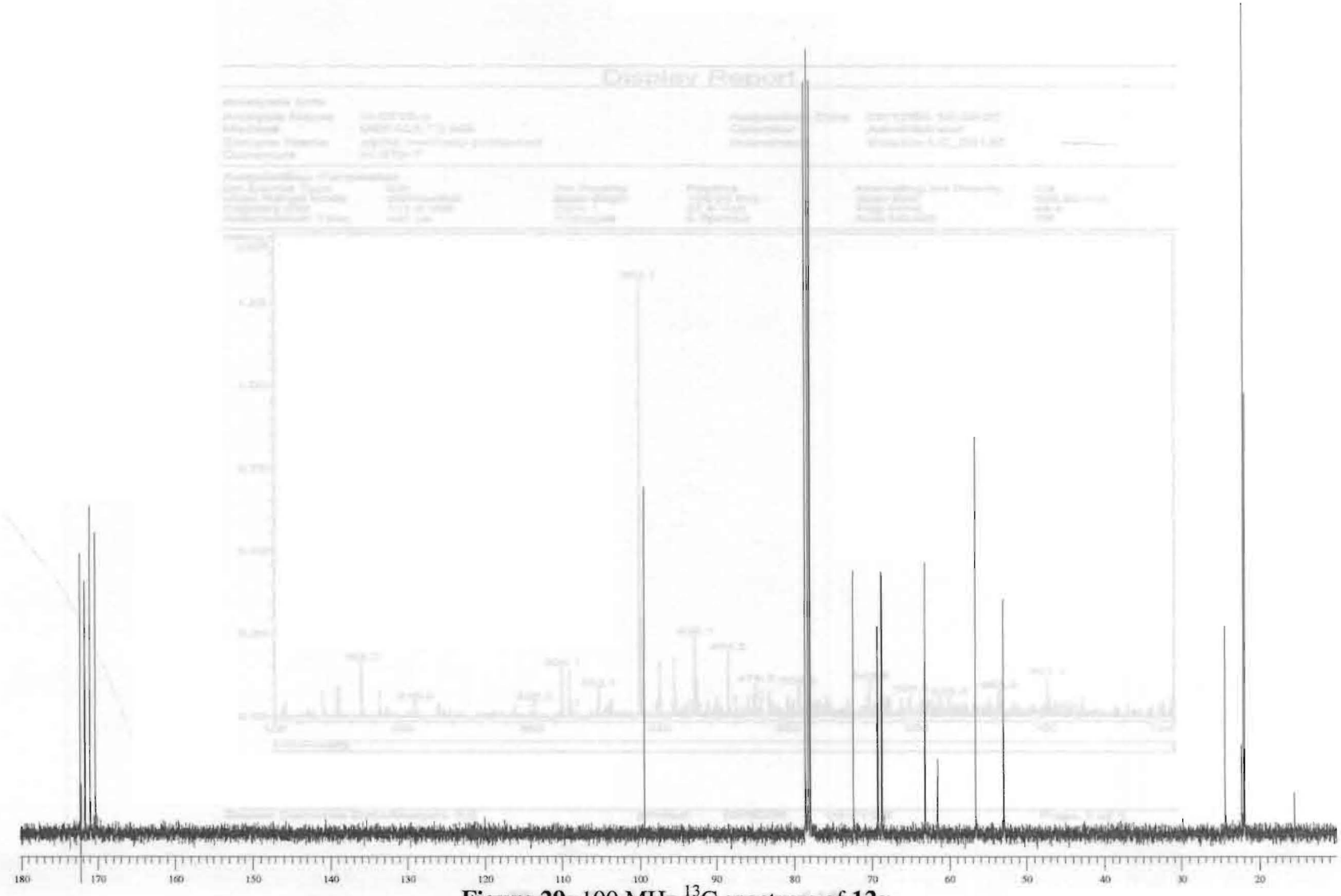

Figure 29: 100 MHz ^{13}C spectrum of **12α**

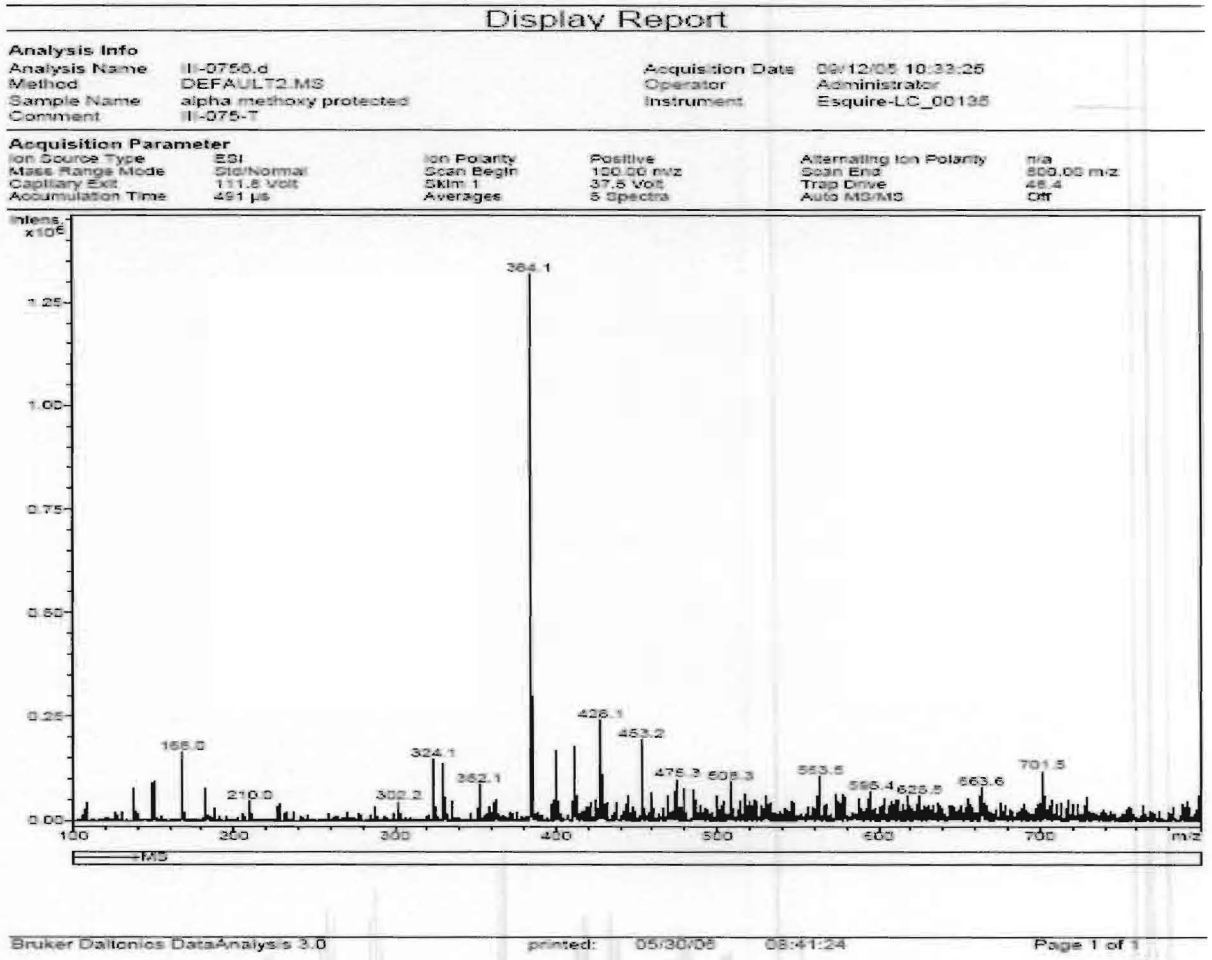

Figure 30: Mass spectrum of **12α**

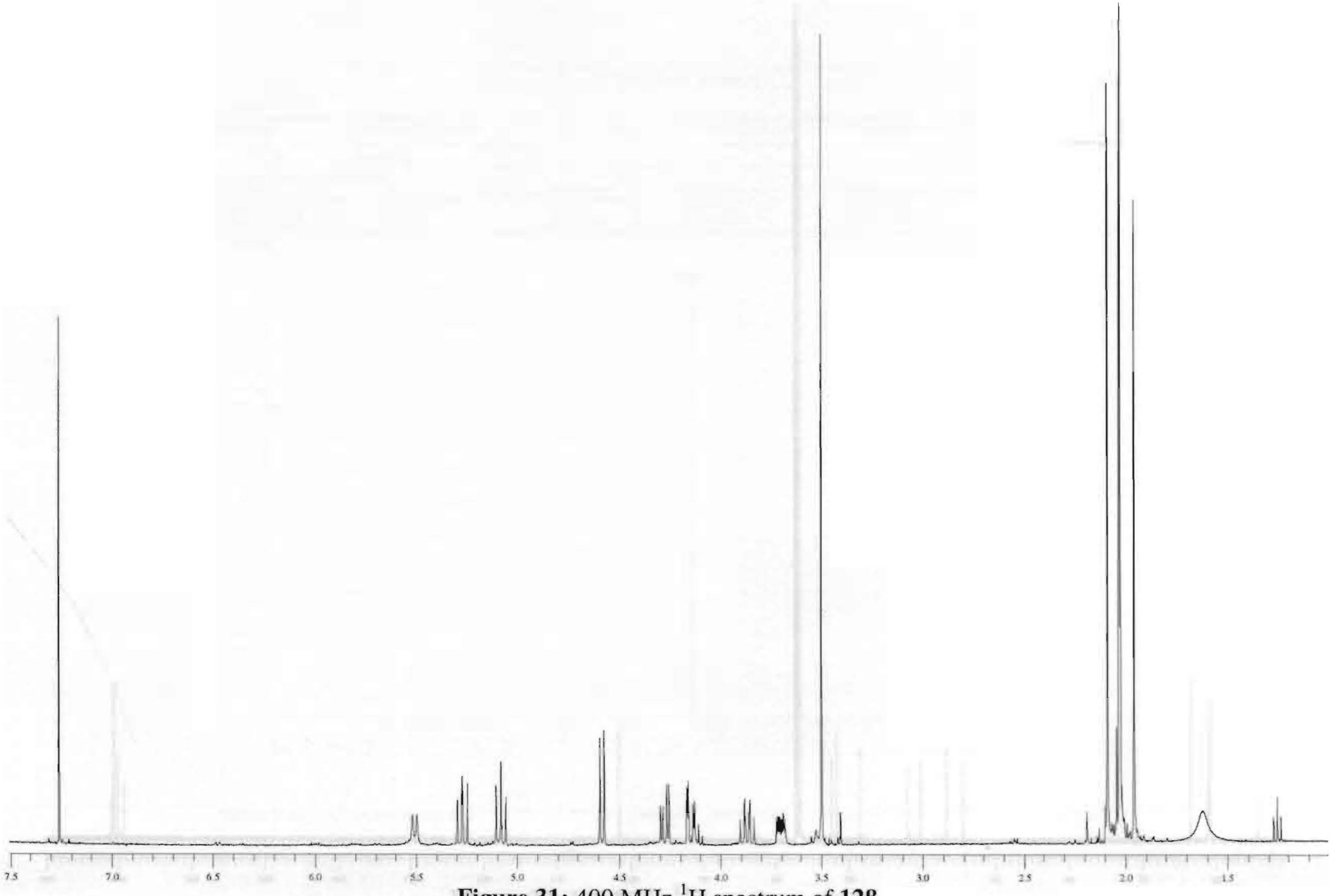

Figure 31: 400 MHz ^{1}H spectrum of **12β**

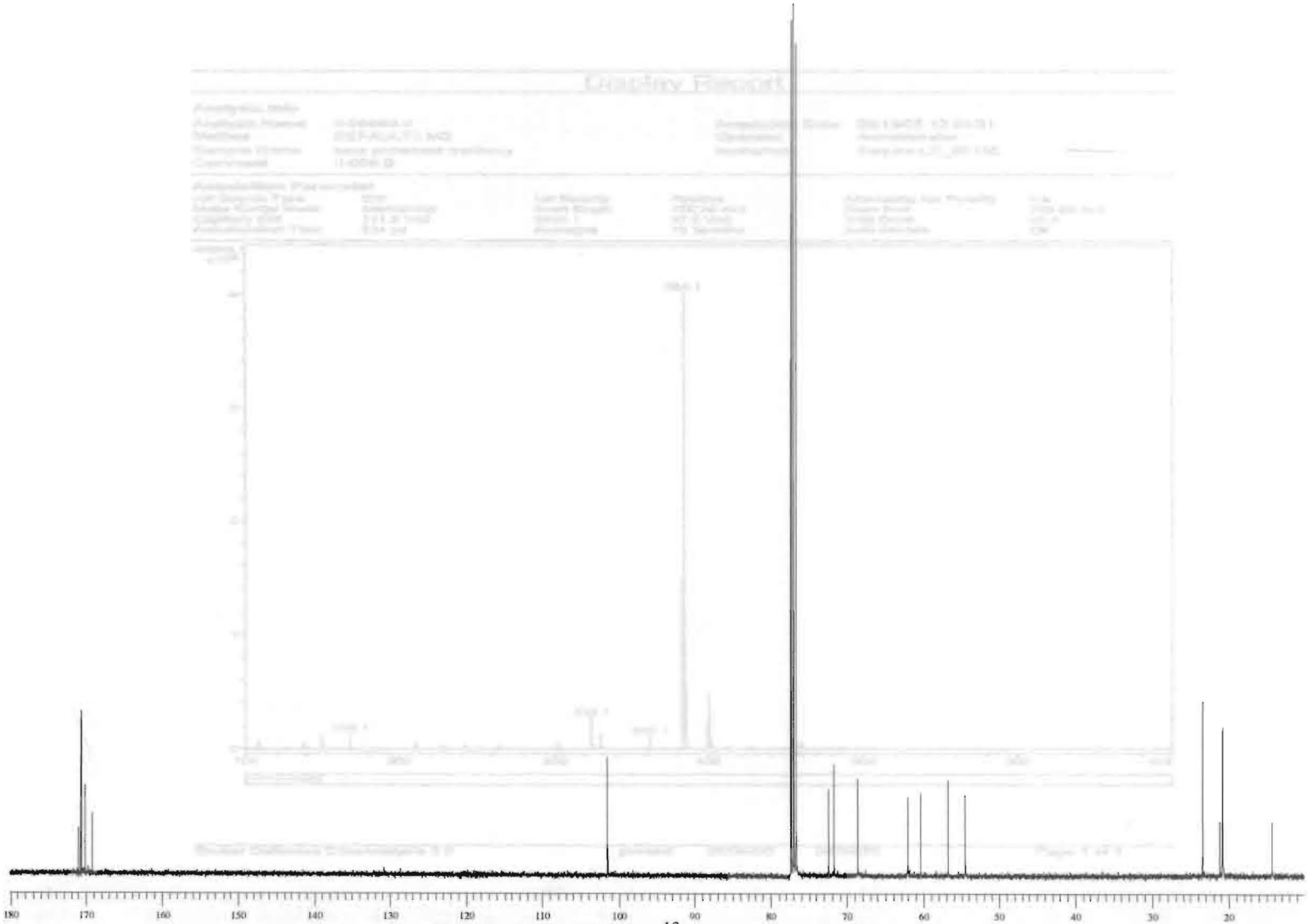

Figure 32: 100 MHz ^{13}C spectrum of **12β**

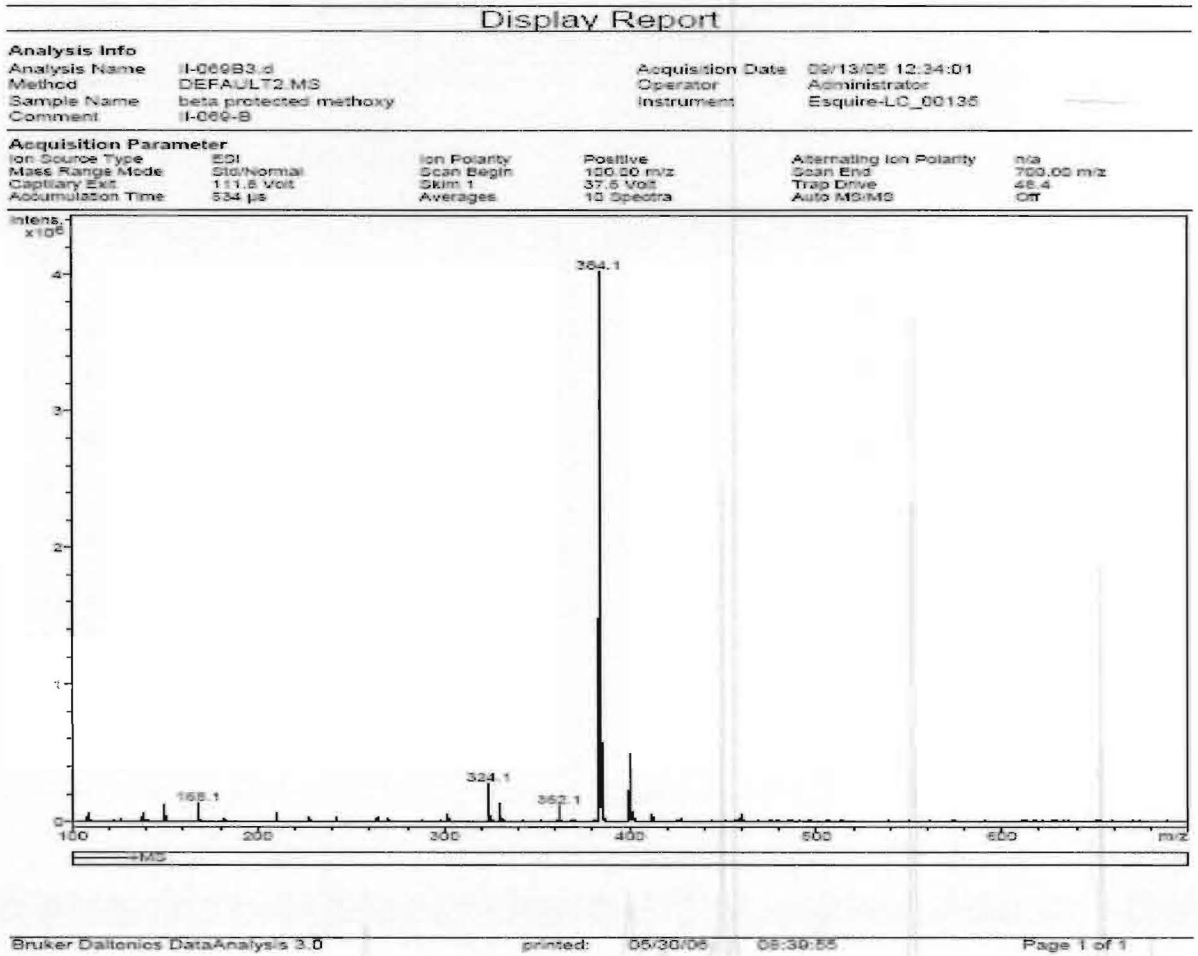

Figure 33: Mass spectrum of **12β**

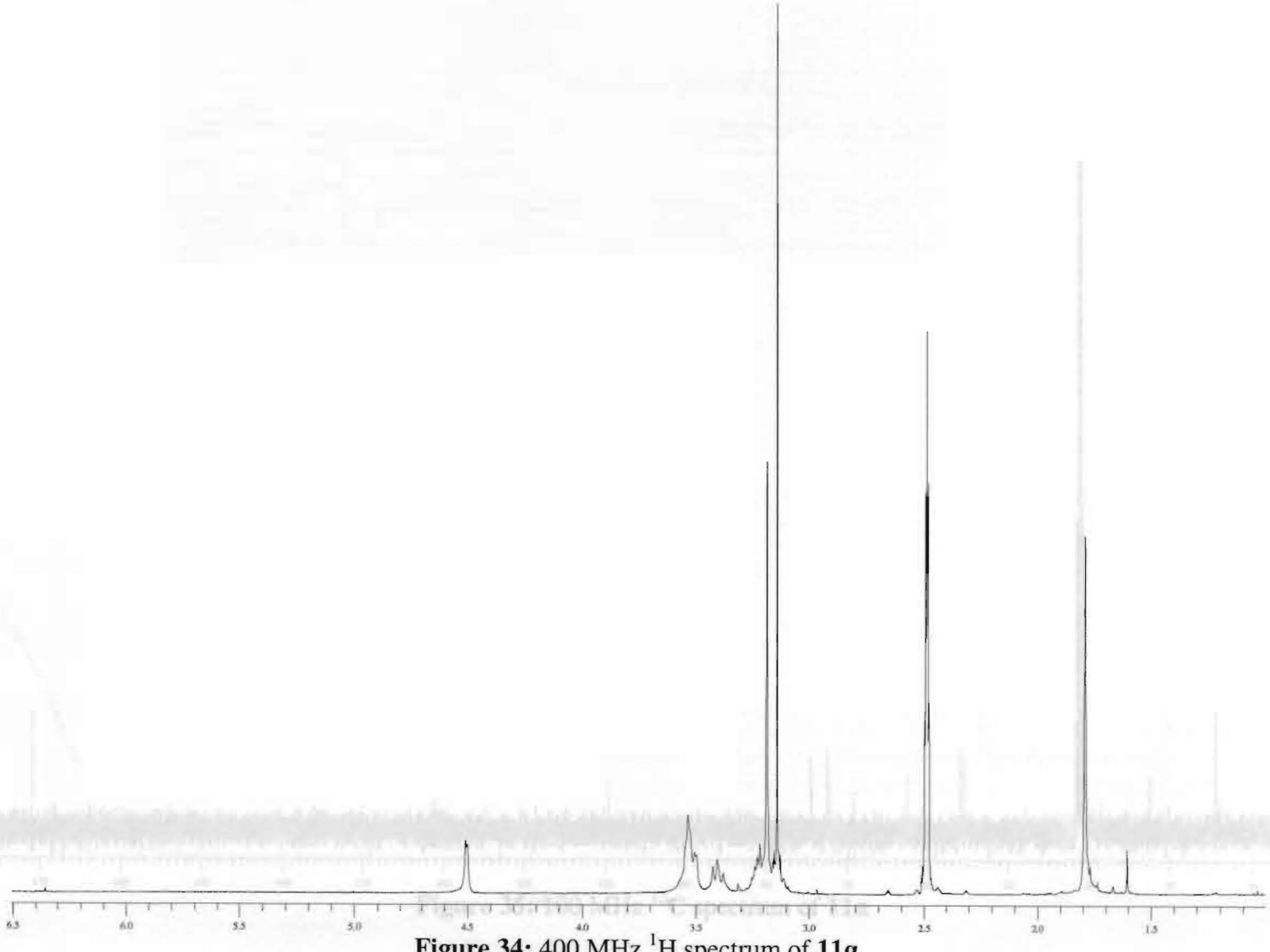

Figure 34: 400 MHz ^{1}H spectrum of **11α**

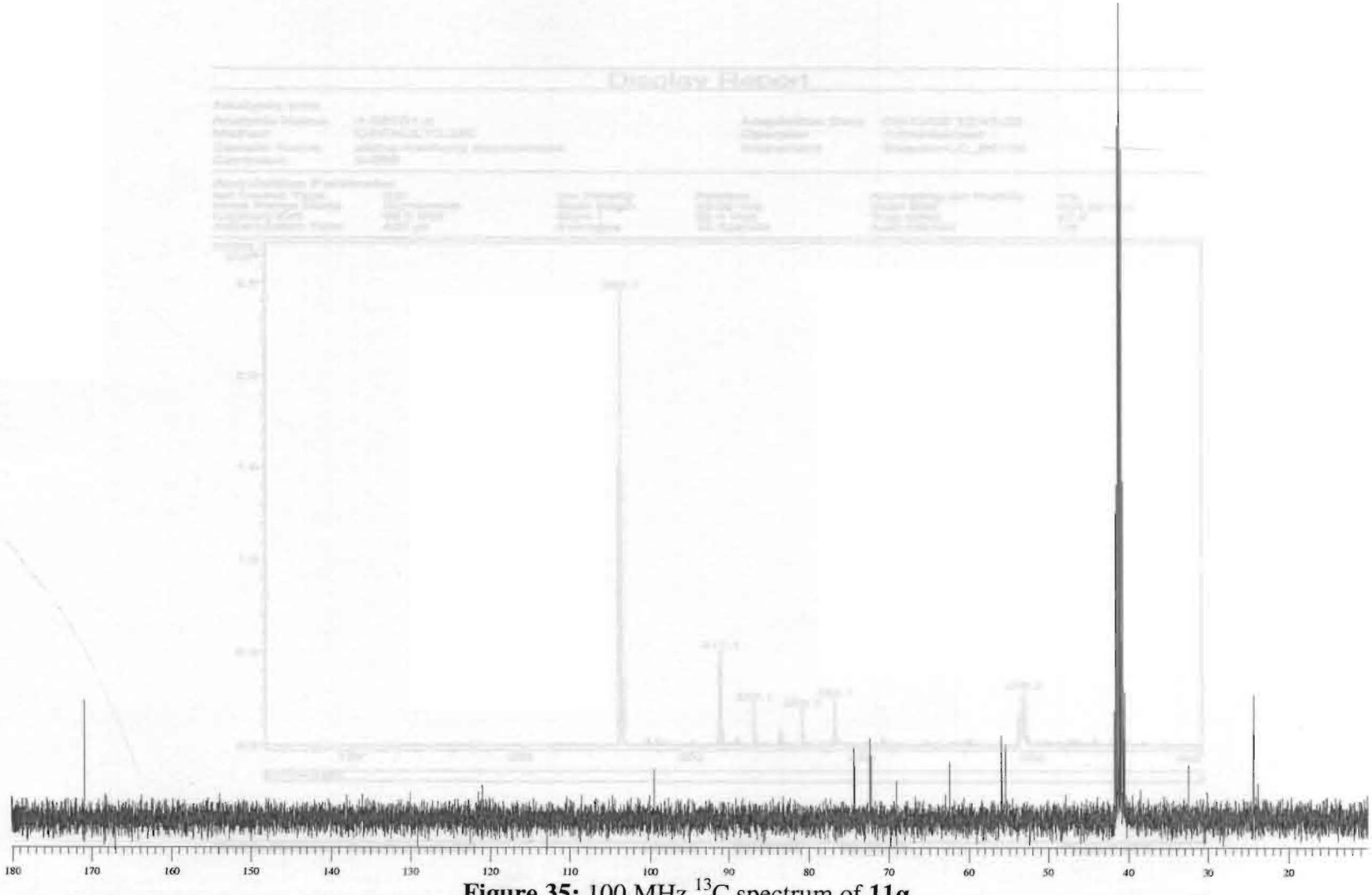

Figure 35: 100 MHz ^{13}C spectrum of **11α**

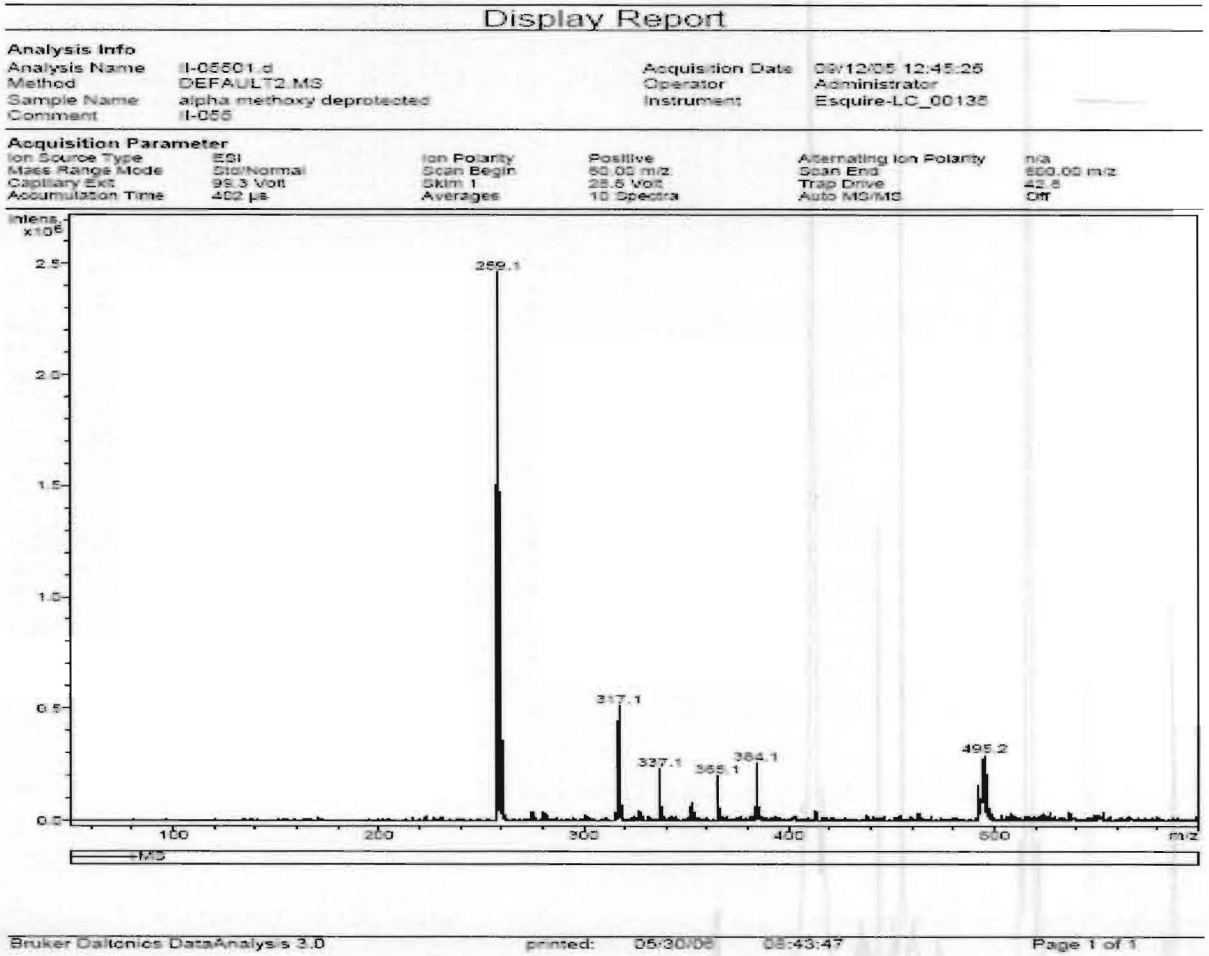

Figure 36: Mass spectrum of **11α**

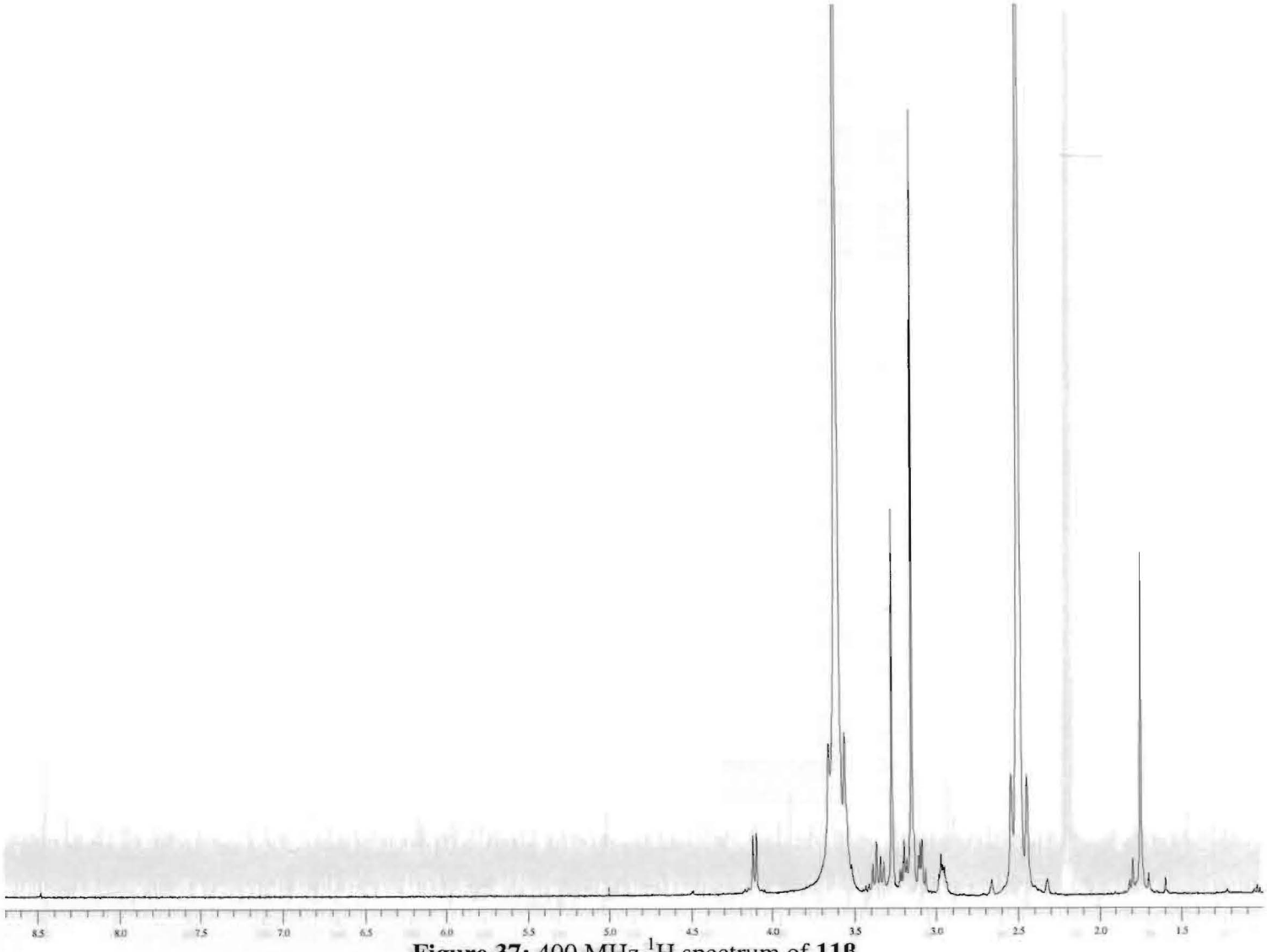

Figure 37: 400 MHz ^{1}H spectrum of **11β**

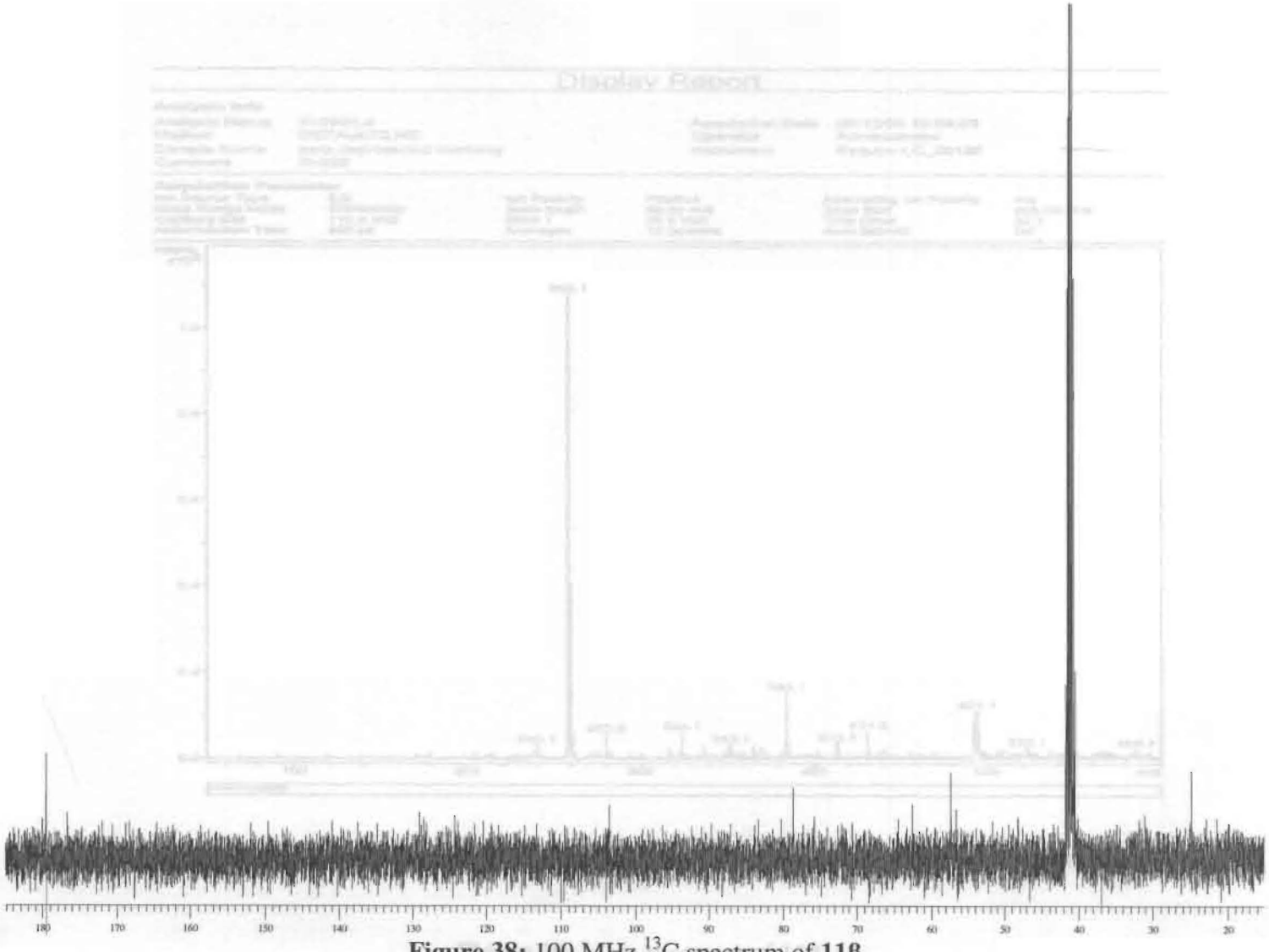

Figure 38: 100 MHz ^{13}C spectrum of **11β**

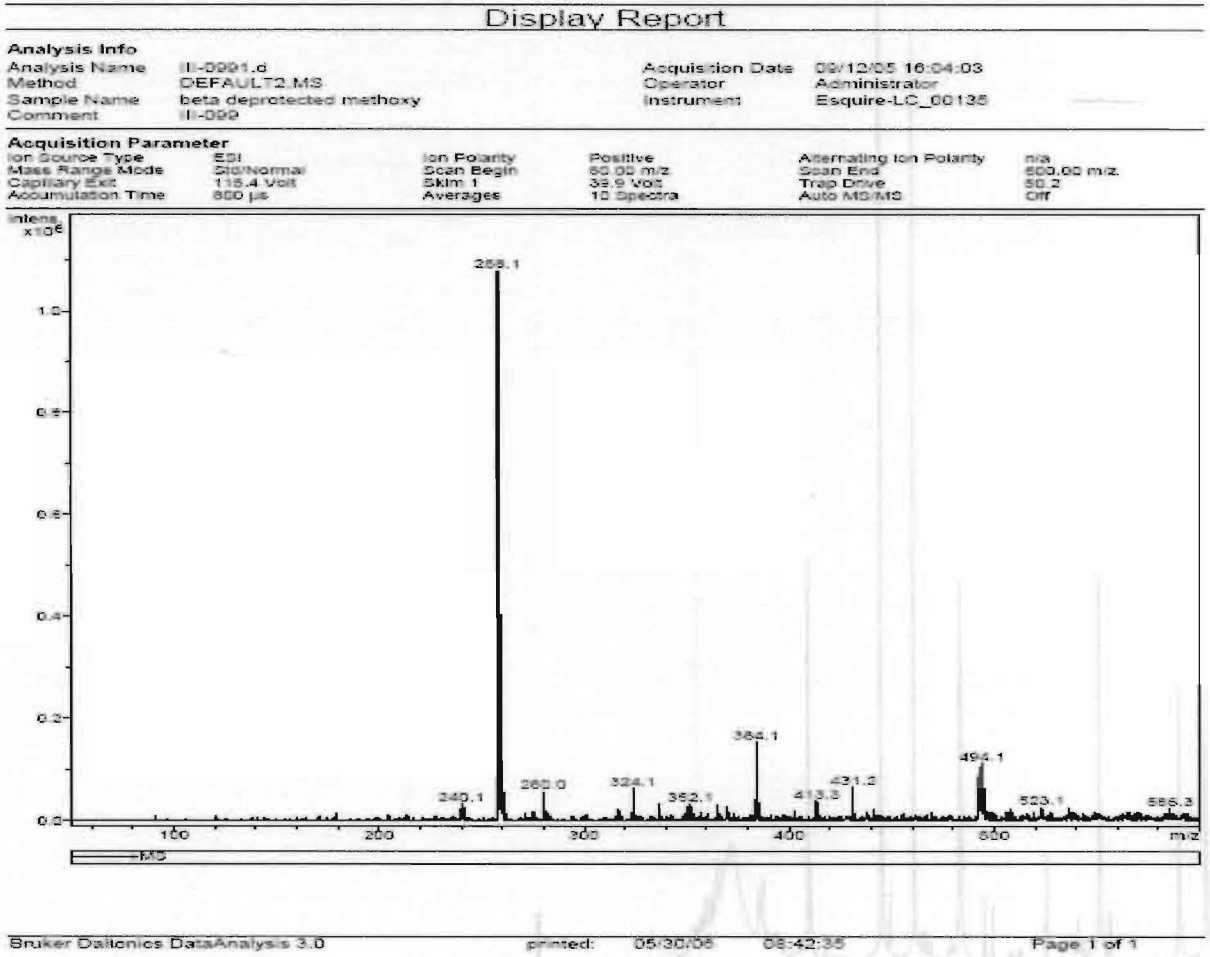

Figure 39: Mass spectrum of **11β**

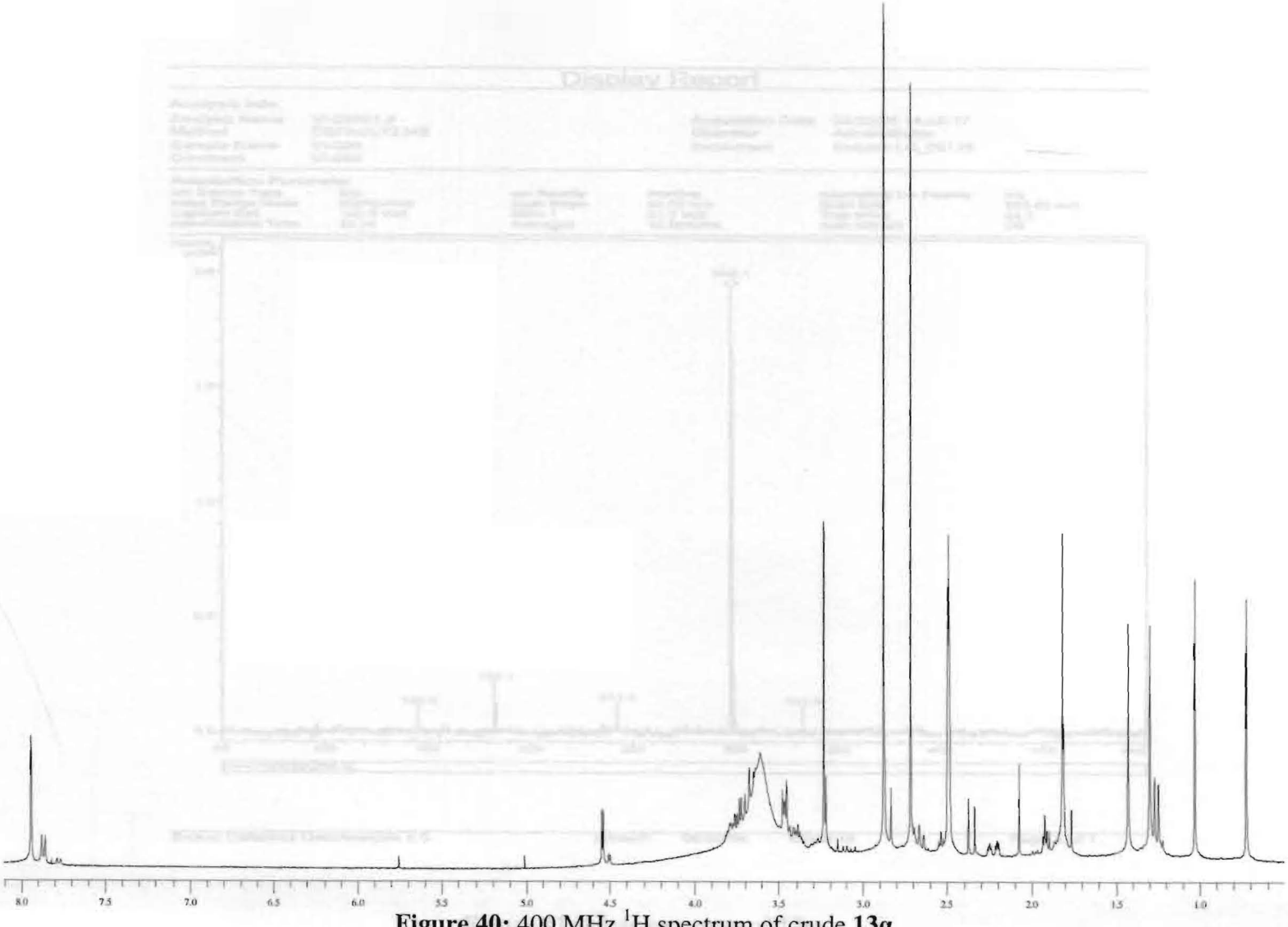

Figure 40: 400 MHz ^{1}H spectrum of crude **13α**

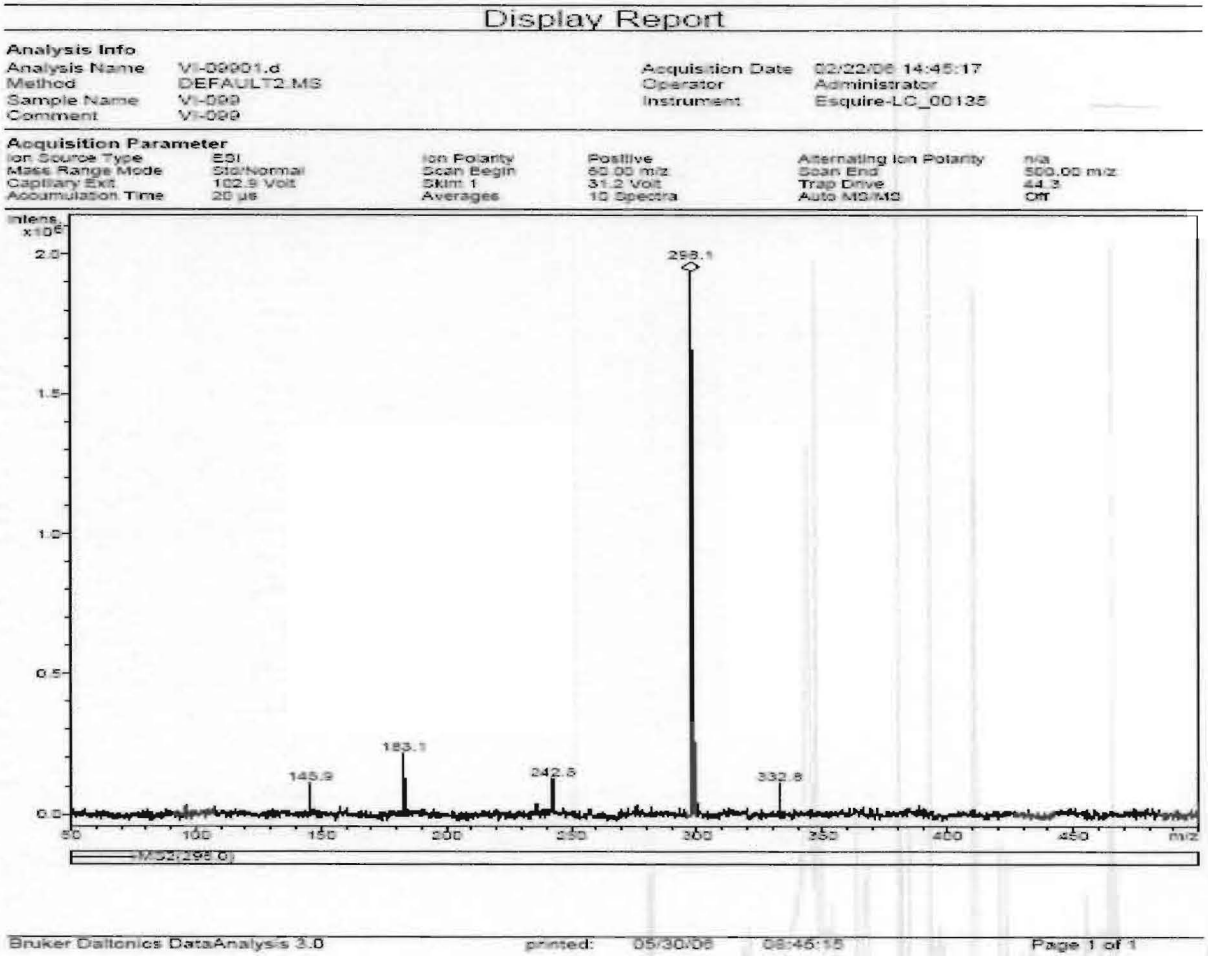

Figure 41: Mass spectrum of **13α**

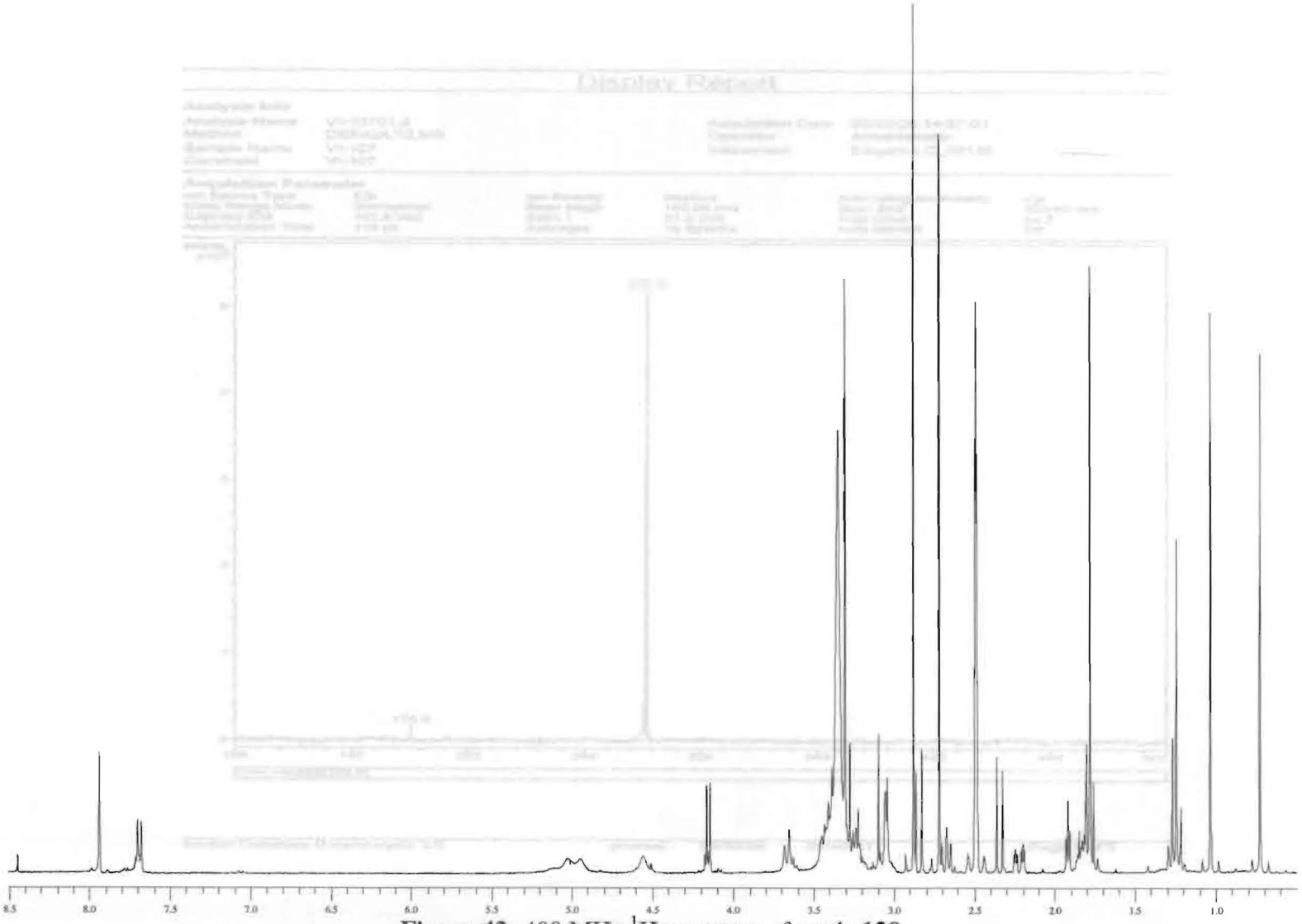

Figure 42: 400 MHz ^{1}H spectrum of crude **13β**

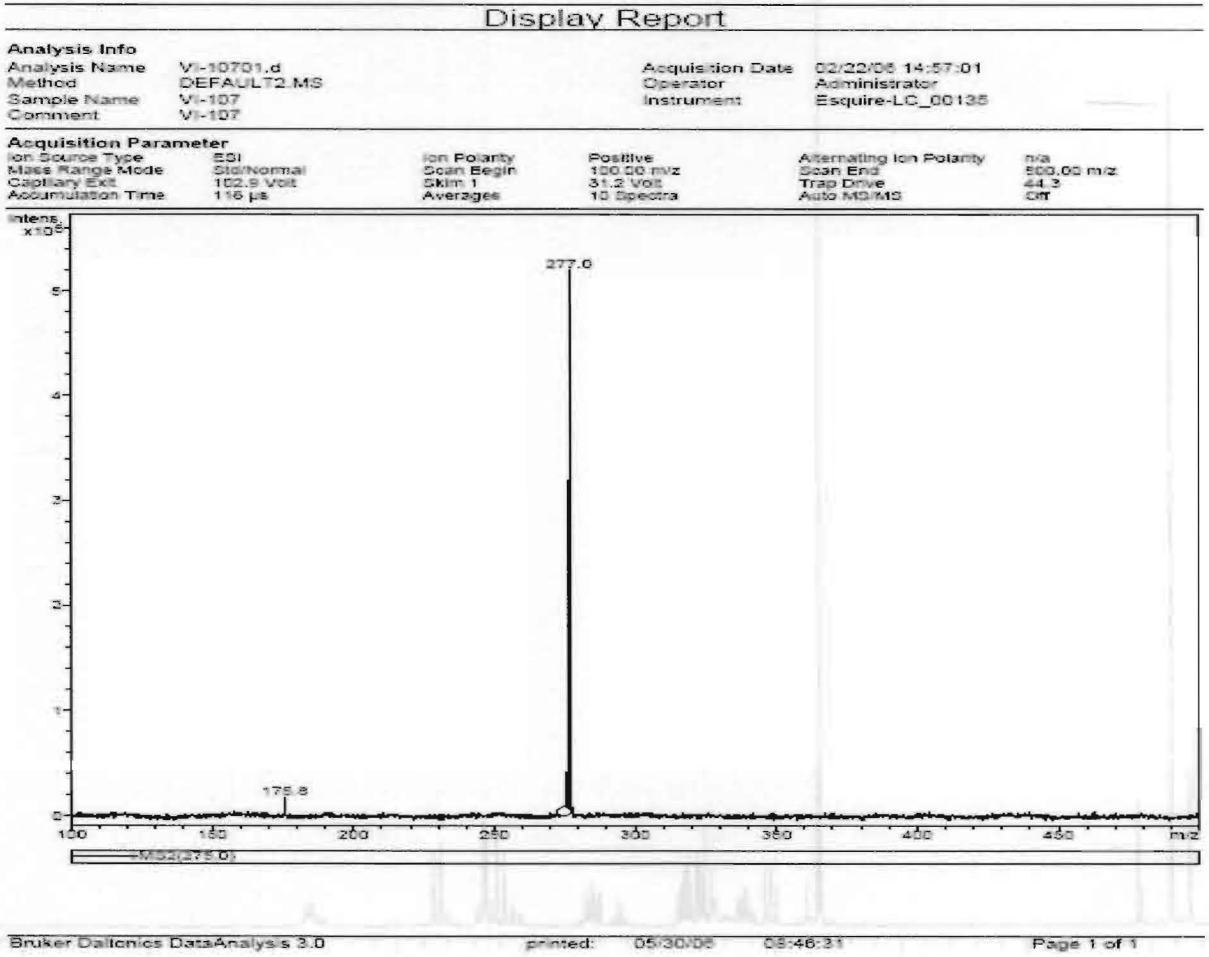

Figure 43: Mass spectrum of **13β**

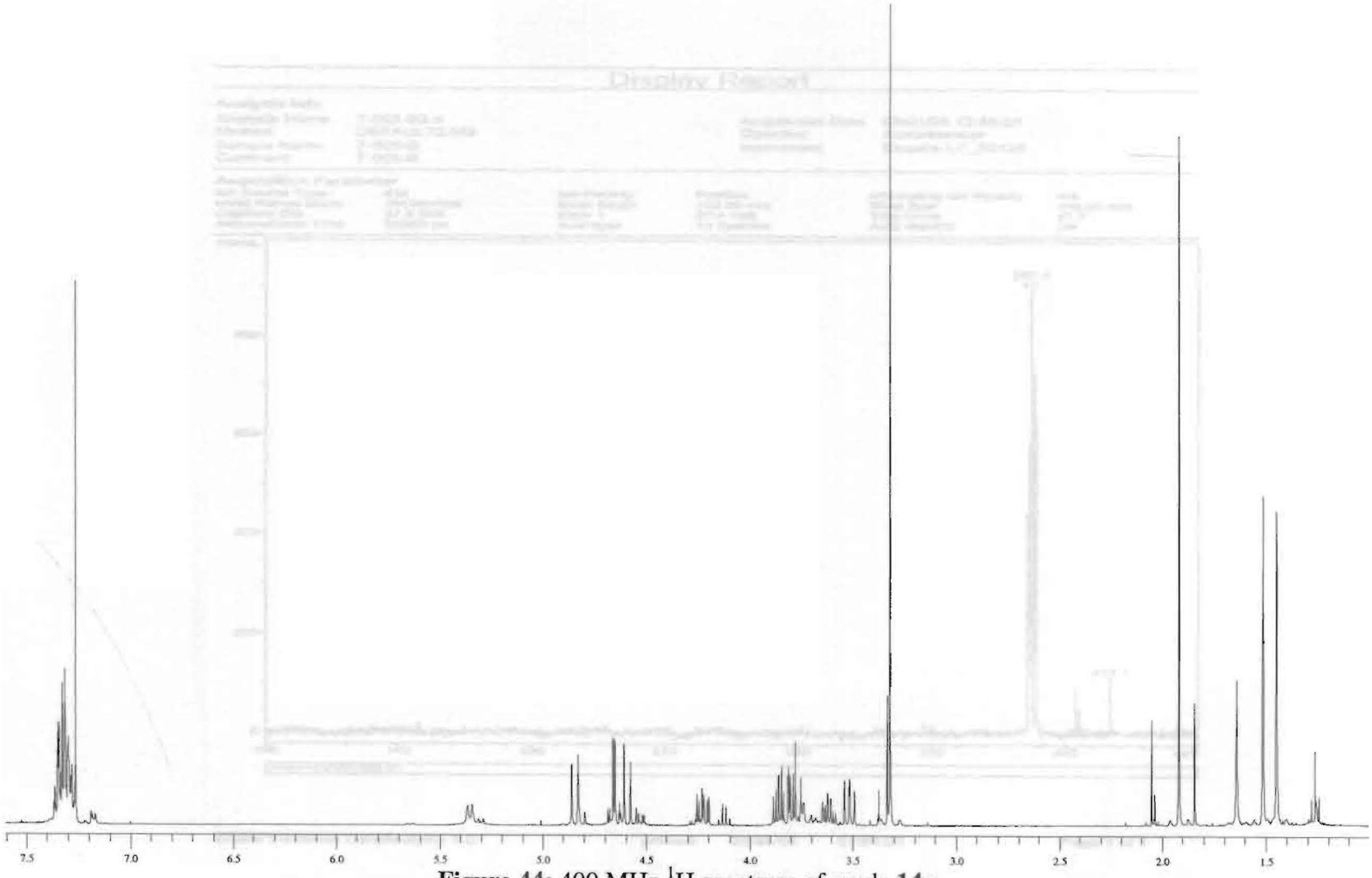

Figure 44: 400 MHz ^{1}H spectrum of crude **14α**

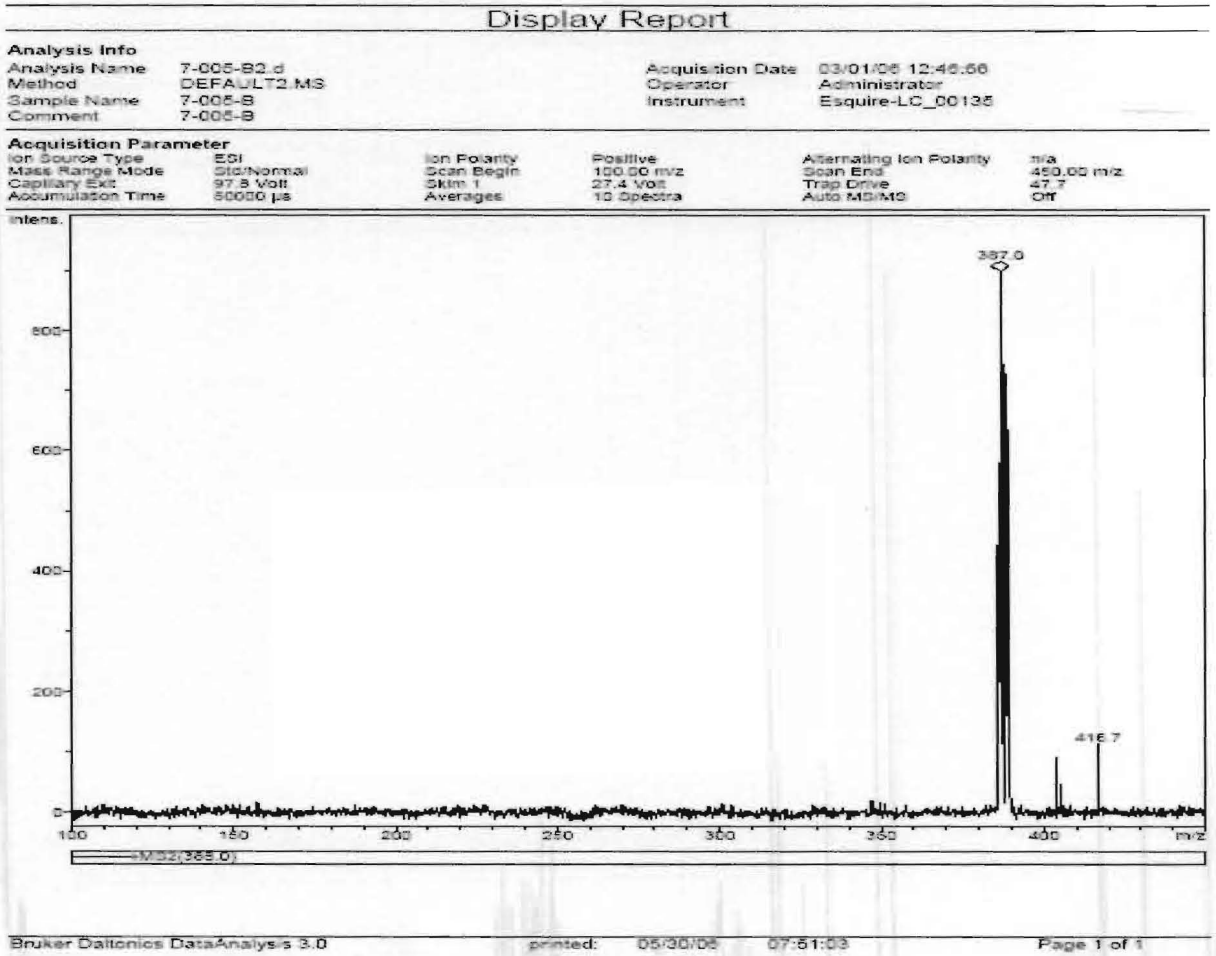

Figure 45: Mass spectrum of **14α**

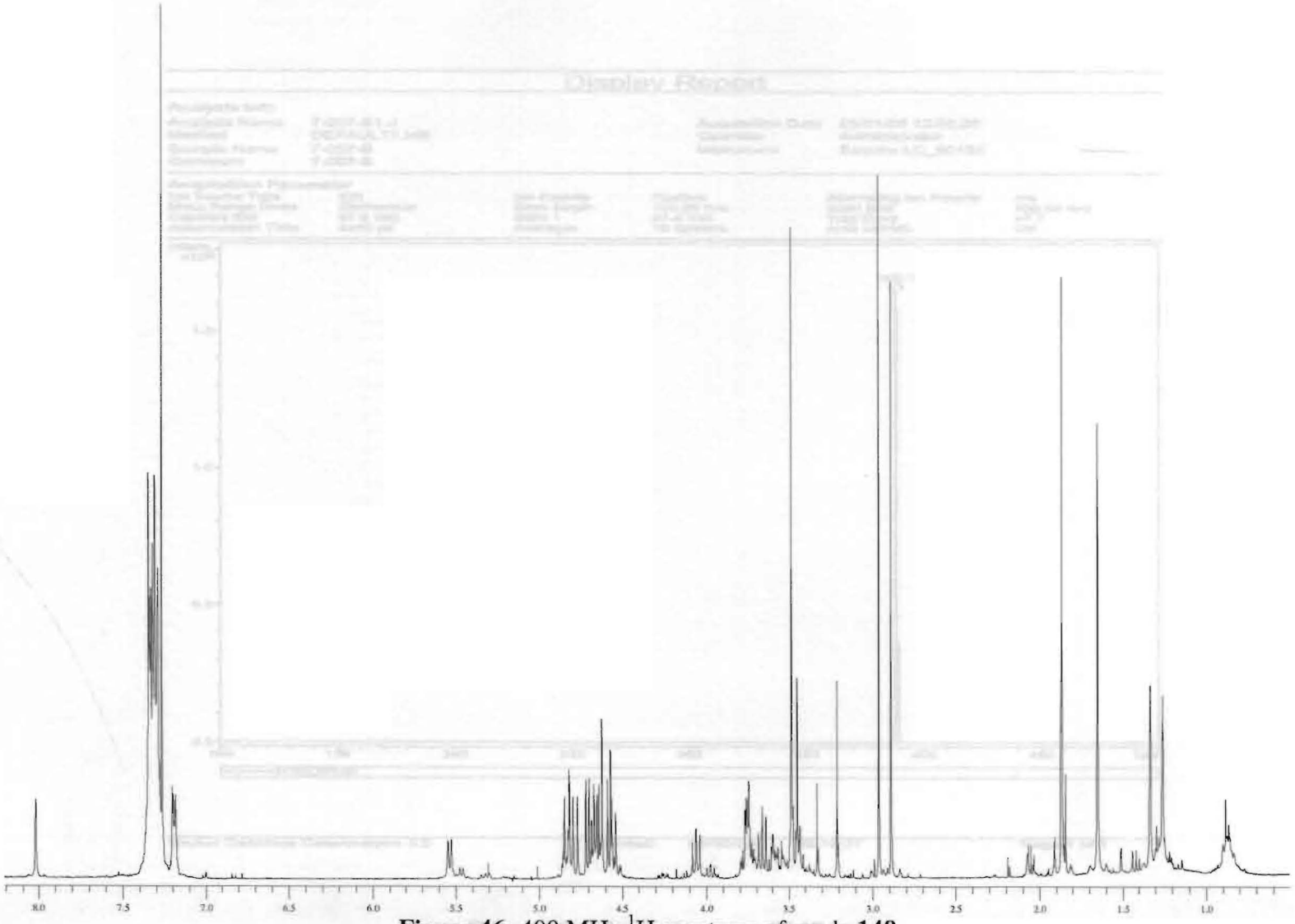

Figure 46: 400 MHz ^{1}H spectrum of crude **14β**

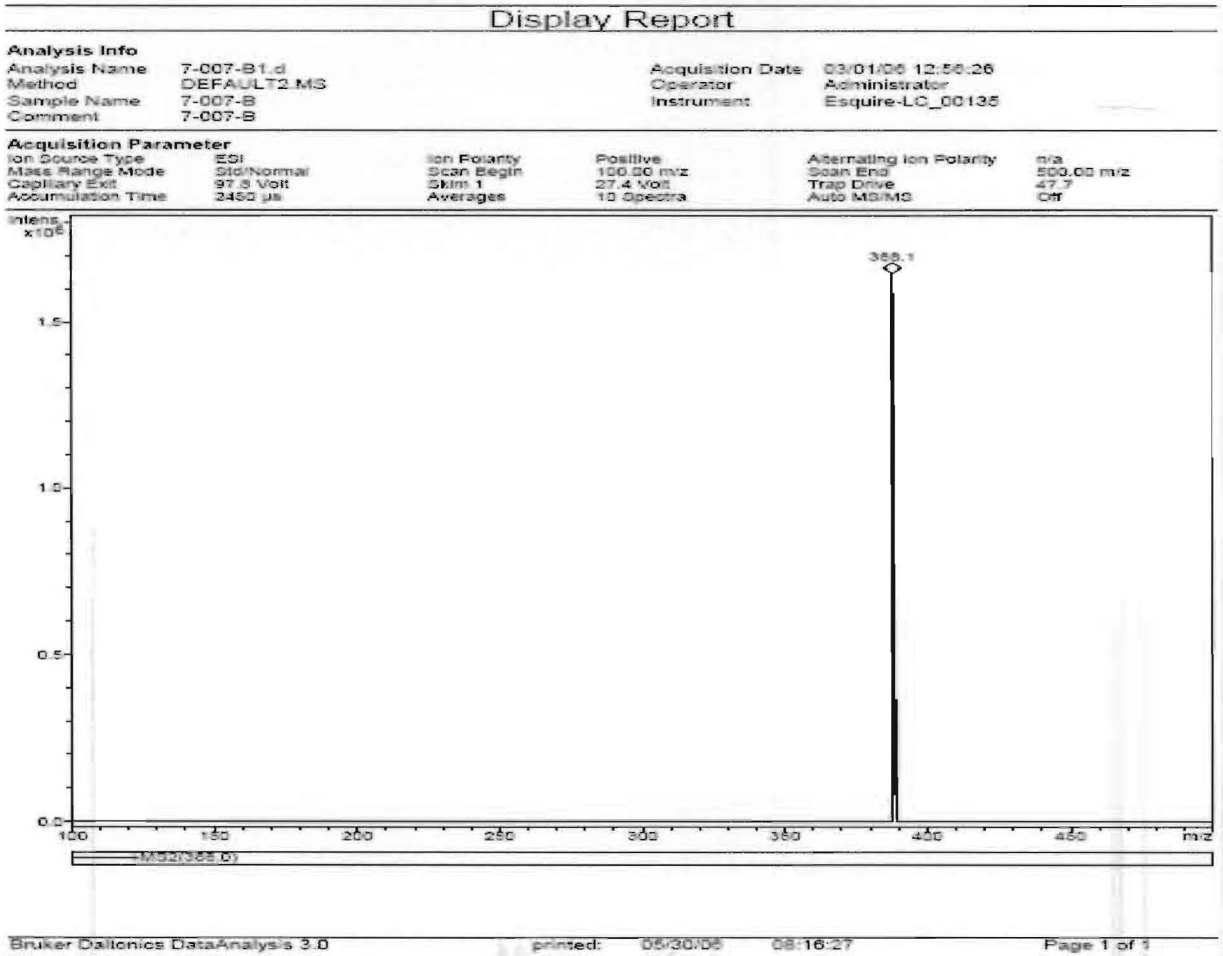

Figure 47: Mass spectrum of **14β**

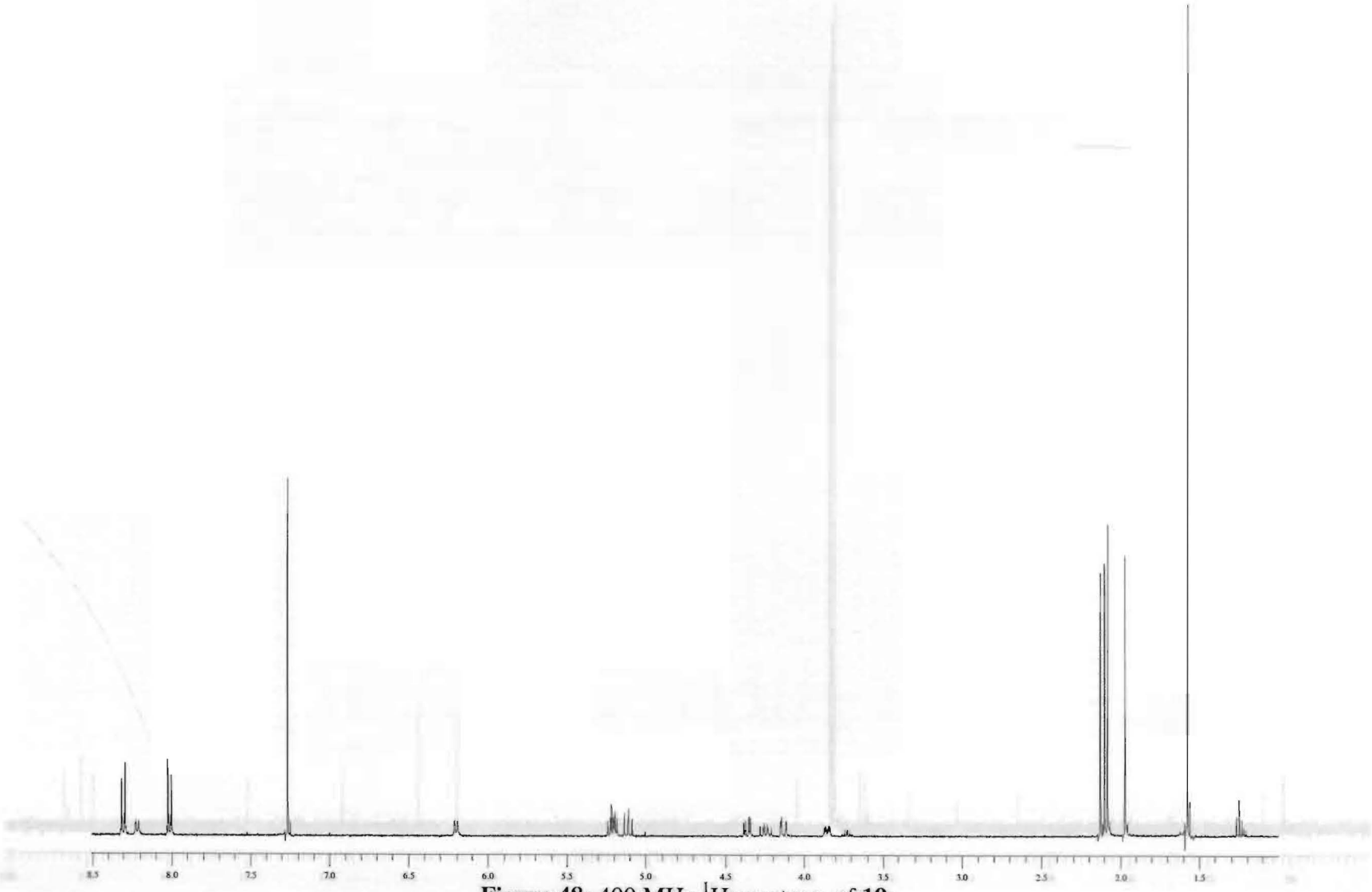

Figure 48: 400 MHz ^{1}H spectrum of **19**

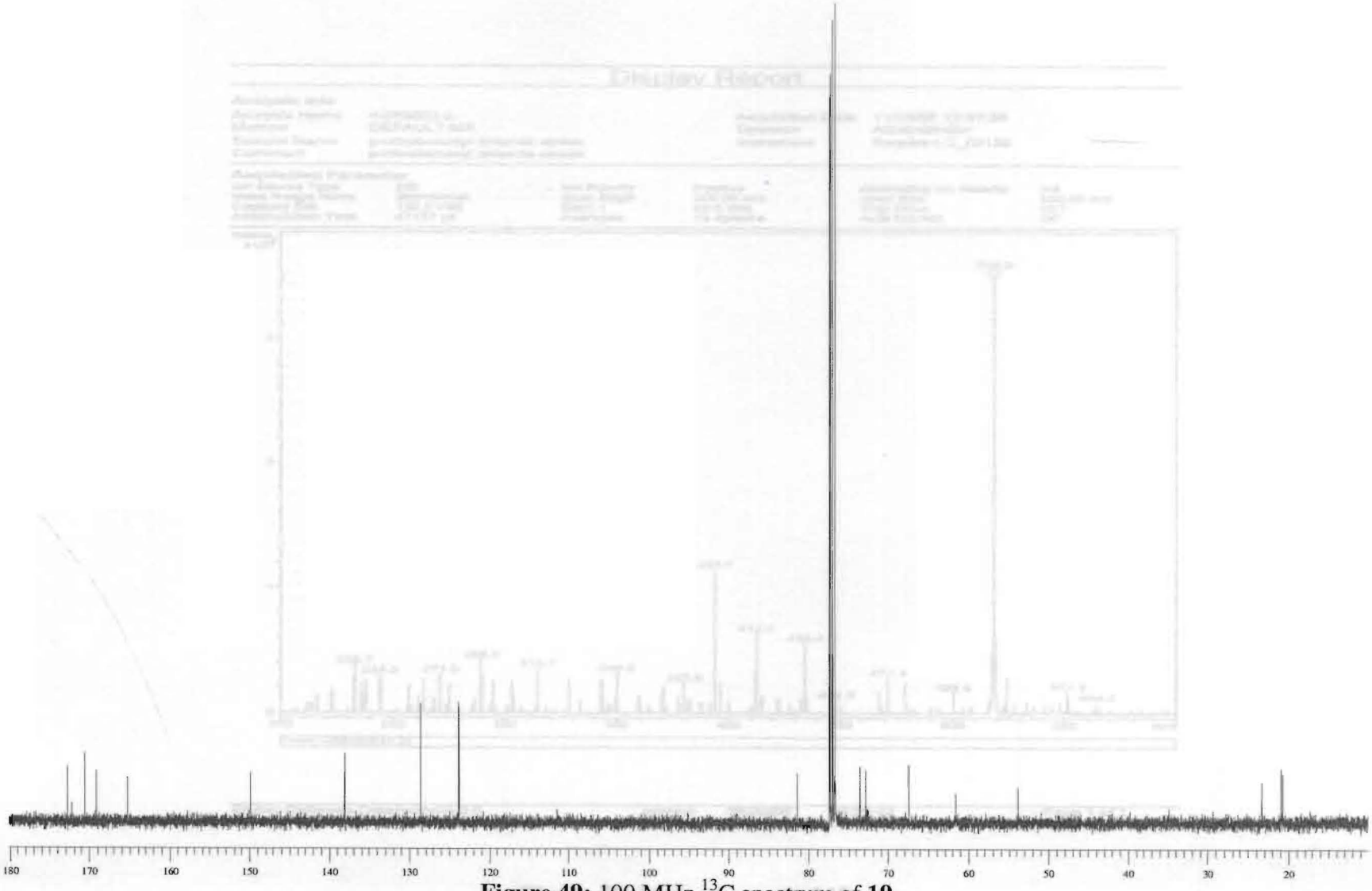

Figure 49: 100 MHz ^{13}C spectrum of **19**

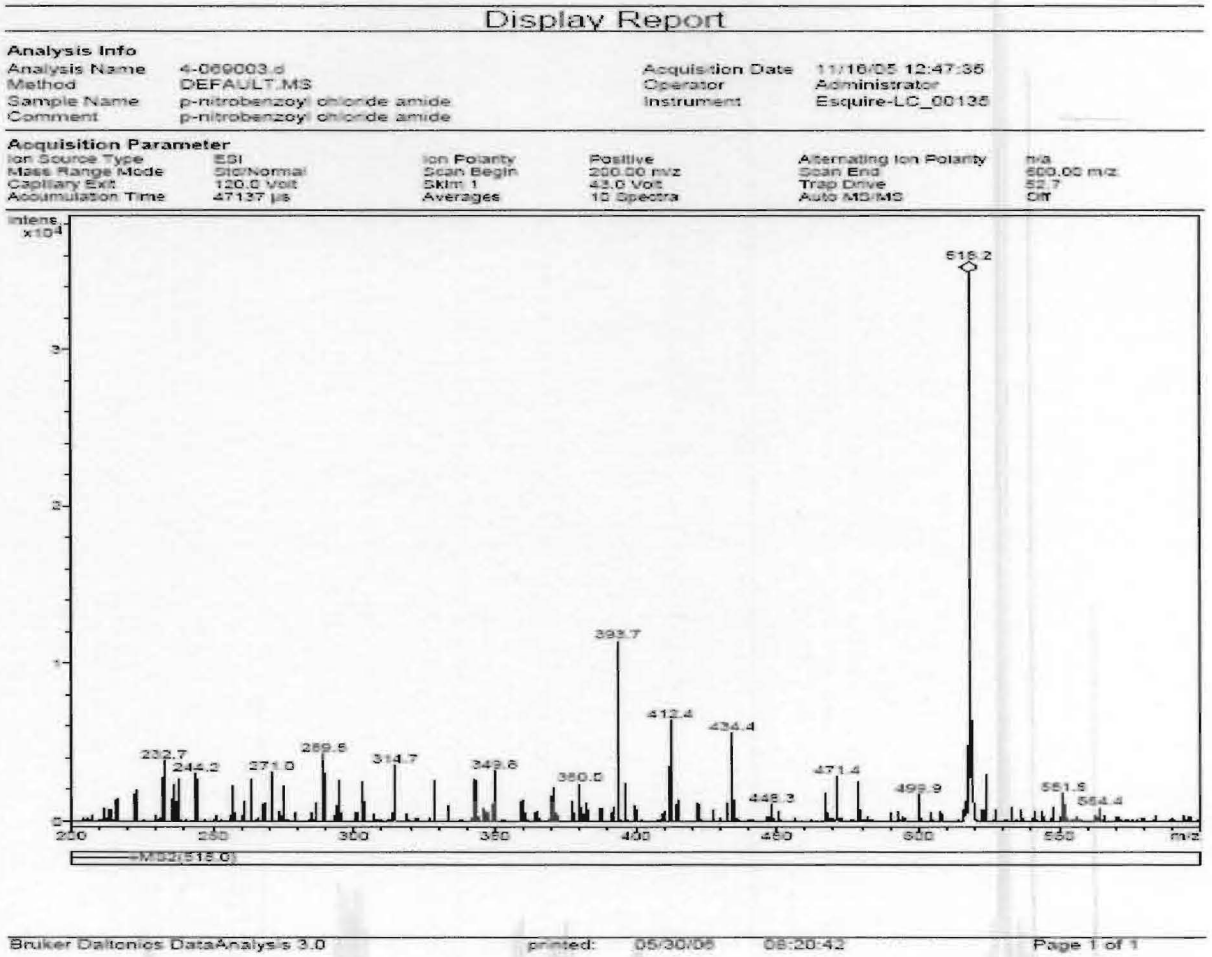

Figure 50: Mass spectrum of **19**

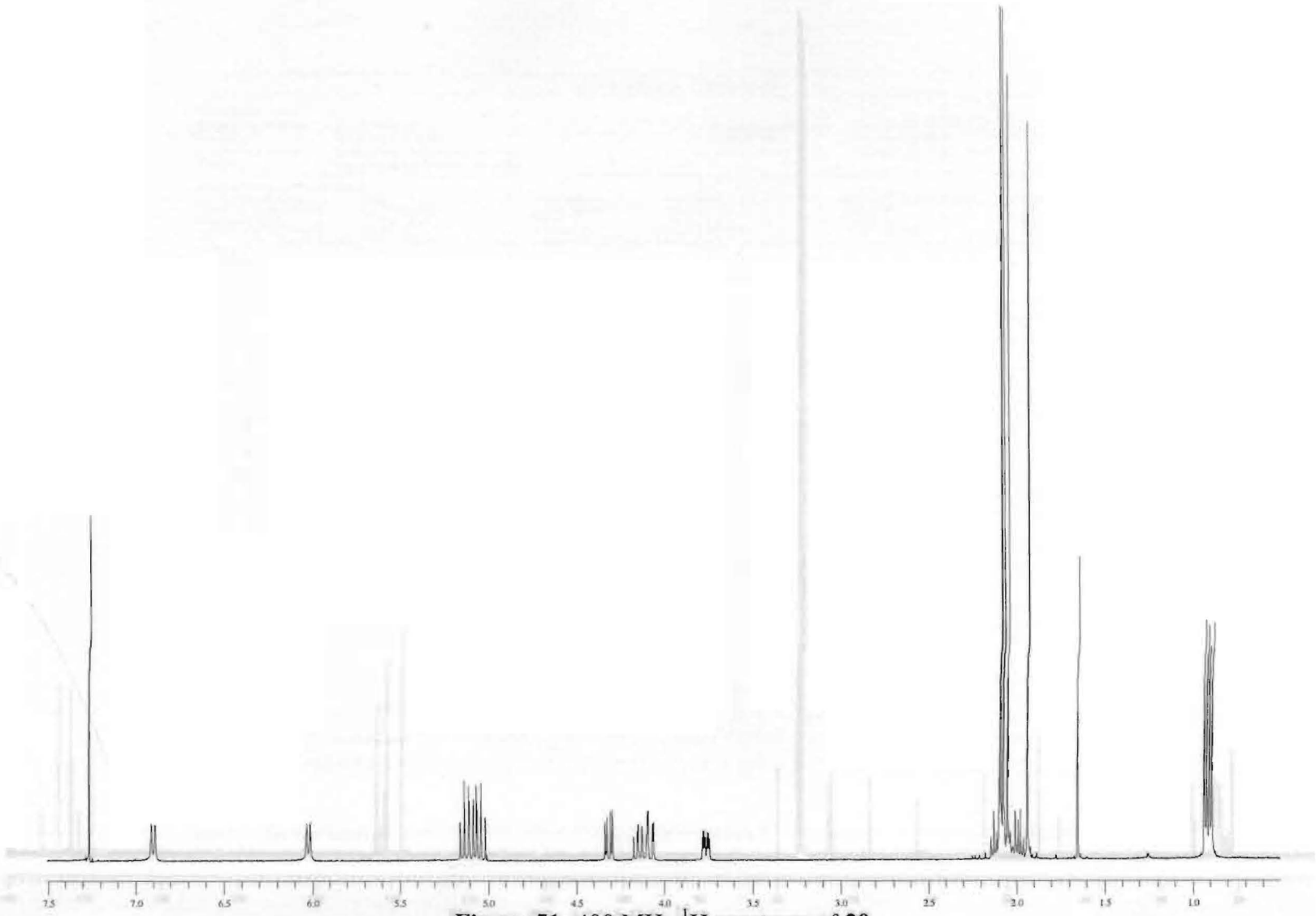

Figure 51: 400 MHz ^{1}H spectrum of **20**

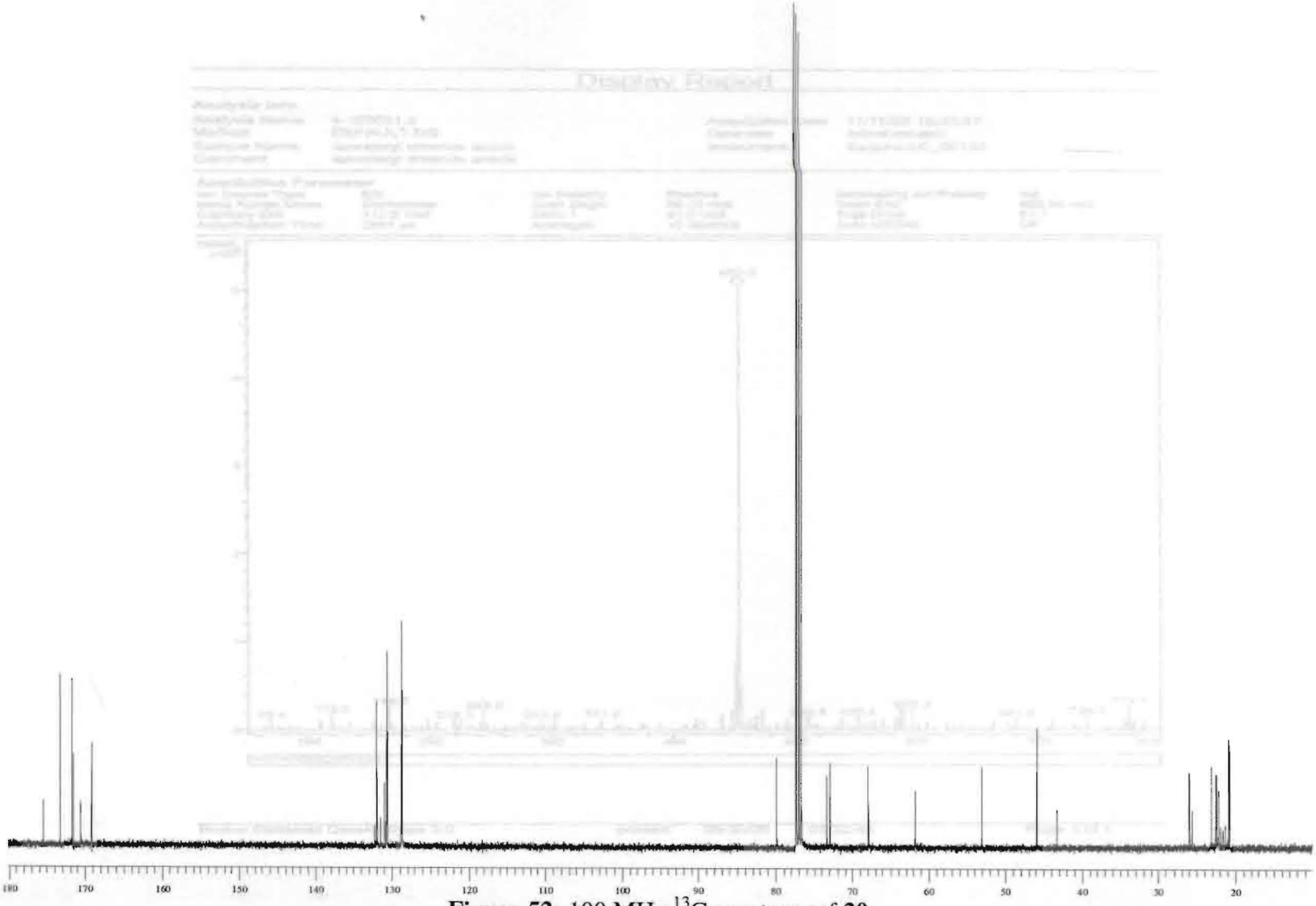

Figure 52: 100 MHz ^{13}C spectrum of **20**

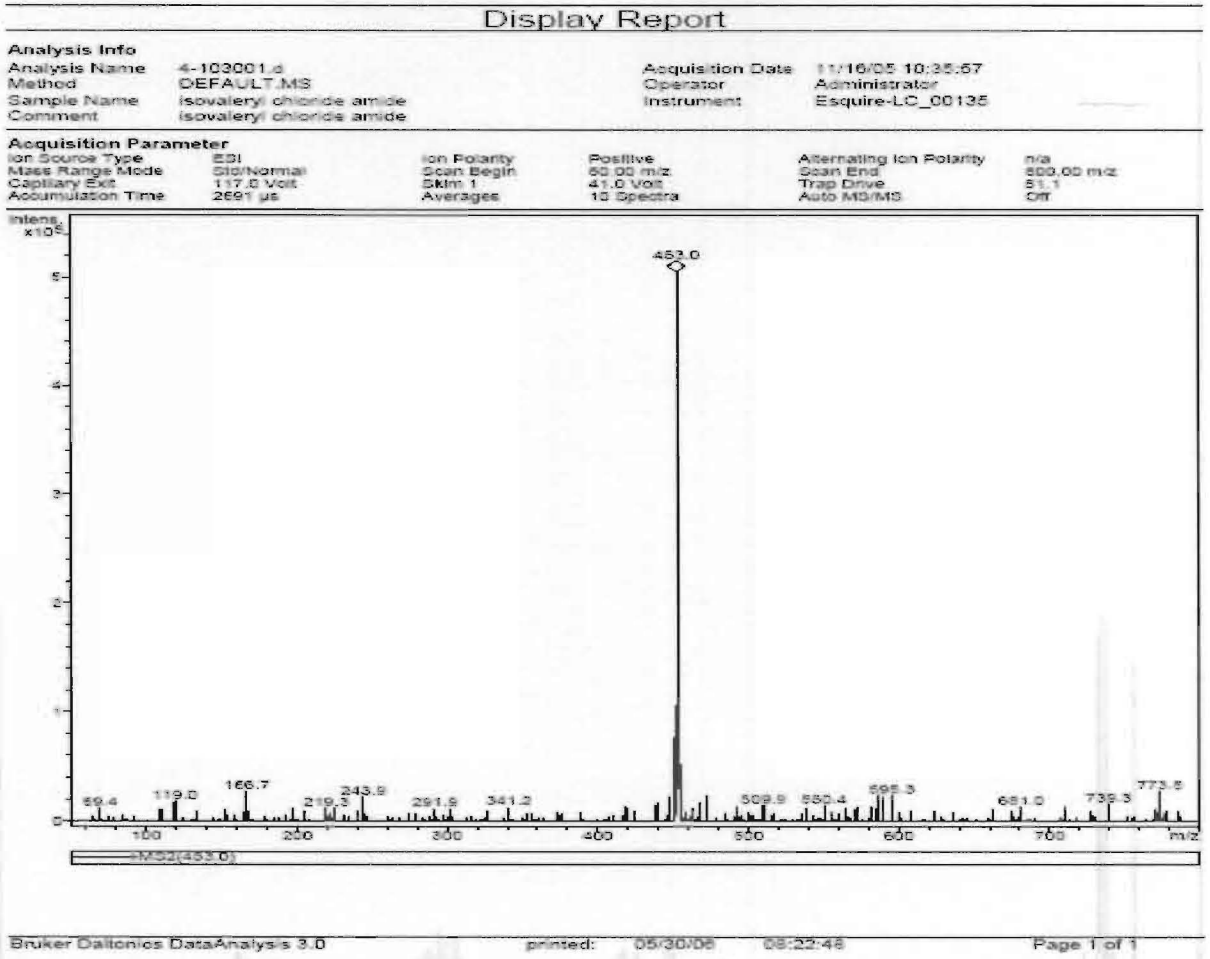

Figure 53: Mass spectrum of **20**

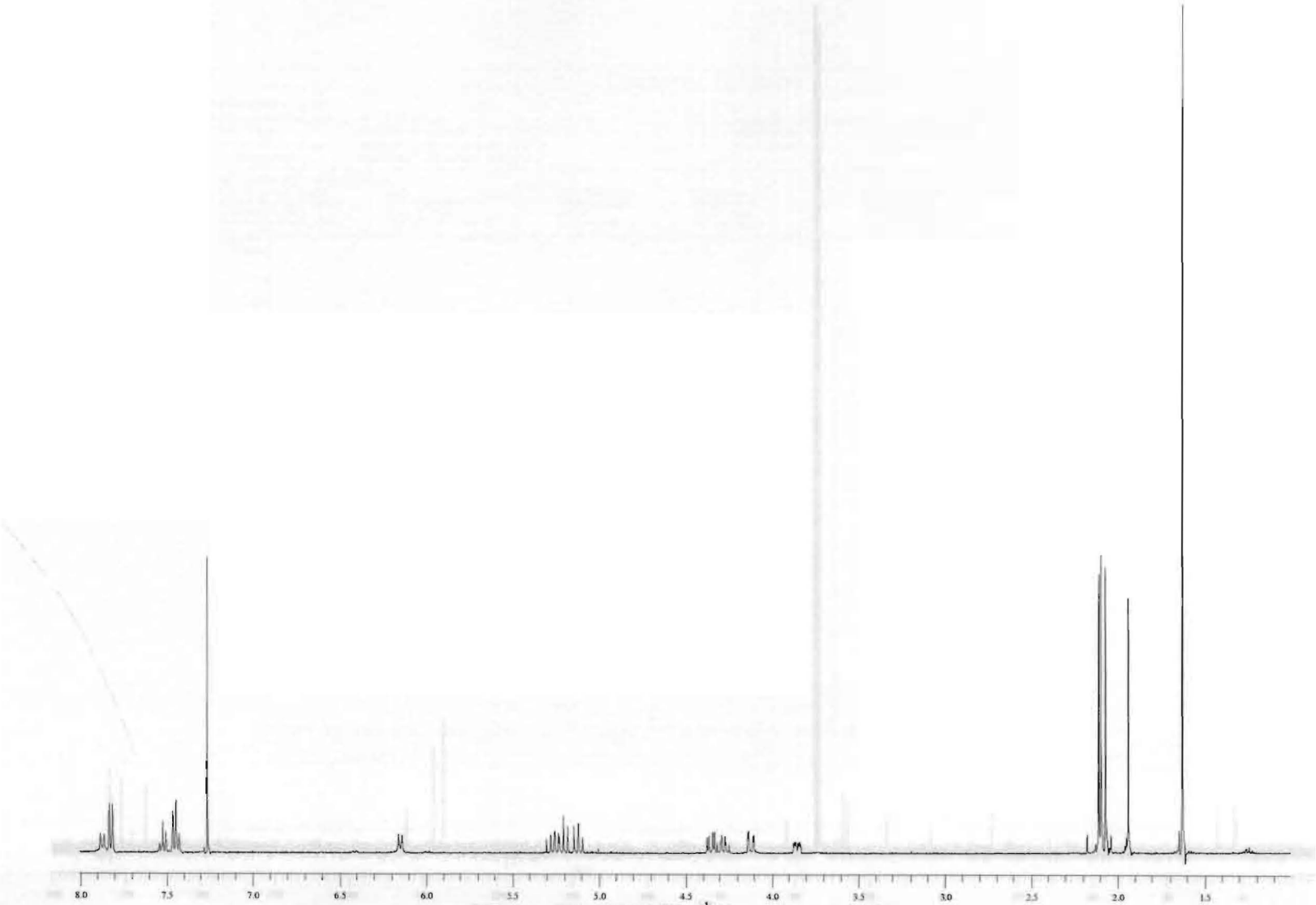

Figure 54: 400 MHz ^{1}H spectrum of **21**

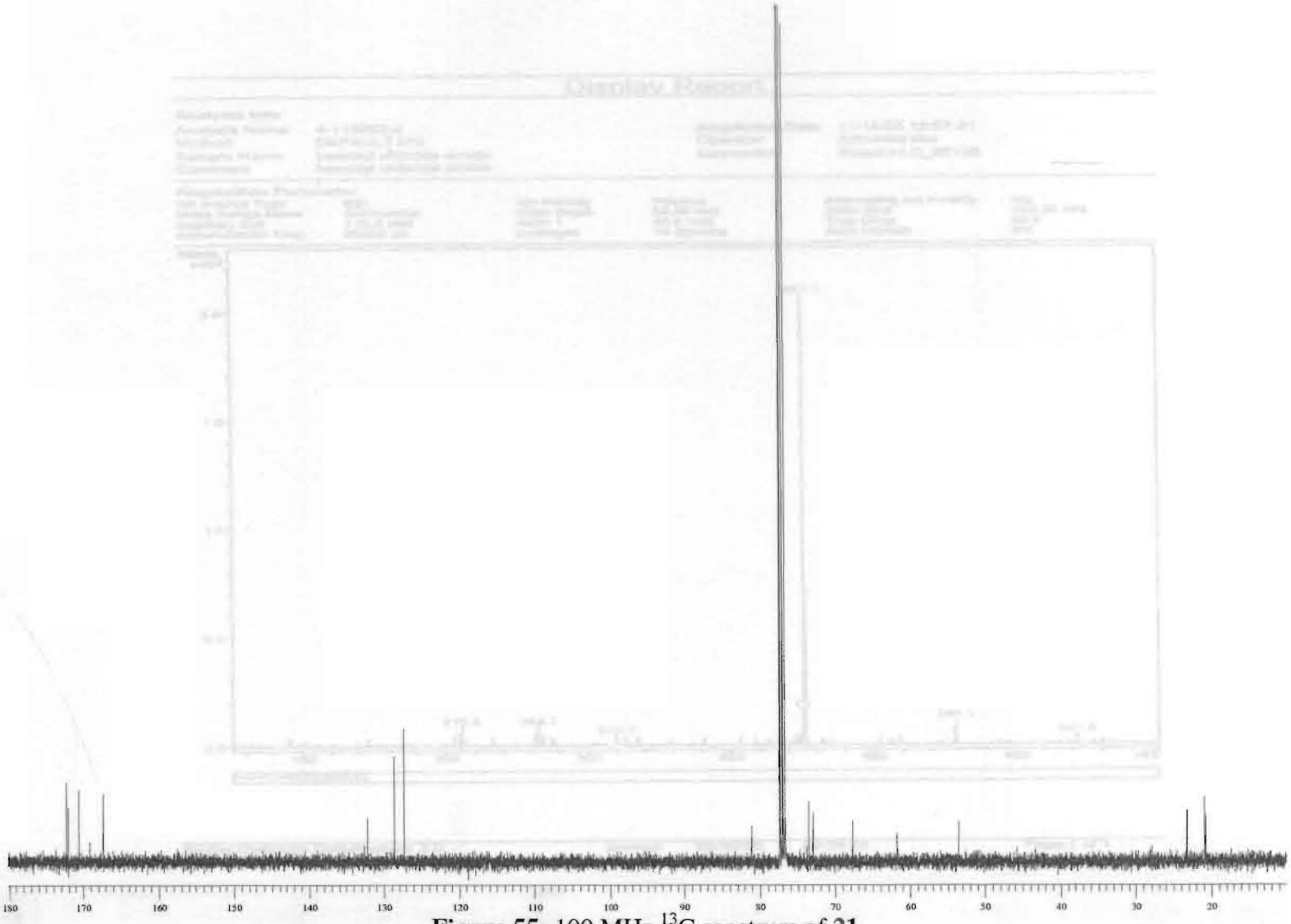

Figure 55: 100 MHz ^{13}C spectrum of **21**

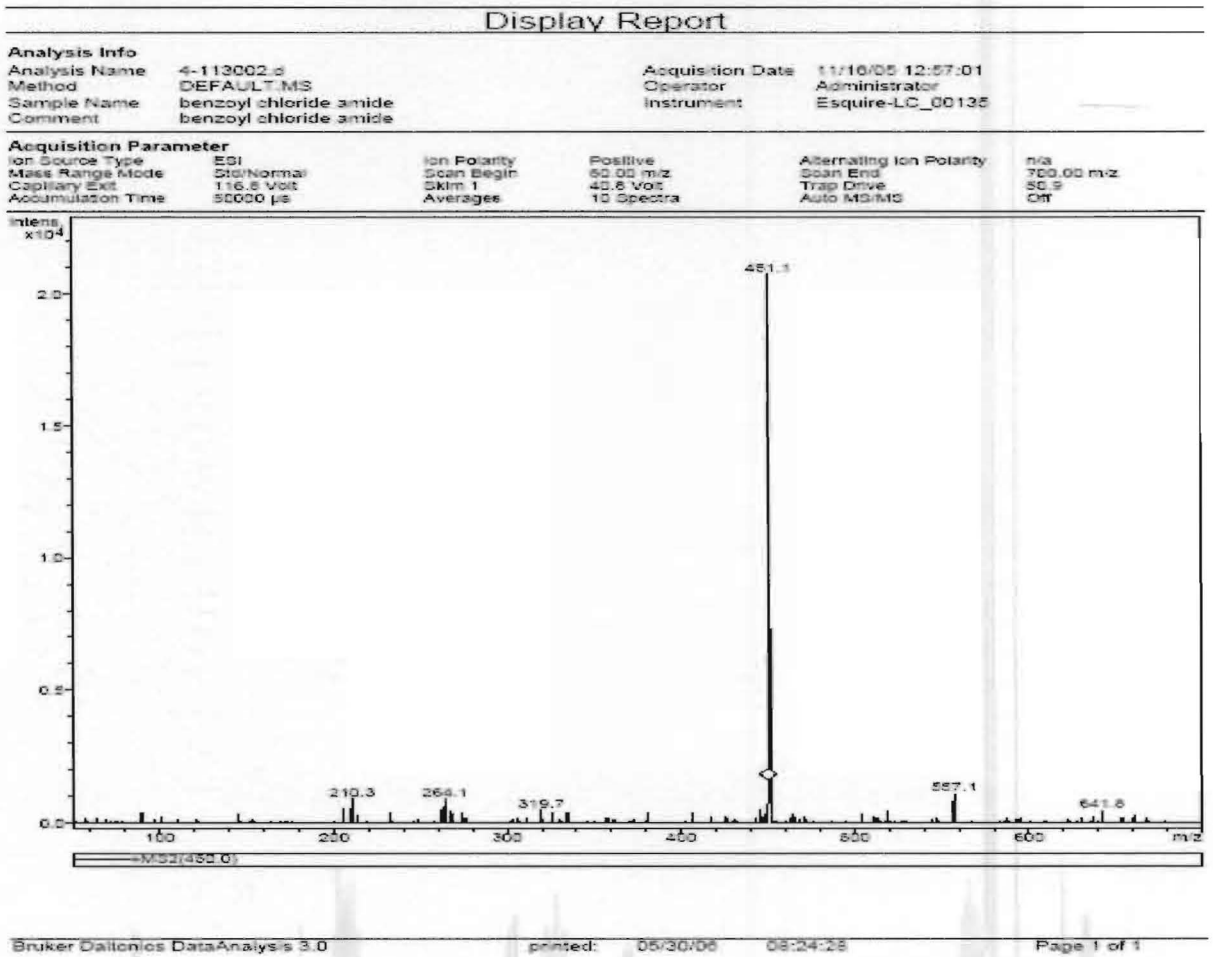

Figure 56: Mass spectrum of **21**

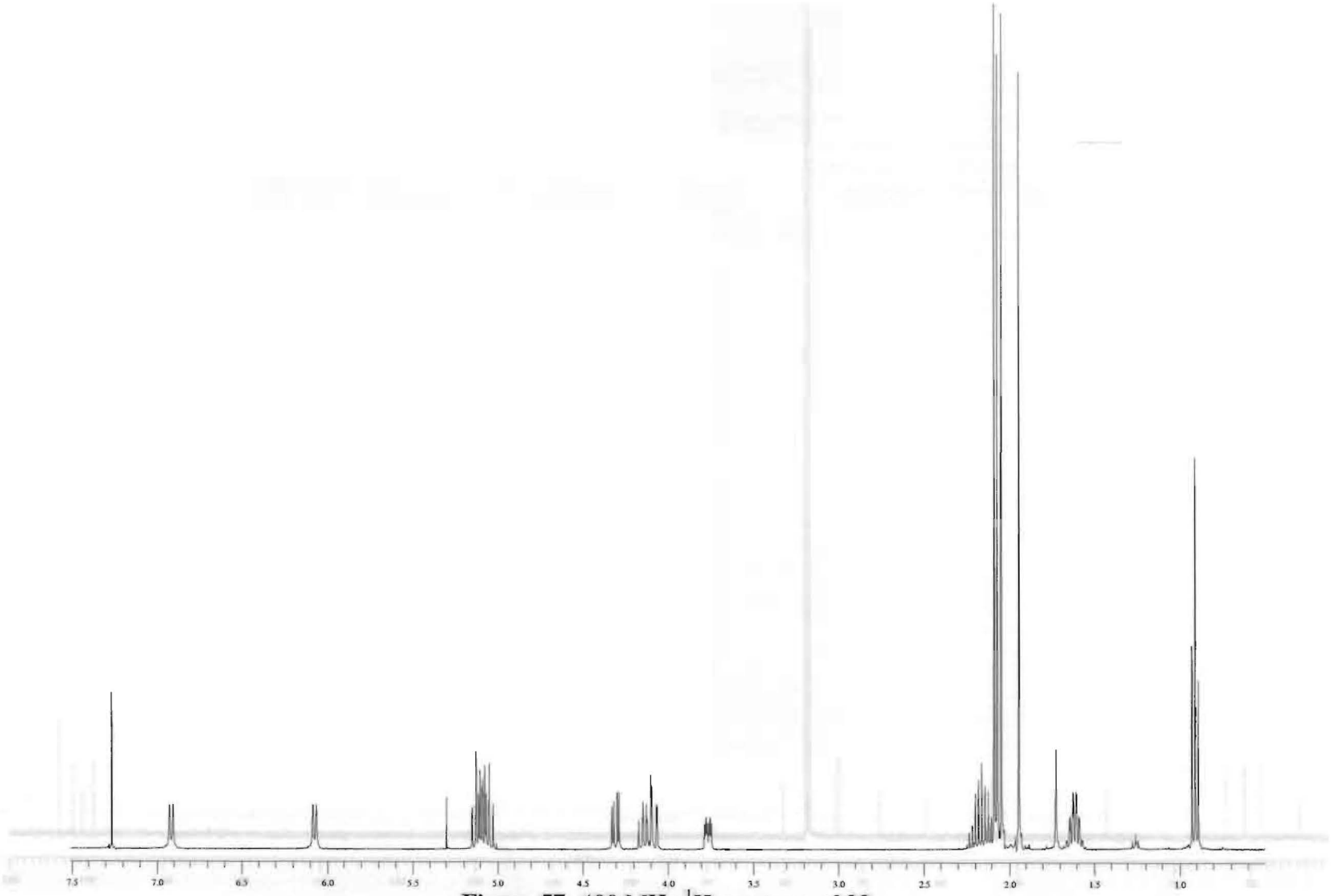

Figure 57: 400 MHz ^{1}H spectrum of **22**

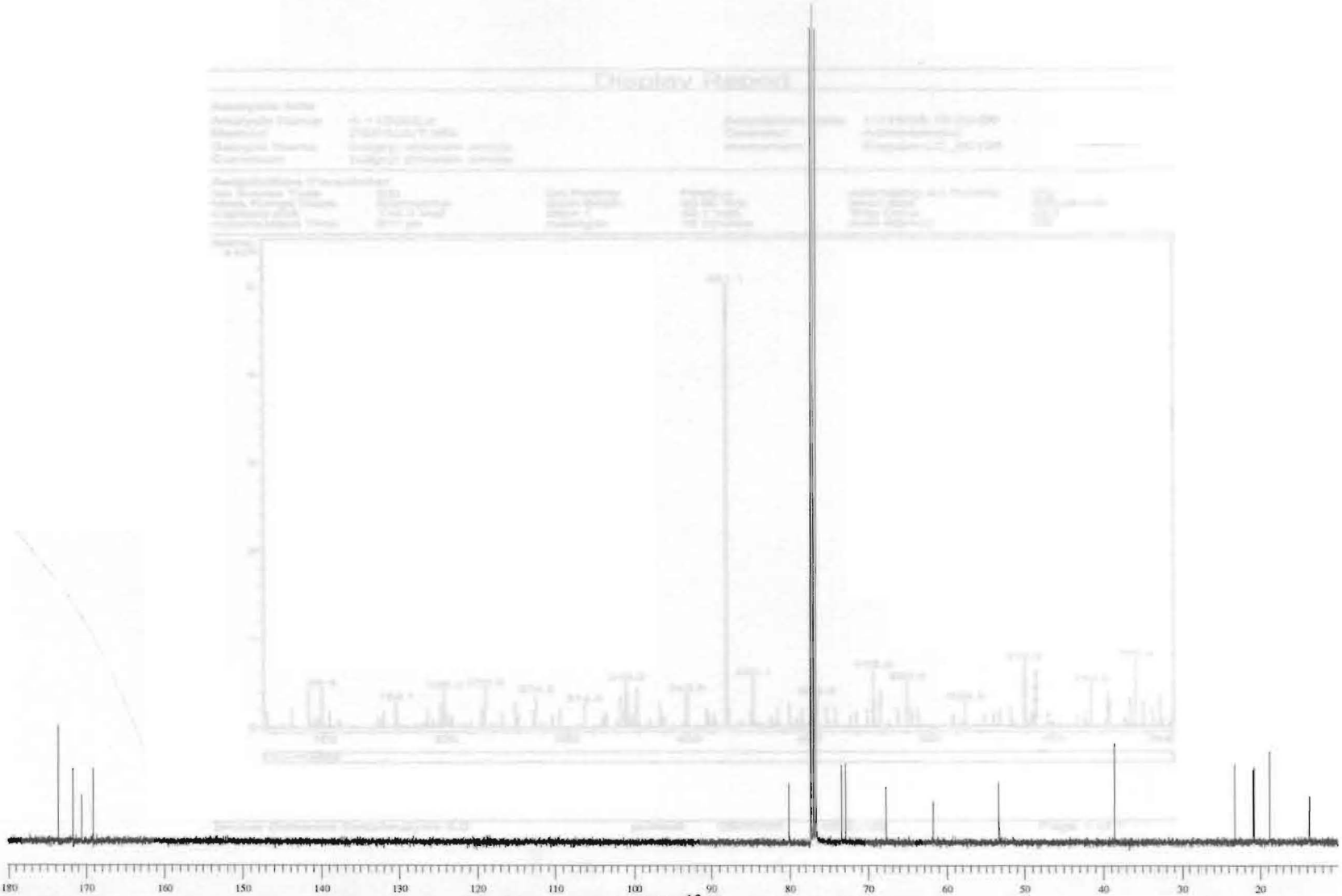

Figure 58: 100 MHz ^{13}C spectrum of **22**

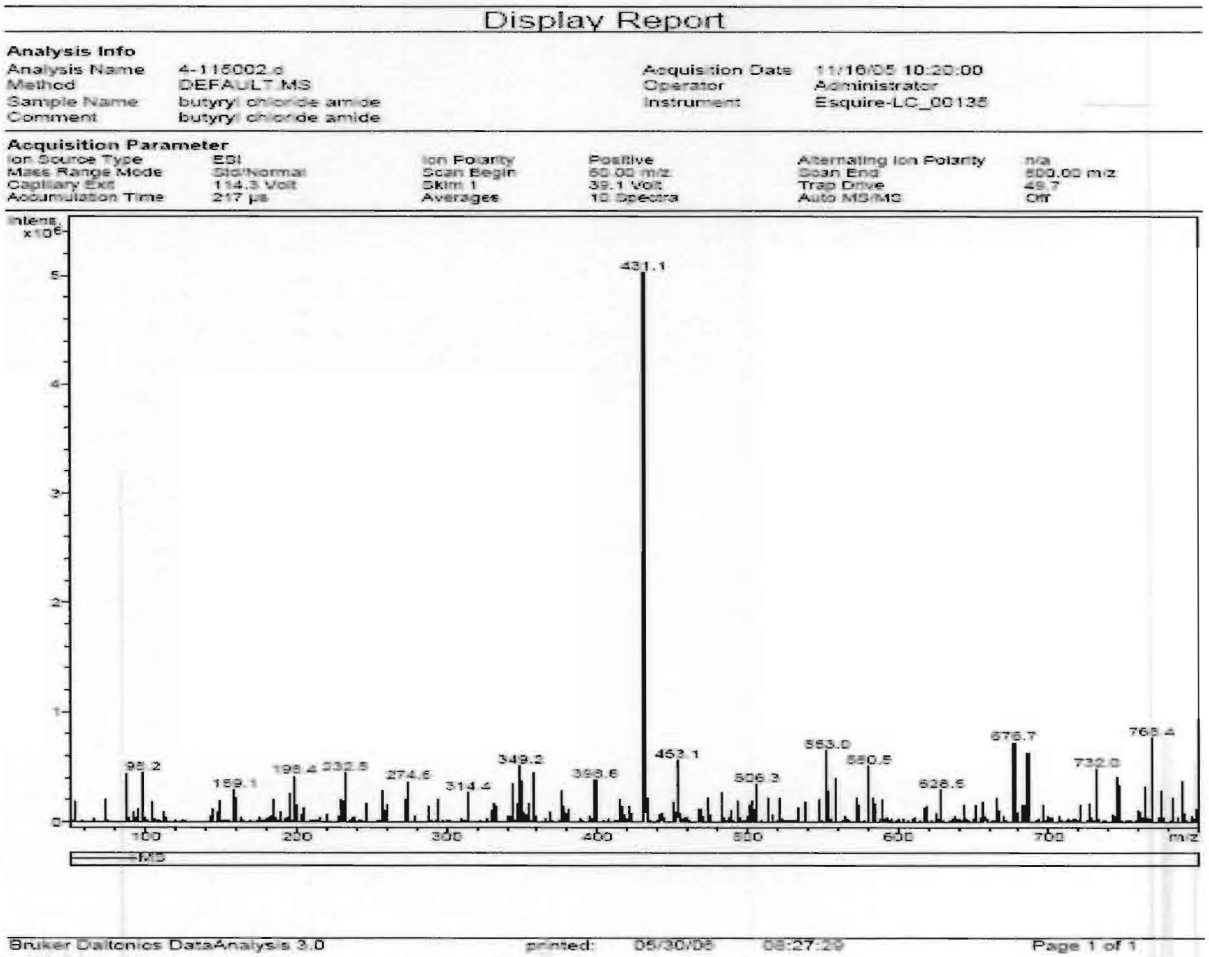

Figure 59: Mass spectrum of **22**

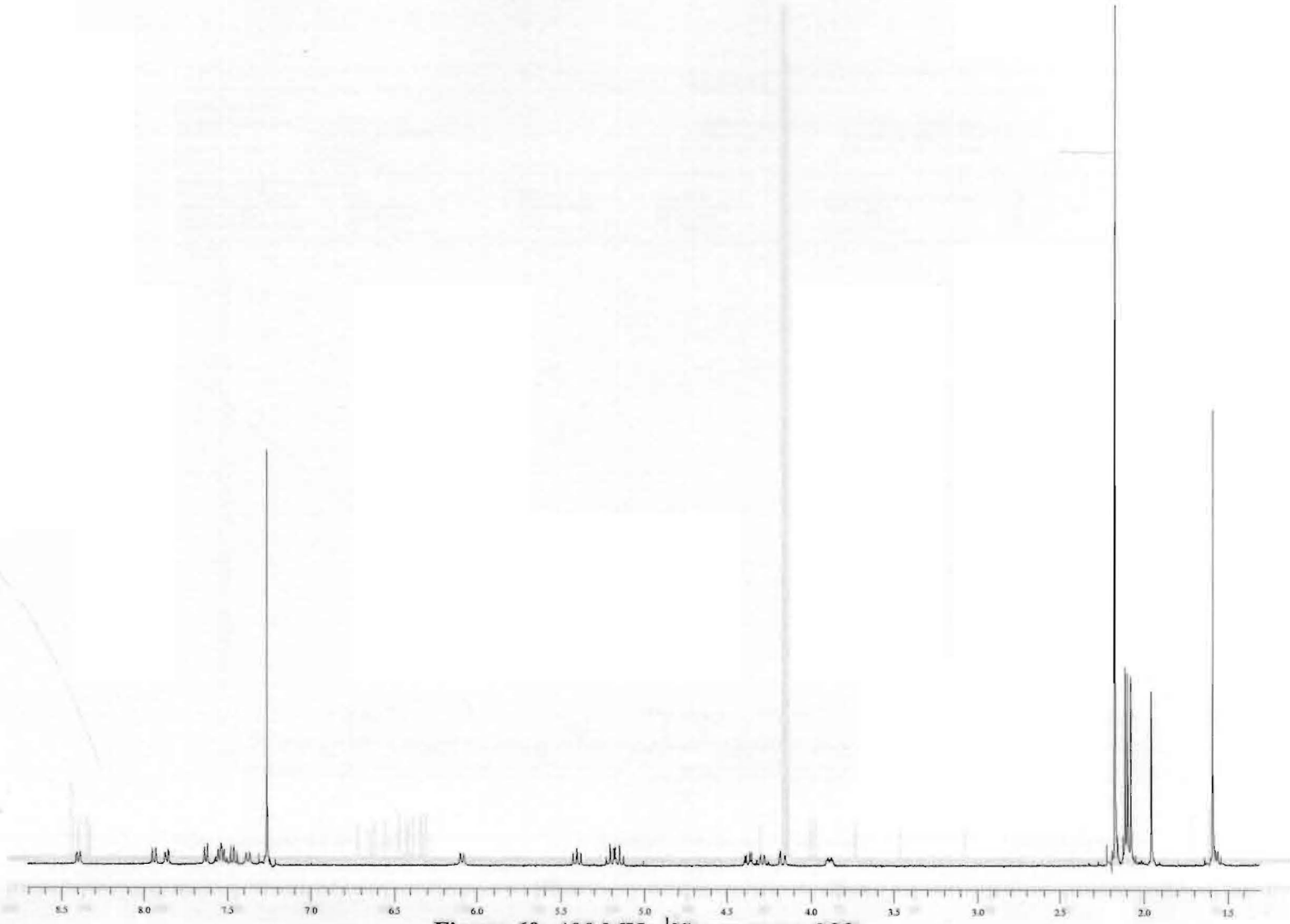

Figure 60: 400 MHz ^{1}H spectrum of **23**

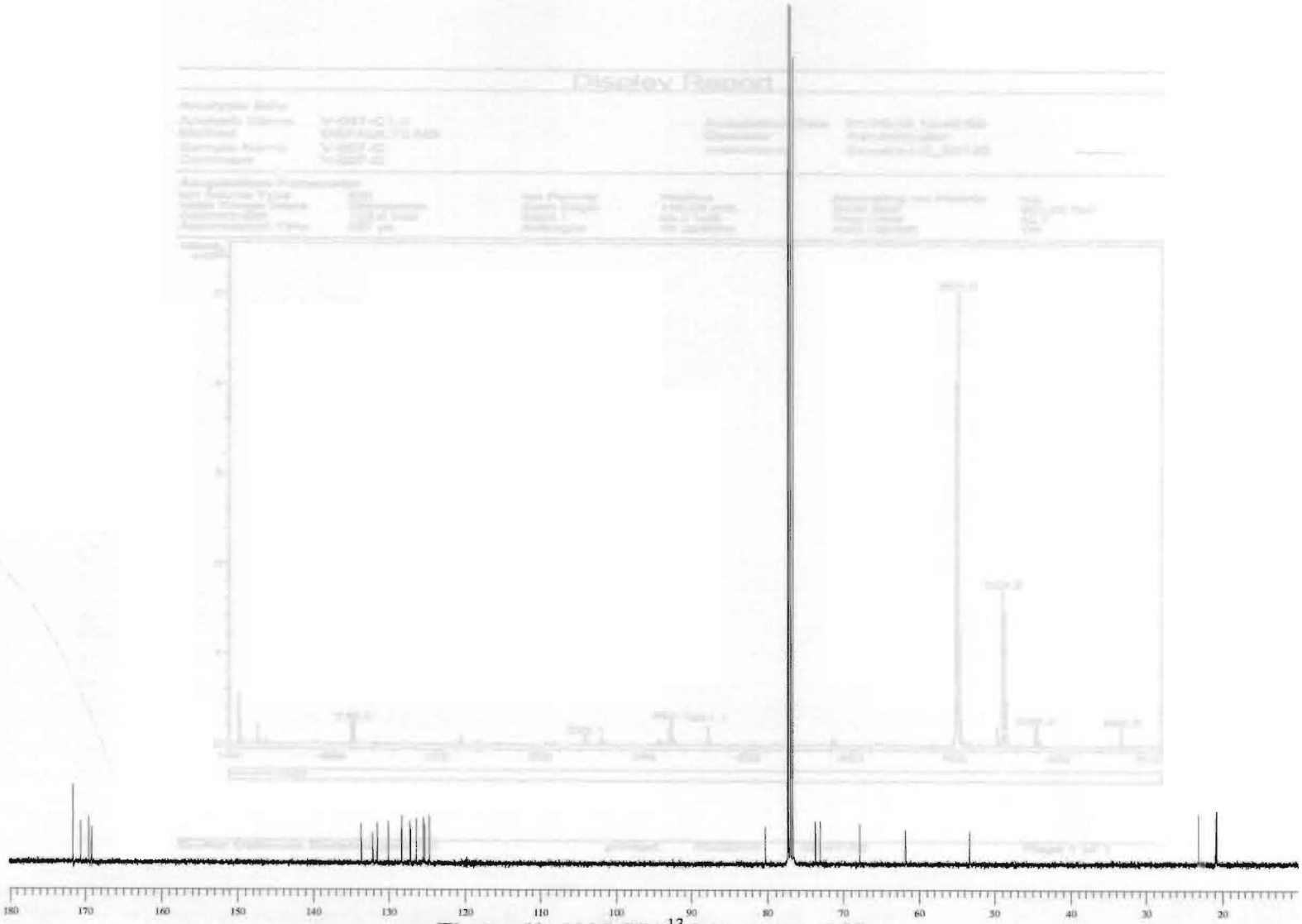

Figure 61: 100 MHz ^{13}C spectrum of **23**

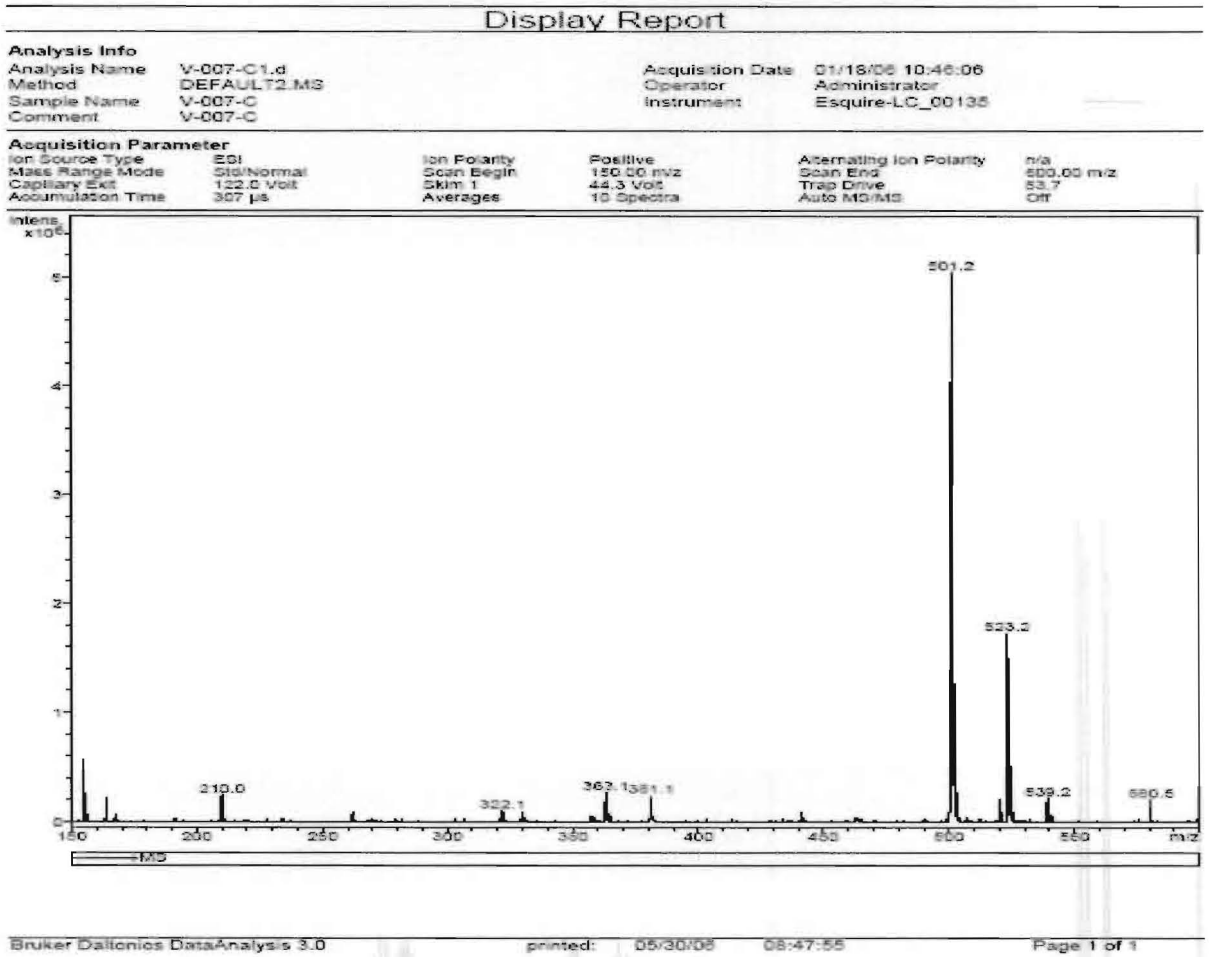

Figure 62: Mass spectrum of **23**

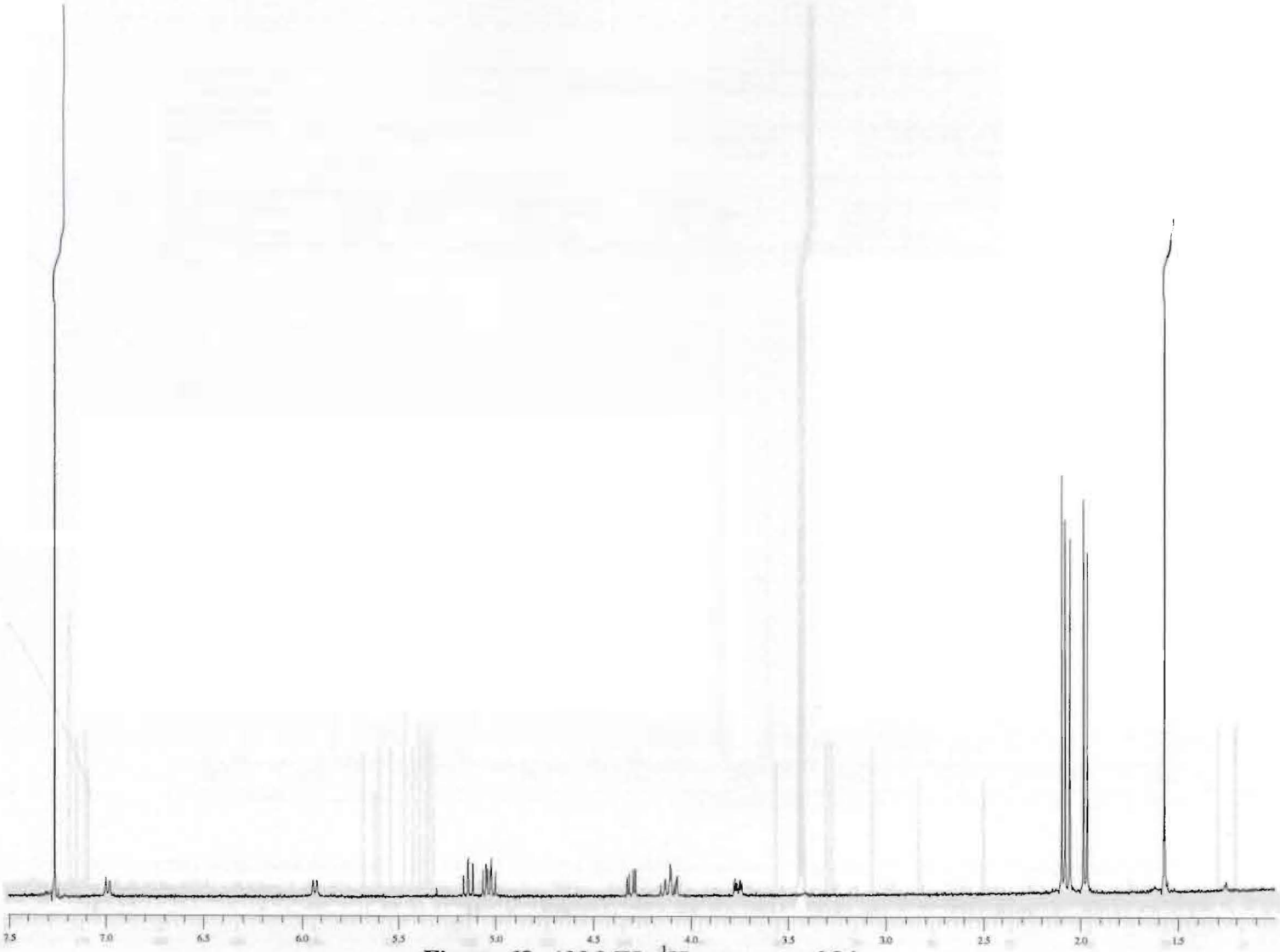

Figure 63: 400 MHz ^{1}H spectrum of **24**

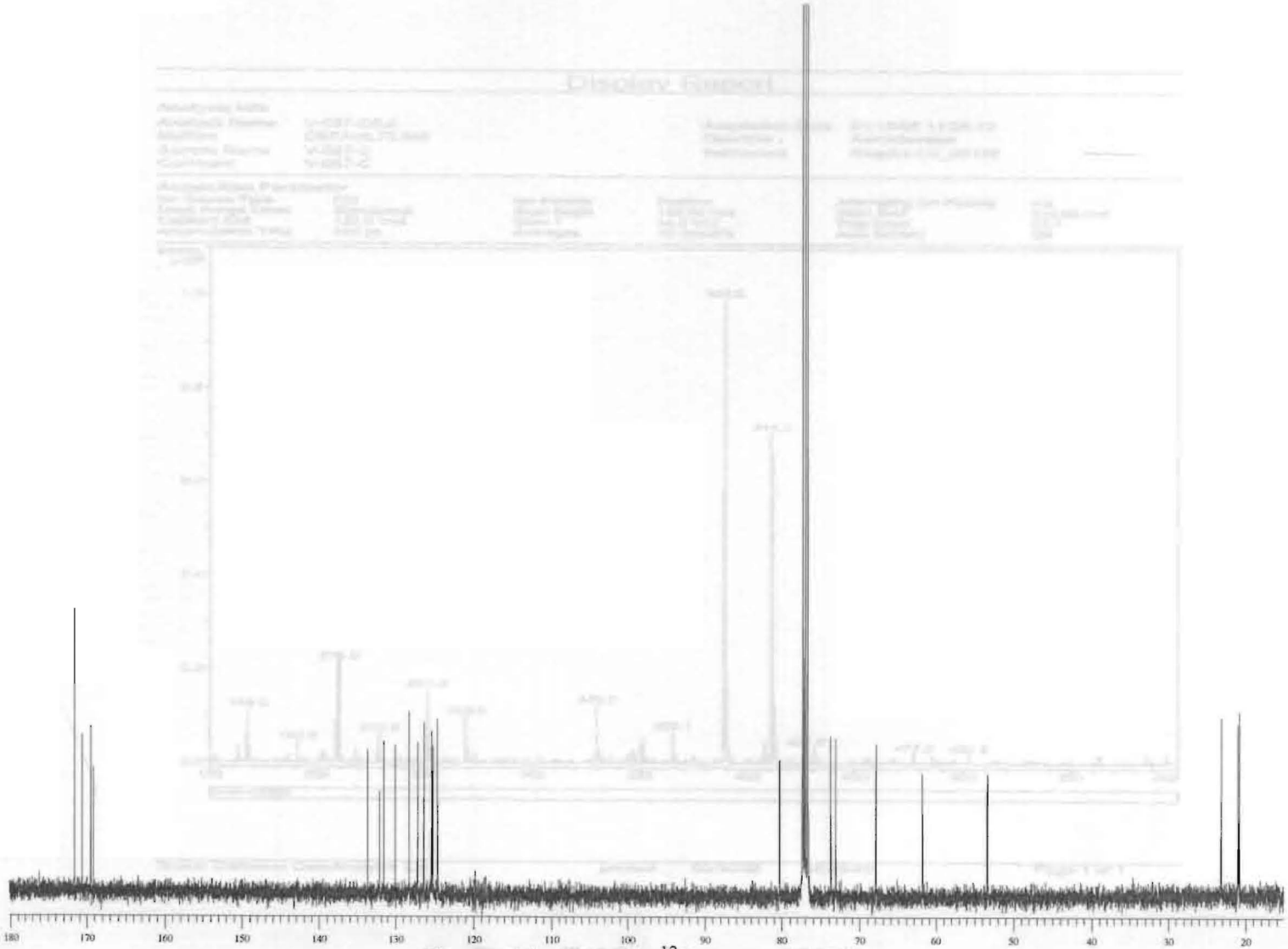

Figure 64: 100 MHz ^{13}C spectrum of **24**

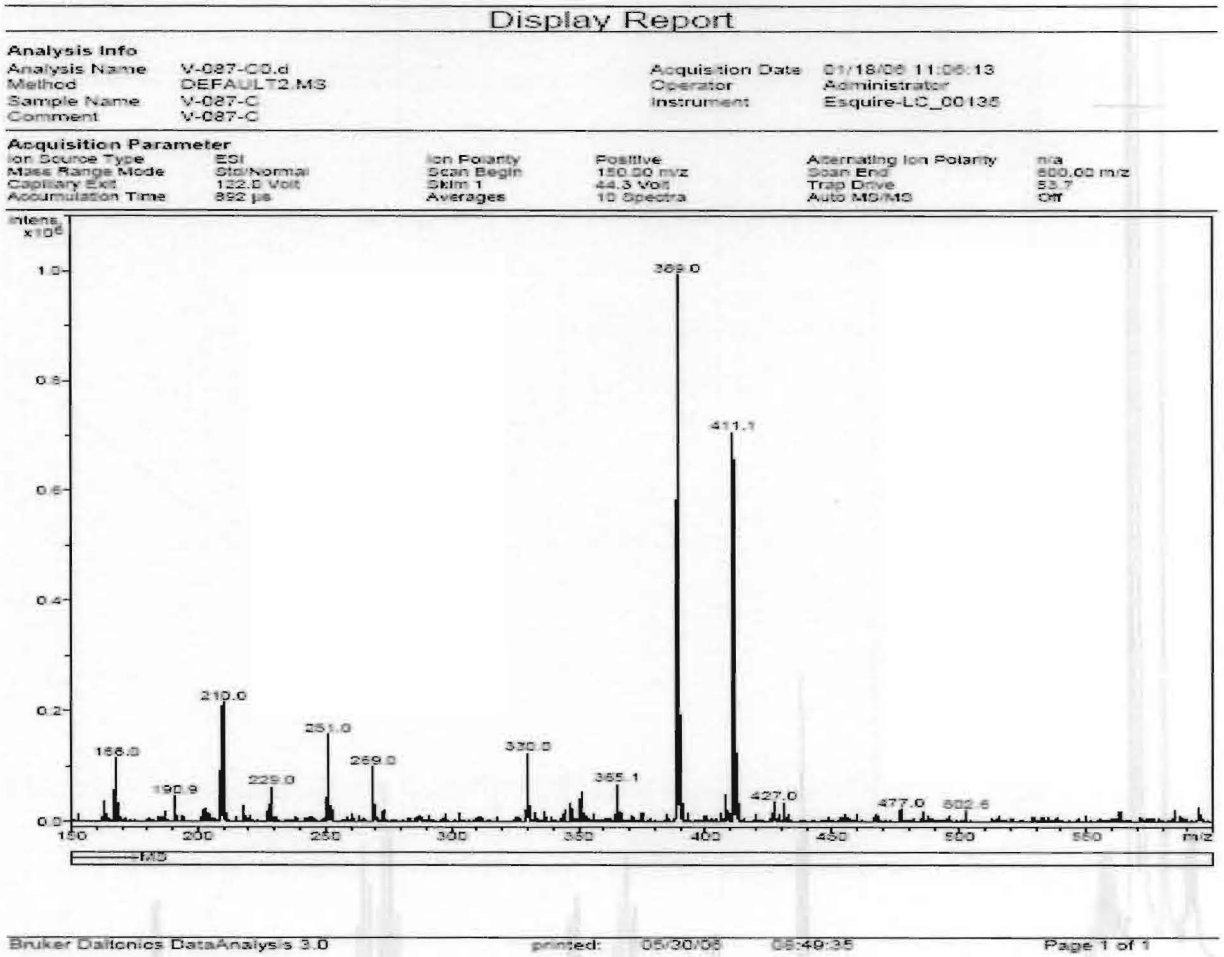

Figure 65: Mass spectrum of **24**

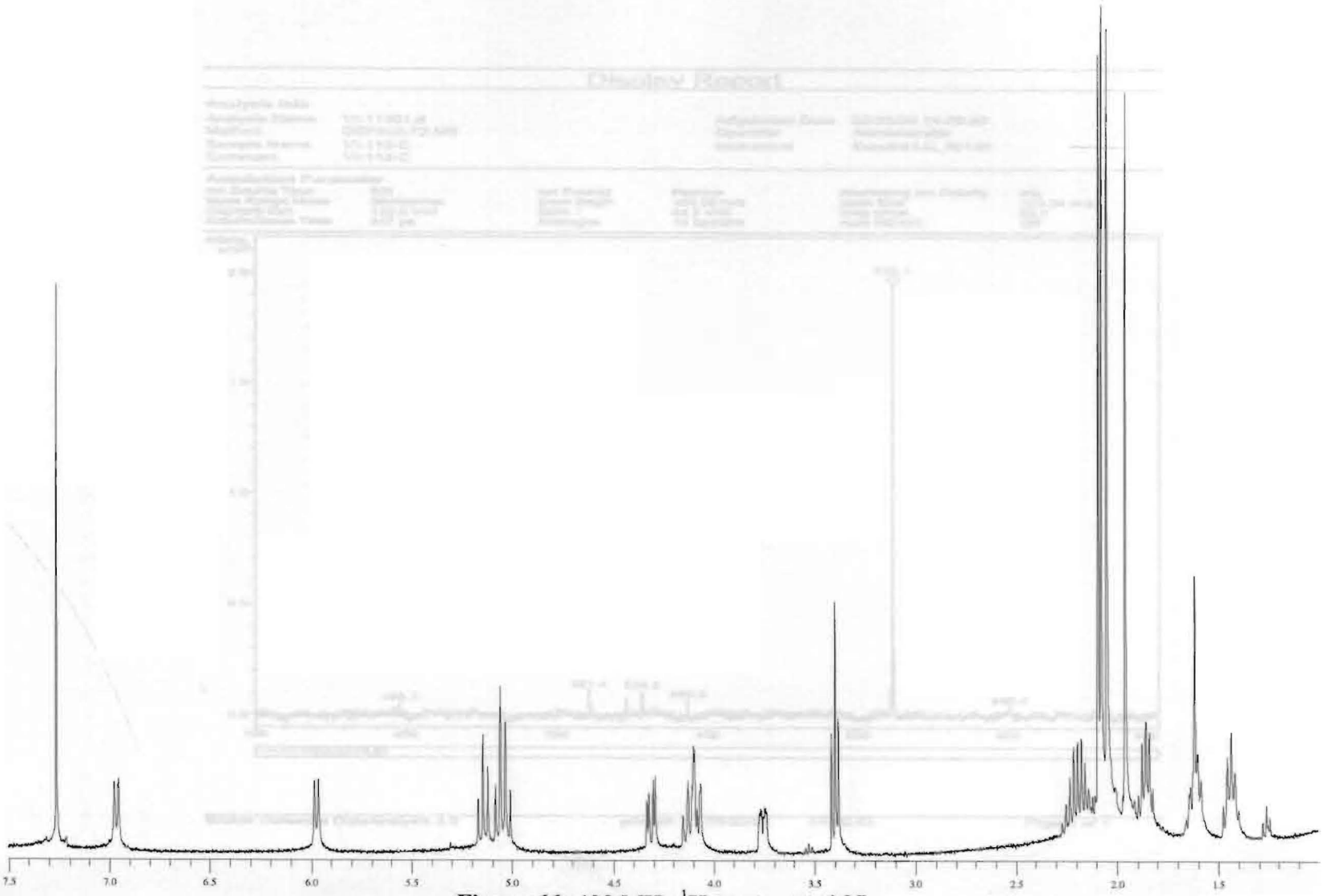

Figure 66: 400 MHz ^{1}H spectrum of **25**

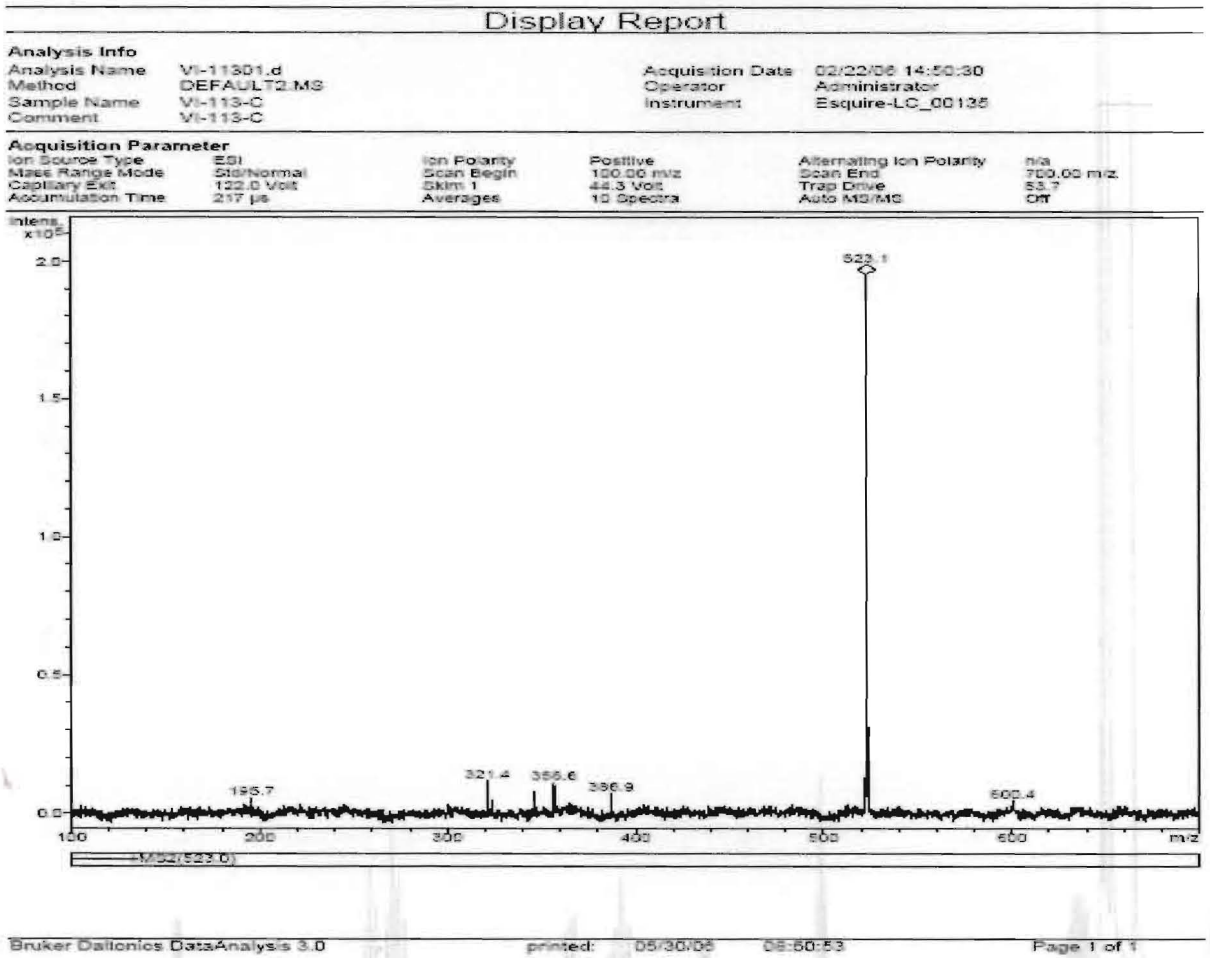

Figure 67: Mass spectrum of **25**

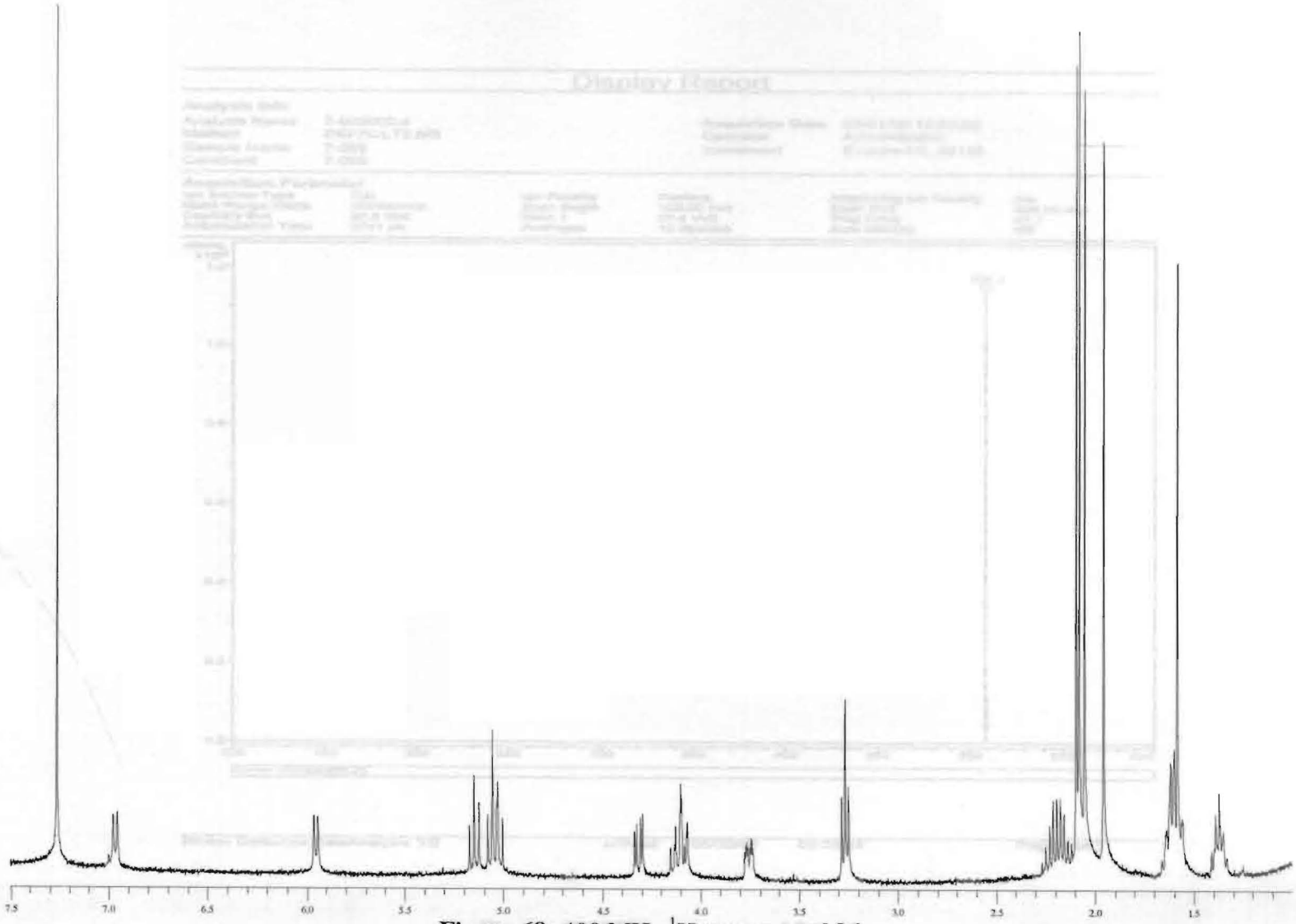

Figure 68: 400 MHz ^{1}H spectrum of **26**

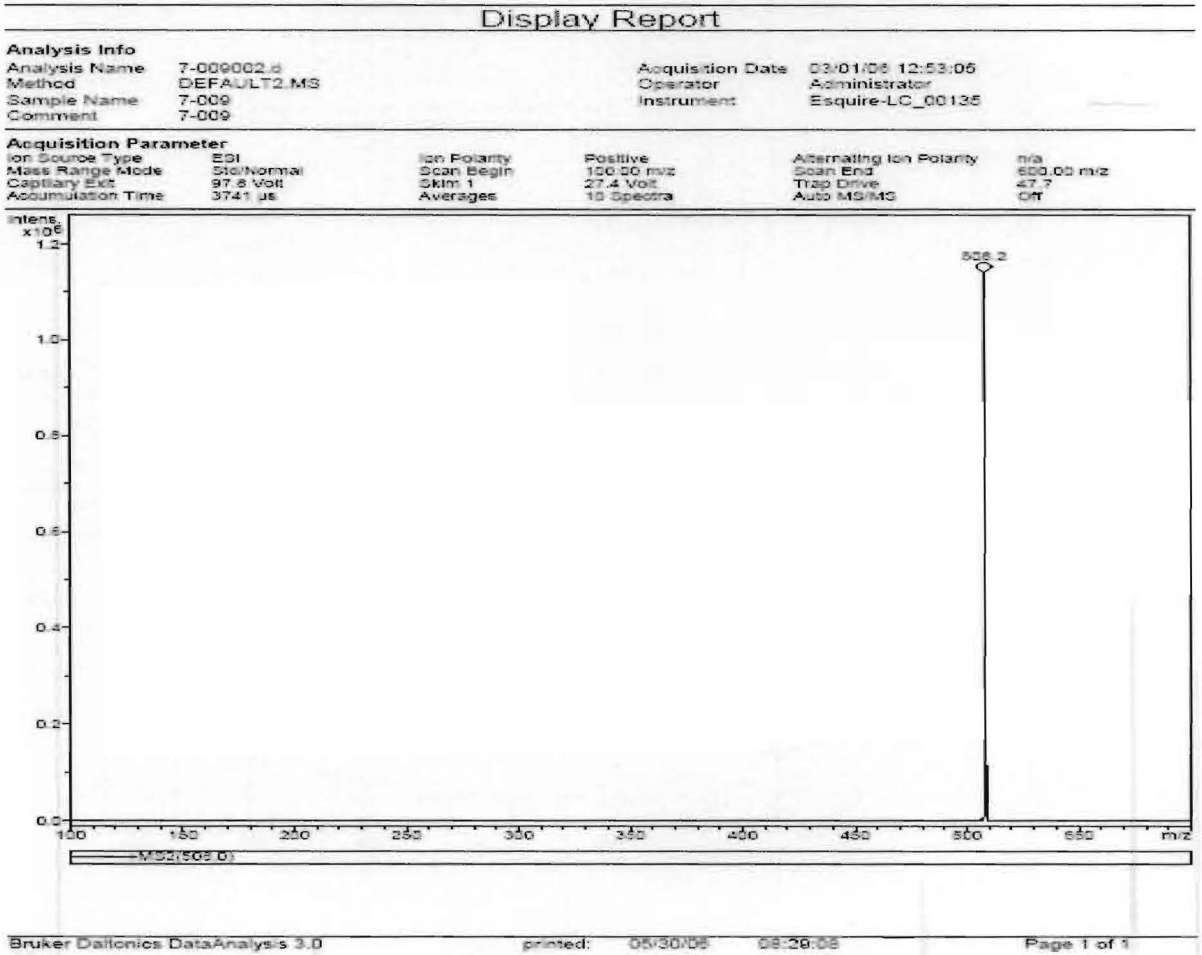

Figure 69: Mass spectrum of **26**

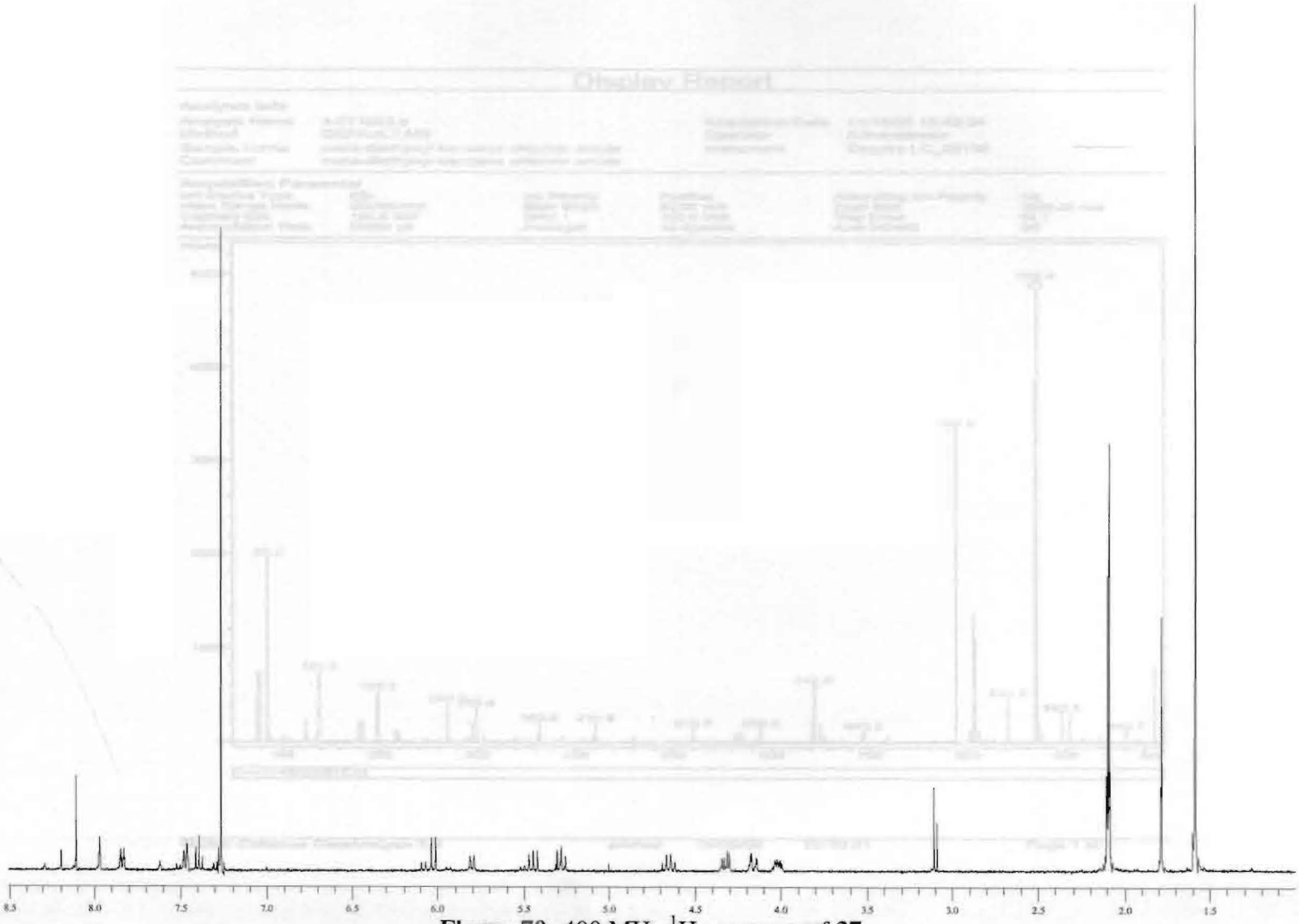

Figure 70: 400 MHz ^{1}H spectrum of **37**

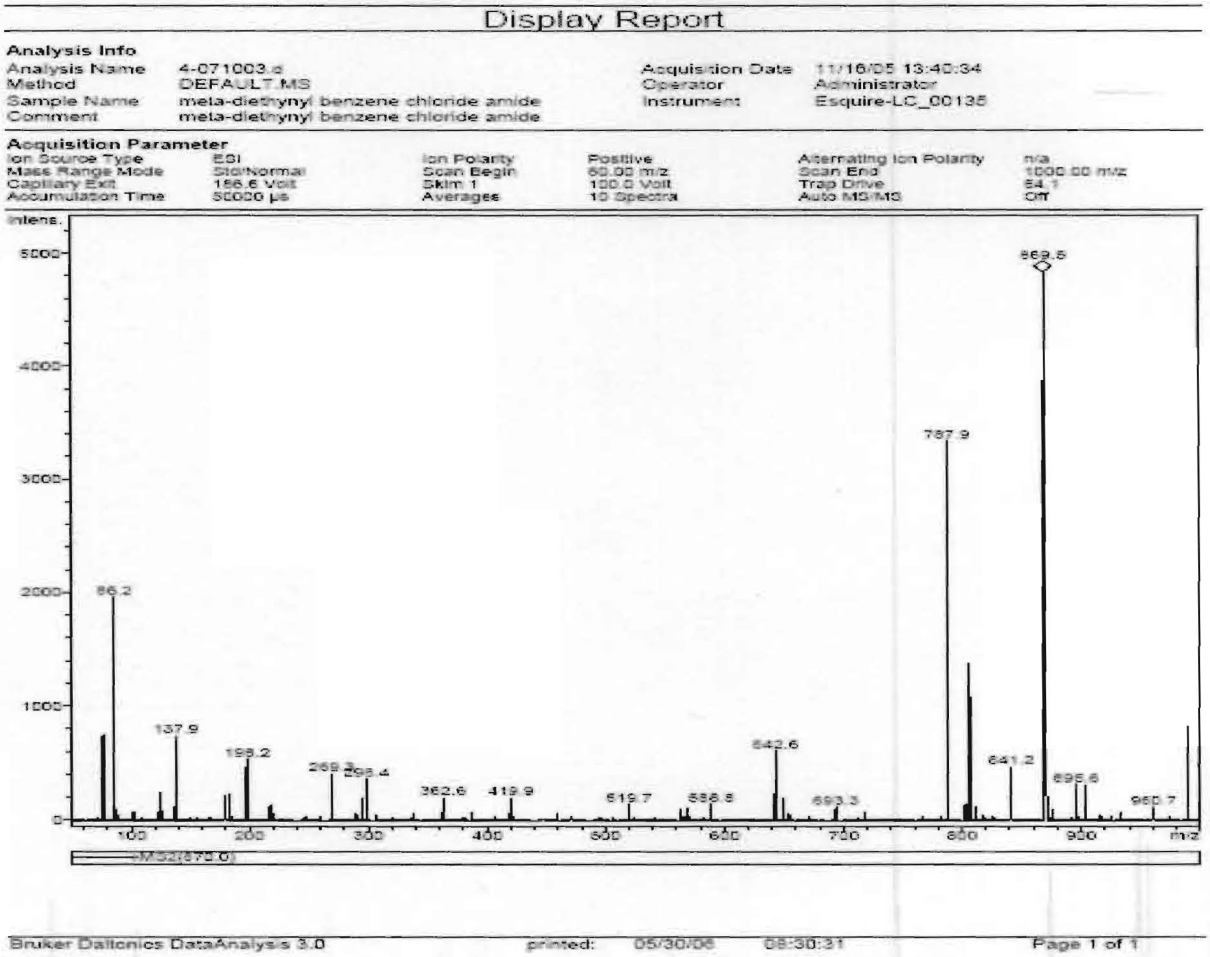

Figure 71: Mass spectrum of **37**

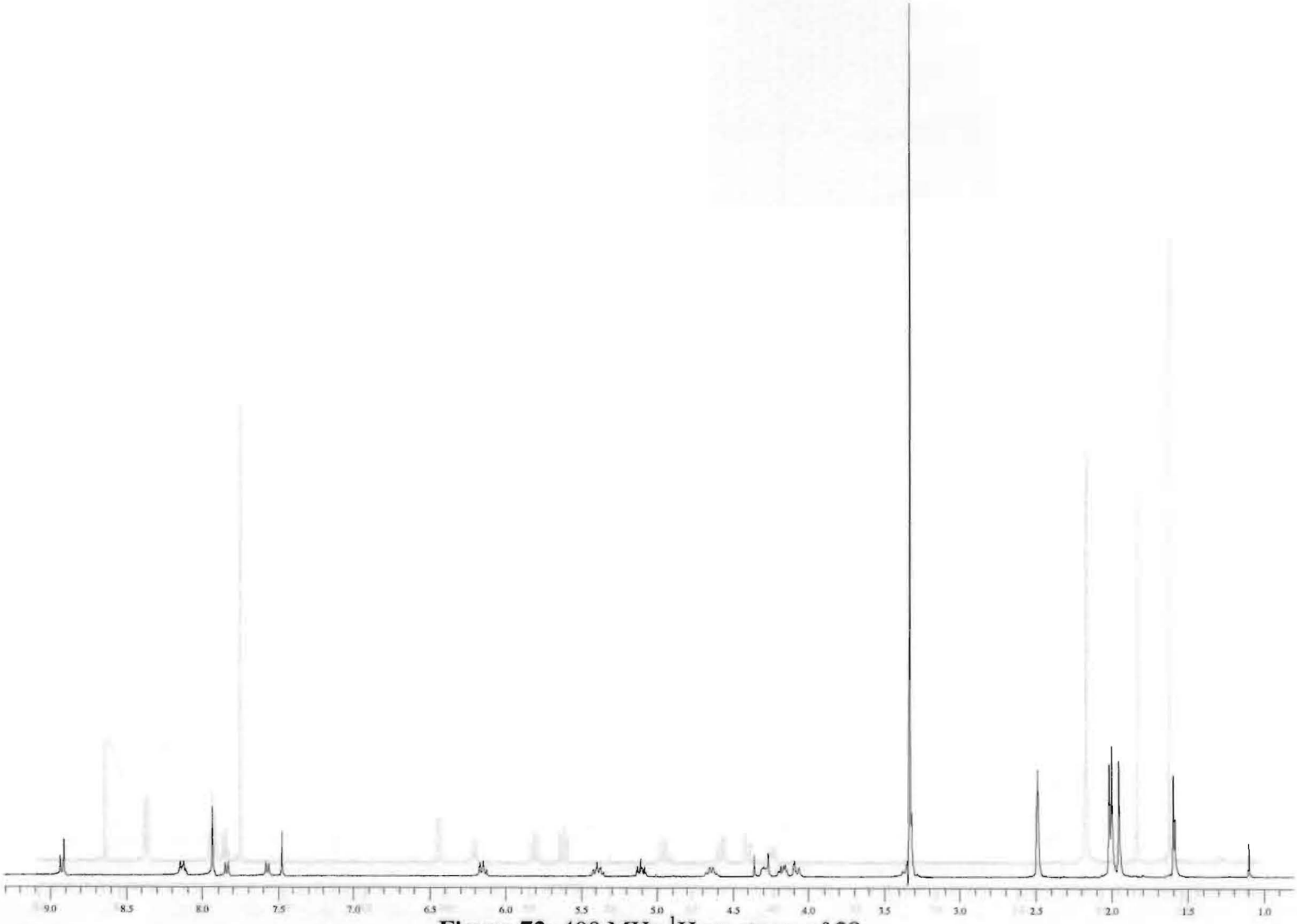

Figure 72: 400 MHz ^{1}H spectrum of **38**

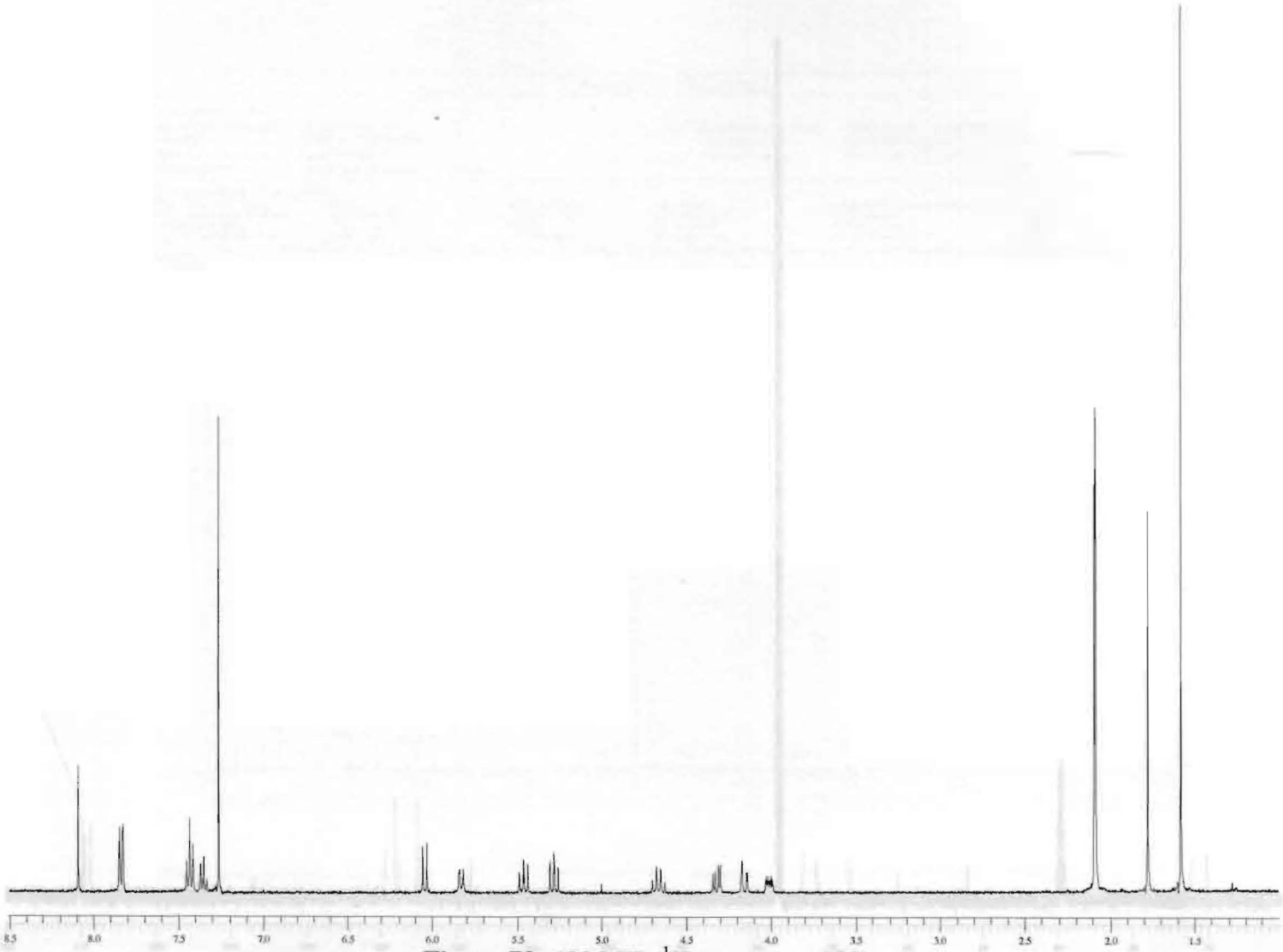

Figure 73: 400 MHz ^{1}H spectrum of **39**

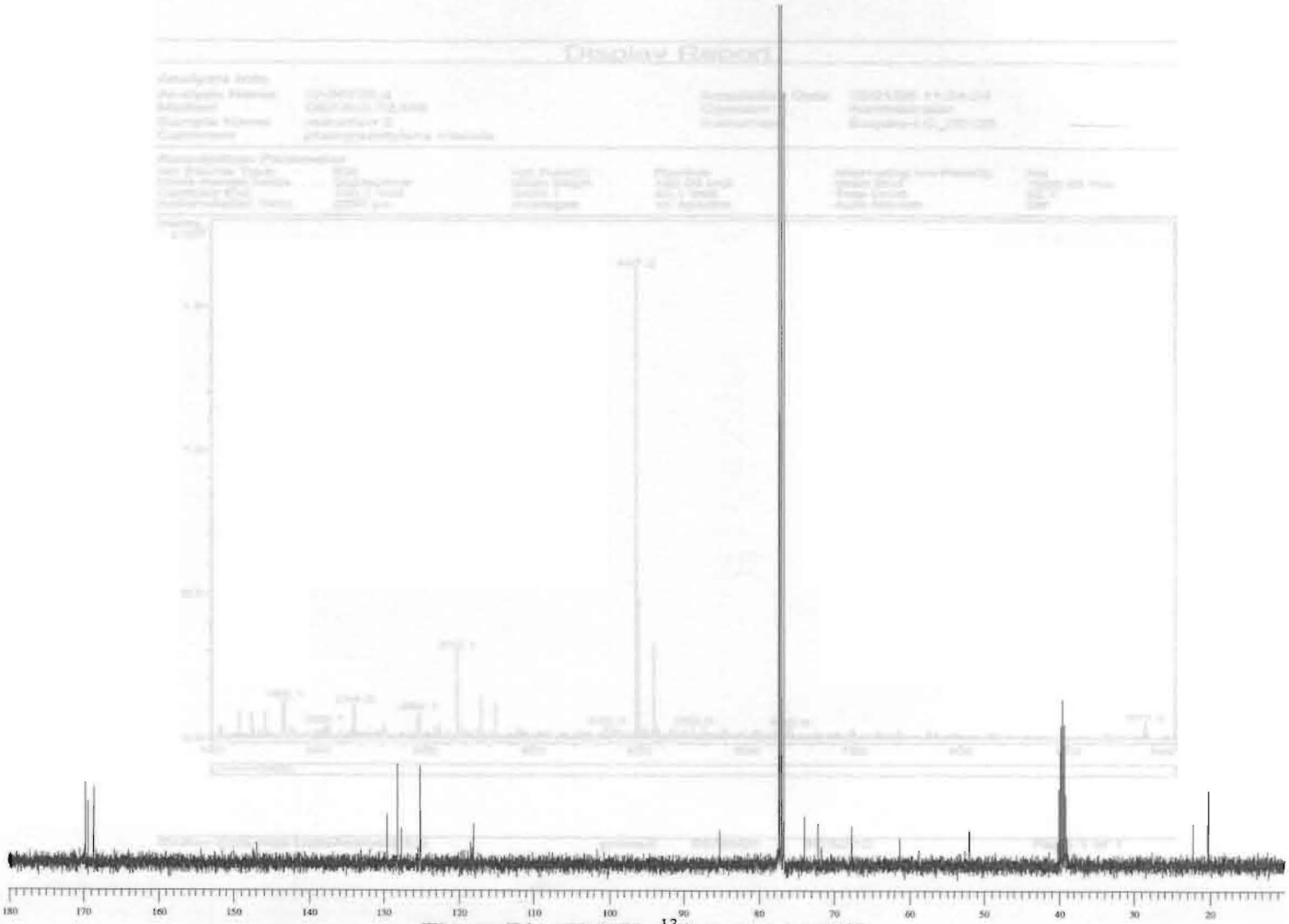

Figure 74: 100 MHz ^{13}C spectrum of **39**

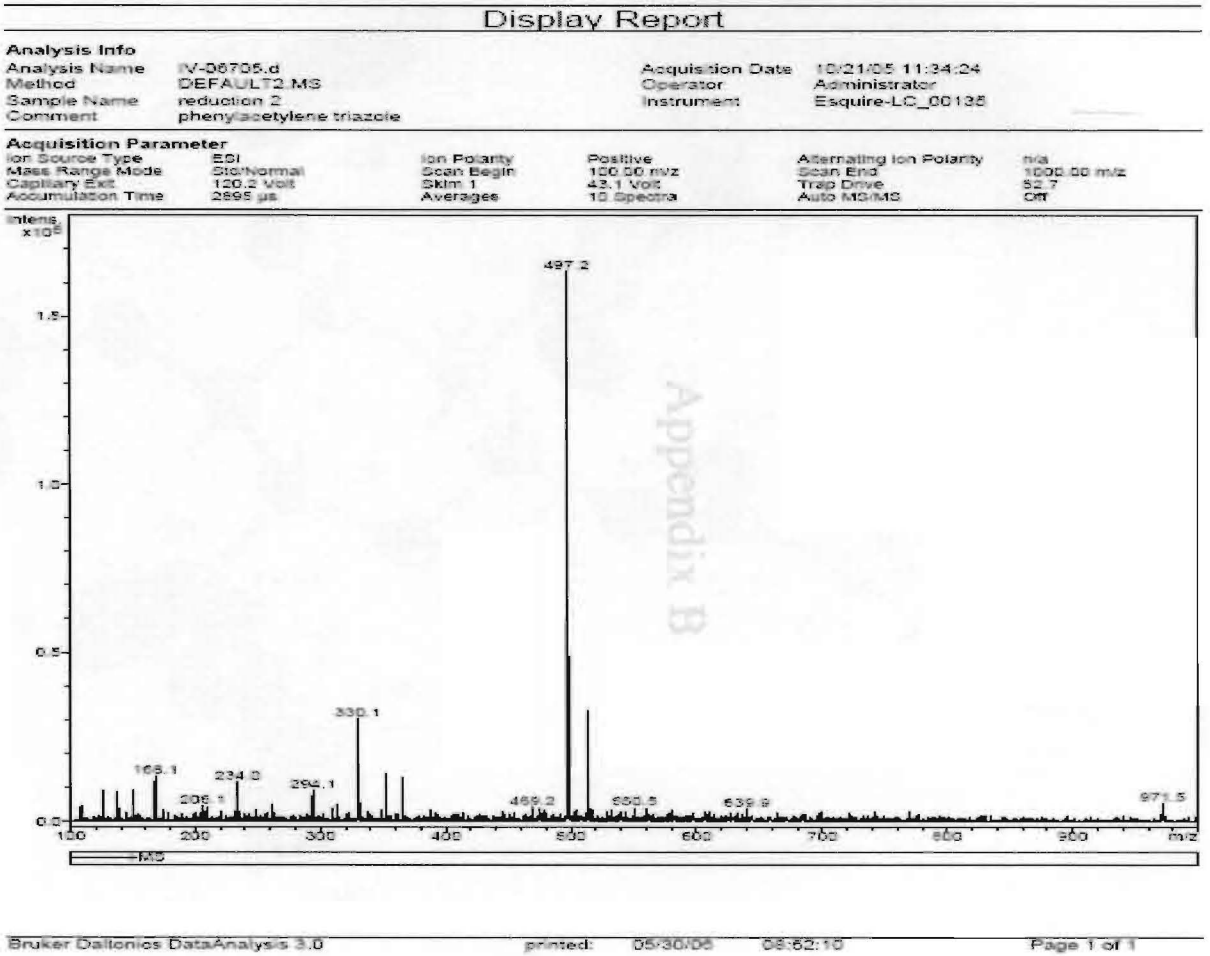

Figure 75: Mass spectrum of **39**

Appendix B

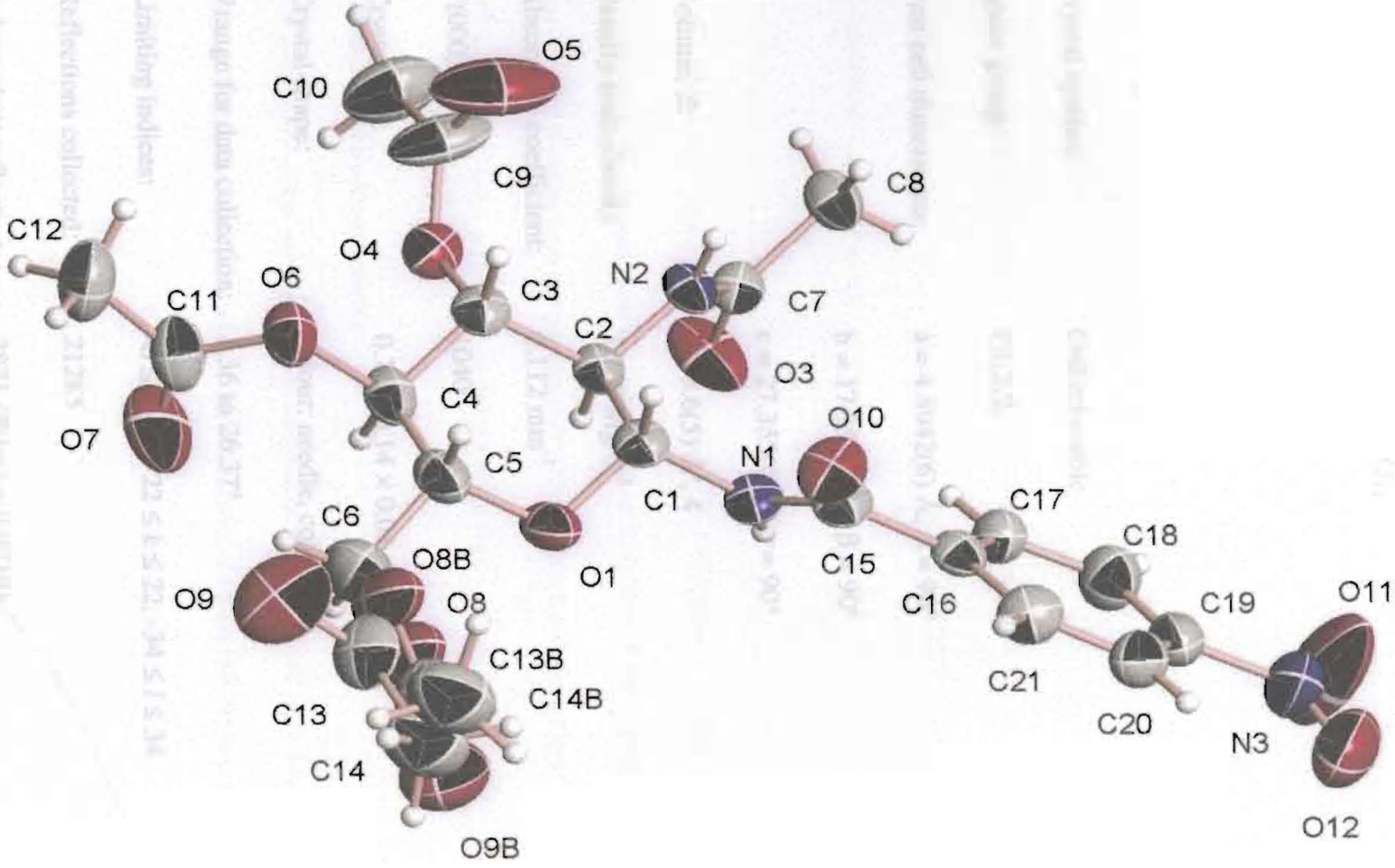

Figure 76: X-Ray crystal structure of **19**

Table 3: Crystal data and structure refinement for **19**

Empirical formula:	$C_{21}H_{25}N_3O_{11}$
Formula weight:	495.44
Temperature:	298(2) K
Wavelength:	0.71073 Å
Crystal system:	Orthorhombic
Space group:	$P2_12_12_1$
Unit cell dimensions:	a = 4.8942(6) Å, α = 90°
	b = 17.953(2) Å, β = 90°
	c = 27.355(4) Å, γ = 90°
Volume, Z:	2403.6(5) $Å^3$, 4
Density (calculated):	1.369 Mg/m^3
Absorption coefficient:	0.112 mm^{-1}
F(000):	1040
Crystal size:	0.71 × 0.14 × 0.08 mm
Crystal shape:	colour: needle, colourless
θ range for data collection:	1.36 to 26.37°
Limiting indices:	$-6 \leq h \leq 6$, $-22 \leq k \leq 22$, $-34 \leq l \leq 34$
Reflections collected:	21285
Independent reflections:	2871 (*R*(int) = 0.0719)

Completeness to $\theta = 26.37°$: 100.0 %

Absorption correction: multi-scan

Max. and min. transmission: 1 and 0.652958

Refinement method: Full-matrix least-squares on F^2

Data / restraints / parameters: 2871 / 57 / 345

Goodness-of-fit on F^2: 1.082

Final R indices [$I>2\sigma(I)$]: R1 = 0.0767, wR2 = 0.1910

R indices (all data): R1 = 0.1139, wR2 = 0.2132

Largest diff. peak and hole: 0.338 and -0.249 e × Å^{-3}

Refinement of F^2 against ALL reflections. The weighted R-factor wR and goodness of fit are based on F^2, conventional R-factors R are based on F, with F set to zero for negative F^2. The threshold expression of $F^2 > 2\sigma(F^2)$ is used only for calculating R-factors

Treatment of hydrogen atoms:

All hydrogen atoms were placed in calculated positions and were isotropically refined with a displacement parameter 1.5 (methyl) or 1.2 times (all others) that of the adjacent carbon atom.

Table 4: Atomic coordinates [$\times 10^4$] and equivalent isotropic displacement parameters [$Å^2 \times 10^3$] for **19**.

U(eq) is defined as one third of the trace of the orthogonalized U_{ij} tensor.

	x	y	z	U(eq)
C(1)	4082(10)	9773(3)	1537(2)	59(1)
C(2)	5507(9)	9179(3)	1251(2)	55(1)
C(3)	4508(11)	8428(3)	1424(2)	65(1)
C(4)	4829(12)	8362(3)	1961(2)	71(2)
C(5)	3653(16)	9016(3)	2226(2)	78(2)
C(6)	4340(30)	9003(5)	2751(3)	126(3)
C(7)	7196(10)	9384(3)	437(2)	60(1)
C(8)	6429(14)	9487(3)	-87(2)	78(2)
C(9)	4958(16)	7467(5)	849(4)	124(3)
C(10)	6830(20)	6932(5)	634(4)	143(4)
C(11)	4730(20)	7199(4)	2374(3)	96(2)
C(12)	3050(20)	6542(4)	2477(3)	127(3)
C(15)	2989(10)	11029(3)	1319(2)	62(1)
C(16)	4021(11)	11736(3)	1114(2)	60(1)
C(17)	6099(14)	11744(3)	772(2)	71(2)
C(18)	6933(18)	12398(4)	568(2)	94(2)
C(19)	5771(16)	13033(4)	720(2)	84(2)
C(20)	3758(17)	13050(3)	1059(3)	89(2)
C(21)	2865(14)	12391(4)	1252(2)	81(2)
N(1)	4834(8)	10502(2)	1389(2)	62(1)
N(3)	6700(30)	13735(4)	501(3)	127(3)
O(1)	4729(9)	9683(2)	2037(1)	77(1)
N(2)	5134(8)	9271(2)	736(1)	59(1)
O(3)	9512(8)	9420(4)	575(2)	109(2)
O(4)	6081(8)	7862(2)	1197(1)	73(1)
O(5)	2809(15)	7601(5)	682(3)	188(4)
O(6)	3413(9)	7701(2)	2112(2)	84(1)
O(7)	6953(15)	7322(4)	2528(2)	142(2)
O(10)	609(8)	10955(3)	1419(2)	89(1)
O(11)	8420(40)	13735(4)	212(3)	269(9)
O(12)	5808(19)	14298(4)	678(3)	153(3)
C(13)	1400(20)	9548(6)	3276(4)	102(3)
C(14)	500(30)	10255(10)	3534(5)	153(6)
O(8)	3520(20)	9643(4)	2993(2)	125(3)
O(9)	571(17)	8965(6)	3367(4)	159(4)
C(13B)	1930(70)	9992(16)	3235(10)	102(3)

C(14B)	-840(110)	10250(40)	3410(18)	153(6)
O(8B)	2040(60)	9384(14)	2968(9)	125(3)
O(9B)	3930(90)	10320(20)	3326(15)	172(17)

All esds (except the esd in the dihedral angle between two l.s. planes) are estimated using the full covariance matrix. The cell esds are taken into account individually in the estimation of esds in distances, angles and torsion angles; correlations between esds in cell parameters are only used when they are defined by crystal symmetry. An approximate (isotropic) treatment of cell esds is used for estimating esds involving l.s. planes.

Table 5: Bond lengths [Å] and angles [deg] for **19**

C(1)-O(1)	1.413(6)
C(1)-N(1)	1.419(6)
C(1)-C(2)	1.496(7)
C(1)-H(1)	0.9800
C(2)-N(2)	1.429(6)
C(2)-C(3)	1.510(7)
C(2)-H(2)	0.9800
C(3)-O(4)	1.419(6)
C(3)-C(4)	1.482(7)
C(3)-H(3)	0.9800
C(4)-O(6)	1.434(6)
C(4)-C(5)	1.495(8)
C(4)-H(4)	0.9800
C(5)-O(1)	1.406(7)
C(5)-C(6)	1.477(9)
C(5)-H(5)	0.9800
C(6)-O(8)	1.385(10)
C(6)-O(8B)	1.44(2)
C(6)-H(6A)	0.9700
C(6)-H(6B)	0.9700
C(7)-O(3)	1.196(6)
C(7)-N(2)	1.315(6)
C(7)-C(8)	1.494(7)
C(8)-H(8A)	0.9600
C(8)-H(8B)	0.9600
C(8)-H(8C)	0.9600
C(9)-O(5)	1.172(10)
C(9)-O(4)	1.307(9)
C(9)-C(10)	1.454(11)
C(10)-H(10A)	0.9600
C(10)-H(10B)	0.9600
C(10)-H(10C)	0.9600
C(11)-O(7)	1.189(10)
C(11)-O(6)	1.320(8)
C(11)-C(12)	1.465(12)
C(12)-H(12A)	0.9600
C(12)-H(12B)	0.9600
C(12)-H(12C)	0.9600
C(15)-O(10)	1.203(6)
C(15)-N(1)	1.321(6)
C(15)-C(16)	1.477(8)
C(16)-C(21)	1.358(8)
C(16)-C(17)	1.383(8)
C(17)-C(18)	1.363(8)
C(17)-H(17)	0.9300

C(18)-C(19)	1.340(9)
C(18)-H(18)	0.9300
C(19)-C(20)	1.353(10)
C(19)-N(3)	1.467(10)
C(20)-C(21)	1.368(9)
C(20)-H(20)	0.9300
C(21)-H(21)	0.9300
N(1)-H(1B)	0.8600
N(3)-O(11)	1.155(14)
N(3)-O(12)	1.204(10)
N(2)-H(2A)	0.8600
C(13)-O(9)	1.149(12)
C(13)-O(8)	1.302(12)
C(13)-C(14)	1.519(17)
C(14)-H(14A)	0.9600
C(14)-H(14B)	0.9600
C(14)-H(14C)	0.9600
C(13B)-O(9B)	1.17(2)
C(13B)-O(8B)	1.31(2)
C(13B)-C(14B)	1.51(2)
C(14B)-H(14D)	0.9600
C(14B)-H(14E)	0.9600
C(14B)-H(14F)	0.9600

O(1)-C(1)-N(1)	108.9(4)
O(1)-C(1)-C(2)	108.7(4)
N(1)-C(1)-C(2)	112.8(4)
O(1)-C(1)-H(1)	108.8
N(1)-C(1)-H(1)	108.8
C(2)-C(1)-H(1)	108.8
N(2)-C(2)-C(1)	111.9(4)
N(2)-C(2)-C(3)	111.8(4)
C(1)-C(2)-C(3)	108.7(4)
N(2)-C(2)-H(2)	108.1
C(1)-C(2)-H(2)	108.1
C(3)-C(2)-H(2)	108.1
O(4)-C(3)-C(4)	108.6(4)
O(4)-C(3)-C(2)	109.0(4)
C(4)-C(3)-C(2)	110.4(4)
O(4)-C(3)-H(3)	109.6
C(4)-C(3)-H(3)	109.6
C(2)-C(3)-H(3)	109.6
O(6)-C(4)-C(3)	107.4(5)
O(6)-C(4)-C(5)	109.0(5)
C(3)-C(4)-C(5)	112.0(4)
O(6)-C(4)-H(4)	109.4

C(3)-C(4)-H(4)	109.4
C(5)-C(4)-H(4)	109.4
O(1)-C(5)-C(6)	106.6(6)
O(1)-C(5)-C(4)	110.3(5)
C(6)-C(5)-C(4)	111.8(6)
O(1)-C(5)-H(5)	109.3
C(6)-C(5)-H(5)	109.3
C(4)-C(5)-H(5)	109.3
O(8)-C(6)-C(5)	112.8(8)
O(8B)-C(6)-C(5)	102.6(14)
O(8)-C(6)-H(6A)	109.0
O(8B)-C(6)-H(6A)	81.8
C(5)-C(6)-H(6A)	109.0
O(8)-C(6)-H(6B)	109.0
O(8B)-C(6)-H(6B)	141.1
C(5)-C(6)-H(6B)	109.0
H(6A)-C(6)-H(6B)	107.8
O(3)-C(7)-N(2)	122.6(5)
O(3)-C(7)-C(8)	122.2(5)
N(2)-C(7)-C(8)	115.1(5)
C(7)-C(8)-H(8A)	109.5
C(7)-C(8)-H(8B)	109.5
H(8A)-C(8)-H(8B)	109.5
C(7)-C(8)-H(8C)	109.5
H(8A)-C(8)-H(8C)	109.5
H(8B)-C(8)-H(8C)	109.5
O(5)-C(9)-O(4)	123.4(8)
O(5)-C(9)-C(10)	122.9(9)
O(4)-C(9)-C(10)	112.8(8)
C(9)-C(10)-H(10A)	109.5
C(9)-C(10)-H(10B)	109.5
H(10A)-C(10)-H(10B)	109.5
C(9)-C(10)-H(10C)	109.5
H(10A)-C(10)-H(10C)	109.5
H(10B)-C(10)-H(10C)	109.5
O(7)-C(11)-O(6)	120.8(8)
O(7)-C(11)-C(12)	126.5(8)
O(6)-C(11)-C(12)	112.5(8)
C(11)-C(12)-H(12A)	109.5
C(11)-C(12)-H(12B)	109.5
H(12A)-C(12)-H(12B)	109.5
C(11)-C(12)-H(12C)	109.5
H(12A)-C(12)-H(12C)	109.5
H(12B)-C(12)-H(12C)	109.5
O(10)-C(15)-N(1)	123.4(6)
O(10)-C(15)-C(16)	120.7(5)

N(1)-C(15)-C(16)	115.9(4)
C(21)-C(16)-C(17)	119.0(5)
C(21)-C(16)-C(15)	119.8(5)
C(17)-C(16)-C(15)	121.1(5)
C(18)-C(17)-C(16)	120.4(6)
C(18)-C(17)-H(17)	119.8
C(16)-C(17)-H(17)	119.8
C(19)-C(18)-C(17)	118.6(7)
C(19)-C(18)-H(18)	120.7
C(17)-C(18)-H(18)	120.7
C(18)-C(19)-C(20)	122.7(6)
C(18)-C(19)-N(3)	118.2(8)
C(20)-C(19)-N(3)	119.1(8)
C(19)-C(20)-C(21)	118.6(6)
C(19)-C(20)-H(20)	120.7
C(21)-C(20)-H(20)	120.7
C(16)-C(21)-C(20)	120.6(6)
C(16)-C(21)-H(21)	119.7
C(20)-C(21)-H(21)	119.7
C(15)-N(1)-C(1)	121.6(4)
C(15)-N(1)-H(1B)	119.2
C(1)-N(1)-H(1B)	119.2
O(11)-N(3)-O(12)	122.7(9)
O(11)-N(3)-C(19)	120.4(10)
O(12)-N(3)-C(19)	116.4(9)
C(5)-O(1)-C(1)	111.6(4)
C(7)-N(2)-C(2)	122.2(4)
C(7)-N(2)-H(2A)	118.9
C(2)-N(2)-H(2A)	118.9
C(9)-O(4)-C(3)	118.6(5)
C(11)-O(6)-C(4)	119.1(6)
O(9)-C(13)-O(8)	122.0(11)
O(9)-C(13)-C(14)	123.9(12)
O(8)-C(13)-C(14)	113.4(12)
C(13)-O(8)-C(6)	113.8(9)
O(9B)-C(13B)-O(8B)	120(3)
O(9B)-C(13B)-C(14B)	122(3)
O(8B)-C(13B)-C(14B)	118(3)
C(13B)-C(14B)-H(14D)	109.5
C(13B)-C(14B)-H(14E)	109.5
H(14D)-C(14B)-H(14E)	109.5
C(13B)-C(14B)-H(14F)	109.5
H(14D)-C(14B)-H(14F)	109.5
H(14E)-C(14B)-H(14F)	109.5
C(13B)-O(8B)-C(6)	131(3)

Table 6: Anisotropic displacement parameters [$Å^2 \times 10^3$] for **19**.

The anisotropic displacement factor exponent takes the form: $-2\pi^2 [(h a^*)^2 U11 + ... + 2 h k a^* b^* U12]$

	U11	U22	U33	U23	U13	U12
C(1)	37(2)	72(3)	68(3)	4(2)	-3(2)	-13(3)
C(2)	32(2)	71(3)	63(3)	11(2)	-5(2)	-7(2)
C(3)	42(3)	76(3)	75(3)	1(3)	-7(3)	-5(3)
C(4)	51(3)	87(4)	75(4)	23(3)	-8(3)	-6(3)
C(5)	82(4)	93(4)	59(3)	13(3)	-7(3)	-18(4)
C(6)	177(10)	123(6)	77(5)	-4(4)	-1(6)	-4(7)
C(7)	44(3)	64(3)	71(3)	5(3)	3(3)	1(2)
C(8)	67(4)	98(4)	67(3)	12(3)	3(3)	3(4)
C(9)	60(4)	117(6)	195(9)	-81(6)	3(5)	-20(4)
C(10)	116(7)	114(6)	199(9)	-64(6)	4(8)	9(6)
C(11)	96(6)	94(5)	98(5)	29(4)	9(5)	28(5)
C(12)	161(9)	92(5)	130(7)	39(4)	14(7)	10(6)
C(15)	37(3)	71(3)	78(4)	-5(3)	-4(3)	-6(3)
C(16)	45(3)	73(3)	61(3)	-1(3)	-12(2)	-4(3)
C(17)	77(4)	69(3)	67(3)	5(3)	0(3)	-5(3)
C(18)	111(6)	90(5)	81(4)	6(4)	14(4)	0(5)
C(19)	96(5)	81(4)	74(4)	13(3)	-15(4)	-17(4)
C(20)	96(5)	72(4)	99(5)	0(3)	-22(5)	10(4)
C(21)	63(4)	90(4)	89(4)	-5(3)	11(3)	1(3)
N(1)	37(2)	73(3)	77(3)	3(2)	0(2)	-13(2)
N(3)	190(9)	82(5)	107(5)	17(4)	-12(6)	-20(6)
O(1)	80(3)	87(2)	63(2)	0(2)	-8(2)	-25(2)
N(2)	36(2)	81(3)	60(2)	9(2)	-9(2)	-6(2)
O(3)	35(2)	200(6)	92(3)	27(3)	-1(2)	-10(3)
O(4)	54(2)	76(2)	90(3)	0(2)	-5(2)	7(2)
O(5)	90(5)	226(9)	248(9)	-134(7)	-37(5)	-2(5)
O(6)	70(2)	89(3)	94(3)	30(2)	-7(2)	-9(2)
O(7)	106(5)	164(6)	156(6)	55(4)	-31(4)	25(5)
O(10)	42(2)	94(3)	132(4)	5(3)	10(2)	-3(2)
O(11)	500(20)	130(5)	172(7)	13(5)	177(13)	-71(9)
O(12)	179(7)	91(4)	188(6)	28(4)	-27(6)	-13(5)
C(13)	81(6)	110(8)	114(7)	27(7)	28(6)	-21(6)
C(14)	178(18)	165(9)	115(9)	-28(8)	-10(10)	24(13)
O(8)	189(9)	102(5)	83(3)	0(4)	27(6)	-53(5)
O(9)	104(6)	169(8)	206(9)	-7(7)	61(6)	-20(6)
C(13B)	81(6)	110(8)	114(7)	27(7)	28(6)	-21(6)

C(14B)	178(18)	165(9)	115(9)	-28(8)	-10(10)	24(13)
O(8B)	189(9)	102(5)	83(3)	0(4)	27(6)	-53(5)
O(9B)	170(30)	150(30)	200(30)	0(20)	-40(30)	-40(30)

Table 7: Hydrogen coordinates ($\times 10^4$) and isotropic displacement parameters ($Å^2 \times 10^3$) for **19**.

	x	y	z	U(eq)
H(1)	2105	9714	1495	71
H(2)	7467	9213	1321	66
H(3)	2580	8367	1337	77
H(4)	6773	8314	2042	85
H(5)	1663	9017	2187	93
H(6A)	3464	8576	2902	151
H(6B)	6295	8945	2788	151
H(8A)	4501	9577	-111	116
H(8B)	6885	9045	-268	116
H(8C)	7410	9903	-220	116
H(10A)	5831	6503	525	214
H(10B)	8159	6784	873	214
H(10C)	7745	7156	360	214
H(12A)	4201	6111	2504	191
H(12B)	1763	6469	2216	191
H(12C)	2078	6614	2778	191
H(17)	6932	11300	680	85
H(18)	8281	12404	328	113
H(20)	2999	13500	1158	107
H(21)	1454	12392	1480	97
H(1B)	6532	10604	1343	75
H(2A)	3507	9252	618	71
H(14A)	-1013	10145	3745	229
H(14B)	-42	10618	3296	229
H(14C)	1990	10447	3725	229
H(14D)	-813	10786	3449	229
H(14E)	-1256	10024	3718	229
H(14F)	-2207	10120	3174	229

Table 8: Hydrogen bonds for **19** [Å and deg].

D-H...A	d(D-H)	d(H...A)	d(D...A)	<(DHA)
N(2)-H(2A)...O(3)#1	0.86	1.98	2.800(6)	158.5
N(1)-H(1B)...O(10)#2	0.86	2.10	2.942(5)	165.0

Symmetry transformations used to generate equivalent atoms:
#1 x-1,y,z #2 x+1,y,z

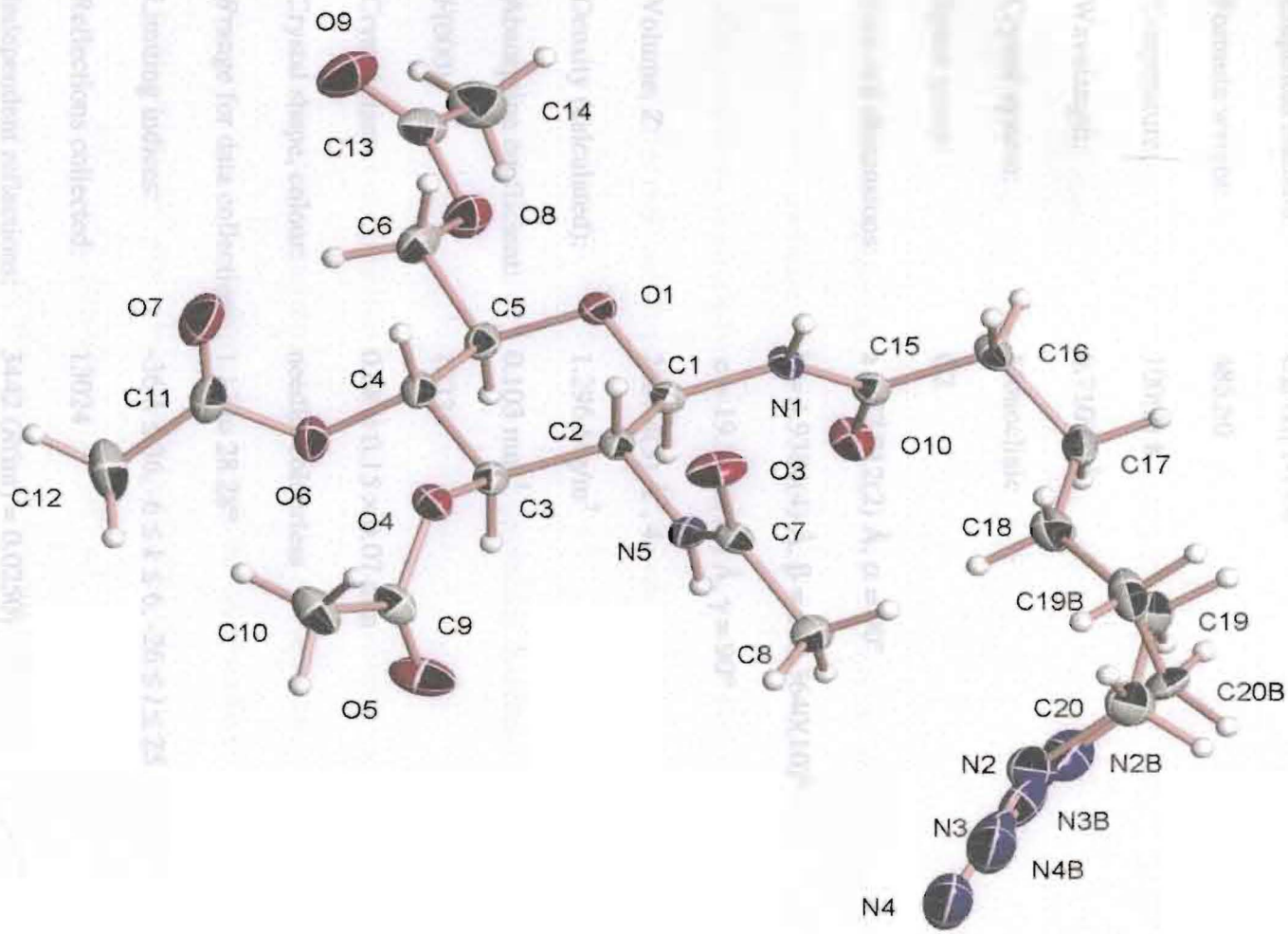

Figure 77: X-Ray crystal structure of **26**

Table 9: Crystal data and structure refinement for **26**

Identification code:	06mz053m
Empirical formula:	$C_{20}H_{31}N_5O_9$
Formula weight:	485.50
Temperature:	100(2) K
Wavelength:	0.71073 Å
Crystal system:	Monoclinic
Space group:	C2
Unit cell dimensions:	a = 27.912(2) Å, α = 90°
	b = 4.9384(4) Å, β = 112.3640(10)°
	c = 19.5130(15) Å, γ = 90°
Volume, *Z*:	2487.4(3) $Å^3$, 4
Density (calculated):	1.296 Mg/m^3
Absorption coefficient:	0.103 mm^{-1}
F(000):	1032
Crystal size:	0.68 × 0.15 × 0.07 mm
Crystal shape, colour:	needle, colourless
θ range for data collection:	1.13 to 28.28°
Limiting indices:	$-36 \le h \le 36$, $-6 \le k \le 6$, $-26 \le l \le 25$
Reflections collected:	13024
Independent reflections:	3442 (*R*(int) = 0.0250)
Completeness to θ = 28.28°:	99.9 %
Absorption correction:	multi-scan

Max. and min. transmission: 0.993 and 0.908

Refinement method: Full-matrix least-squares on F^2

Data / restraints / parameters: 3442 / 55 / 345

Goodness-of-fit on F^2: 1.102

Final R indices [$I>2\sigma(I)$]: R1 = 0.0421, wR2 = 0.1014

R indices (all data): R1 = 0.0444, wR2 = 0.1028

Largest diff. peak and hole: 0.358 and -0.198 e × Å^{-3}

Refinement of F^2 against ALL reflections. The weighted R-factor wR and goodness of fit are based on F^2, conventional R-factors R are based on F, with F set to zero for negative F^2. The threshold expression of $F^2 > 2\sigma(F^2)$ is used only for calculating R-factors

Comments: The tail end of the azidopentane chain is disordered over two positions, the occupancy ratio refined to 0.841(5) to 0.159(5). Equivalent 1,2-distances within the disordered part of the molecule as well as the distance between the first and third N-atom of the azide group were restraint to be the same within a standard deviation of 0.02. The anisotropic displacement parameters of neighboring disordered atoms were restraint to be similar using SIMU and DELU commands (SIMU standard deviation for 1,2 and 1,3 distances: 0.01, DELU standard deviations: s = 0.04, st = 0.08). Further the second and third N atoms of the azide were restraint to have the same anisotropic displacement parameters as their disordered counterparts.

Treatment of hydrogen atoms:

All hydrogen atoms were placed in calculated positions and were isotropically refined with a displacement parameter 1.5 (methyl) or 1.2 times (all others) that of the adjacent carbon atom.

Table 10: Atomic coordinates [$\times 10^4$] and equivalent isotropic displacement parameters [$Å^2 \times 10^3$] for **26**.

U(eq) is defined as one third of the trace of the orthogonalized U_{ij} tensor.

	x	y	z	U(eq)
C(1)	3537(1)	7779(4)	3027(1)	17(1)
C(2)	3332(1)	9508(4)	2319(1)	17(1)
C(3)	3576(1)	8470(4)	1790(1)	19(1)
C(4)	4162(1)	8290(5)	2166(1)	22(1)
C(5)	4330(1)	6776(5)	2906(1)	22(1)
C(6)	4911(1)	6985(5)	3322(1)	29(1)
C(7)	2463(1)	11528(4)	1822(1)	18(1)
C(8)	1888(1)	10954(5)	1514(1)	24(1)
C(9)	3189(1)	9452(5)	490(1)	24(1)
C(10)	3211(1)	11421(6)	-76(1)	34(1)
C(11)	4676(1)	7991(5)	1424(1)	28(1)
C(12)	4745(1)	6317(7)	826(2)	45(1)
C(13)	5561(1)	5043(6)	4371(1)	32(1)
C(14)	5676(1)	2983(7)	4971(2)	44(1)
C(15)	3130(1)	6818(4)	3900(1)	19(1)
C(16)	2889(1)	8024(5)	4406(1)	22(1)
C(17)	2332(1)	7054(6)	4196(1)	31(1)
C(18)	1968(1)	7867(7)	3429(1)	38(1)
C(19)	1408(1)	7030(9)	3317(2)	39(1)
C(20)	1020(1)	7672(9)	2547(2)	43(1)
N(2)	1122(1)	5786(9)	2013(2)	40(1)
N(3)	894(2)	6236(8)	1363(3)	38(1)
N(4)	697(1)	6514(9)	740(2)	53(1)
C(19B)	1404(5)	9000(30)	3102(9)	39(4)
C(20B)	1119(6)	6330(30)	2982(10)	33(4)
N(2B)	1186(6)	4560(30)	2383(9)	40(4)

N(3B)	1015(8)	5590(50)	1784(13)	38(1)
N(4B)	818(13)	6720(80)	1239(17)	53(1)
N(1)	3325(1)	8628(4)	3551(1)	18(1)
O(1)	4091(1)	8026(3)	3357(1)	21(1)
N(5)	2773(1)	9346(4)	1982(1)	18(1)
O(3)	2633(1)	13853(3)	1920(1)	31(1)
O(4)	3476(1)	10351(3)	1188(1)	22(1)
O(5)	2962(1)	7337(4)	370(1)	39(1)
O(6)	4332(1)	6779(4)	1665(1)	27(1)
O(7)	4888(1)	10074(5)	1670(1)	44(1)
O(8)	5052(1)	5049(4)	3922(1)	32(1)
O(9)	5868(1)	6545(5)	4274(1)	45(1)
O(10)	3146(1)	4351(3)	3814(1)	26(1)

All esds (except the esd in the dihedral angle between two l.s. planes) are estimated using the full covariance matrix. The cell esds are taken into account individually in the estimation of esds in distances, angles and torsion angles; correlations between esds in cell parameters are only used when they are defined by crystal symmetry. An approximate (isotropic) treatment of cell esds is used for estimating esds involving l.s. planes.

Table 11: Bond lengths [Å] and angles [deg] for **26**.

C(1)-N(1)	1.425(2)
C(1)-O(1)	1.436(2)
C(1)-C(2)	1.537(3)
C(1)-H(1)	1.0000
C(2)-N(5)	1.447(2)
C(2)-C(3)	1.526(3)
C(2)-H(2)	1.0000
C(3)-O(4)	1.440(2)
C(3)-C(4)	1.519(3)
C(3)-H(3)	1.0000
C(4)-O(6)	1.446(2)
C(4)-C(5)	1.533(3)
C(4)-H(4)	1.0000
C(5)-O(1)	1.431(2)
C(5)-C(6)	1.517(3)
C(5)-H(5)	1.0000
C(6)-O(8)	1.445(3)
C(6)-H(6A)	0.9900
C(6)-H(6B)	0.9900
C(7)-O(3)	1.229(3)
C(7)-N(5)	1.342(3)
C(7)-C(8)	1.510(3)
C(8)-H(8A)	0.9800
C(8)-H(8B)	0.9800
C(8)-H(8C)	0.9800
C(9)-O(5)	1.198(3)
C(9)-O(4)	1.365(3)
C(9)-C(10)	1.490(3)
C(10)-H(10A)	0.9800
C(10)-H(10B)	0.9800
C(10)-H(10C)	0.9800
C(11)-O(7)	1.193(3)
C(11)-O(6)	1.356(3)
C(11)-C(12)	1.502(4)
C(12)-H(12A)	0.9800
C(12)-H(12B)	0.9800
C(12)-H(12C)	0.9800
C(13)-O(9)	1.202(3)
C(13)-O(8)	1.357(3)
C(13)-C(14)	1.491(4)
C(14)-H(14A)	0.9800
C(14)-H(14B)	0.9800
C(14)-H(14C)	0.9800
C(15)-O(10)	1.233(3)
C(15)-N(1)	1.355(3)

C(15)-C(16)	1.512(3)
C(16)-C(17)	1.526(3)
C(16)-H(16A)	0.9900
C(16)-H(16B)	0.9900
C(17)-C(18)	1.508(3)
C(17)-H(17A)	0.9900
C(17)-H(17B)	0.9900
C(18)-C(19)	1.552(4)
C(18)-C(19B)	1.562(14)
C(18)-H(18A)	0.9900
C(18)-H(18B)	0.9900
C(19)-C(20)	1.514(5)
C(19)-H(19A)	0.9900
C(19)-H(19B)	0.9900
C(20)-N(2)	1.504(5)
C(20)-H(20A)	0.9900
C(20)-H(20B)	0.9900
N(2)-N(3)	1.204(5)
N(3)-N(4)	1.135(6)
C(19B)-C(20B)	1.510(16)
C(19B)-H(19C)	0.9900
C(19B)-H(19D)	0.9900
C(20B)-N(2B)	1.527(15)
C(20B)-H(20C)	0.9900
C(20B)-H(20D)	0.9900
N(2B)-N(3B)	1.196(17)
N(3B)-N(4B)	1.138(18)
N(1)-H(1A)	0.8800
N(5)-H(5A)	0.8800
N(1)-C(1)-O(1)	108.87(15)
N(1)-C(1)-C(2)	111.56(16)
O(1)-C(1)-C(2)	108.92(15)
N(1)-C(1)-H(1)	109.1
O(1)-C(1)-H(1)	109.1
C(2)-C(1)-H(1)	109.1
N(5)-C(2)-C(3)	110.84(15)
N(5)-C(2)-C(1)	110.23(15)
C(3)-C(2)-C(1)	108.18(16)
N(5)-C(2)-H(2)	109.2
C(3)-C(2)-H(2)	109.2
C(1)-C(2)-H(2)	109.2
O(4)-C(3)-C(4)	105.71(15)
O(4)-C(3)-C(2)	109.70(16)
C(4)-C(3)-C(2)	111.70(15)
O(4)-C(3)-H(3)	109.9

C(4)-C(3)-H(3)	109.9
C(2)-C(3)-H(3)	109.9
O(6)-C(4)-C(3)	105.93(16)
O(6)-C(4)-C(5)	108.94(17)
C(3)-C(4)-C(5)	111.67(16)
O(6)-C(4)-H(4)	110.1
C(3)-C(4)-H(4)	110.1
C(5)-C(4)-H(4)	110.1
O(1)-C(5)-C(6)	107.29(16)
O(1)-C(5)-C(4)	108.82(17)
C(6)-C(5)-C(4)	110.55(17)
O(1)-C(5)-H(5)	110.0
C(6)-C(5)-H(5)	110.0
C(4)-C(5)-H(5)	110.0
O(8)-C(6)-C(5)	107.03(18)
O(8)-C(6)-H(6A)	110.3
C(5)-C(6)-H(6A)	110.3
O(8)-C(6)-H(6B)	110.3
C(5)-C(6)-H(6B)	110.3
H(6A)-C(6)-H(6B)	108.6
O(3)-C(7)-N(5)	122.45(18)
O(3)-C(7)-C(8)	121.78(19)
N(5)-C(7)-C(8)	115.76(18)
C(7)-C(8)-H(8A)	109.5
C(7)-C(8)-H(8B)	109.5
H(8A)-C(8)-H(8B)	109.5
C(7)-C(8)-H(8C)	109.5
H(8A)-C(8)-H(8C)	109.5
H(8B)-C(8)-H(8C)	109.5
O(5)-C(9)-O(4)	123.0(2)
O(5)-C(9)-C(10)	126.3(2)
O(4)-C(9)-C(10)	110.7(2)
C(9)-C(10)-H(10A)	109.5
C(9)-C(10)-H(10B)	109.5
H(10A)-C(10)-H(10B)	109.5
C(9)-C(10)-H(10C)	109.5
H(10A)-C(10)-H(10C)	109.5
H(10B)-C(10)-H(10C)	109.5
O(7)-C(11)-O(6)	123.4(2)
O(7)-C(11)-C(12)	126.5(2)
O(6)-C(11)-C(12)	110.1(2)
C(11)-C(12)-H(12A)	109.5
C(11)-C(12)-H(12B)	109.5
H(12A)-C(12)-H(12B)	109.5
C(11)-C(12)-H(12C)	109.5
H(12A)-C(12)-H(12C)	109.5

H(12B)-C(12)-H(12C)	109.5
O(9)-C(13)-O(8)	122.1(2)
O(9)-C(13)-C(14)	126.3(2)
O(8)-C(13)-C(14)	111.6(2)
C(13)-C(14)-H(14A)	109.5
C(13)-C(14)-H(14B)	109.5
H(14A)-C(14)-H(14B)	109.5
C(13)-C(14)-H(14C)	109.5
H(14A)-C(14)-H(14C)	109.5
H(14B)-C(14)-H(14C)	109.5
O(10)-C(15)-N(1)	122.75(19)
O(10)-C(15)-C(16)	121.7(2)
N(1)-C(15)-C(16)	115.52(19)
C(15)-C(16)-C(17)	111.26(17)
C(15)-C(16)-H(16A)	109.4
C(17)-C(16)-H(16A)	109.4
C(15)-C(16)-H(16B)	109.4
C(17)-C(16)-H(16B)	109.4
H(16A)-C(16)-H(16B)	108.0
C(18)-C(17)-C(16)	114.52(19)
C(18)-C(17)-H(17A)	108.6
C(16)-C(17)-H(17A)	108.6
C(18)-C(17)-H(17B)	108.6
C(16)-C(17)-H(17B)	108.6
H(17A)-C(17)-H(17B)	107.6
C(17)-C(18)-C(19)	109.4(2)
C(17)-C(18)-C(19B)	134.0(6)
C(17)-C(18)-H(18A)	109.8
C(19)-C(18)-H(18A)	109.8
C(19B)-C(18)-H(18A)	113.1
C(17)-C(18)-H(18B)	109.8
C(19)-C(18)-H(18B)	109.8
C(19B)-C(18)-H(18B)	71.5
H(18A)-C(18)-H(18B)	108.3
C(20)-C(19)-C(18)	112.7(3)
C(20)-C(19)-H(19A)	109.0
C(18)-C(19)-H(19A)	109.0
C(20)-C(19)-H(19B)	109.0
C(18)-C(19)-H(19B)	109.0
H(19A)-C(19)-H(19B)	107.8
N(2)-C(20)-C(19)	107.8(3)
N(2)-C(20)-H(20A)	110.2
C(19)-C(20)-H(20A)	110.2
N(2)-C(20)-H(20B)	110.2
C(19)-C(20)-H(20B)	110.2
H(20A)-C(20)-H(20B)	108.5

N(3)-N(2)-C(20)	116.8(4)
N(4)-N(3)-N(2)	175.2(5)
C(20B)-C(19B)-C(18)	98.0(11)
C(20B)-C(19B)-H(19C)	112.2
C(18)-C(19B)-H(19C)	112.2
C(20B)-C(19B)-H(19D)	112.2
C(18)-C(19B)-H(19D)	112.2
H(19C)-C(19B)-H(19D)	109.8
C(19B)-C(20B)-N(2B)	114.1(13)
C(19B)-C(20B)-H(20C)	108.7
N(2B)-C(20B)-H(20C)	108.7
C(19B)-C(20B)-H(20D)	108.7
N(2B)-C(20B)-H(20D)	108.7
H(20C)-C(20B)-H(20D)	107.6
N(3B)-N(2B)-C(20B)	112.7(19)
N(4B)-N(3B)-N(2B)	173(3)
C(15)-N(1)-C(1)	121.42(17)
C(15)-N(1)-H(1A)	119.3
C(1)-N(1)-H(1A)	119.3
C(5)-O(1)-C(1)	111.26(14)
C(7)-N(5)-C(2)	123.33(17)
C(7)-N(5)-H(5A)	118.3
C(2)-N(5)-H(5A)	118.3
C(9)-O(4)-C(3)	117.58(17)
C(11)-O(6)-C(4)	117.59(18)
C(13)-O(8)-C(6)	114.78(19)

Table 12: Anisotropic displacement parameters [$Å^2 \times 10^3$] for **26**.

The anisotropic displacement factor exponent takes the form: -2 π2 [(h a*)^2 U11 + ... + 2 h k a* b* U12]

	U11	U22	U33	U23	U13	U12
C(1)	19(1)	13(1)	20(1)	-2(1)	8(1)	0(1)
C(2)	19(1)	13(1)	22(1)	-2(1)	10(1)	-1(1)
C(3)	21(1)	16(1)	21(1)	-2(1)	10(1)	-2(1)
C(4)	23(1)	20(1)	26(1)	-3(1)	13(1)	-2(1)
C(5)	19(1)	21(1)	27(1)	-2(1)	11(1)	1(1)
C(6)	20(1)	32(1)	34(1)	1(1)	10(1)	1(1)
C(7)	24(1)	14(1)	17(1)	-1(1)	7(1)	0(1)
C(8)	23(1)	20(1)	28(1)	-2(1)	9(1)	2(1)
C(9)	30(1)	21(1)	23(1)	-1(1)	11(1)	7(1)
C(10)	51(1)	29(1)	25(1)	1(1)	18(1)	3(1)
C(11)	24(1)	34(1)	31(1)	7(1)	16(1)	6(1)
C(12)	56(2)	48(2)	47(2)	1(1)	38(1)	7(2)
C(13)	23(1)	36(1)	34(1)	-13(1)	6(1)	7(1)
C(14)	35(1)	53(2)	35(1)	-1(1)	2(1)	11(1)
C(15)	21(1)	18(1)	19(1)	-2(1)	7(1)	1(1)
C(16)	30(1)	19(1)	19(1)	0(1)	12(1)	-2(1)
C(17)	35(1)	34(1)	33(1)	-7(1)	23(1)	-10(1)
C(18)	29(1)	54(2)	32(1)	-11(1)	12(1)	2(1)
C(19)	29(2)	56(2)	40(2)	-14(2)	20(1)	-4(2)
C(20)	26(1)	56(2)	45(2)	-16(2)	12(1)	6(2)
N(2)	29(2)	46(2)	44(2)	-10(2)	13(1)	7(2)
N(3)	21(2)	36(2)	60(3)	3(2)	18(2)	4(1)
N(4)	39(2)	82(3)	43(2)	4(2)	20(1)	-2(2)
C(19B)	54(10)	33(10)	44(9)	-7(8)	36(8)	-7(8)
C(20B)	24(7)	38(9)	38(9)	-11(8)	12(7)	-17(7)
N(2B)	38(8)	24(7)	62(10)	-5(8)	24(7)	2(6)
N(3B)	21(2)	36(2)	60(3)	3(2)	18(2)	4(1)
N(4B)	39(2)	82(3)	43(2)	4(2)	20(1)	-2(2)
N(1)	24(1)	12(1)	21(1)	-4(1)	11(1)	-1(1)
O(1)	19(1)	23(1)	23(1)	-5(1)	8(1)	-1(1)
N(5)	20(1)	12(1)	23(1)	-2(1)	9(1)	-3(1)
O(3)	29(1)	12(1)	42(1)	-1(1)	3(1)	-1(1)
O(4)	29(1)	18(1)	21(1)	-1(1)	12(1)	-4(1)
O(5)	53(1)	22(1)	30(1)	-3(1)	4(1)	-5(1)
O(6)	31(1)	25(1)	35(1)	-4(1)	22(1)	-1(1)
O(7)	40(1)	45(1)	56(1)	-3(1)	30(1)	-13(1)

O(8)	22(1)	39(1)	33(1)	3(1)	7(1)	5(1)
O(9)	22(1)	51(1)	56(1)	-2(1)	6(1)	1(1)
O(10)	39(1)	14(1)	30(1)	1(1)	17(1)	0(1)

Table 13: Hydrogen coordinates ($\times 10^4$) and isotropic displacement parameters ($Å^2 \times 10^3$) for **26**.

	x	y	z	U(eq)
H(1)	3443	5841	2895	20
H(2)	3437	11437	2449	21
H(3)	3430	6653	1593	23
H(4)	4317	10146	2244	26
H(5)	4224	4832	2819	26
H(6A)	5094	6566	2987	34
H(6B)	5008	8839	3519	34
H(8A)	1724	11953	1801	36
H(8B)	1831	9008	1547	36
H(8C)	1736	11527	995	36
H(10A)	2964	10880	-566	50
H(10B)	3562	11446	-77	50
H(10C)	3122	13232	44	50
H(12A)	4428	6398	377	67
H(12B)	4815	4434	992	67
H(12C)	5036	7028	717	67
H(14A)	6026	2273	5094	66
H(14B)	5425	1498	4801	66
H(14C)	5651	3824	5411	66
H(16A)	2893	10023	4373	26
H(16B)	3096	7500	4924	26
H(17A)	2333	5054	4233	37
H(17B)	2198	7783	4560	37
H(18A)	2072	6966	3054	46
H(18B)	1986	9850	3368	46
H(19A)	1400	5061	3407	47
H(19B)	1305	7985	3686	47
H(20A)	662	7415	2525	51
H(20B)	1059	9577	2418	51
H(19C)	1327	10174	3459	46
H(19D)	1330	9995	2632	46

H(20C)	745	6698	2845	40
H(20D)	1243	5317	3455	40
H(1A)	3320	10364	3650	22
H(5A)	2628	7735	1876	22

Table 14: Hydrogen bonds for **26** [Å and deg].

D-H...A	d(D-H)	d(H...A)	d(D...A)	<(DHA)
N(1)-H(1A)...O(10)#1	0.88	2.08	2.949(2)	168.3
N(5)-H(5A)...O(3)#2	0.88	1.92	2.737(2)	153.9

Symmetry transformations used to generate equivalent atoms:
#1 x,y+1,z #2 x,y-1,z